THE ROLE OF TETRASPANIN 6 IN COLORECTAL CANCER

by

Regina Andrijes

A thesis submitted to the University of Birmingham for the degree of

DOCTOR OF PHILOSOPHY

Institute of Cancer and Genomics

College of Medical and Dental Sciences

University of Birmingham

October 2018

ABSTRACT

Colorectal cancer is one of the most common cancer types and the second leading cause of cancer-related deaths worldwide. Poor survival of patients highlights the importance of identification of novel prognostic markers. The work in this thesis presents Tspan6 as a potential candidate. Tspan6 is a poorly studied member of the tetraspanin family of proteins that has been implicated in cancer initiation, progression and metastasis. The expression of Tspan6 in a cohort of genetically profiled colorectal adenocarcinomas in this study demonstrated that Tspan6 expression is significantly reduced in tumours vs. adjacent non-cancerous tissues. To illustrate the role of Tspan6 in colorectal cancer (CRC) Tspan6 KO mice carrying $APC^{min/+}$ allele were generated. It was found that loss of *Tspan6* gene accentuates APC-driven tumorigenesis *in vivo*. Specifically, these animals developed larger numbers of intestinal and colonic polyps. Interestingly, these polyps were significantly bigger in size and presented with a more severe neoplastic phenotype. The RNAseq analysis of polyps derived from $APC^{min/+}$ and $APC^{min/+}$Tspan6 KO showed substantial enrichment of differentially expressed genes within the MAPK signalling pathway. Additionally, our experiments with intestinal organoids derived from Tspan6 KO mice and a Caco-2 CRC cell model confirmed the important role of Tspan6 in EGFR-dependent signalling in colonic epithelium via a pathway involving autocrine production of TGF-α. Furthermore, it was demonstrated that Tspan6 regulates the production of EVs through the involvement of an adapter protein syntenin-1, an established partner of Tspan6 which is known to play a critical role in biogenesis of multivesicular bodies (MVBs) and exosomal production. Therefore, it is hypothesised that the Tspan6-syntenin-1 complex plays a critical role in suppressing of colorectal tumorigenesis by controlling autocrine secretion of EGFR ligands via

extracellular vesicles. The better understanding of the Tspan6-dependent mechanisms of EGFR regulation can underpin further development of EGFR-targeting therapy and improve survival of CRC patients.

I dedicate this thesis to my mother, Luiza,

and my siblings, Viorika and Artjom,

who always love, understand and support me.

ACKNOWLEDGEMENTS

This PhD is undoubtedly one of the biggest achievements in my life. The whole journey has been a mixture of failure and success, excitement and frustration, discouragement and motivation, but overall very rewarding in my life. I would like to thank everyone who has helped me on the way. Firstly, I would like to express my gratitude to my PhD supervisors, Dr Fedor Berditchevski, Dr Andrew Beggs and Dr Chris Tselepis for the advice, guidance, constructive criticism, your help, support and encouragement. A special thank you to Dr Rahul Hejmadi and my friend and colleague Dr Maha Ibrahim for helping me with pathology examination and scoring of samples. I am grateful to Celina Whalley for helping me with RNA sequencing and all the members of Beggs lab for being helpful, kind and friendly. A special thank you to Richard Horniblow for consulting me, willingness to proof read countless pages of my reports and thesis and becoming a good friend in the process.

I would like to thank all the staff, colleagues and fellow students of the Institute of Cancer and Genomics, you all have made this place a second home to me. I am also thankful to all the members of our laboratory, Maryam, Jing, and especially Isaac. Thank you for the stimulating discussions, for all the long hours we shared in the lab and the fun we had outside the lab, I could not ask for a better team to work with.

I wish to express my eternal gratitude to Vera Novitskaia for always being there for me, for teaching, advising and listening. You have become my dearest friend, a shoulder to cry on, you have provided me with strength and motivation and taught me invaluable life lessons. I would like to thank all my friends in the UK and in Estonia for your unconditional friendship. Especially to my best friend Kristina, who

has shared with me the moments of happiness, when I was accepted to the program, the moments of frustration, when I was writing my thesis, and been there for me for over 18 years of my life. I would also like to express my gratitude, appreciation and love to Andrea for believing in me, supporting me and making me happy.

And finally, I would like to thank my whole family: my mother, sister and brother for supporting me not only during my PhD but throughout my life. I would not be here if it was not for you.

TABLE OF CONTENTS

LIST OF FIGURES

LIST OF TABLES

ABBREVIATIONS

15-PGDH	15-Hydroxyprostaglandin Dehydrogenase
ACS	American Cancer Society
AOM	Azoxymethane
AP-2	Adaptor Protein 2
APC	Adenomatous Polyposis Coli
APP	amyloid precursor protein
AREG	Amphiregulin
ARF6	ADP-Ribosylation Factor 6
ATCC	ADP-Ribosylation Factor 6
BMP	Bone Morphogenic Protein
BSA	Bovine Serum Albumin
BTC	Betacellulin
CAP	Cancer Associated Polyp
CDK8	cyclin-dependent kinase 8
CFP	Cancer Free Polyp
CFTR	cystic fibrosis transmembrane receptor
CIMP	The CpG Island Methylator Phenotype
CIN	Chromosomal Instability
CK1α	Casein Kinase 1
CM	Conditioned Media
CO-IP	Co-immunoprecipitation
COX-2	Cyclooxygenase-2
CRC	Colorectal Cancer
CS	Cowden Syndrome
CTLA-4	Cytotoxic T Lymphocyte Antigen-4
CTX	Cetuximab
DMAB	3,2′-Dimethyl-4-Aminobiphenyl
DMEM	Dulbecco’s modified Eagle’s medium

DMH	1,2-Dimethylhydrazine
DMSO	Dimethyl Sulfoxide
DNA	Deoxyribonucleic Acid
Dvl	Dishevelled
ECM	Extracellular Matrix
EDTA	Ethylenediaminetetraacetic Acid
EGF	Epidermal Growth Factor
EGFR	Epidermal Growth Factor Receptor
EMVI	Extramural Vascular Invasion
ENU	Ethylnitrosourea
EPGN	Epigen
EREG	Epiregulin
ERK	Extracellular-Signal-Regulated Kinase
ESCRT	Endosomal Sorting Complex Required for Transport
EV	Extracellular Vesicle
FAP	Familial Adenomatous Polyposis
FCS	Foetal Calf Serum
FFPE	Formalin Fixed Paraffin Embedded
FGF	Fibroblast Growth Factor
FGFR	Fibroblast Growth Factor Receptor
Fz	Frizzled
GAB	GRB2-Associated Binder
GAPDH	Glyceraldehyde 3-Phosphate Dehydrogenase
GITR	Glucocorticoid-Induced TNF Receptor Related Protein
GITR	Gastrointestinal Tract
GPCR	G-Protein Coupled Receptors
GSK3β	Glycogen Synthase Kinase 3 Beta
HB-EGF	Heparin-Binding Epidermal Growth Factor
HBRC	Human Biomaterials Resource Centre

HCV	Hepatitis C Virus
HMPS	Hereditary Mixed Polyposis
HNPCC	Hereditary Non-Polyposis Colorectal Cancer
HSPG	Heparan Sulfate Proteoglycan
IF	Immunofluorescence
IFN-β	Interferon Beta
IL-5	Interleukin-5
ILV	Intraluminal Vesicles
IQ	2-Amino-33-Methylimidazo [4,5-f] Quinoline
IRS	Insulin Receptor Substrate
ISC	Intestinal Stem Cells
JNK	c-Jun-N-Terminal Kinase
JPS	Juvenile Polyposis
KO	Knockout
Lag-3	lymphocyte activation gene-3
LEF	Lymphoid Enhancer Family
LEL	Large Extracellular Loop
LGR5	Leucine-Rich Repeat-Containing G-Protein Coupled Receptor 5
lngRNA	Long non-coding RNA
LOH	Loss of Heterozygosity
LPT	Lapatinib
LRP	Lipoprotein-Receptor-Related Protein
MAM	Methylazoxymethanol
MAPK	Mitogen-Activated Protein Kinase
MDCK	Madin-Darby canine kidney
MIN	Multiple Intestinal Neoplasia
miRNA	MicroRNA
MLH1	MutL Homolog 1
MMR	Mismatch Repair Machinery

MNNG	N-Methyl-N′-Nitro-N-Nitrosoguanidine
MNU	Methylnitrosourea
mRNA	Messenger RNA
MSH2	MutS Protein Homolog 2
MSI-H	High Microsatellite Instability
MSI-L	Low Microsatellite Instability
MSS	Microsatellite Stable
MUTYH	mutY DNA Glycosylase
MVB	Multivesicular Body
Nedd4	Neural Precursor Cell Expressed Developmentally Down-Regulated Protein 4
NFAT	Nuclear Factor of Activated T Cells
NF-κB	Nuclear Factor Kappa-Light-Chain-Enhancer of Activated B Cells
NGS	Next Generation Sequencing
NHS	National Health Service
NK	Natural Killer
NLK	Nemo-like Kinase
NRG	Neuregulin
NTA	Nanoparticle Tracking Analysis
OD	Optical Density
PBS	Phosphate Suffer Saline
PBS-0	Modified Phosphate Buffered Saline
PCP	Planar Cell Polarity
PD-1	Programmed Cell Death Protein
PDGF-R	Platelet- Derived Growth Factor Receptor
PD-L1	Programmed Cell Death Protein ligand
PDZ	Postsynaptic density-95, Disc large, ZO-1
PEI	Polyethyleimine
PFA	Paraformaldehyde
PhIP	2-Amino-1-Methyl-6-Phenylimidazo [4,5-b]-Pyridine

PI3K	Phosphoinositide 3-Kinase
PI4K	Phosphatidylinositol 4-Kinase
PIK3CA	Phosphatidylinositol-4,5-Bisphosphate 3-Kinase Catalytic Subunit Alpha
PIP3	Phosphatidylinositol -3, -4, -5 Triphosphate
PJS	Peutz Jeghers Syndrome
PKC	Protein Kinase C
PKG	cGMP-Dependent Kinase G
PLD2	Phospholipase D2
PPAP	Polymerase Proofreading-Associated Polyposis
PSG	Pregnancy-Specific Glycoproteins
PTEN	Phosphatidylinositol 3,4,5-Trisphosphate 3-Phosphatase and Dualspecificity Protein Phosphatase
RAB27	Ras-Related Protein Rab-27
RhoA	RAS homologue-gene family member A
RLR	Retinoic Acid-Inducible Gene I-Like Receptor
RNAseq	RNA Sequencing
RNF43	Ring Finger 43
RTK	Receptor Tyrosine Kinase
SDS-PAGE	Sodium Dodecyl Sulphate-Poliacrylamide Gel Electrophoresis
SEER	Surveillance, Epidemiology, and End Results
SEL	Small Extracellular Loop
SeV	Sendai Virus
shRNA	Short Hairpin RNA
siRNA	Small Interfering RNA
SSA	Sessile Serrated Adenoma
STAR	Short Tandem Repeat
TA	Transit Amplifying (cells)
TAK 1	TGF-β activated kinase 1
TBST	Tris-Buffered Saline - Tween 20®
TCF	T-Cell Factor

TERM/TEM	Tetraspanin Enriched Microdomain
TGF-α	Transforming Factor Alpha
TGF-β	Transforming Factor Beta
TIM-3	T Cell Immunoglobulin and Mucin Containing Protein-3
TIMP-1	Tissue Inhibitor of Metalloproteinase 1
TNFR	TNF Receptor
Treg	T Regulatory Cell
Tspan6	Tetraspanin-6
VEGF-R	Vascular Endothelial Growth Factor Recepor
WHO	World Health Organisation
WT	Wild Type
ZO-1	Zona Occludin-1

1 INTRODUCTION

1.1 Colorectal cancer

1.1.1 Definition

Cancer is a collective term for a group of disorders that result from dysregulated cell growth (WHO 2015). Transformed cells proliferate in an aberrant manner, independent of cell control signals, leading to dysregulation in balance of cell proliferation and apoptosis. Newly formed, neoplastic cell populations can invade locally and frequently metastasise to other organs causing significant morbidity and ultimately death. The majority of solid tumours are highly heterogeneous and molecular mechanisms underlying oncogenesis differ for different types of cancer (Ruddon 2003). Colorectal cancer (CRC) is a malignant tumour that arises as a result of complex genetic or epigenetic alterations of epithelial stem cells of the colon or rectum. CRC is initiated within the intestinal mucosa - the lining of the luminal surface of the large intestine. These cells are constantly exposed to toxins from intestinal contents, including the colonic microbiota and digesta alongside the constant sloughing of the outermost cells during gastro-intestinal transit of food undergoing digestion. To avoid the aggregation of damaged cells in the colon, a self-renewal mechanism of the colonic epithelial cells takes place at a high rate (Creamer, Shorter *et al.* 1961).

1.1.2 Types of cancers in the colon and rectum

The most common form of CRC is adenocarcinoma, accounting for more than 96% of all colorectal cancers. This type of cancer is initiated within the intestinal gland cells that line the inside of the colon or rectum. Less common types of tumours

developing in the colorectum are carcinoid tumours that are initiated in the hormone producing cells of the colon; lymphomas – starting in immune cells – typically arising in lymph nodes, but rarely occur in colon, rectum and other organs; sarcomas – tumours arising in blood vessels, muscle and connective tissue (ACS 2018). This study is focussed on characterising adenocarcinoma of the intestine and colon.

1.1.3 Colorectal cancer incidence

CRC is the fourth most common type of cancer diagnosed in the United Kingdom, second most common cancer in Europe and third most common in the world and represents 12% of all diagnosed cancers in UK (SEER Research Data 1973-2015 2018, Cancer Research UK 2015, Ferlay, Soerjomataram *et al.* 2015). The mean age of CRC diagnosis in 2015 was 85-89 years. Gender distribution of CRC is skewed towards the male population with a 55% in men vs. 45% in women.

1.1.4 Colorectal cancer mortality and survival

CRC is the second largest cause of cancer-related death in the UK, with approximately 16,000 lives every year (Cancer Research UK 2015). The most recent statistics indicate that at least 59% of men and 58% of women will survive their disease for 5 years after diagnosis. Remarkably, in the last 40 years the survival rate has more than doubled. The ten-year survival for both men and women has increased from 22% in 1971-1972 to 56% and 57% in 2010-2011 for men and women respectively. This prominent increase in the survival rate is closely linked to the emergence of nation-wide screening programs. The National Health Service (NHS) launched a screening program in England in 2006, in Wales in 2008, and in Northern Ireland in 2010, with the aim of detecting the disease at its earliest stage of development. Detection of CRC precursor lesions, or early stage cancer allows for

five-year survival of 90%, compared to 10% diagnosed at the latest stage. This data exemplifies the impact the screening process has made on the diagnosis and detection of the disease. Additionally, major improvements have occurred due to the development of personalised treatments. This increases the chances of patient response to treatment and lowers the incidence of side effects as opposed to chemo- and radiotherapies.

1.1.5 The worldwide distribution of colorectal cancer

CRC is the third most common type of cancer worldwide with 1.36 million people diagnosed in 2012. CRC accounted for approximately 694,000 deaths in 2012, comprising 8% of all cancer related deaths in the world (GLOBOCAN, 2012). However, the worldwide distribution of CRC incidence is not uniform. The highest incidence has been recorded in European countries, North America and Oceania; and the lowest incidence is seen in some countries of South and Central Asia and Africa (Brenner *et al.*, 2014). Age-standardised incidence by region for 2008 shows a 10-fold difference in incidence in both men and women in Central Africa compared to Australia and New Zealand (Figure 1-1). This pattern demonstrates that CRC is a disease of more developed countries. Indeed, countries of the developed world account for 63% of all CRC cases (Janout and Kollarova, 2001).

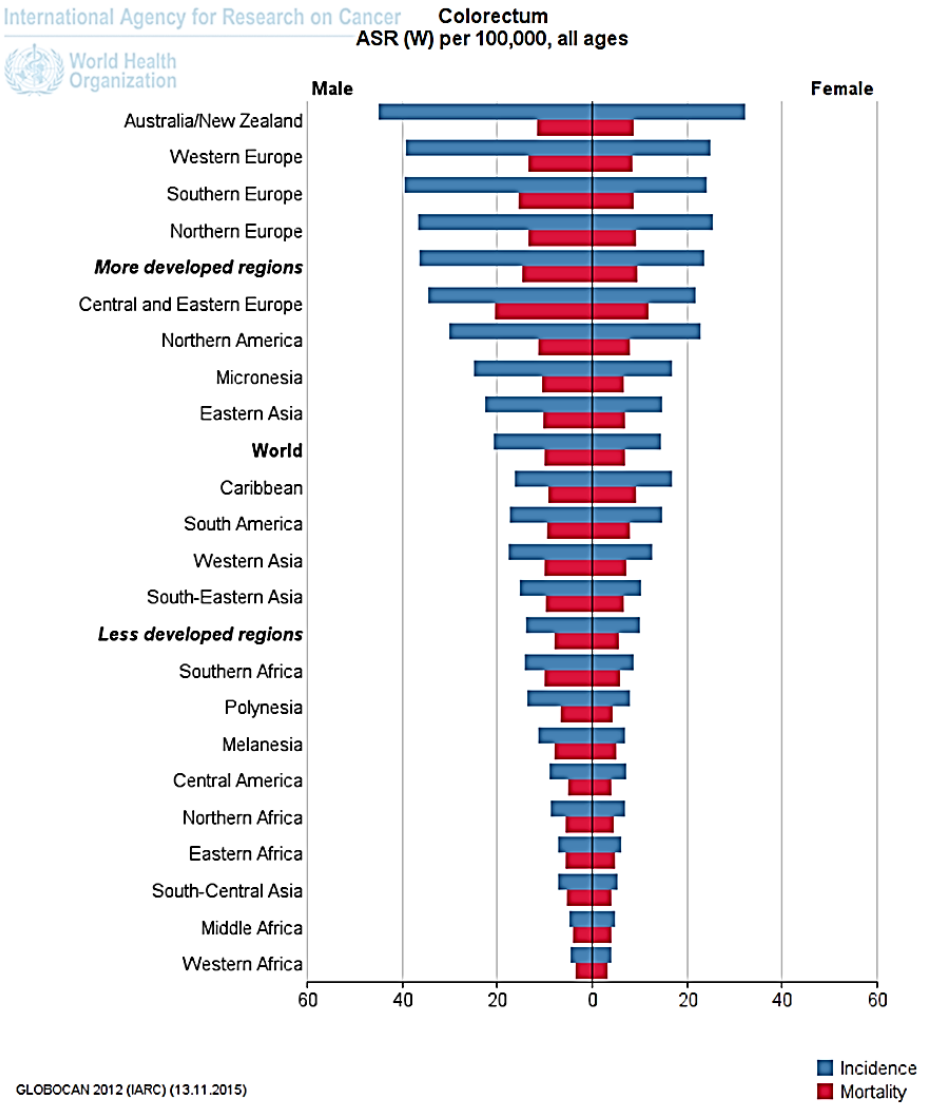

Figure 1-1. Age standardised incidence and mortality rates in males and females in the world in 2012. Numbers represent the number of colorectal cases per 100,000 individuals. In more developed regions incidence of colorectal cancers is up to 10-fold higher. Figure is reproduced from Ferlay J, Soerjomataram I *et al.* 2013.

1.1.6 Colorectal cancer risk factors

Both genetic and environmental factors play a role in aetiology of colorectal cancer. The majority of CRCs are sporadic and account for 75%-85% of all CRC cases. These develop as a result of accumulation of somatic mutations, and as such risk of CRC development increases with age (Fredericks, Dealtry *et al.* 2015, Noone, Howlader *et al.* 2018). Risk further increases in individuals with one or more affected family members, and accounts for more than 20% of CRC cases (Valle 2014, Armelao, de Pretis 2014). The group of CRCs that are characterised by inherited germline mutations are collectively known as hereditary type of colorectal cancer and account for 3%-5% of CRC patients (Kuipers, Grady *et al.* 2015). The two most common hereditary syndromes that significantly increase the lifetime risk of CRC development are familial adenomatous polyposis (FAP) or hereditary non-polyposis colorectal cancer (HNPCC), also known as Lynch syndrome. Other hereditary colorectal cancer syndromes include MUTYH-associated with mutations in the mutY DNA glycosylase (MUTYH) gene, polymerase proofreading-associated polyposis (PPAP), juvenile polyposis (JPS), hereditary mixed polyposis (HMPS), Cowden syndrome (CS), Peutz Jeghers syndrome, and serrated polyposis (Talseth-Palmer 2017, Tomlinson 2015, Church 2004). Individuals with FAP are at 100% risk of developing colorectal cancer, unless they undergo prophylactic colectomy, and for patients with HNPCC-related mutations lifetime risk of CRC is as high as 80% (Colussi, Brandi *et al.* 2013). CRC developed in patients with FAP or HNPCC is characterised by an early onset, at 40-50 years of age (Fredericks, Dealtry *et al.* 2015, Kuipers, Grady *et al.* 2015). Additionally, there is an increased risk of developing CRC in individuals with inflammatory bowel disease (IBD), which accounts for 1% of CRC incidences (Jess, Rungoe *et al.* 2012, Kuipers, Grady *et al.*

2015).

1.1.6.1 Familial adenomatous polyposis

Familial adenomatous polyposis (FAP) is an autosomal dominant inherited disease and is caused by mutations in adenomatous polyposis coli (APC) gene, which plays a central role in Wnt signalling (Vasen, Tomlinson *et al.* 2015) (see below). FAP is characterised by the appearance of hundreds to thousands of adenomatous polyps in the colon. Most of these patients will develop benign adenomas, but some will progressively accumulate additional mutations, resulting in the transformation of benign to malignant lesions. To date more than 300 APC mutations have been identified in individuals with FAP (Waller, Findeis *et al.* 2016). These mutations result in a truncated form of the protein with aberrant function. The vast majority of these mutations are nonsense and frameshift mutations, but insertions and deletions also occur. Nearly a third of germline mutations in APC occur at codons 1061 and 1309. As many as 5% of FAP patients carry a deletion mutation at codon 1061, and 10% of patients have the deletion at codon 1309. Other germline mutations in APC are evenly distributed between codons 200 and 1600 (Half, Bercovich *et al.* 2009). Progression to malignancy requires additional genetic alterations in APC, and commonly FAP patients acquire a somatic mutation in the wild-type parental allele or loss of heterozygosity (LOH) at this locus, strongly supporting Knudson's two-hit hypothesis (Knudson 1971).

1.1.6.2 Lynch Syndrome

Lynch syndrome or HNPCC is the most common form of hereditary colorectal cancer, accounting for 4-5% of CRC cases and is an autosomal dominant inherited condition (Fredericks, Dealtry *et al.* 2015, Kinzler, Vogelstein 1996). In contrast to

numerous polyp manifestations in FAP patients, HNPCC is characterised by the absence or a small number of polyps with distinct histopathological features: polyps appear to be mucinous, poorly differentiated and often with lymphocytic infiltrate (Sarosiek, Stelmaszuk 2018, Seth, Ager *et al.* 2018). Germline mutations in HNPCC patients occur in genes of DNA mismatch repair machinery (MMR). Mutations in five genes have been identified to date: *MLH1, MSH2, MSH6, PMS2 or EPCAM* (Kuipers, Grady *et al.* 2015). Aberrant function of the MMR system results in sequential accumulation of multiple mutations in both coding and non-coding microsatellite sequences of DNA. This leads to high level of microsatellite instability (MSI-H) phenotype in HNPCC patients (Le, Ansari *et al.* 2017). This in turn, dramatically accelerates the mutation rate in other tumour-suppressor and/or oncogenes, leading to rapid cancer development. The most common mutations are found in *MSH2* and *MLH1*, 36%-60% and 25-50% respectively (Dowty, Win *et al.* 2013). Mutations in these genes account for 95% of Lynch syndrome alterations (Colussi, Brandi *et al.* 2013).

1.1.6.3 Environmental risk factors

Among non-modifiable risk factors, such as age, gender and family history of the disease, there are variety of risk factors that are greatly associated with the modern westernised lifestyle, including tobacco smoking, alcohol consumption, physical inactivity, obesity, and diet high in fat, red and processed meat and low consumption of dietary fibre. In the United Kingdom, 54% of colorectal cancers are tightly correlated to lifestyle and could be prevented (CRUK, 2015). Hence, environmental and lifestyle factors play an important role in the development of colorectal cancer. Risk factors associated with colorectal cancer, and factors that

have been reported to be preventative of CRC, predominantly lifestyle factors, are presented in Table 1-1. It is predicted that 11% of CRC cases in UK are caused by the high incidence of obesity, smoking and alcohol consumption coupled with low levels of physical activity (Cancer Research UK 2015).

Table 1-1. Overview of risk and preventive factors of colorectal cancer. Table is reproduced from Brenner, Kloor *et al.* 2014.

Overview of risk and preventive factors of colorectal cancer	
	Risk
Sociodemographic factors	
Older age	↑↑↑
Male sex	↑↑
Medical factors	
Family history	↑↑
Inflammatory bowel disease	↑↑
Diabetes	↑
Helicobacter pylori infection	(↑)
Other infections	(↑)
Large bowel endoscopy	↓↓
Hormone replacement therapy	↓
Aspirin	↓
Statins	(↓)
Lifestyle factors	
Smoking	↑
Excessive alcohol consumption	↑
Obesity	↑
Physical activity	↓
Diet factors	
High consumption of red and processed	↑
Fruit and vegetables	(↓)
Cereal fibre and whole grain	(↓)
Fish	(↓)
Dairy products	(↓)

↑↑↑ very strong risk increase
↑↑ strong risk increase
↑ moderate risk increase
↓↓ strong risk reduction
↓ moderate risk reduction
( ) not fully established associations

Approximately 70% of CRC burden can be reduced by change in dietary habits (Haggar, Boushey 2009). A strong association of CRC development has been seen in individuals that consume higher than average amounts of red and processed meat as well as animal fat, with 13% of CRC cases in UK are believed to be caused by meat consumption (Cancer Research UK 2015, Haggar, Boushey 2009, Boyle, Langman 2000). The presence of haem iron in red meat is thought to be the causative agent of CRC development (Fonseca-Nunes, Jakszyn *et al.* 2013, Kabat, Miller *et al.* 2007). High temperatures used in production of processed meat results in production of heterocyclic amines and polycyclic aromatic hydrocarbons, both of which are believed to have carcinogenic properties. Consumption of animal fat is believed to cause a dysbiosis in the colon, favouring bacteria capable of degrading bile salts to potentially carcinogenic N-nitroso compounds (Larsson, Wolk 2006). Consumption of dietary fibre plays a significant role in prevention of CRC (Parkin, Boyd 2011, Aune, Chan *et al.* 2011). It is estimated that an increase in dietary fibre intake could reduce CRC incidence by 28% in UK (Cancer Research UK 2015).

1.1.7 Treatment of colorectal cancer

For patients diagnosed with colon or rectal cancer surgical removal of the tumour is often the main treatment. For treatment of advanced rectal tumours, a neoadjuvant (preoperative) radiotherapy or chemoradiotherapy with 5-fluorouracil or capecitabine is often used to facilitate tumour shrinking and prevent spreading to other tissues. It has been shown that neoadjuvant treatment is effective in reducing local recurrence, however it does not have a significant impact on overall survival (Kuipers, Grady *et al.* 2015, van Gijn, Marijnen *et al.* 2011). Adjuvant (postoperative) chemotherapy is commonly used for stage III tumours (Labianca, Nordlinger *et al.*

2013). Drugs used to treat CRC include 5-Fluorouracil, capecitabine, irinotecan, oxaliplatin, trifluridine and tipiracil. Often, two or more of these drugs are combined to increase the efficacy of the treatment. Sometimes, chemotherapeutic drugs are used in combination with targeted therapies. Three major groups of drugs for targeted therapies of CRC are monoclonal antibodies against EGFR (cetuximab and panitumumab), monoclonal antibodies and small-molecule based compound against VEGF-A (bevacizumab and ziv-aflibercept respectively), and small-molecule based multikinase inhibitor (regorafenib) targeting receptor tyrosine kinases (RTKs), such as EGFR, vascular endothelial growth factor receptor (VEGFR1/2/3), platelet-derived growth factor receptor-β (PDGF-R), fibroblast growth factor receptor (FGFR), as well as c-KIT, RET and BRAF (Wilhelm, Dumas *et al.* 2011). Anti-EGFR therapies are commonly used for metastatic colorectal adenocarcinomas that express high levels of EGFR and do not carry mutations in downstream effectors of the EGFR signalling pathway including KRAS, NRAS or BRAF. Anti-VEGF-A treatment is commonly used to prevent angiogenesis of tumours and restrict access of oxygen and nutrients (Willett, Boucher *et al.* 2004). Regorafenib is used in cases of advanced CRC when other drugs proved to be ineffective. It targets multiple angiogenic, stromal and oncogenic RTK (Ettrich, Seufferlein 2018).

Immunotherapy has also been employed to manipulate the tumour microenvironment via tumour infiltrating lymphocytes. Current immunotherapies include immune checkpoint inhibitors directed against cytotoxic T lymphocyte antigen-4 (CTLA-4) and programmed cell death protein (PD-1)/PD-1 ligand (PD-L1) (Gong, Chehrazi-Raffle *et al.* 2018). A number of novel targets are currently in the development and trial stages for applications in colorectal and other tumours,

targeting T cell immunoglobulin and mucin containing protein-3 (TIM-3), lymphocyte activation gene-3 (Lag-3), OX40 (CD134), glucocorticoid-induced TNF receptor (TNFR)-related protein (GITR, CD357), 4-1BB (CD137), CD40, and CD70 (Jager, Halama *et al.* 2016). Interestingly, only colorectal tumours with a high level of microsatellite instability (MSI-H) have been shown to effectively respond to current immunotherapies due to somatic hypermutations that lead to expression of larger amount of neoantigens available for immune clearing (Le, Uram *et al.* 2015).

Despite the wide range of treatments available the survival of patients with advanced tumours has not improved in the last two decades, thus necessitating a deeper understanding and characterising colorectal adenocarcinoma development and progression.

1.2 Molecular basis of CRC

1.2.1 The anatomical structure of the colon

The intestine is anatomically divided into the small intestine and the colon. The innermost layer of intestine, the mucosa, is lined with rapidly renewing epithelial cells. The proliferative cells reside in the crypts of Lieberkühn – epithelial invaginations in the underlying intestinal tissue. The crypts contain self-renewing stem cells and their progeny – transit amplifying (TA) cells. TA cells divide four to five times before leaving the crypt, migrating upwards, following terminal differentiation into one of the four differentiated types of cells – mucus-secreting goblet cells, hormone-secreting enteroendocrine cells, absorptive enterocytes and Paneth cells (Figure 1-2) (van der Flier, Clevers 2009). Paneth cells are the only differentiated type of cells that escape migration and participate in antibacterial defence and innate immunity (Clevers, Bevins 2013). Three days after terminal differentiation cells undergo apoptosis and

anoikis with the exception of Paneth cells that are long-lived and reside at the bottom of the crypt between 2 and 3 months. The colonic surface lacks villi and is flat. The cellular organisation of the colonic epithelium is comparable to small intestine with the exception of Paneth cells that are absent in the colon (van der Flier, Clevers 2009). Of note, small intestinal cancers are rare, affecting around 1,500 individuals compared to 41,300 cases of large bowel cancers yearly in the UK, around 30% of colorectal cancers occur in ascending colon, 10% in transverse, 15% in descending, 25% in sigmoid and 20% in rectum (Cancer Research UK 2015).

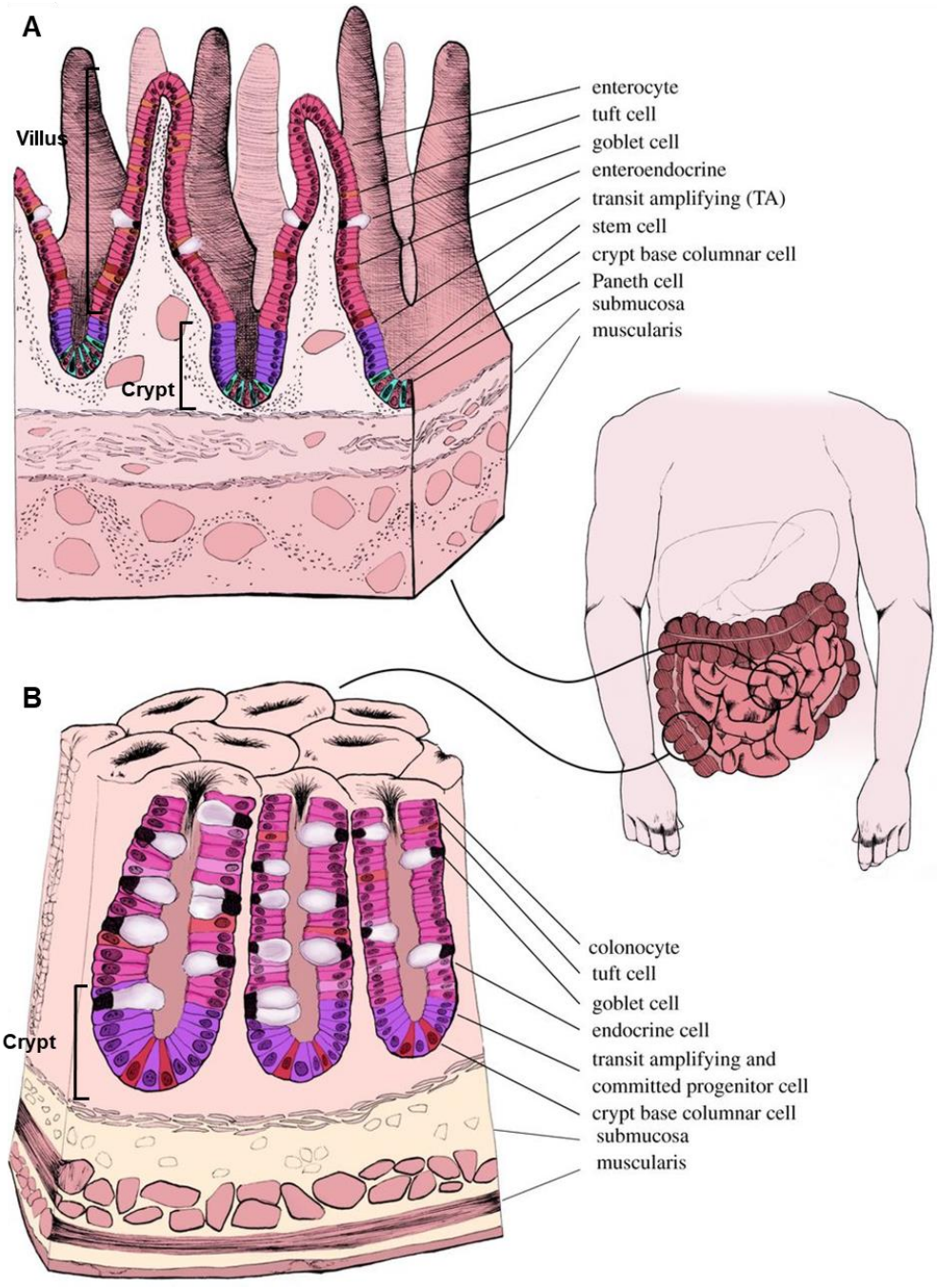

Figure 1-2. Anatomy of the small and large intestine. (A) The architecture of mucosal layer of the small intestine consists of crypts (bottom) and villi (protruding into the intestinal lumen). The stem cells and Paneth cells reside at the bottom of the crypt, transit amplifying (TA) cells are migrating up the crypt and terminally differentiated cells (enterocytes, tuft cells, Goblet cells, enteroendocrine cells) are located at the villus compartment. **(B)** The surface of the colonic epithelium is flat and does not have villi. Crypts of the colon lack Paneth cells, but contain crypt base columnar secretory cells. The mature colonic epithelium contains high proportion of Goblet cells. Figure is reproduced and modified from Fair, Colquhoun *et al.* 2018.

1.2.2 Molecular pathways of colorectal carcinogenesis

There are two well characterised pathways underlying tumorigenic transformation of colonic epithelial cells: the conventional adenoma-carcinoma sequence, proposed by Fearon and Vogelstein, and the serrated pathway. Adenoma-carcinoma sequence describes molecular events that give rise to formation of adenomatous polyps (precursor lesions) which develop into carcinomas. The vast majority of sporadic colorectal cancers (up to 90%) start their development in this way; and are typically initiated by mutations in adenomatous polyposis coli (APC) gene (Fearon, Eric R. 2011, Moran, Ortega *et al.* 2010, Leslie, Carey *et al.* 2002). Genetic alterations at the later stages of tumorigenesis include point mutations of tumour-suppressor (*TP53, DCC, SMAD2/4, TGF-βRII)* and oncogenes *(KRAS, PIK3CA, BRAF, CTNNB1, HER-2/ERBB2)* and amplification of chromosomal segments (gains of chromosomes and chromosome arms 7, 8q, 13, and 20q), large chromosomal deletions or translocations (losses of chromosomes 4q, 8p, 17p, and 18q) (Camps, Grade *et al.* 2008). The serrated neoplasia pathway has been identified recently and accounts for 15% to 30% of all CRCs (Kim, S. Y., Kim 2018). The serrated pathway is characterised by somatic mutations in *BRAF* or *KRAS* in early stages of polyp development and by excessive CpG island promoter hypermethylation resulting in epigenetic silencing of tumour-suppressor genes, e.g. *MLH1* (Kedrin, Gala 2015). The serrated pathway is further stratified by the degree of microsatellite instability (MSI) into MSI-H (high) or MSI-L (low) (Yamane, Scapulatempo-Neto *et al.* 2014). Microsatellite instability is also a common feature of the conventional pathway in colorectal carcinogenesis.

1.2.3 Adenoma-Carcinoma sequence

In 1990, Fearon and Vogelstein proposed a model of molecular pathogenesis of colorectal carcinoma development – adenoma-carcinoma sequence (Fearon, Vogelstein 1990). The key principal of this process is the requirement of multiple genetic hits, caused by chromosomal instability (CIN), harbouring mutations in critical genes, such as *APC*, *KRAS*, *TP53* and *TGF-β* pathway genes (Arends 2013). However, it is being widely recognised that it is the total accumulation of mutations rather than the sequence that is required for successful malignant carcinoma formation. An early stage of colorectal tumorigenesis is characterised by mutations in adenomatous polyposis coli gene (*APC*) and formation of dysplastic adenomas (Kinzler and Vogelstein, 1996). *APC* is a tumour suppressor gene and encodes a protein with multiple functions, implicated in differentiation, adhesion, polarity, migration, development, apoptosis, and chromosomal segregation (Leslie, Carey *et al.* 2002). The protein is located at the basolateral membrane of the colonic epithelial cells. Its expression levels increase as cells migrate up from the crypt base. APC plays a central role in the Wnt signalling pathway (see below). Disruption of APC abrogates its ability to negatively regulate Wnt signal transduction resulting in constitutive activation of the latter. Truncated APC, in the context of CRC, loses its binding ability to β-catenin, leading to β-catenin accumulation in the cytoplasm. Subsequently, β-catenin is translocated to the nucleus where the protein binds to T-cell factor (TCF)/lymphoid enhancer (LEF) family of transcription factors and activates gene transcription that stimulates cell growth and inhibits apoptosis. Loss of function mutations in the *APC* gene occur in over 80% of colon adenocarcinomas (Fredericks, Dealtry *et al.* 2015). Downregulation of the APC function can be also achieved through epigenetic silencing via hypermethylation of the APC gene

promoter (Segditsas and Tomlinson, 2006).

Although the hyperactivation of Wnt signalling results in increased cellular proliferation, additional molecular changes are required for cellular transformation to progress from adenoma to malignant type of lesion. The second step towards progression of CRC is activation of the *KRAS* gene leading to advanced adenomatous lesions. *KRAS* is a proto-oncogene that encodes a small protein with GTPase activity which plays an important role in controlling cell proliferation and differentiation (Leslie, Carey *et al.* 2002). Mutations in *KRAS* decrease its GTPase activity resulting in constitutive activation of downstream signalling pathways (e.g. Ras/Raf/MEK/ERK pathway), leading to increased proliferation and inhibition of apoptosis (Lemieux *et al.*, 2015). *KRAS* is mutated in approximately 30% of colorectal adenomas and 30%-42% of colorectal cancers (Liu, Jakubowski *et al.* 2011).

The progression to late adenoma often is associated with allelic loss of 18q, and generally occurs due to chromosomal instability and deficiency in mismatch repair mechanisms. A number of tumour suppressor genes are located to this chromosomal region, including *DCC*, *SMAD2, SMAD4*, and *Cables*. SMAD2 and SMAD4, are key components of TGF-β signalling pathway, which in turn negatively regulates epithelial cell growth (Leslie, Carey *et al.* 2002). Genetic alterations and/or loss of *SMAD4* or *SMAD2* promote enhanced transcription of genes involved in cell growth and proliferation (Zhao, Mishra *et al.* 2018, Fleming, Jorissen *et al.* 2013). Allelic loss of 18q has been identified in 70% of colorectal cancers (Arends 2013). Interestingly, the loss of SMAD4 does not initiate tumour formation, indicating the

important role in tumour progression initiated by other gene alterations, such as *APC* and KRAS (Zhao, Mishra *et al.* 2018).

Dysfunction of P53 plays a major role in progression of late stage adenomas to carcinomas. *TP53* is an important tumour-suppressor gene that maintains genomic integrity. P53 appears to be mutated in up to 75% of colorectal cancers, typically through combination of missense mutations and loss of heterozygosity of chromosome 17p (Markowitz, Bertagnolli 2009). Recently published analysis of colorectal adenomas revealed the enrichment of mutations in *TP53*, *FBXW7*, *PIK3CA, KIAA1804* and *SMAD2* exclusively in cancer associated polyps (CAPs) compared to cancer free polyps (CFPs), highlighting the role of these genes in malignant transformation of benign adenomas in the colon epithelium (Druliner, Wang *et al.* 2018).

1.2.4 Serrated Pathway

Approximately 10% of all colorectal cancers are derived through the serrated pathway which is manifested by the formation of serrated group of polyps (sessile serrated adenomas, traditional serrated and mixed polyps) (Yamane, Scapulatempo-Neto *et al.* 2014, Sweetser, Smyrk *et al.* 2013). Serrated polyps exhibit hyperplasia and lack of dysplasia on a cytological level, i.e. the crypt epithelium tends to fold in. It is believed to result from cell aggregation and failure of apoptosis and anoikis, however, the molecular basis of serration has not been fully determined (Kim, Kim 2018, Patai, Molnar *et al.* 2013). Commonly observed genetic alterations in the serrated pathway are BRAF or KRAS mutations, hypermethylation of tumour-suppressor gene promoters, resulting in epigenetic silencing (CIMP – CpG island methylator phenotype), and microsatellite instability (Kedrin, Gala 2015).

Conventional adenoma-carcinoma and the serrated pathways are compared in Figure 1-3, highlighting the key molecular and histological differences. BRAF is a serine/threonine tyrosine kinase that functions downstream of KRAS in a signal transduction pathway leading to activation of MAP kinases. Mutations in either of these genes lead to constitutive MAPK pathway activation resulting in uncontrolled proliferation, cell survival, invasion and metastasis (Rustgi 2013, Chan, Zhao *et al.* 2003, Heinemann, Stintzing *et al.* 2009). BRAF and KRAS mutations are mutually exclusive, and alterations in BRAF have been shown to occur at a higher frequency than KRAS mutations in serrated adenomas (Larki, Gharib *et al.* 2017, Kedrin, Gala 2015). This emphasises BRAF to be a hallmark of serrated colorectal carcinomas. The most frequent mutation in BRAF is V600E and appears to be mutated in approximately 82% of serrated carcinomas (Patai, Molnar *et al.* 2013).

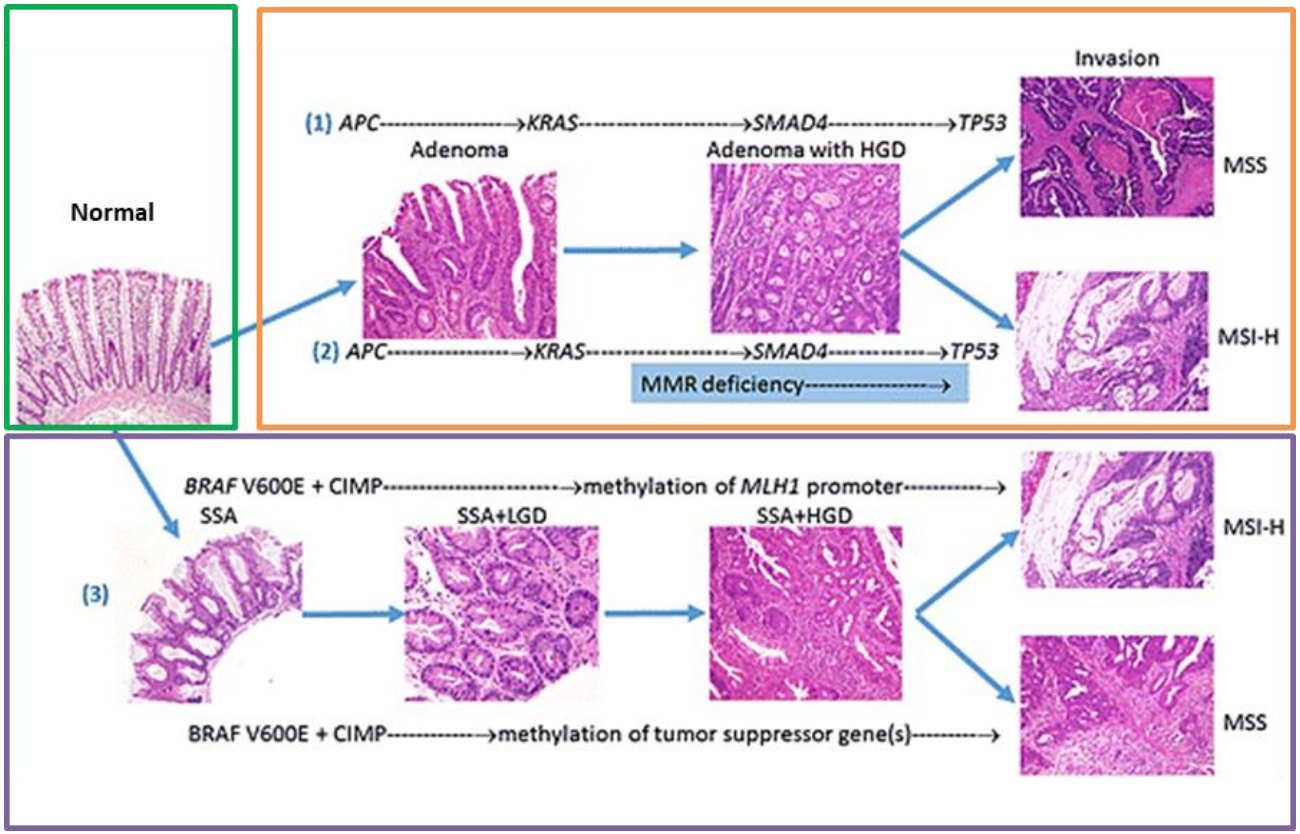

Figure 1-3. Schematic comparison of key events in conventional and serrated colorectal carcinogenesis. 1) Conventional, or adenoma-carcinoma sequence, is initiated by loss of function of *APC*, followed by activation mutation in *KRAS* gene. Mutations in *SMAD4* result in high grade dysplasia (HGD). Inactivation of tumour suppressor gene *TP53* results in microsatellite stable (MSS) cancer. 2) Mismatch repair (MMR) protein deficiency results in MSI-high (MSI-H) cancers. 3) The serrated pathway typically is initiated by mutations in BRAF gene and CpG island methylation phenotype (CIMP) resulting in sessile serrated adenomas (SSA). MSI-H cancers result from methylation in MLH1 promoter; MSS cancers result from methylation events in tumour suppressor genes. The figure is reproduced from Gonzalez, Washington *et al.* 2017.

Hypermethylation of CpG islands flanking promoters of tumour-suppressor genes is often found in various cancers. CpG island methylator phenotype (CIMP) is found to be present in 20-30% of colorectal cancers, and in up to 80% of serrated colorectal carcinomas (Advani, Advani *et al.* 2018, Rhee, Kim *et al.* 2016).

Another hallmark of CRC is microsatellite instability (MSI) (Yamane, Scapulatempo-Neto *et al.* 2014). MSI is caused by the loss of MMR genes, resulting in increased susceptibility to accumulating mutations within microsatellite regions (Markowitz, Bertagnolli 2009). Approximately 15-20% of sporadic colorectal cancers have a high status of microsatellite instability (MSI-H) (Colussi, Brandi *et al.* 2013). Interestingly, several studies have shown that patients with CRC associated with microsatellite instability have no response to chemotherapy (Testa, Pelosi *et al.* 2018, Chang, Chang *et al.* 2017, Marmol, Sanchez-de-Diego *et al.* 2017).

1.3 Signal transduction pathways in colorectal cancer

Multiple intracellular signalling pathways tightly regulate cellular activity and homeostasis. Signalling cascades, such as Wnt/β-catenin, EGFR/MAPK, Notch, myc, TGF-β and p53 are found to be dysregulated in CRCs. Deregulation of these signalling pathways contributes to cellular malignancy, cancer initiation, progression and metastasis. Hyperactivation of Wnt and EGFR mediated signalling cascades is associated with initiation of colorectal carcinogenesis and are discussed below.

1.3.1 Wnt signalling

The Wnt signalling pathway controls a wide range of biological processes throughout embryonic development and adult life. It is one of the key mechanisms of the colonic cell renewal that controls cell proliferation, cell polarity and determines

cell fate (Wiese, Nusse *et al.* 2018, Katoh 2017, Fuerer, Nusse *et al.* 2008). Impaired Wnt signalling is associated with the majority of colorectal cancers, highlighting its importance in cancer development and progression (Krausova, Korinek 2014, Polakis 2012). Wnt signalling activation is determined by Wnt binding to receptors on the surface of the cell membrane. Wnt ligands belong to the large family of secreted glycoproteins that are highly conserved throughout the organisms. To date, 19 human Wnt ligands have been identified. Although Wnt ligands are structurally related, they can trigger different signalling pathways (Baarsma, Konigshoff *et al.* 2013, Miller 2002). Some Wnt ligands (Wnt1, Wnt3a, Wnt8) preferentially activate canonical, or β-catenin dependent pathway; others (Wnt4, Wnt5a and Wnt11) can activate non-canonical pathways (MacDonald, Tamai *et al.* 2009). However, the Wnt signalling framework is more complex and Wnt activity is context dependent.

1.3.1.1 Canonical Wnt signalling

The canonical Wnt pathway has been comprehensively studied and is best characterised. The hallmark of the canonical Wnt signalling is the accumulation of β-catenin in the cytoplasm and its subsequent nuclear translocation. β-catenin is a multifunctional protein, first described as a part of cadherin-based junctions and plays a role in developmental and homeostatic processes. β-catenin stability in the cell is tightly regulated by phosphorylation events. Specifically, phosphorylation of tyrosine residues (Tyr831 and Tyr860) by Src kinase and serine (Ser846) by CK1α promotes dissociation of β-catenin from E-cadherin. Consequently, β-catenin is transferred into the cytoplasm where it is captured by the degradation complex consisting of Axin, APC, glycogen synthase kinase 3β (GSK3β), casein kinase 1 (CK1α) (Figure 1-4.A) (Liu, Li *et al.* 2002). Sequential phosphorylation of N-terminal Serine/Threonine

residues (Ser33, Ser37, Thr41 and Ser45) targets β-catenin for ubiquitination and subsequent degradation by 26S proteasomes (Amit, Hatzubai *et al.* 2002).

Activation of the canonical pathway is mediated by Wnt binding to the receptor complex that consists of one of the transmembrane Frizzled (Fz) receptors and co-receptor low-density lipoprotein-receptor-related protein (LRP5/6). This interaction induces the phosphorylation of LRP5/6 by CK1α and GSK3β, which in turn facilitates translocation of Axin from the destruction complex to the membrane (Figure 1-4.B) (Nayak, Bhattacharyya *et al.* 2016, Komiya, Habas 2008). Additionally, cytoplasmic phosphoprotein Dishevelled (Dvl) is also recruited to the receptor complex, inhibiting the kinase activity of GSK3β. Axin recruitment to the Wnt/Fz/LRP receptor complex results in disruption of the destruction complex and stabilisation of β-catenin (Rao, Kuhl 2010, MacDonald, Tamai *et al.* 2009). Subsequently, β-catenin is translocated to the nucleus where it acts as a co-transcriptional activator by forming a complex with LEF/TCF family members to activate transcription of Wnt target genes (Table 1-2). Among them are genes that play role in cell differentiation, cell signalling, proliferation, and adhesion (Behrens 2005).

In addition to colorectal cancer the dysregulation of the canonical Wnt signalling has been implicated in a number of other malignancies, including melanoma, hepatocellular carcinoma, prostate, thyroid, and ovarian cancer. A range of mutations that lead to β-catenin stabilisation have been reported. In rare cases of CRC with wild-type APC, other components of Wnt signalling cascade are mutated, such as Axin1/2 and β-catenin (Nusse, Clevers 2017, Schneikert, Behrens 2007). In addition, mutations in negative regulators of the Frizzled receptor – E3 ubiquitin

ligases Rnf43 and Znrf3 were identified in multiple carcinomas (Assie, Letouze *et al.* 2014, Wu, Jiao *et al.* 2011).

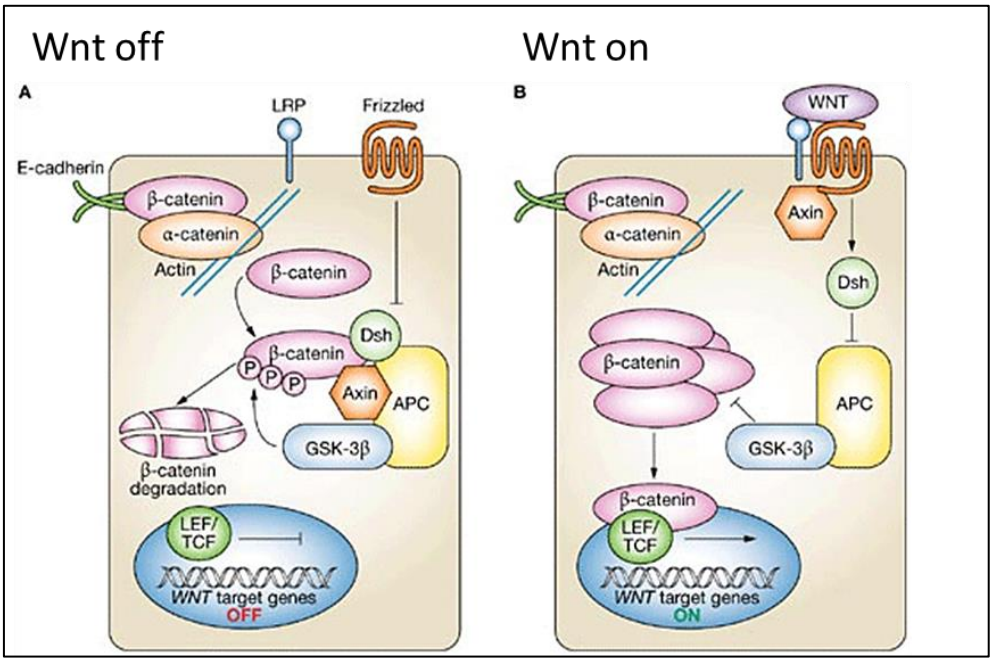

Figure 1-4. Schematic representation of canonical Wnt signal transduction pathway. (A) In the absence of Wnt ligands, β-catenin intracellular levels are regulated by β-catenin destruction complex, consisting of APC, Axin, GSK3β, and other. Axin and APC bind to β-catenin, GSK3β phosphorylates its N-terminal Ser/Thr residues, resulting in proteosomal degradation of β-catenin. **(B)** Upon binding of Wnts to receptor complex Frizzled/LRP5/6 (Fz/LRP), Axin from the β-catenin destruction complex is recruited to the membrane. Kinase activity of GSK3β is inhibited. β-catenin accumulates in the cytoplasm, translocates to the nucleus, where it initiates transcriptional activation of Wnt target genes in complex with LEF/TCF. The image is reproduced from Reya, Clevers 2005**.**

Table 1-2 Target gene of β-catenin and their function in cancer initiation and progression. Table reproduced from Huang, Du 2008.

β-catenin target genes related to cancer

Function	Target gene
Cell proliferation	C-myc; Cyclin D1
Inhibition of apoptosis	MDR1/PGP; COX-2; PPARδ
Tumor progression	MMPs; uPAR,Upa; CD44; Laminin γ2; Nr-CAM
Growth factors	c-met; VEGF; WISP-1; BMP-4
Transcription factors	c-jun, fra-1; ITF-2; Id2; AF17
Negative feedback targets	Conductin; Tcf-1; Nkd

1.3.1.2 Non-canonical Wnt signalling pathways

Alternative Wnt signalling pathways are mediated via β-catenin and LRP independent routes. A variety of non-canonical pathways have been reported, with the two most investigated cascades being planar cell polarity (PCP) and Wnt/Ca^{2+} pathways (Figure 1-5). Planar cell polarity is a term that describes the spatial organisation of cellular components in a two-dimensional plane. PCP is activated by Wnt4, Wnt5a or Wnt11 through various Frizzled receptors and mediated by Dishevelled proteins (Komiya, Habas 2008). The Fz/Dvl complex activates c-Jun-N-terminal kinase (JNK) and Rho-associated kinase (RhoA kinase) which results in actin cytoskeleton reorganisation (Rao, Kuhl 2010). These phenomena are known to control the orientation of hairs and bristles (Yang, Mlodzik 2015). The Wnt/Ca^{2+} pathway is mediated by the interaction of Wnt5a with Frizzled-2. This interaction allows for the increase of intracellular levels of Ca^{2+} via inactivation of cGMP-dependent kinase G (PKG), which in turn activates phospholipase C (PLC). PLC triggers release of intracellular levels of Ca^{2+}, which in turn activates calcium dependent proteins, including protein kinase C (PKC) and Ca^{2+}/calmodulin-dependent protein kinase II (CaMKII) (Komiya, Habas 2008). CaMKII is required for

the activation of nuclear factor of activated T cells (NFAT), promoting transcription of genes necessary for ventral cell fate determination; and for activation of TGF-β activated kinase 1 (TAK 1) and Nemo-like kinase (NLK). PKC is known to regulate actin cytoskeleton reorganisation, resulting in tissue separation during gastrulation typically via activation of small GTPase Cdc42 (Komiya, Habas 2008). This pathway is involved in cancer, inflammation and neurodegeneration (Hapak, Rothlin *et al.* 2018, Gomez-Orte, Saenz-Narciso *et al.* 2013). Both PCP and Ca^{2+} pathways were reported to antagonise canonical WNT signalling (Mazzotta, Neves *et al.* 2016, Rao, Kuhl 2010).

Although the canonical signalling pathway plays a central role in CRC, the non-canonical Wnt-mediated pathways may also contribute to carcinogenesis. It was demonstrated that inactivation of RhoA results in colon cancer metastasis in mice (Rodrigues, Macaya *et al.* 2014). In addition, Wnt5a driven non-canonical Wnt signalling positively regulates expression of tumour suppressor 15-hydroxyprostaglandin dehydrogenase (15-PGDH) in colon adenocarcinomas (Mehdawi, Prasad *et al.* 2016). In summary, both the canonical and non-canonical Wnt signalling pathways may contribute to colorectal carcinogenesis by utilising different mechanisms and demonstrate complexity and heterogeneity of CRCs.

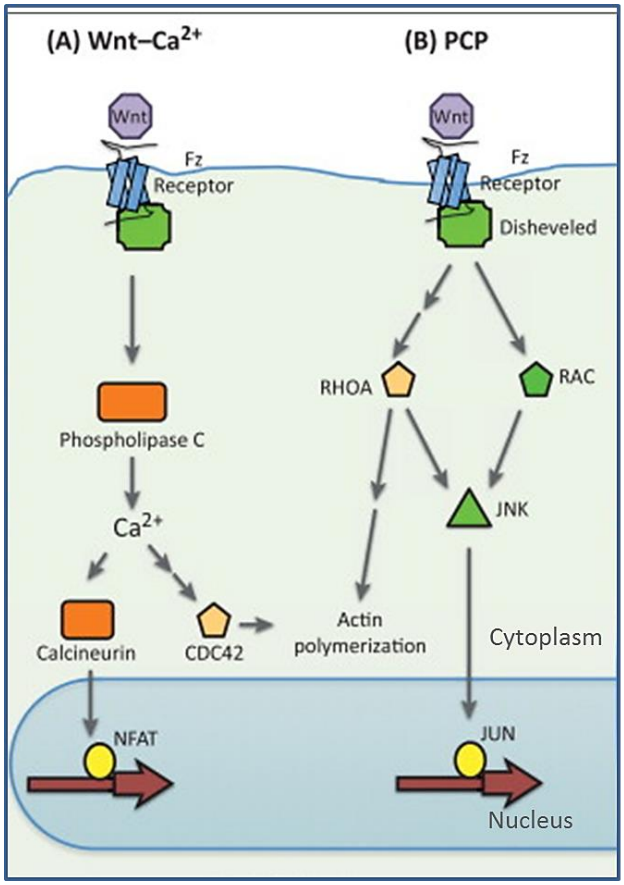

Figure 1-5. Schematic representation of Wnt-Ca^{2+} and planar cell polarity pathways activated by Wnt. (A) Wnt-Ca^{2+} pathway is initiated by Wnt binding to Frizzled (Fz). It results in activation of phospholipase C, which releases intracellular Ca2+ required for activation of calcium-dependent proteins. **(B)** Planar cell polarity pathway is activated by Wnt interaction with Fz/Dvl (Dishevelled) complex. It activates a cascade that has the small GTPases RAC1 and RHOA, and JNK kinase as downstream effectors that control rearrangements in the cytoskeleton and gene expression. Figure reproduced from Gomez-Orte, Saenz-Narciso *et al.* 2013.

1.3.2 EGFR signalling in colorectal cancer

Another important signalling pathway that is often upregulated in many cancers, including CRC, is the EGFR pathway. Epidermal growth factor receptor (EGFR) belongs to the tyrosine kinase receptor family that mediates a number of cellular processes, such as cell proliferation, survival, migration, and resistance to apoptosis (Mitchell, Luwor *et al.* 2018, Krasinskas 2011). Signal transduction is initiated by interaction between the growth factors and the receptor extracellular ligand-binding domain that leads to activation of various downstream effectors. Cascades that are activated through EGFR are presented in Figure 1-6. The Ras/MAPK, PI3K/Akt, and JAK/STAT pathways are the main intracellular pathways activated by EGFR and are involved in development of CRC. Known EGFR ligands include epidermal growth factor (EGF), heparin-binding (HB)-EGF, transforming factor alpha (TGF-α), amphiregulin (AREG), betacellulin, epiregulin (EREG) and epigen (Wilson, Mill *et al.* 2012). Different EGFR ligands bind with different affinities to the receptor and result in different downstream effects of EGFR signalling (Mitchell, Luwor *et al.* 2018, Ronan, Macdonald-Obermann *et al.* 2016). The EGFR ligands are detailed in Table 1-3.

The mitogen-activated protein kinase (MAPK) pathway is crucial for cell proliferation and survival, and it is also important for intestinal epithelial cell differentiation (Tang, Liu *et al.* 2016). The MAPK pathway is initiated by binding of ligands to EGFR, which results in receptor dimerisation and auto-phosphorylation of EGFR cytoplasmic domain, followed by downstream phosphorylation relay to Ras and MAPK extracellular regulated kinases 1 and 2 (ERK1/2). Activated ERKs are then imported into the nucleus where they phosphorylate specific transcription factors

involved in cell proliferation (Figure 1-6) (Liebmann 2001).

The phosphatidylinositol 3-kinase (PI3K)/Akt pathway regulates cell growth, apoptosis resistance, invasion, and migration and is also activated through EGFR (Castellano, Downward 2010, Scaltriti, Baselga 2006). PI3K can be directly recruited to the receptor dimer but requires EGFR dimerization with HER-3 receptor. The recruitment is facilitated by the docking proteins insulin receptor substrate (IRS) or GRB2-associated binder (GAB). The catalytic subunit of PI3K generates phosphatidylinositol -3, -4, -5 trisphosphate (PIP3) which is responsible for recruitment of serine/threonine kinase Akt. Activated Akt phosphorylates a number of factors responsible for cell survival, proliferation and motility (Scaltriti, Baselga 2006). Oncogenic activation of this pathway is known to contribute to pathogenesis and malignant progression of colorectal carcinoma lesions.

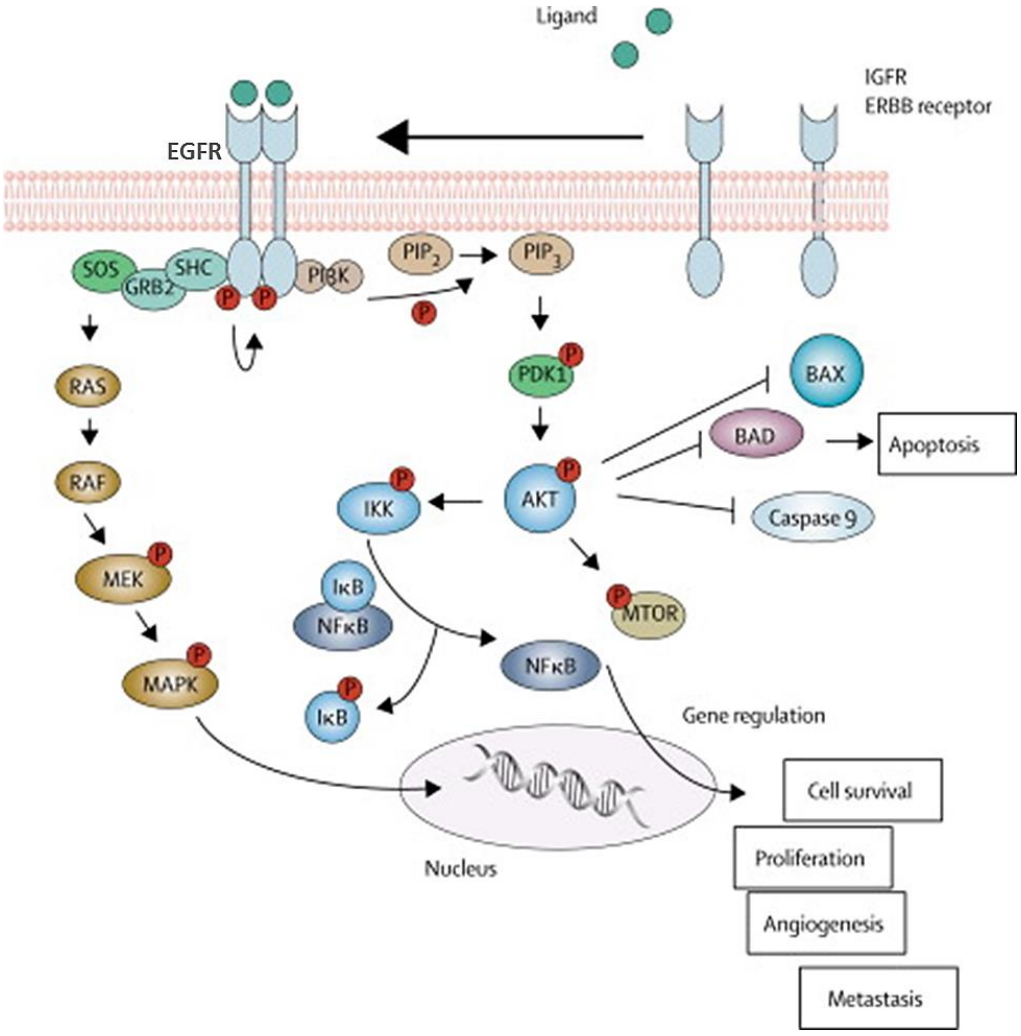

Figure 1-6. Schematic representation of Ras/MAPK and PI3K/Akt pathways activated by ligand binding to EGFR. Upon ligand binding, EGFR is dimerised and auto-phosphorylated at cytoplasmic domain, which provides a binding site for the adaptor proteins Grb2 and Sos either directly or through the association with the adaptor molecule Shc. This complex formation leads to conformational modification of Sos and recruitment of GTPase exchange factor (RasGEF) to the complex. This promotes activation of Ras (Ras-GTP) which in turn activated Raf, that through intermediate steps phosphorylates MAPK extracellular regulated kinases 1 and 2 (ERK1/2). Activated ERKs are then imported into nucleus where they phosphorylate specific transcription factors involved in cell proliferation. PI3K is recruited to the receptor dimer, resulting in activation of phosphatidylinositol -3, -4, -5 triphosphate (PIP3) followed by phosphorylation of phosphoinositide-dependent kinase-1 (PDK1) and control activation of serine/threonine kinase Akt, which in turn can activate mTOR and NFκB pathways and inhibits apoptosis. Image is reproduced from Hougardy, Maduro *et al.* 2005**.**

Table 1-3. EGFR ligands, specificity to ErbB family of tyrosine kinase receptors and affinity. Table is reproduced and modified from Mitchell, Luwor *et al.* 2018**.**

EGF-family ligands	Receptor specificity	Affinity class
EGF	EGFR	High
TGF-α	EGFR	High
AREG	EGFR	Low
EREG	EGFR, ERBB4	Low
HB-EGF	EGFR, ERBB4	High
BTC	EGFR, ERBB4	High
EPGN	EGFR, ERBB3, ERBB4	Low
NRG	ERBB3, ERBB4	High

Although EGFR mutations are uncommon in CRC, they may be acquired as a resistance mechanism to the anti-EGFR therapy (Zhao, Wang *et al.* 2017, Arena, Bellosillo *et al.* 2015). The hyperactivation of EGFR signalling in CRC is frequently occurring due to EGFR gene amplification and three- to fivefold increase in copy number is seen in approximately 50% of CRC (Krasinskas 2011). In addition, as mentioned earlier, EGFR downstream effectors are frequently mutated in CRC; KRAS is mutated in up to 40% of cases, BRAF in up to 22%, PIK3CA in approximately 18%, and PTEN in 13% to 19% of CRC (summarised in Table 1-4) (Krasinskas 2011). It has been noted that ligands, such as EREG and AREG, are often overexpressed in CRCs and contribute to carcinogenesis of intestinal epithelium (Mitchell, Luwor *et al.* 2018). The overexpression of EGFR ligands is also linked to development of metastases (Sasaki, Hiroki *et al.* 2013). For example, elevated expression of betacellulin (BTC), epigen, TGF-α, AREG and EGF was observed in a significant proportion of metastatic CRC and this correlated with poor prognosis in anti-EGFR treatment with cetuximab (Khelwatty, Essapen *et al.* 2017). Interestingly, in other studies the expression of AREG and EREG was associated with a better response to cetuximab and panitumumab therapy (Qu, Sandmann *et al.* 2016, Zhai, Yu *et al.* 2017, Ronan, Macdonald-Obermann *et al.* 2016). Another recent report demonstrated a positive correlation of expression of EGFR ligands (TGF-α, BTC, EGF and HB-EGF) with disease-free survival (Yun, Kwak *et al.* 2018). These conflicting reports of association of EGFR ligands expression and response to the anti-EGFR treatment highlights the importance for further stratification of CRC tumours and need to identify more reliable biomarkers of CRC prognosis.

Table 1-4. Frequency of mutations in the EGFR/MAPK pathway and their impact on clinical outcome. Table reproduced from Krasinskas 2011.

Component (gene/protein)	Protein function	Defect in CRC	Frequency	Impact	
				Prognostic	Predictive (to anti-EGFR therapy)
EGFR/EGFR	Transmembrane tyrosine kinase receptor	Protein expression	25–90%	Controversial	No correlation
		Mutation	Rare	Unknown	Unknown
		Increased copy number	0–50%*	Uncertain	Uncertain
KRas/K-Ras	GDP-/GTP-binding protein; facilitates ligand-dependent signaling	Activating mutation (codons 12, 13, 61, 146); leads to activation of MAPK pathway	30–40%	Controversial	No response (if K-Ras is mutated)
BRAF/B-Raf	Serine-threonine protein kinase downstream of KRas	Activating mutation (V600E)	5–12%	Poor prognosis in MSS tumours	No response (if BRAF is mutated)
PIK3CA/PI3K	A key signal transducer in the PI3K-AKT pathway	Activating mutation (exons 9 and 20)	14–18%	Poor prognosis in K-Ras wt tumours	No response (if exon 20 is mutated)
PTEN/PTEN	A protein tyrosine phosphatase enzyme; inactivates PI3K pathway	Loss of protein expression; mutation; LOH	13–19%	Poor prognosis in K-Ras wt tumours	No response (possibly)

1.4 Mouse models of CRC

Human CRCs are extremely heterogenous and complex. Thus, a large number of murine models have been developed in an attempt to recapitulate aetiology, pathology, and clinical progression of human disease and to address specific research questions.

The most commonly used model of CRC was established in an ethylnitrosourea (ENU) mutagenesis screen (Moser, Pitot *et al.* 1990). These mice are predisposed to multiple intestinal neoplasia (MIN) due to a truncating mutation in *APC* gene in codon 850, hence were named APC^{min} (Su, Kinzler *et al.* 1992). Homozygous $APC^{min/min}$ mice are embryonically lethal, confirming the crucial role of Wnt signalling in development. Heterozygous $APC^{min/+}$ develop up to 30 polyps, predominantly in the small intestine (Tong, Yang *et al.* 2011). The $APC^{min/+}$ has been used in numerous studies aimed to assess a multistep progression in colorectal cancer, chemoprevention, inflammation-associated tumorigenesis and anti-cancer host immune responses (Wang, Lu, Zhang 2015, Jackstadt, Sansom 2015, Yamada, Mori 2007, Kettunen, Kettunen *et al.* 2003). Other models with mutated *APC* gene were generated using homologous recombination of embryonic stem cells. The intestinal polyps that develop in these mice are histologically similar, however the number of polyps varies significantly between the models (summarised in Table 1-5). Interestingly, these polyps predominantly develop in the small intestine similarly to $APC^{min/+}$ mice.

Table 1-5. Mouse models of CRC with APC truncations. Table adapted and modified from Tong, Yang *et al.* 2011.

APC mutants	Mutation site	Polyps/mouse		Tumour histopathology	Reference
		Small intestine	Colon		
APC$^{min/+}$	truncating mutation at codon 850 (ENU induced)	~30	~3	Benign adenomas	(Moser, Pitot *et al.* 1990)
***Apc*$^{\Delta716}$**	truncating mutation at codon 716	~300	~3	Benign adenomas	(Oshima, Oshima *et al.* 1995)
***Apc*^{1638N}**	truncating mutation at codon 1638 (neomycin insertion in exon 15)	~3	~0	Benign adenomas	(Pretlow, Edelmann *et al.* 2003)
***Apc*^{1638T}**	truncating mutation at codon 1638 (hygromycin insertion in exon 15)	0	0	Benign adenomas	(Pretlow, Edelmann *et al.* 2003)
***Apc*$^{\Delta14}$**	frameshift at codon 580	~65	~4	Benign adenomas	(Colnot, Niwa-Kawakita *et al.* 2004)
***Apc*^{1309}**	frameshift at codon 1309	~35	~3	Benign adenomas	(Quesada, Kimata *et al.* 1998)
***Apc*$^{\Delta580}$**	frameshift at codon 580 and a truncation at codon 605	~120		Benign adenomas	(Kuraguchi, Wang *et al.* 2006)
***Apc*$^{\Delta474}$**	frameshift at codon 474	~30	~3	Benign adenomas	(Sasai, Masaki *et al.* 2000)
***Apc*$^{1322T/+}$**	truncating mutation at codon 1322	~200	~3	Benign adenomas	(Pollard, Deheragoda *et al.* 2009)

Since APC-based mouse models predominantly result in the formation of intestinal adenomas in mice, researchers were prompted to generate other models that would recapitulate the phenotype of invasive carcinomas. As such, APC mutant mice were crossed with mice carrying mutations that are associated with more advanced stages of human adenomas or carcinomas, including *KRAS, SMAD2, SMAD4, TP53, FBXW&7,* and *TGF-βR2*. These experiments confirmed that a second mutation can accentuate the "APC-deficient" phenotype. For instance, APC-heterozygous mice expressing constitutively active KRAS ($Kras^{G12D}$) present with high grade dysplasia throughout the intestine (Haigis, Kendall *et al.* 2008). Heterozygous deletion of PTEN in $APC^{min/+}$ mice results in formation of invasive carcinomas, showing the important role of the PIK3A/Akt pathway in CRC (Shao, Washington *et al.* 2007). In addition, the expression of hypomorphic allele $Egfr^{wa2}$ and the antimorphic allele $Egfr^{wa5}$ reduced the multiplicity of adenomatous polyps in $APC^{min/+}$ mice, demonstrating the important role of EGFR in adenoma formation (Dahlhoff, Horst *et al.* 2008, Roberts, Min *et al.* 2002). Other genes, known as modifiers of Min affect the tumour burden (Mom-1/2/3/5/7, Foxl-1, Cox-1, Cox-2, Mbd4, EphB2, EphB3, EphB4), location (Smad3, Smad4, EphB3, EphB4, ERα) and invasion (Smad4, TGF-β, Smad4, EphB2) of the $APC^{min/+}$ phenotype (Young, Ordonez *et al.* 2013). The transgenic expression of EGFR ligands also accentuates $APC^{min/+}$ phenotype in mice. As such, the expression of HB-EGF promotes formation of serrated adenomas in the caecum of $APC^{min/+}$ mice (Bongers, Muniz *et al.* 2012). The expression of BTC transgene results in increased adenoma burden in $APC^{min/+}$ mice (Dahlhoff, Horst *et al.* 2008), while TGF-α transgene enhances adenoma formation in the jejunum in this model (Bilger, Sullivan *et al.* 2008). These findings

once again demonstrate that extracellular activation of EGFR plays an important role in colorectal carcinogenesis in APC-deficient lesions. In addition to APC models, a number of models with gene mutations involved in HNPCC-related carcinogenesis, including Msh2, Msh6, Mlh1 have been established (McIntyre, Buczacki *et al.* 2015, Tong, Yang *et al.* 2011).

Apart from genetically generated models, chemically induced carcinogenesis is also widely used in studies with mice and is a rapid, reproducible model which mimics 'Fearon and Vogelstein' adenoma-carcinoma sequence. A variety of carcinogens are available including azoxymethane (AOM), methylazoxymethanol (MAM), 1,2-dimethylhydrazine (DMH), 2-amino-1-methyl-6-phenylimidazo [4,5-b]-pyridine (PhIP) and 2-amino-33-methylimidazo [4,5-f] quinoline (IQ), 3,2′-dimethyl-4-aminobiphenyl (DMAB), methylnitrosourea (MNU) and N-methyl-N′-nitro-N-nitrosoguanidine (MNNG) (Tong, Yang *et al.* 2011). A selection of genetically modified mouse models for colorectal cancers, including rationale, strategy, advantages and disadvantages of each model are summarised in Table 1-6. In summary, a wide variety of mouse models are available to study colorectal carcinogenesis and careful consideration must be taken for selection of an appropriate model to address a specific research question.

Table 1-6. Genetically modified mouse models of CRC. Table adapted and modified from McIntyre, Buczacki *et al.* 2015.

Mouse allele	Rationale	Strategy	Advantages	Disadvantages	Reference
$APC^{Min/+}$	N/A	Germline truncating mutation (N- terminus)	Model of human familial adenomatous polyposis (FAP) syndrome and >80% of sporadic CRCs contain mutations	Developed hundreds of low-grade adenomas	(Moser, Pitot *et al.* 1990, Su, Kinzler *et al.* 1992)
	Ethylnitrosurea (ENU) mutagenesis screen	Loss of heterozygosity occurs at wildtype allele in tumours	Short-lived for rapid studies Tumour multiplicity easily quantifiable	Short-lived as tumour burden causes obstruction, prolapse and bleeding Short life-span means that adenomas do not acquire sufficient mutations to progress to adenocarcinoma and metastasise Tumours predominantly located in small rather than large intestine	(Halberg, Waggoner *et al.* 2009, Chen, X., Halberg *et al.* 2008)
$Msh2^{-/-}$	Msh2 mutations common in CRC	Germline knockout	Model of Hereditary non-polyposis CRC (HNPCC) or Lynch Syndrome (3% of all CRCs)	Msh2 mutation in all cells of body and mice are predisposed to lymphomas	(Reitmair, Schmits *et al.* 1995)

Villin-Cre/Msh2^{LoxP}	To restrict malignancy to intestine to prevent lymphoma	Conditional Cre recombinase expressed from promoter of intestinal specific gene (Villin)	Developed intestinal adenomas and adenocarcinomas No deaths from lymphoma	Do not develop metastases	(Kucherlapati, Lee *et al.* 2010)
APC$^{580S/580S}$	To model advanced CRC by restricting tumours to colon and reducing tumour burden	Conditional Adenoviral Cre recombinase is administered through the anus to inactivate APC	Live >1 year. Developed two or three intestinal adenomas Some mice developed adenocarcinomas	Do not develop metastases Conditional allele (unactivated) reduces APC expression in all cells, like APC$^{fl/fl}$ which results in development of life-limiting hepatocellular carcinomas by 14 months	(Shibata, Toyama *et al.* 1997)
APC$^{lox15/+}$; Fabpl-Cre	To model advanced CRC by restricting tumours to the colon and reducing tumour burden	Conditional Cre recombinase expressed in the distal small intestinal and colonic epithelia to inactivate APC	Live >1 year. Developed two or three intestinal adenomas Some mice developed adenocarcinomas	Do not develop metastases	(Robanus-Maandag, Koelink *et al.* 2010)
APC$^{Min/+}$ Trp53$^{-/-}$	To model advanced CRC through addition of cooperating gene mutations	Germline mutations in APC and Trp53		Do not develop metastases	(Clarke, Cummings *et al.* 1995)

$APC^{2lox14/+}$ K-RasLSL-G12D and Fabpl-Cre	To model advanced CRC through addition of cooperating gene mutations	Conditional Cre recombinase expressed in the distal small intestine/colonic epithelia and results in constitutive activation of K-Ras and inactivation of APC	Developed more adenocarcinomas than single mutant (APC or K-Ras alone) control mice	Do not develop metastases	(Haigis, Kendall *et al.* 2008)
APC mutant with disruption of TgfbR2, Smad2 or Sm ad4	To model advanced CRC through addition of cooperating gene mutations		Developed more adenocarcinomas than single mutant control mice.	Do not develop metastases	(Hamamoto, Beppu *et al.* 2002, Munoz, Upton *et al.* 2006, Takaku, Oshima *et al.* 1998)
$APC^{Min/+}$ Villin Cre $Fbxw7^{(\Delta G)}$	To model advanced CRC through addition of cooperating gene mutations	Germline mutation of APC Conditional mutation of Fbxw7 Cre recombinase expressed from promoter of intestinal specific gene (Villin)	Decreased lifespan Increased tumour burden Fbxw7 null control mice developed adenomas by 9-10 months of age	Do not develop adenocarcinomas or metastases	(Babaei-Jadidi, Li *et al.* 2011)

$APC^{CKO/CKO}$ - LSL-G12D; $K\text{-}Ras^{tm4tyj/+}$	To model advanced CRC through addition of cooperating mutations. To restrict tumours to the colon and reduce tumour burden	Adenoviral Cre solution administered via the anus to simultaneously disrupt APC and activate K-Ras	Developed adenocarcinomas after five months Developed metastases to distant organs after six months e.g. liver In vivo monitoring via colonoscopy	Labour intensive mouse surgery required to clamp a section of colon to deliver Adenoviral Cre-solution to the colon via the anus	(Hung, Maricevich *et al.* 2010)
Carcinogen-induced mouse model	Sporadic colorectal cancer	Chemicals supplemented with food	Easy and reproducible. DMH/AOM/MAM have relatively high colorectal tumour incidence. IQ, PhIP, DMAB, MNNG or MNU target multiple organs and exhibit a low tumour incidence.	The tumours are not metastatic.	(Tong, Yang *et al.* 2011)

1.5 Organoids as a model of colorectal cancer and normal intestinal epithelium

Conventional experimental models that are utilised in cancer research extend from *in vitro* to *in vivo* systems. Whilst these models contributed to a significant progress in understanding of the disease there are a number of limitations that do not allow the comprehensive characterisation of individual tumours and the development of novel more specific and robust therapies for CRC. For example, the derivation of cell lines is often achieved by immortalisation using viral infections or exogenous expression of oncogenes, thus making them susceptible to a genetic drift. In addition, established cell lines are maintained out of the context of a specific tissue architecture and physiological properties of the tissue (Young, Madeleine, Reed 2016). Animal models, on the other hand, provide insights into more physiological context of a disease, including immune responses and vasculature components. However, they may not be representatives of human disease and can be costly (Young, Madeleine, Reed 2016). The knowledge that intestinal cancers arise from intestinal stem cells (ISC) and not short-lived trans-amplifying cells has made the organoid system increasingly attractive for CRC studies and is widely applied in developmental studies (Barker, Ridgway *et al.* 2009).

Intestinal and colonic organoids can be derived from ISCs or from isolated intestinal and colonic crypt structures in media containing growth factors and inhibitors mimicking mesenchymal signals (Sato, Vries *et al.* 2009, Sato, Stange *et al.* 2011). Organoids cultured in 3D ECM or Matrigel™ form three-dimensional structures which recapitulate tissue cellular composition and organisation *ex vivo*. Due to continuous cell renewal properties of ISCs, organoids are long lived and can

be sub-cultured indefinitely. In addition, it has been shown that organoids maintain gene expression profile identical to freshly isolated crypts after extended propagation (Sato, T., Vries *et al.* 2009). Intestinal organoids form structures with a central lumen lined by villus-like epithelium and several surrounding crypt-like domains protruding into extracellular matrix; apoptotic cells are shed into the central lumen. Organoids recapitulate all epithelial cell subtypes of intestine, including stem cells, Paneth cells, enterocytes, enteroendocrine cells and Goblet cells (Date, Sato 2015, Middendorp, Schneeberger *et al.* 2014). Interestingly, cell organisation in organoids is identical to that seen *in vivo* with stem cells and Paneth cells residing at the bottom of crypts, whereas terminally differentiated enterocytes are migrating towards the lumen (Figure 1-7).

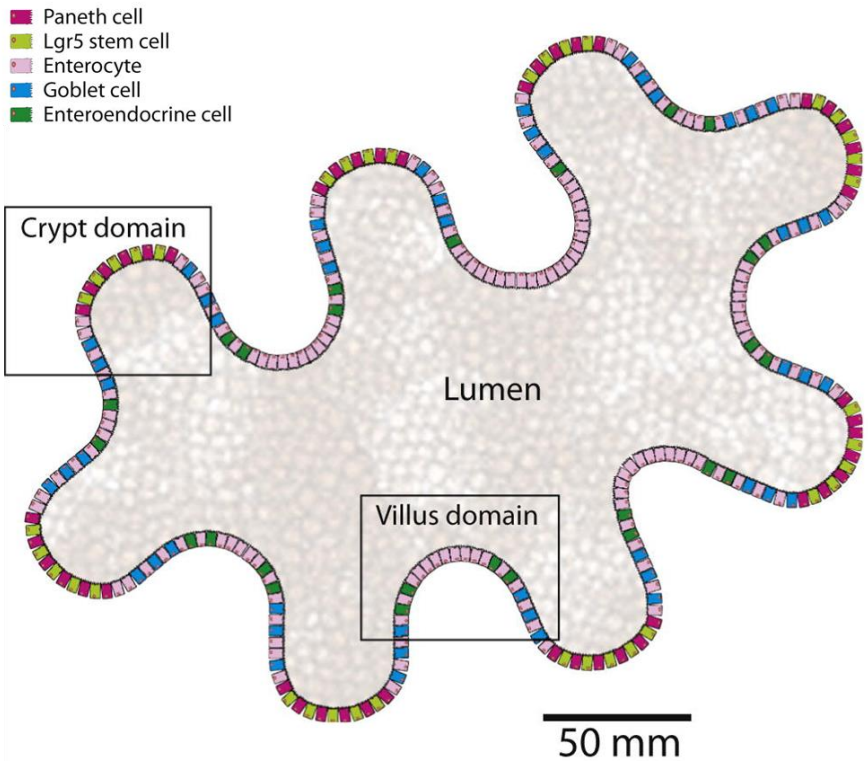

Figure 1-7. Schematic representation of intestinal organoid with crypt domains protruding into ECM and villus domains facing central lumen, corresponding to the intestinal architecture. Stem cells (Lgr5+) and Paneth cells are located at the crypt bottom, differentiated cells comprise of enterocytes, Goblet cells and enteroendocrine cells. Figure reproduced and modified from Roeselers, Ponomarenko *et al.* 2013.

The mouse intestinal organoids are cultured in serum-free conditions in the presence of growth factors that facilitate stem cell renewal and differentiation, including R-Spondin-1, EGF, and Noggin (Sato, Stange *et al.* 2011, Jung, Sato *et al.* 2011). Mouse colonic crypts lack Paneth cells, that are the major intrinsic source of Wnt3a required for ISCs, therefore for culture of mouse colon organoids additional Wnt3a ligands are required in the media (Clevers, Bevins 2013, Sato, Toshiro, van Es *et al.* 2010). To successfully culture human intestinal and colon organoids p38 and TGF-β inhibitors are required (Sato, Stange *et al.* 2011). R-spondin-1 is an agonist of Wnt signalling that inhibits degradation of Wnt receptors through

interaction with Rnf43/Znrf3 transmembrane E3 ubiquitin ligases, therefore inducing prolonged Wnt-mediated signalling in ISCs (Koo, Spit *et al.* 2012, Hao, Jiang *et al.* 2016). Activation of EGFR is also required for the long-term culture of intestinal organoids to contribute to stem cell maintenance and division of TA cells (Matano, Date *et al.* 2015). Noggin is an effective antagonist of BMP signalling; the latter induces cell differentiation through activation of p38 and SMAD-1 and SMAD-4 signalling cascades. It has been shown that depletion of Noggin from organoid cultures results in Lgr5+ stem cell loss and attenuation of organoid proliferation (Sato, Vries *et al.* 2009).

The organoid model has been recognised as a powerful system for basic and translational studies. It represents an excellent genetically stable tool to study cell interactions, stem cell biology, as well as development of personalised therapies, drug screening and correction of mutations. Widely used techniques of genetic manipulation including lentiviral, electroporation-based transfection, gene silencing with shRNAs and CRISPR/Cas9 are applicable to organoids and provide further advantages to the model. For instance, CRISPR/Cas9 technology was used in human normal intestinal organoids to engineer CRC organoids by sequential induction of mutations in tumour driving mutations characterised in classic adenoma-carcinoma sequence (Matano, Date *et al.* 2015). Organoids have also proven to be powerful and more reliable than 2D cell culture models in drug screening (Vlachogiannis, Hedayat *et al.* 2018, Schutte, Risch *et al.* 2017, Francies, Barthorpe *et al.* 2016, Longati, Jia *et al.* 2013). In addition, ‘CRC organoid biobanks’ have been formed to store organoids derived from CRC patients, which would greatly benefit CRC focused research, potentially leading to identification of novel gene interactions

and personalised therapy (van de Wetering, Francies *et al.* 2015).

In summary, intestinal and colonic organoids represent a robust, reproducible, genetically stable model that is suitable for basic research and has many applications in translational research. The utilisation of organoids will allow reduction in animal models used and benefit the understanding of tumour development prospectively leading to personalised medicine.

1.6 Tetraspanins

1.6.1 Overview

Tetraspanins are a large family of small transmembrane glycoproteins that are evolutionarily conserved among protozoan and metazoan organisms (Boavida, Qin *et al.* 2013, Huang, Yuan *et al.* 2005). Tetraspanins are expressed in nearly all cells of the human body and multiple members of the tetraspanin superfamily are expressed in each cell (Levy, Shoham 2005). The human genome has 33 genes encoding tetraspanin proteins. Tetraspanins have been implicated in a wide array of physiological functions including immune, reproductive, and urogenital systems (Yeung, Hickey *et al.* 2018, Yang, Sari *et al.* 2016, Schroder, Lullmann-Rauch *et al.* 2009, Wright, Geary *et al.* 2004, Le Naour, Rubinstein *et al.* 2000).

1.6.2 Tetraspanin structure

Four transmembrane domains of tetraspanins link together two extracellular loops – a large extracellular loop (LEL) and a small extracellular loop (SEL) (demonstrated in Figure 1-10). Tetraspanins have a number of characteristic structural features that distinguish them from other classes of four transmembrane domain proteins including a number of conserved residues in the extracellular

domain and polar residues in the transmembrane region. Highly polar residues – Asn, Gln and Glu – in transmembrane domains 1, 3 and 4 are 70%-90% conserved among all tetraspanins (Hemler 2005, Stipp, Kolesnikova *et al.* 2003). These residues are crucial for the formation of strong hydrogen bonds between each other or other residues contributing to the stabilisation of the transmembrane domain tertiary structure. There is also evidence that transmembrane region 1 of the tetraspanin CD82 is crucial for the biosynthesis and delivery of the protein to the cell surface through interaction with calnexin, an endoplasmic reticulum (ER) molecular chaperone (Cannon, Cresswell 2001).

Extracellular domains of tetraspanins present with a higher variation in size and sequence. It is thought that the large extracellular loop (LEL) is structurally similar among all tetraspanins: comprising of three helices and a variable region which determines the functional characteristic of each tetraspanin and contains nearly all known tetraspanin protein-protein interaction sites (Seigneuret, Delaguillaumie *et al.* 2001). Specifically, residues crucial for Hepatitis C Virus (HCV) E2 glycoprotein binding to tetraspanin CD81 were mapped to the hypervariable region of the LEL of CD81 (Kitadokoro, Bordo *et al.* 2001, Drummer, Wilson *et al.* 2002). The variable region of LEL is stabilised by two to four disulphide bonds and involves a conserved cysteine-cysteine-glycine (CCG) motif – another hallmark of the tetraspanin structure. The SEL of the tetraspanins has not been studied in great detail and little is known of its contribution to the function of tetraspanins. It is predicted that ~70% of tetraspanins share similar features of SEL – it is enriched in hydrophobic residues, predicted to form a β-strand region that interacts with the LEL conserved subdomain groove as has been shown for tetraspanins CD81 and

uroplakins (UPIa and UPIb) (Seigneuret 2006, Seigneuret, Delaguillaumie *et al.* 2001, Min, Wang *et al.* 2006, Kitadokoro, Bordo *et al.* 2001). All tetraspanins are characterised by the presence of a variable number of cysteine residues at the predicted cytoplasmic portions, and where investigated these cysteines are found to be palmitoylated (Berditchevski, Odintsova *et al.* 2002, Charrin, Manie *et al.* 2002, Yang, Claas *et al.* 2002). Palmitoylation is required for the efficient tetraspanin-tetraspanin interaction as well as association with other proteins that are organised into the tetraspanin enriched microdomain (TEM/TERM) (Levy, Shoham 2005, Hemler 2005). In 2016, the first crystal structure of full-length tetraspanin CD81 was resolved (Zimmerman, Kelly *et al.* 2016). This work revealed that transmembrane domains are organised in the 'cone-like' structure, where transmembrane domains 1 and 2 are separated from transmembranes 3 and 4 at the membrane, and a cholesterol molecule can bind the interface of the formed cavity resulting in the conformational change of the LEL (Figure 1-8). It is suggested that such a conformational shift determines binding ability of CD81 to its partner proteins, membrane localisation and has consequent effects on the regulation of cellular function of tetraspanins (Matthews, Szyroka *et al.* 2017). However, it remains unclear if this feature is common for other tetraspanins and additional work must be carried out.

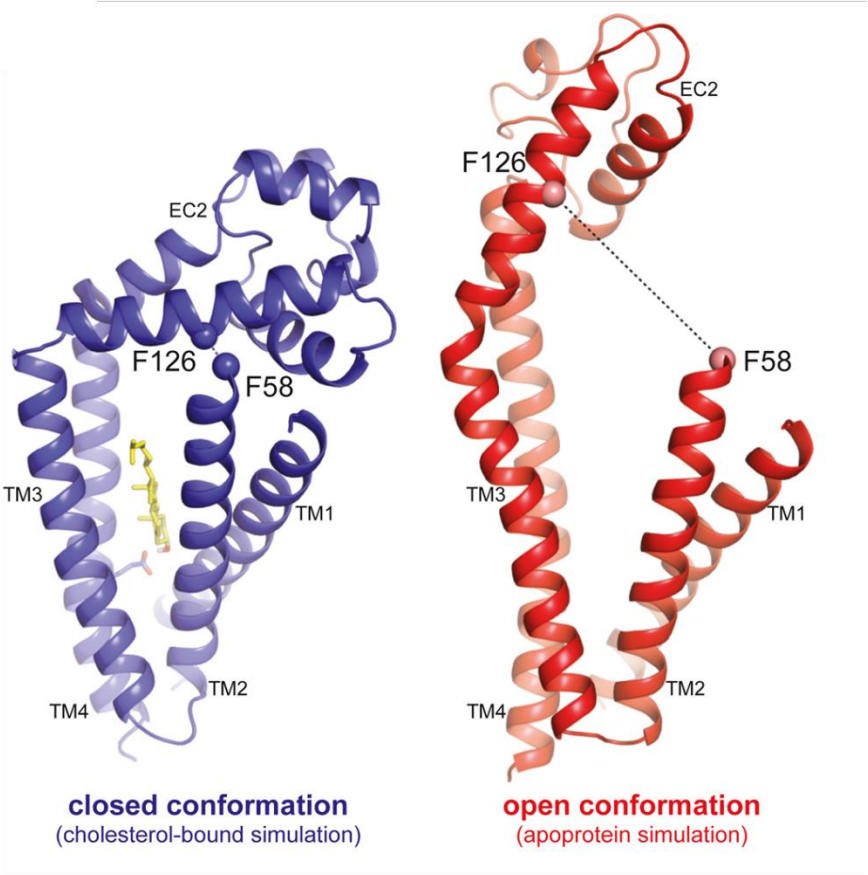

Figure 1-8. Crystal structure of tetraspanin CD81. Four transmembrane domains of CD81 (TM1-TM4) form a cone-like structure in the membrane. Molecular dynamic simulation suggests binding of cholesterol molecule (yellow) to the intramembrane cavity resulting in a conformation change of the LEL. Figure is reproduced from Zimmerman, Kelly *et al.* 2016.

1.6.3 Tetraspanin function

Functionally tetraspanins are implicated in the modulation of signalling pathways underlying cell adhesion, proliferation, motility, host-parasite interactions, and cell fusion (van Deventer, Dunlock *et al.* 2017). Specific functions of tetraspanins are determined by multiple *cis*- interactions with partner proteins, resulting in modulation of their signal transduction potential (e.g. integrins, receptor tyrosine kinases), intracellular trafficking (integrins, ADAM10) and clustering at the cell surface (integrins, EWI-2). Hence, tetraspanins are considered as molecular

facilitators (Hemler 2014, Charrin, Jouannet *et al.* 2014, Charrin, Manie *et al.* 2003). In addition to their function in *cis-,* several tetraspanin proteins were shown to function as receptors (in *trans*-) for a number of soluble ligands. Specifically, CD9 was reported as a receptor for pregnancy-specific glycoproteins (PSGs), CD63 – for tissue inhibitor of metalloproteinase 1 (TIMP-1), Tspan12 – for Norrin, and CD82 - for a transmembrane protein DARC (Moore, Dveksler 2014, Aaberg-Jessen, Sorensen *et al.* 2018, Lai, Zhang *et al.* 2017, Hur, Choi *et al.* 2016).

Tetraspanins and their partner proteins are organised into microdomains and specific clustering is crucial for molecular function of membrane proteins. The generally accepted model of TEMs/TERMs proposes heterotypic associations between multiple tetraspanins and their partners (Hopf, Colwell *et al.* 2012, Charrin, le Naour *et al.* 2009, Levy, Shoham 2005). However, recently it was demonstrated by super-resolution microscopy that tetraspanins form nanoclusters of ~10 homotypic tetraspanin molecules that overlap with nanoclusters of partner proteins and rarely overlap with clusters formed by other tetraspanins (Zuidscherwoude, Gottfert *et al.* 2015).

One of the best studied examples of how tetraspanins affect function of the associated receptors is tetraspanin-dependent regulation of laminin-binding integrins (α3β1, α6β1, α6β4 and α7β1) by CD151 (Kazarov, Yang *et al.* 2002, Sterk, Geuijen *et al.* 2002, Sawada, Yoshimoto *et al.* 2003, Berditchevski 2001, Yang, Claas *et al.* 2002). The CD151-integrin interaction is mediated by the LEL of CD151 and results in the conformational change of integrins from an inactive to an active state (Figure 1-9) (Haeuw, Goetsch *et al.* 2011). Strikingly, inactivation of CD151 was shown to

impair integrin-mediated cell adhesion, thus supporting a role for CD151 in the regulation of integrin-mediated adhesion strengthening (Nishiuchi, Sanzen *et al.* 2005). The functional importance of CD151 is further demonstrated in individuals with a CD151 nonsense mutation that results in hereditary nephritic syndrome (leading to kidney failure) and epidermolysis bullosa (fragile skin) (Karamatic Crew, Burton *et al.* 2004). This phenotype was associated with the deficient assembly of the basement membrane in these organs. Importantly, certain variants of epidermolysis bullosa were associated with deficiencies in α6– and β4–integrin subunits (Ashton, Sorelli *et al.* 2001). Accordingly, CD151-KO in FVB/N mice has also caused significant renal defects, strengthening the role of CD151 in regulation of integrin function (Sachs, Kreft *et al.* 2006, Baleato, Guthrie *et al.* 2008). Furthermore, histologically similar kidney and skin abnormalities were observed in α3-, α6-, and β4-KO mice (Belkin, Stepp 2000).

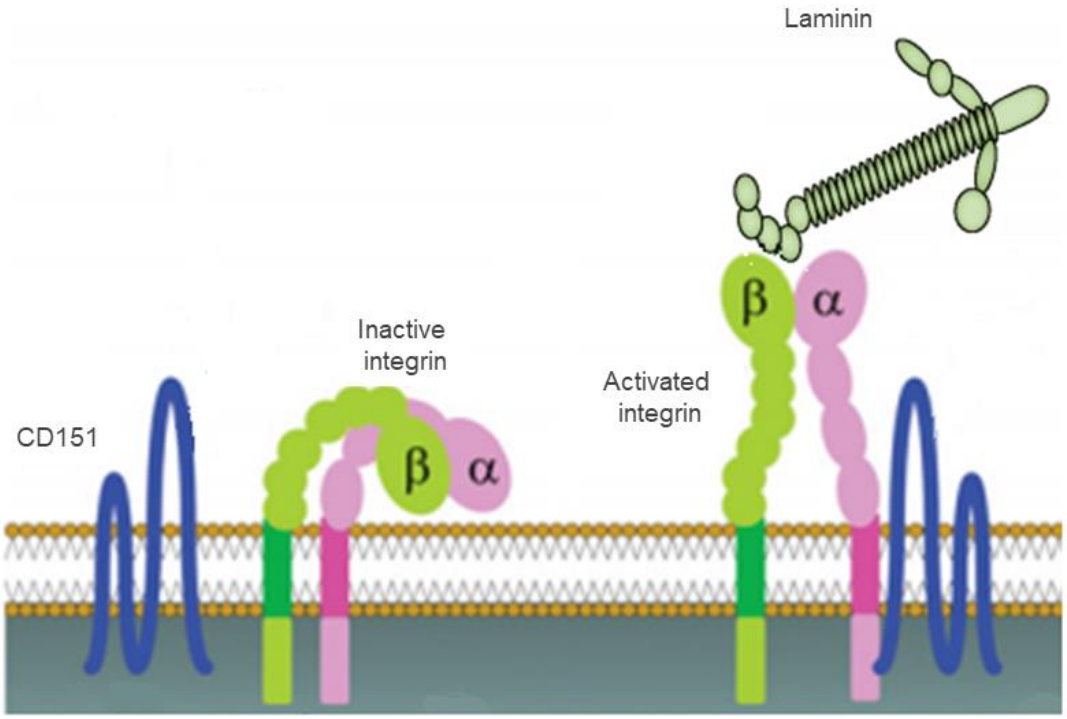

Figure 1-9. Schematic representation of CD151-integrin interaction on the cell surface. The association of integrins with CD151 results in a conformational change of integrins into an active state and adhesion to extracellular laminins. Figure is adapted and modified from Haeuw, Goetsch *et al.* 2011.

The role of tetraspanins in the intracellular trafficking of the associated proteins is best exemplified by studies focussed on CD81 and its partner CD19 (Cherukuri, Shoham *et al.* 2004, Levy 2014, Vences-Catalan, Rajapaksa *et al.* 2012). The interaction of CD81 and CD19, a B cell specific immunoglobulin domain containing protein, occurs through the LEL of CD81 during biosynthesis in the ER (Shoham, Rajapaksa *et al.* 2006). It has been shown that CD81 deficient mice have approximately a 50% reduction of CD19 expression on the surface of B cells (Miyazaki, Muller *et al.* 1997, Tsitsikov, Gutierrez-Ramos *et al.* 1997, Maecker, Levy 1997). Interestingly, CD19 expression was lost in an individual with mutated CD81

due to deficient trafficking of the protein from the ER to the Golgi (van Zelm, Smet *et al.* 2010). Loss of CD19 expression on B cells results in immunodeficiency, characterised by impaired antibody responses (Shoham, Rajapaksa *et al.* 2003).

Similarly, tetraspanins of the TspanC8 group have been shown to regulate intracellular trafficking and the maturation of matrix metalloprotease ADAM10 (Saint-Pol, Eschenbrenner *et al.* 2017, Matthews, Koo *et al.* 2018). The subgroup of TspanC8s consists of six tetraspanins (Tspan5, Tspan10, Tspan14, Tspan15, Tspan17 and Tspan33), characterised by eight cysteine residues in their LEL. It has been shown that TspanC8s specifically interact with ADAM10 via their LEL, and facilitate trafficking of ADAM10 from the ER to the plasma membrane and the removal of its inhibitory pro-domain (Noy, Yang *et al.* 2016, Haining, Yang *et al.* 2012, Prox, Willenbrock *et al.* 2012). Expression of ADAM10 was significantly reduced in erythrocytes in the Tspan33-KO mouse model (Haining, Yang *et al.* 2012). In addition to their role in endocytic trafficking of ADAM10, different TspanC8s, which appear to bind to different regions of ADAM10, determine the specificity of ADAM10 towards different substrates. For example, complex of Tspan15/ADAM10 promotes cleavage of N-cadherin, whereas Tspan14/ADAM10 and Tspan5/ADAM10 promote cleavage of Notch (Matthews, Szyroka *et al.* 2017, Jouannet, Saint-Pol *et al.* 2016, Haining, Yang *et al.* 2012, Zhou, Fujiwara *et al.* 2014, Ruiz-Garcia, Lopez-Lopez *et al.* 2016).

Tspan12 regulates multimerization of Frizzled-4/Lrp5 complex at the membrane facilitating β-catenin stabilisation and enhanced Norrin-induced Wnt signalling in retinal vasculature (Lai, Zhang *et al.* 2017, Junge, Yang *et al.* 2009).

Frizzled-4 forms a complex with its co-receptors Lrp5 or Lrp6 and activates the canonical Wnt signalling pathway in response to Wnt ligands or Norrin (structurally unrelated to Wnt cysteine-knot like growth factor) (Bang, Kim *et al.* 2018). The mouse KO model for Tspan12 exhibited impaired vascular development in the retina, a phenotype that was also demonstrated in mice deficient for Frizzled-4, Lrp5 and Norrin (Junge, Yang *et al.* 2009). Interestingly, Tspan12 mutations result in familial exudative vitreoretinopathy (blindness disorder) due to impaired retinal vasculature development (Nikopoulos, Venselaar *et al.* 2010, Poulter, Ali *et al.* 2010).

Tetraspanins have been shown to associate with multiple signalling molecules, including G-protein coupled receptors (GPCRs), EGFR, c-MET, C-Kit, ADAM10 and ADAM17, protein kinase C (PKC), and phosphatidylinositol 4-kinase (PI4K) (Termini, Gillette 2017). For instance, in the context of EGFR signalling CD82 has been shown to negatively regulate ligand-induced receptor dimerization and endocytosis (Odintsova, Voortman *et al.* 2003, Berditchevski, Odintsova 2016, Danglot, Chaineau *et al.* 2010). In addition, CD9 was reported to mediate EGFR signalling and was shown to inhibit proteolytic cleavage of TGF-α (Murayama, Shinomura *et al.* 2008, Shi, Fan *et al.* 2000). Another study demonstrated that CD9 promotes trafficking of pro-TGF-α to the cell surface from the Golgi (Imhof, Gasper *et al.* 2008). Furthermore, it has been shown that tetraspanin CD82 expression results in Wnt signalling inhibition through decreased phosphorylation of β-catenin and its intracellular re-distribution to E-cadherin complexes (Abe, Sugiura *et al.* 2008, Chigita, Sugiura *et al.* 2012). Another study has also demonstrated the role of CD63 in regulating β-catenin stabilisation via Akt-dependent GSK3β inhibition (Seubert, Cui *et al.* 2015).

1.6.4 Tetraspanins and colorectal cancer

Tetraspanins are associated with the development and progression of various cancers including CRC (Hemler 2014, Wang, Li *et al.* 2011, Romanska, Berditchevski 2011). Specifically, Tspan8 (C0-029), Tspan12, CD151 and Tspan1 have been shown to be upregulated in colorectal carcinomas and this is associated with a poor prognosis (Richardson, Jennings *et al.* 2011, Hashida, Takabayashi *et al.* 2003, Liu, Chen *et al.* 2017, Greco, Bralet *et al.* 2010, Chen, Zhu *et al.* 2009). However, expression of CD9, CD82, and uroplakin UPKIa are positively regulated with patient survival (Hashida, Takabayashi *et al.* 2003, He, Kong *et al.* 2014). Interestingly, Tspan8 has been proposed as a potential target for radio-immunotherapy in CRC using mouse monoclonal antibodies which are proven to effectively inhibit tumour growth in preclinical mouse models (Maisonial-Besset, Witkowski *et al.* 2017). The molecular functions of these tetraspanins in the context of colorectal cancer have not been well investigated in detail. Tspan8 and CD151 were shown to regulate cell motility through integrin and E-cadherin modulation thus linking their functions to metastasis of CRC cells (Malla, Pandrangi *et al.* 2018, Kohno, Hasegawa *et al.* 2002, Zhu, Ailane *et al.* 2017, Guo, Xia *et al.* 2012). Tspan12 was shown to promote β-catenin signalling through the association with LRP5 and Fzd4 and stabilisation of the complex (Knoblich, Wang *et al.* 2014, Junge, Yang *et al.* 2009). Therefore, it is important to investigate molecular functions of tetraspanins associated with CRC to fully unravel their potential implications not only in diagnostics but also in treatment and disease management.

1.6.5 Tetraspanin 6

Tetraspanin 6 (Tspan6) was first isolated from a human glioma cDNA by

Maeda *et al.* in 1998 (Maeda *et al.*, 1998). Tspan6 comprises of 245 amino acids and displays all key features of the tetraspanin proteins. In the LEL Tspan6 has a predicted N-linked glycosylation site at residue Asn134 (Figure 1-10). EST database analysis suggested that Tspan6 is expressed at high levels in brain and at lower levels in colon, lung, pancreas, prostate, retina, and melanocytes (Todd *et al.*, 1998).

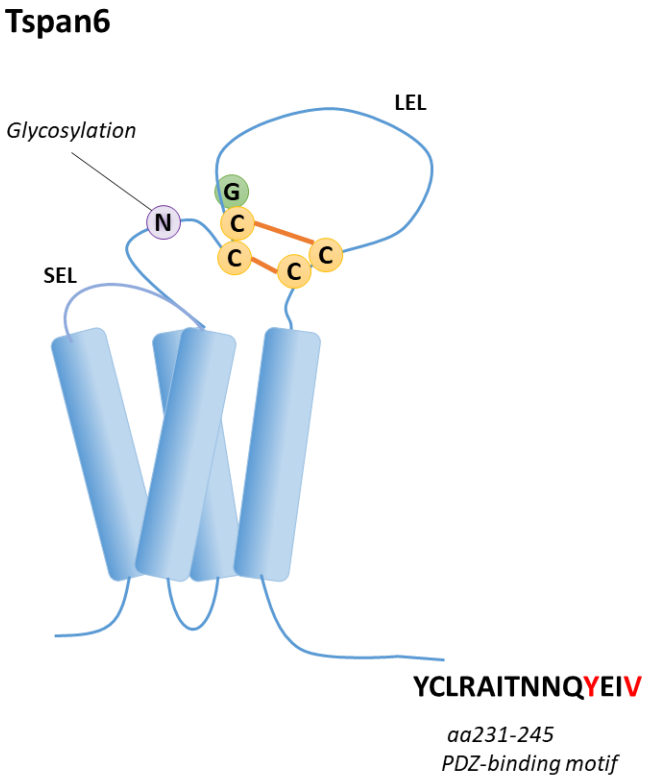

Figure 1-10. Schematic representation of Tspan6. The transmembrane domains form a cone-shaped structure, large extracellular loop (LEL) contains conserved CCG motif, where cysteines (C) form di-sulphide bonds, and Asn134 (N) glycosylation site. The N-terminus of Tspan-6 contains PDZ-binding motif.

Tspan6 is a poorly studied tetraspanin and little is known about its contribution to cellular processes. Early studies have shown that Tspan6 is localised to adherence junctions (Yamazaki, Okawa *et al.* 2008). In 2012, Tspan6 was demonstrated to play a role in retinoic acid-inducible gene I-like receptor- (RLR-) inducible immune response to Sendai virus (SeV) infection through association with mitochondrial antiviral signalosome (MAVS) resulting in negative regulation of IFN-stimulated response element, NF-κB, and IFN-β signalling (Wang, Tong *et al.* 2012). More recently Tspan6 expression was shown to negatively correlate with the onset of sporadic Alzheimer's disease (Salas, Callaerts-Vegh *et al.* 2017). At the cellular level

Tspan6 was implicated in the biogenesis of multivesicular bodies (MVBs) and can stimulate exosome production through the recruitment of an adaptor protein, syntenin-1 (Guix, Sannerud *et al.* 2017). Tspan6 was also reported as a potential stimulator of autophagy identified in a high-throughput short hairpin RNA (shRNA) screen (Strohecker, Joshi *et al.* 2015). Moreover, Tspan6 was found to be expressed on exosomes isolated from the LIM1863 colon carcinoma cell line (Tauro, Greening *et al.* 2012).

Tspan6 expression was studied in CRC patients. The authors reported that higher expression of Tspan6 in tumours associated with better survival, although not significantly (n=30, p=0.60), suggesting that Tspan6 may be considered as a potential colon cancer biomarker (Chiang Sum-Fu, Tsai Ming-Hung, Tang Reiping, *et al.* 2014). More recently, analysis of mRNA expression in 597 CRC cases has demonstrated positive correlation of high Tspan6 expression and patient survival (p=0.0356) (Figure 1-11) (Uhlen, Zhang *et al.* 2017). In addition, Tspan6 expression was reported to associate with complete response to neoadjuvant therapy in locally advanced rectal cancers (Chauvin, Wang *et al.* 2018). Growing evidence implicating Tspan6 in the development of CRC encouraged us to study in more detail how Tspan6 may be involved in this disease.

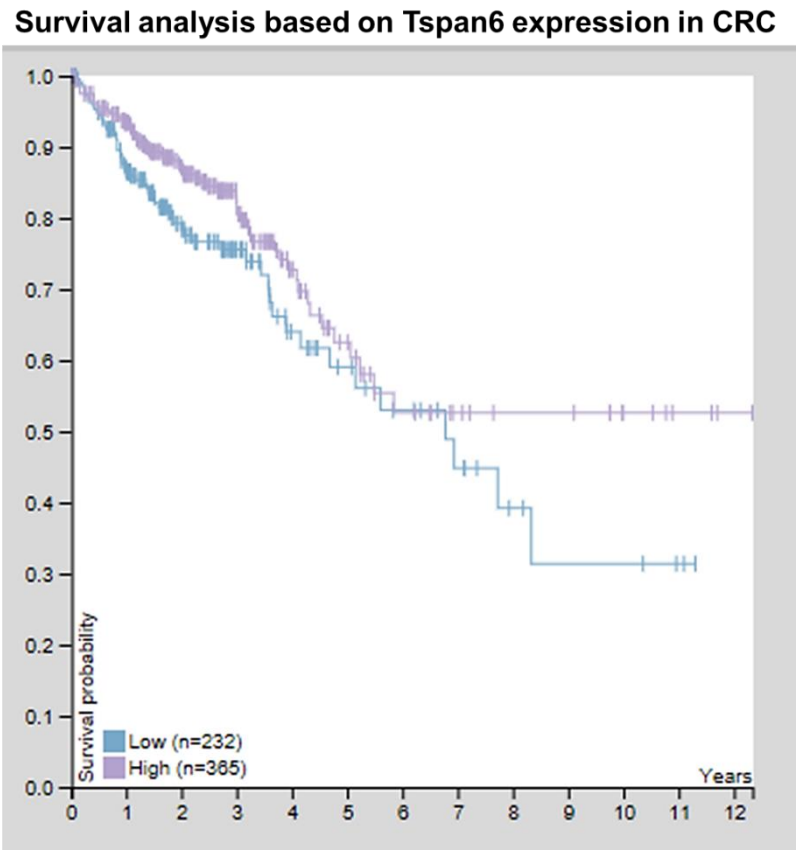

Figure 1-11. CRC patient survival with Tspan6-high (purple) and Tspan6-low (blue) expression of mRNA transcript in CRC tumours. High expression of Tspan6 favours overall 5-year survival of CRC patients (63% vs 59% in Tspan6-high and Tspan6-low expressing tumours respectively, p=0.0356). Figure reproduced from Human Protein Atlas 2017.

1.6.6 Tetraspanins, extracellular vesicles and exosomes

It has been proposed that tetraspanins can also regulate carcinogenesis via exosomes – nanovesicles that function as a powerful tool of communication between various cell types in the tumour microenvironment (Malla, Pandrangi *et al.* 2018, Lu, Li *et al.* 2017). Exosomes are small bi-lipid membrane vesicles, 30nm to 100nm in diameter, and are enriched in cholesterol, sphingomyelin, ceramide, tetraspanin proteins, plasma membrane proteins, signalling molecules and genetic material including mRNAs, miRNAs, and lncRNAs (Bastos, Ruivo *et al.* 2018, Toh, Lai *et al.* 2018). The content of exosomes varies greatly depending on the cell of origin and it is becoming more evident that the biogenesis and cargo sorting into exosomes is a tightly regulated process.

Exosomes are derived from the endocytic pathway through the formation of multivesicular bodies (MVBs) (Alenquer, Amorim 2015). The endocytic pathway is considered as a mechanism of protein recycling and degradation, and exosomes were believed to be means of disposing of redundant cellular waste; however it is becoming more evident that exosomes have important biological function in mediating cellular communication (Nagarajah 2016).

The maturation of endosomes is associated with acidification of the intraluminal compartment and formation of multiple intraluminal vesicles (ILVs), resulting in a late endosome or MVB. Furthermore, late endocytic organelles are directed into one of the two pathways: 1) fusion with lysosomes for protein degradation or 2) fusion with plasma membrane for exosomal release (Figure 1-12). Rab GTPases have been shown to mediate endosome and MVB fate, for example Rab5 facilitates recycling of early endosomes to the plasma membrane, Rab7

promotes maturation of early endosomes to late endosomes and MVB formation, and Rab11, Rab27a/b, Rab35 target MVBs to the plasma membrane, followed by fusion and exosome release (McGough, Vincent 2016, Alenquer, Amorim 2015). The content of exosomes is variable and the sorting of proteins into exosomes is not fully understood. One of the best studied mechanisms requires Endosomal Sorting Complex Required for Transport (ESCRT) complex and is implicated in ILV formation and maturation of early endosomes. ESCRT machinery contains up to 30 different proteins and is subclassified into five complexes (Juan, Furthauer 2018, Colombo, Moita *et al.* 2013). It is unclear which ESCRT machineries are involved in exosomal production, however the components of ESCRT-I and -III, including Alix and Tsg101, have been reportedly identified as exosomal markers (Juan, Furthauer 2018). ALIX has been reported to recruit PDZ-domain-binding cargo proteins, such as syndecans, tetraspanin CD63 and Frizzled receptors into MVBs through association with syntenin-1 (McGough, Vincent 2016, Baietti, Zhang *et al.* 2012, Latysheva, Muratov *et al.* 2006). Syntenin-1 is an adaptor protein that interacts with partner proteins via one of its PDZ (PSD95/Dlg/ZO-1) domains (Sarkar, Boukerche *et al.* 2004). The Alix/Syntenin/Syndecan complex plays a crucial role in exosome cargo sorting and ILV formation (Juan, Furthauer 2018). Syntenin-1 binds to the cytoplasmic tail of the transmembrane heparan sulfate proteoglycan (HSPG) syndecan via its PDZ domain, the endoglycosidase heparanase cleaves heparan sulfate side chains of syndecan, resulting in syndecan clustering and recruitment of alix-ESCRT complex to the N-terminal domain of syntenin to facilitate budding and cleavage (Baietti, Zhang *et al.* 2012, Ghossoub, Lembo *et al.* 2014). The Alix/Syntenin-1 complex was also shown to interact with the small GTPase ADP-Ribosylation Factor 6 (ARF6) via direct

association with syntenin-1 and with the aid of the phospholipase D2 (PLD2) regulates ILV production in endosomes (Ghossoub, Lembo *et al.* 2014). Interestingly, syntenin-1 has been reported to be upregulated in several cancers, including melanoma, glioma, breast cancer, urothelial cell carcinoma, and small cell lung carcinoma; its elevated expression in breast cancer and melanoma is negatively regulated with patient survival (Kegelman, Das *et al.* 2015). Moreover, syntenin-1 is speculated to affect HSPG aggregation, which in turn has been reported to be crucial for cancer-derived exosomes (Fares, Kashyap *et al.* 2016, Christianson, Svensson *et al.* 2013). The role of tetraspanins in ESCRT-dependent EV biogenesis is not fully understood. It is believed that tetraspanins may regulate an alternative, ESCRT-independent exosome biogenesis. As such, upon depletion of ESCRT complex proteins, human epithelial cells Hep2, HeLa and melanocytic MNT-1 cells, were able to generate CD63 enriched extracellular vesicles (EVs) (Colombo, Moita *et al.* 2013, van Niel, G., Charrin *et al.* 2011, Stuffers, Sem Wegner *et al.* 2009).

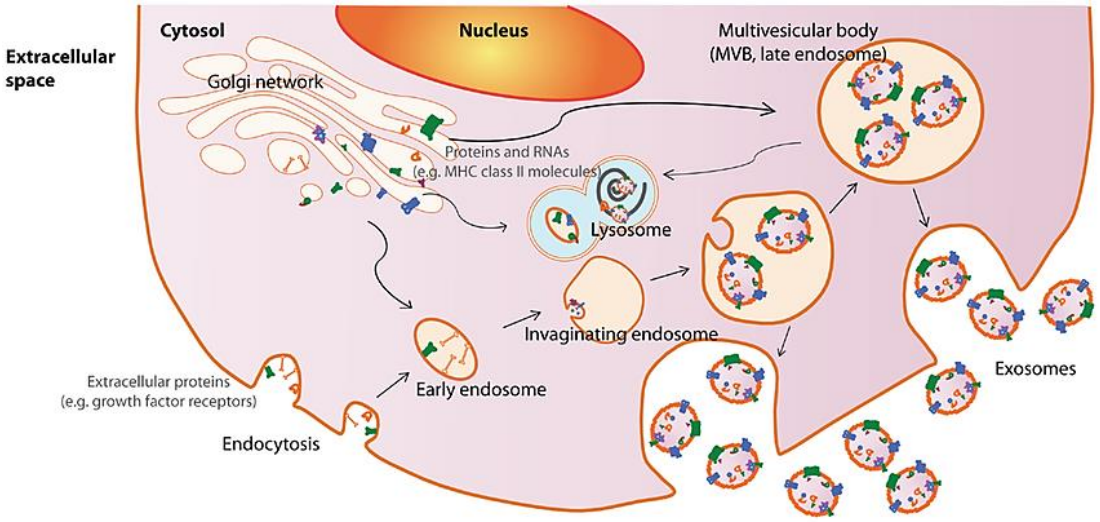

Figure 1-12. Schematic representation of exosome biogenesis. Exosome biogenesis starts with plasma membrane invaginations, formation of early endosomes, followed by formation of intraluminal vesicles (ILVs) within the endosome, maturation to late endosome/multivesicular body (MVB) that can be targeted for lysosomal degradation or fusion with plasma membrane for exosome release. Figure reproduced from Zhang, B., Yin *et al.* 2014.

The enrichment of tetraspanin proteins on exosomes suggests that individual tetraspanins and, perhaps, TEMs/TERMs as a whole play an important role in functionality of exosomes. Cytoplasmic portions of several tetraspanins have endocytic trafficking signals which may be responsible for their recruitment to late endocytic organelles and, subsequently, to exosomes (Berditchevski, Odintsova 2007). For example, it has been shown that the C-terminus of CD63 contains tyrosine-based sorting motif YEVM that binds to adaptor proteins AP-2 and AP-3, facilitating clathrin-dependent internalisation of CD63 enriched TEMs/TERMs (Berditchevski, Odintsova 2007, Rous, Reaves *et al.* 2002). The putative tyrosine-based C-terminal motif YXXØ (Tyr-Xaa-Xaa-Ø, where Ø represents of an amino acid with a bulky hydrophobic side chain) is a common feature of 13 human tetraspanins (Berditchevski, Odintsova 2007). Importantly, various tetraspanins have been shown

to internalise into endosomes with their partner proteins, thus, suggesting their involvement in the recruitment of the partners to exosomal membranes. As such, tetraspanin CD82 internalises in a complex with EGFR and immunoglobulin protein EWI-2 (Zhang, Lane *et al.* 2003). Similarly, tetraspanins CD82 and CD9 facilitate endocytosis of E-cadherin and β-catenin (Chairoungdua, Smith *et al.* 2010). Other examples include CD81-dependent recruitment of Wnt11 into EVs in murine cancer-associated fibroblasts (Luga, Zhang *et al.* 2012); the role of tetraspanin CD9 in sorting of CD10 metalloproteinase cargo recruitment to EVs in B-cells (Mazurov, Barbashova *et al.* 2013); the involvement of Tspan8 in selective recruitment of vascular cell adhesion molecule 1 (VCAM-1) and integrin α4 in pancreatic adenocarcinoma cells (Nazarenko, Rana *et al.* 2010); and the role of CD81 in sorting of MHC class molecules, B cell receptor, intercellular adhesion molecule 1 (ICAM-1) and Rac into EVs (Perez-Hernandez, Gutierrez-Vazquez *et al.* 2013).

Exosomes are currently accepted as important messengers for cellular communication and regulation of biological processes associated with tumour initiation, progression and metastasis (Bastos, Ruivo *et al.* 2018). For instance, melanoma-derived exosomes were reported to contain high levels of vascular endothelial growth factor (VEGF) and IL-8 resulting in enhanced angiogenesis and immunosuppression in tumours (Ekstrom, Bergenfelz *et al.* 2014). Additionally, exosomes derived from cancer were shown to promote tumour metastasis by conditioning a pre-metastatic niche in distal organs for pancreatic cancer (liver metastasis) and melanoma (lung and liver metastasis) (Hoshino, Costa-Silva *et al.* 2015, Costa-Silva, Aiello *et al.* 2015). Furthermore, cancer-derived exosomes have been reported to modulate immune cell recruitment and response, favouring tumour

formation and progression (Mincheva-Nilsson, Baranov 2014). In colorectal cancers, exosomes were reported to contain multiple miRNAs (let-7a, miR-1229, miR-1246, miR-150, miR-21, miR-223, and miR-23a), that are elevated in CRC patients and considered as biomarkers of CRC (Ogata-Kawata, Izumiya *et al.* 2014). Furthermore, exosomes containing miRNA miR-4772-3p were shown to positively correlate with a better outcome of adjuvant therapy and decreased risk of tumour recurrence in stage II and stage III CRCs (Liu, Eng *et al.* 2016). MicroRNA-210-containing exosomes showed the ability to promote epithelial-mesenchymal transition (EMT) and tumour invasion (Bigagli, Luceri *et al.* 2016). Interestingly, tetraspanins have been implicated in sorting RNAs into EVs. As such, Tspan8 expressing cells were shown to enrich secreted exosomes in 285 mRNA and miRNA transcripts (Nazarenko, Rana *et al.* 2010). Exosomes have also been implicated to play a role in chemo- and drug resistance. For instance, tumour-derived exosomes were shown to be enriched in ΔNp73 mRNA, a transcript of which inhibits the tumour suppressor function of TP53, promoting chemoresistance to oxaliplatin in the colon cancer cell line HCT116 (Soldevilla, Rodriguez *et al.* 2014). A more recent study demonstrated that exosomes derived from KRAS mutant cells can induce drug resistance to anti-EGFR treatment with cetuximab in cetuximab-sensitive, namely Caco-2 cells (Zhang, Zhang *et al.* 2017).

In summary, exosomes play an important role in tumour development, progression and metastasis, and investigating how individual tetraspanins modulate their composition and function may lead to better understanding a better understanding of their role in the context of a specific disease.

1.7 Research Objectives

Tetraspanin 6 (Tspan6) is a poorly studied protein of the tetraspanin family of transmembrane proteins with no defined cellular function. While changes in expression of Tspan6 in CRC have been reported, the contribution of the protein in development of the disease has not been investigated. The aim of this project was to examine the role of Tspan6 in normal epithelium and in the progression to CRC. In this study, the biological effects of Tspan6 expression on tissue homeostasis and its role in the early stages of carcinogenesis and underlying mechanisms were addressed. The hypothesis of this project proposes that Tspan6 expression in CRC negatively regulates tumorigenesis by modulating EGFR-dependent signalling through interaction with syntenin-1 and limiting production of exosomes containing EGFR ligands.

1.7.1 Aims

The specific aims of this study were as follows:

1) To examine Tspan6 expression and distribution in CRC;
2) To determine the involvement of Tspan6 in colorectal carcinogenesis using Tspan6 KO mouse model;
3) To examine cellular functions of Tspan6 in intestinal epithelial cells.

2 MATERIALS AND METHODS

2.1 Cell culture methods

2.1.1 Mammalian cell lines

Mammalian cell lines used in this project are listed in the Table 2-1. All cells were obtained from American Type Culture Collection (ATCC) unless stated otherwise.

Table 2-1. Mammalian cells used in the project

Cell Line	Source	Tissue	Cell type
HEK293T	ATCC®	Human Embryonic Kidney	Epithelial
Caco-2	gifted	Human Colorectal adenocarcinoma	Epithelial
L cells	ATCC®	Murine Subcutaneous Connective Tissue	Fibroblast
L-Wnt3a cells	ATCC®	Murine Subcutaneous Connective Tissue	Fibroblast
HA-R-Spondin-1-Fc 293 cells	Amsbio	Human Embryonic Kidney	Epithelial
L-WNR cells	ATCC®	Murine Subcutaneous Connective Tissue	Fibroblast

2.1.2 Cell line authentication

Caco-2 cells were kindly provided by Dr Chris Tselepis (University of Birmingham). Caco-2 cells were authenticated by multiplex PCR and short tandem repeat (STR) DNA profiling analysis using GenePrint® 10 System (Promega). The DNA was isolated from Caco-2 cells and ten loci were amplified using multiplex PCR according to the manufacturer's instructions. The resulted STR profile was matched to Caco-2 STR profile published on the ATCC website and 87.5% match was identified against the cells used in these studies (Figure 2-1). The obtained STR

profile did not match other cell lines in the database (ATCC), confirming the authenticity and purity of the Caco-2 cell line.

A

Caco-2 Expected STR profile (*ATCC)	
STR Locus	**Alleles**
TH01	6
D5S818	12, 13
D13S317	11, 13, 14
D7S820	11, 12
D16S539	12, 13
CSF1PO	11
Amelogenin	X
vWA	16, 18
TPOX	9, 11

B

Sample STR profile	
STR Locus	**Alleles**
TH01	6
D5S818	12
D13S317	13, 14
D7S820	11, 12
D16S539	12, 13
CSF1PO	11
Amelogenin	X
vWA	16, 18
TPOX	9

C

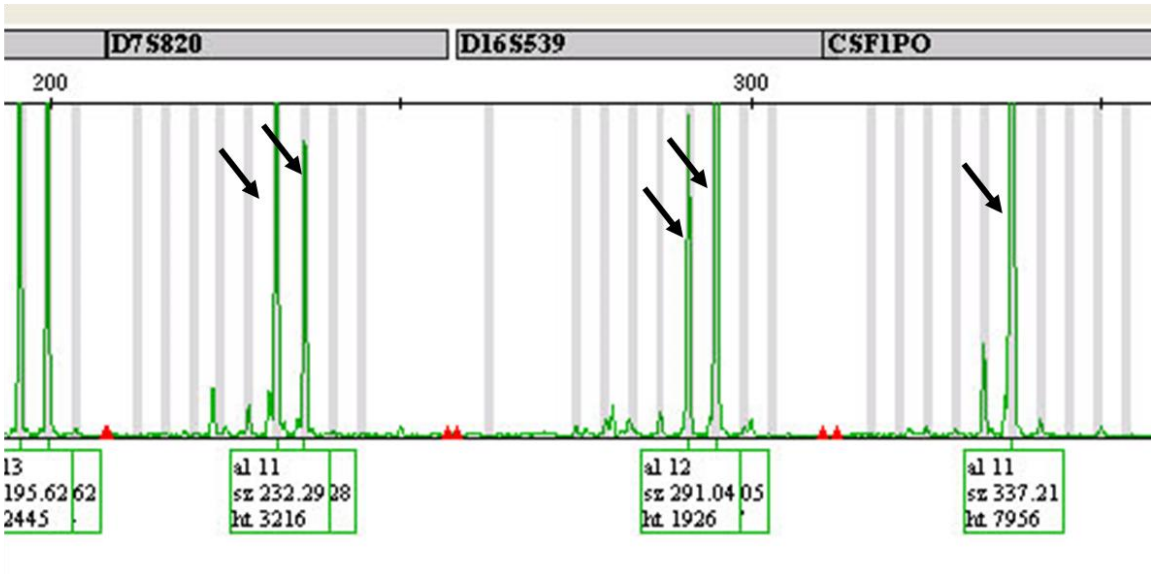

Figure 2-1. Authentication of the Caco-2 cell line. **(A)** The expected STR profile of Caco-2 cell line with alleles of nine DNA loci. **(B)** The STR profile of Caco-2 experimental cells with identified alleles for nine DNA loci shows 87.5% match to the expected profile. **(C)** The example of allele amplification profile in Caco-2 experimental cells for locus D7S820, D16S539 and CSF1PO. Black arrows indicate amplified alleles of named loci with annotations below.

2.1.3 Mammalian cell line culture

All cells were cultured in high glucose (4500 mg/l) Dulbecco's Modified Eagle's Medium (DMEM) (Gibco), supplemented with 10% (v/v) Foetal Calf Serum (FCS)

(Gibco) and 50 U/ml Penicillin / 50 µg/ml Streptomycin (Gibco). Stably transfected Caco-2 cells were maintained in the presence of 2 µg/ml puromycin (Sigma-Aldrich), L-Wnt3a cells were grown in 0.4 mg/mL Geneticin® (G418), HA-R-Spondin-1-Fc 293T cells - in 300 µg/ml Zeocin, and L-WNR cells - in 0.5 mg/ml Hygromycin B and 0.5 mg/ml Geneticin® (G418). All cell lines were cultured at 37°C, in a humidified incubator (Galaxy R CO2 Incubators, RS Biotech) in 5% CO2 atmosphere. Cells were passaged when they reached 80% confluency. For passaging, growth medium was removed, and cells were washed with sterile phosphate buffered saline (PBS) to remove all traces of serum. To detach cells from a plastic surface of the flask/plate, they were incubated with 0.05% Trypsin-EDTA (Gibco) for 5 min at 37°C. Subsequently dislodged cells were resuspended in fresh growth medium and pelleted by centrifuging at 190 x *g* for 3 min in Heraeus Megafuge 40 (ThermoFisher Scientific). After resuspension cells were plated at required density (1:5 for Caco-2 or 1:10 for HEK293T, L Cells, L-Wnt3a cells, Noggin-secreting 293 cells, and HA-R-Spondin-1-Fc 293 cells, L-WNR cells). Growth media was changed every three days.

2.1.4 Cryopreservation of cell lines

For cryopreservation, cells (collected as described above) were resuspended in freezing solution (10% (v/v) dimethyl sulfoxide (DMSO) (Sigma-Aldrich) and 90% (v/v) FCS). The suspension of $1x10^6$ cells/ml was subsequently frozen in 1 ml CryoTube™ vials (Nunc) at -80°C for at least 24h before transferring to liquid nitrogen for long term storage. Cells were recovered by thawing in a water bath for 2 min at 37°C. Thawed cell suspension was transferred to a tube with 9 ml of pre-warmed complete growth medium and pelleted by centrifugation at 190 x *g* for 3 min. Cells were resuspended in fresh medium and seeded in T25 tissue culture flask.

Cells were incubated at 37°C, in humidified 5% CO_2 atmosphere for at least 48h before further manipulation.

2.1.5 Caco-2 3D culture

Caco-2 3D colonies were plated on polymerised growth factor reducedMatrigel™ (BD Bioscience) supplemented with 0.4 mg/ml Matrigel™ in complete growth medium or in DMEM supplemented with 10% FCS in 8-well chamber LabTek (Thermo Fisher Scientific). Each well was pre-coated with 45 µl of 100% Matrigel™ and incubated for 15 min in the incubator at 37°C for Matrigel™ to solidify. Subsequently, $6x10^3$ cells were mixed with 0.4 mg/ml Matrigel™ in DMEM and added to each Matrigel™ coated well. Cells were incubated at 37°C, in humidified incubator (Galaxy R CO2 Incubators, RS Biotech) in 5% CO_2 atmosphere.

For the experiments involving EGF and cetuximab cells were plated on Matrigel™-coated LabTek in 0.4 mg/ml Matrigel™ in complete growth medium. After 24 hours 10 ng/ml of EGF or 25 µg/ml cetuximab were added and cells were incubated in cell incubator at 37°C for 5 days. Fresh media containing EGF or cetuximab was added every two days. The growth of colonies was examined using phase-contrast microscopy (Nikon) and images of 25 fields were taken for subsequent analysis. The diameter of colonies and lumens were measured using ImageJ Software. Approximately 150 colonies per condition were analysed.

2.2 Organoid culture

2.2.1 Organoid derivation

Mouse intestine and colon were collected into ice-cold PBS. The intestine was cut into 3cm pieces and villi were scraped using a coverslip. Then tissue was cut into

2-3 mm sections and placed in a Falcon tube with modified ice-cold PBS (PBS-0) (Sigma-Aldrich) and vigorously shaken for 3 min to remove contaminating villi. This process was repeated until the supernatant was clear. Subsequently, intestinal tissue was incubated in 25ml of gentle cell dissociation reagent (StemCell Technologies) for 15 min on a rocker at room temperature to separate the crypts and villi from the intestinal basal surface. The crypts were then isolated from villi by centrifugation at 300 x *g* 5 min. The supernatant was discarded and pellets resuspended in 10 ml of ice-cold PBS and centrifuged for 2 min at 150x*g* to remove single cells. Crypts were then counted and resuspended in Matrigel™ (~200 crypts/50µl of Matrigel™). Crypt-Matrigel™ suspension was then pipetted into the centre of the pre-warmed 24-well in the dome-shaped droplet. Subsequently, the plate was incubated for 15 min to allow Matrigel to solidify. Then, 500 µl of Intesticult™ organoid growth medium (StemCell Technologies) was added to each well. Organoids were incubated in a CO_2-incubator for 7-8 days and media was changed every 3 days. To evaluate EGFR-dependent organoid growth, organoids were cultured in mouse intestinal organoid media: Advanced DMEM/F-12 (Gibco) supplemented with 20% (v/v) R-Spondin-1 conditioned medium, 100 ng/ml Noggin (Peprotech), 1xB27 (ThermoFisher Scientific), 1xN2 (ThermoFisher Scientific), 1.25 mM N-Acetyl Cysteine (Sigma-Aldrich), 10mM Nicotinamide (Sigma-Aldrich), 100µg/ml Primocin (Vivogen) and in the presence (control) or absence of 50 ng/ml EGF (Peprotech). Organoids were cultured for 7 days and the growth was examined using phase-contrast microscopy (Nikon) every three days of culture.

2.2.2 Mouse intestinal organoid passaging and maintenance

For passaging, organoids were collected into a 15ml tube and gently washed

by pipetting with 10ml ice-cold PBS-0. Organoids were pelleted by centrifugation at 300 x *g* for 5 min. The supernatant and excess Matrigel™ were removed and discarded. Organoids were then resuspended in 1ml of ice-cold PBS-0 and mechanically disrupted by pipetting. Once the suspension appeared cloudy and no large structures were detected, the suspension was checked under microscope to identify crypt-like structures. Subsequently, cells were further washed twice with ice-cold PBS-0, resuspended in the required amount of Matrigel and plated on pre-warmed 24-well plate as described above and overlaid with 750 µl of growth medium. Each well, containing approximately 50-100 organoids was split into three wells.

2.2.3 Organoid embedding into paraffin blocks

Organoids were fixed with 4% paraformaldehyde/3% sucrose/PBS (PFA) supplemented with 1mM $CaCl_2$ and 0.5 mM $MgCl_2$ for 30 minutes at room temperature. PFA fixed samples were then washed with PBS three times for 5 minutes. Organoids were resuspended in 3% low-melting-point agarose (Sigma-Aldrich). After agarose polymerisation, the pellets were fixed in 10% formalin buffered saline (Sigma-Aldrich) for 4 hours followed by two 30-minute wash in PBS. Samples were dehydrated in graded alcohol (75% - 1hr, 95% - 1hr, 100% - 1hr) and alcohol was replaced with xylene for 1hr, followed by 2hr incubation in paraffin bath at 60°C. Samples were then embedded into fresh paraffin using HistoStar™ (ThermoFisher Scientific) and stored at room temperature.

2.2.4 Organoid size measure

Organoids derived from C57Bl/6J wild-type, Tspan6 KO, $APC^{min/+}$, and $APC^{min/+}Tspan6^{-/y}$ mice were imaged using phase-contrast microscopy after five days in culture. Approximately 10 fields were taken for analysis. Images were analysed

using ImageJ software as shown in Figure 2-2. The Fast Fourier Transform (FFT) algorithm was first used to filter out large structures (down to 200 pixels) and smoothen small particles. Following this, the threshold level was corrected for each image to highlight organoids structures. The algorithm of particle analysis was used to measure organoid area (pixel^2), filtering out particles smaller than 1000 pixel^2. The area of organoids was measured and presented as average area (pixel2) of organoid per genotype. More than 100 organoids per genotype were measured.

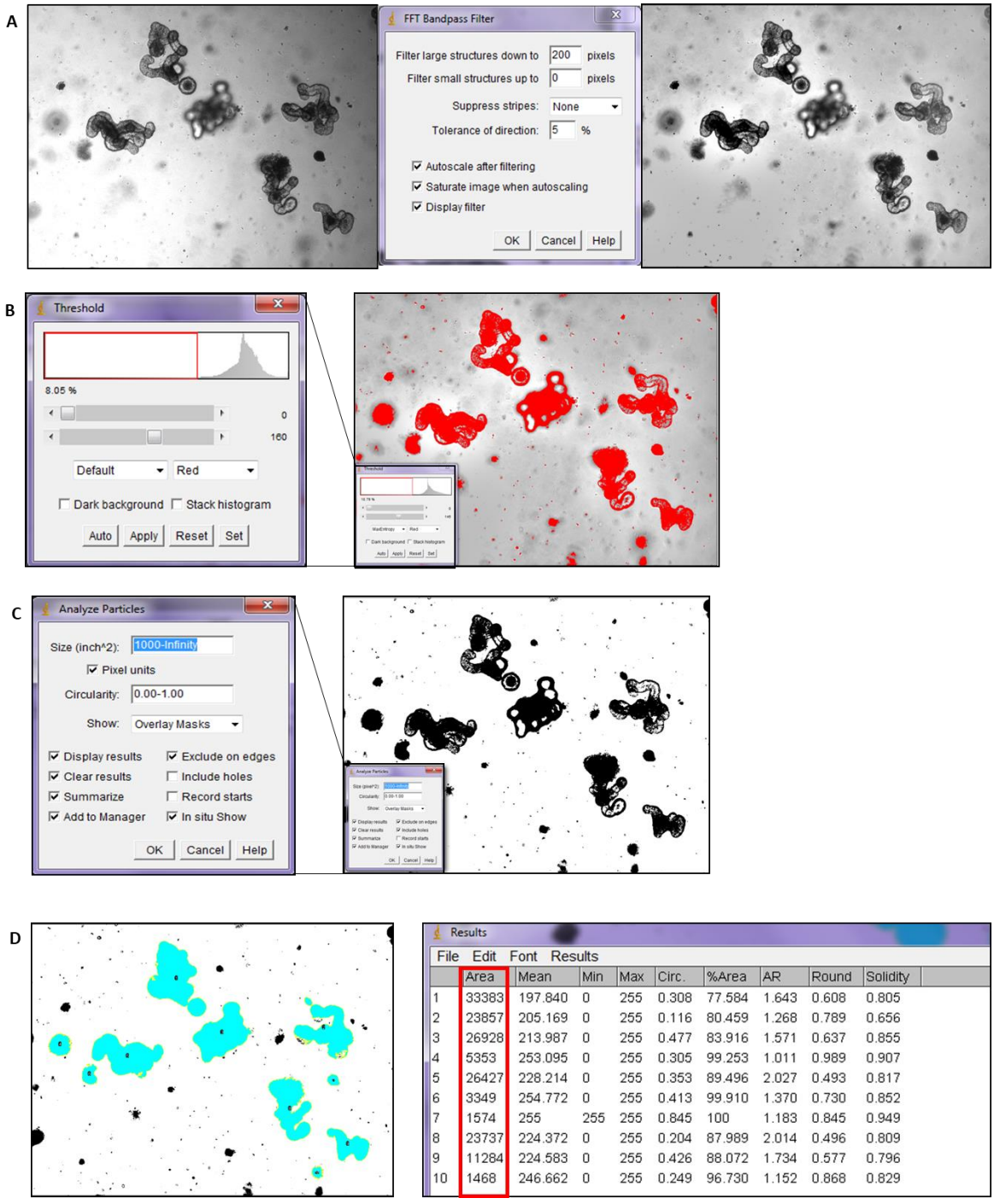

Figure 2-2. ImageJ algorithm for organoid size measure. **(A)** The FFT Bandpass filter was corrected to reduce the image complexity and smoothen small objects in the field. **(B)** Threshold for each image was corrected to isolate organoids from the background. **(C)** The particle analysis was run to detect structures >1000 pixel^2. **(D)** Analysed structured were overlaid with masks and area of organoid and other statistical values shown in result window.

2.3 Cell transfection

2.3.1 Stable gene expression cell line establishment

Stable expression of FLAG-Tspan6 in Caco-2 cells was established using lentiviral transduction. The vectors psPAX2 and pMD2.G were provided by D. Trono (Geneva, Switzerland); the pLVx-Flag-Tspan6 (puro) plasmid was provided by Dr. Berditchevski. Lentiviral particles were produced using PEI-based (polyethyleimine) transfection protocol on 70% confluent HEK293T (Yang, S., Zhou *et al.* 2017). The HEK293T cells were plated on 6cm plate and incubated at 37°C until 70% confluency was reached. Immediately prior to transfection, 3.2ml of fresh media was added to the cells. To transfect cells, 8 µg total DNA (3.6 µg psPAX; 1.8 µg pMD2.G; 2.6 µg pLVx-puro/ pLVx-Flag-Tspan6) was mixed with 800 µl of serum free, antibiotic free DMEM. The mix was vortexed, and 12 µg of PEI was added to the mixture, vortexed and incubated for 10min at room temperature. Subsequently, the DNA/PEI mix was added to the HEK293T cells, the total volume of media was 4 ml. Following 16-hour incubation, media was exchanged for the fresh complete growth medium and incubated for 24 hours to produce viral particles. Virus containing supernatant was harvested and supplemented with polybrene (1 µg/ml). The supernatant was filtered using 0.22 µm filter (Millipore) and added to Caco-2 cells following 24 hours incubation. To increase the efficiency of lentiviral gene transduction, infection of target cells was repeated. For stable gene transduction, selection with 2 µg/ml puromycin started 48 hours after the last infection cycle. Transfection efficiency was determined by Western blot analysis using polyclonal anti-TSPAN6 antibody (Thermo Fisher Scientific) and monoclonal anti-FLAG antibody (Sigma-Aldrich).

2.3.2 siRNA gene silencing

Transfection of Caco-2 cells was carried out using Lipofectamine™ RNAiMAX Reagent (Invitrogen) as per manufactures instructions in a 24-well format. The reverse transfection procedure was utilised. Predesigned small interfering RNA directed against syntenin-1 (Eurofins MWG Operon) and a non-targeting siRNA control (Qiagen) were used to knockdown gene expression at 10 nM final concentration. For each well to be transfected 6pmol siRNA was diluted into 50 µl of Opti-MEM® (Thermo Fischer Scientific) and mixed by pipetting. Separately, 3 µl of Lipofectamine™ RNAiMAX was diluted in 50 µl of Opti-MEM®. Diluted siRNA mix and diluted Lipofectamine RNAiMAX were mixed and incubated for 5min at room temperature. Subsequently, siRNA-Lipofectamine complexes were added to each well containing $3x10^5$ Caco-2 cells in 500 µl antibiotic free media. Following 24-hour incubation at 37°C in a CO_2 incubator cells were detached using TrypLE Express enzyme (Gibco) for 5 min at 37°C and plated in 0.2 mg/ml Matrigel™ on pre-coated with 100% Matrigel 48-well plates. Growth of colonies was examined using phase-contrast microscopy and protein expression knockdown was examined by Western Blot.

2.4 Conditioned media production

2.4.1 Wnt3a and WNR conditioned media

Mouse fibroblast L cells expressing Wnt3a (or co-expressing Wnt3a, R-Spondin-3 and Noggin) were passaged at 1:10 dilution once a week at 90% confluency. Wnt3A conditioned medium was prepared according to the manufacturers protocol. Briefly, cells were cultured in DMEM/FCS media in five 15 cm tissue culture dishes for 4 days after subculture (1:10). Subsequently, the media

was collected, filtered through 0.2 µm filter and stored at 4°C (marked as the “batch 1). Cells were cultured in fresh growth medium for further 3 days, collected and sterile filtered as described above (batch 2). Media from batch 1 and batch 2 were mixed at 1:1 ratio, filtered through 0.2 µm filter system and stored at 4°C for up to 4 weeks.

2.4.2 R-Spondin-1 conditioned media

The 293T cells expressing HA-R-Spondin-1-Fc were passaged at 1:10 dilution once a week at 80% confluency. For conditioned medium, cells were expanded in complete growth medium in T-225 (225 cm^2 area) tissue culture flask. Once cells reached 80% confluence, the media was changed to Advanced DMEM/F-12 containing GlutaMAX and cultured for further 7-10 days. Subsequently, the supernatant was collected, and cells and debris were removed by centrifuging at 3,000 x g for 15 min at 4°C. The supernatant was sterile filtered through a 0.2 µm filtering system and stored at 4°C for up to 4 weeks. The activity of conditioned medium was determined by performing Luciferase TopFlash assay.

2.5 Protein analysis

2.5.1 Extraction of whole-protein lysates from cells

For Western blot analysis whole cell lysates were prepared. Cells ($1x10^6$) were lysed in 100 µl 1x Laemmli (63mM Tris-HCl pH 6.8 2.1 ml, 10% v/v glycerol, 2% w/v SDS) supplemented with 1x Protease/Phosphatase Inhibitor Cocktail (Cell Signalling Technologies). Subsequently lysates were heated at 95°C for 5min, sonicated and centrifuged for 10min at 16000 x *g* at 4°C in MicroCL 17 Microcentrifuge (ThermoFisher Scientific).

2.5.2 Extraction of whole-protein lysates from organoids

Organoids were collected into Eppendorf tubes in ice-cold PBS-0 containing 1x protease/phosphatase inhibitor cocktail (Cell Signalling Technologies) and centrifuged at max speed for 20 seconds at 4°C. The supernatant and separated Matrigel™ were removed and organoids were washed in 1ml of PBS-0/ protease/phosphatase inhibitor cocktail. The pellet was lysed in 1x Laemmli (63mM Tris-HCl pH 6.8 2.1 ml, 10% v/v glycerol, 2% w/v SDS) supplemented with 1x protease/phosphatase inhibitor Cocktail. Subsequently lysates were heated at 95°C for 5min, sonicated and centrifuged for 10min at 16000 x *g* at 4°C.

2.5.3 SDS-PAGE and Western Blot analysis

Equal amounts of whole cell lysates (~40 µg of total protein) were resolved in SDS-PAGE (sodium dodecyl sulphate-polyacrylamide gel electrophoresis) gels. For signalling experiments samples were reduced by adding 5% v/v β-mercaptoethanol (SigmaAldrich). Samples were loaded on 10% SDS-PAGE and resolved at 13 mAmp using Bio-Rad electrophoretic equipment and 1x SDS/Tris/Glycine running buffer (GeneFlow). The resolved proteins were then transferred onto nitrocellulose membrane at 40V at 4°C overnight using 1x Tris/Glycine transfer buffer (Geneflow). The membrane was briefly washed in TBST and blocked using 5% w/v skimmed milk powder in TBST by incubation for 1 hour at room temperature. Subsequently, membranes were probed with appropriate primary antibodies (Table 2-2) overnight at 4°C diluted in 3% w/v BSA-TBST-3mM NaN_2. After washing with TBST (3x 5 min), membranes were incubated with secondary antibody conjugated with fluorescent dye (i.e. goat anti-mouse Ab IRDye 680LT, or goat anti-rabbit Ab IRDye 800CW (LI-COR)) for 1 hour at room temperature. Then, membranes were washed with TBST

2x 5min and dH_2O 1x 5 min proteins were visualized and the signal was quantified using Odyssey®CLx Infrared Imaging System (LI-COR). The protein expression was normalised to expression of housekeeping proteins (β-actin, β-tubulin, or GAPDH).

Table 2-2. Primary antibodies used in the project

Primary antibodies	Host	Source	Dilution
Tspan6	Rabbit	Thermo Scientific (cat #AP9224)	1:500
p-EGFR-Y1045	Rabbit	Cell Signalling Technologies (Cat# 2237S)	1:500
p-EGFR-Y1068	Rabbit	Cell Signalling Technologies (Cat# 2234)	1:700
EGFR	Mouse	Thermo Scientific (Cat# MS-665-P0)	1:700
p-β-catenin T41/S45	Rabbit	Cell Signalling Technologies (Cat# 9565)	1:500
p-β-catenin S552	Rabbit	Cell Signalling Technologies (Cat# 5651)	1:1000
β-catenin	Mouse	BD Laboratories (Cat# 610153)	1:2000
p-ERK T202/Y204	Rabbit	Cell Signalling Technologies (Cat# 9101)	1:1000
ERK1/2	Rabbit	Cell Signalling Technologies (Cat# 9102)	1:1000
p-Src family Y527	Rabbit	Cell Signalling Technologies (Cat# 2105)	1:1000
Src	Rabbit	Cell Signalling Technologies (Cat# 2108)	1:1000
p-p38 T180/Y182	Rabbit	Cell Signalling Technologies (Cat# 4511)	1:1000
p38 MAPK	Rabbit	Cell Signalling Technologies (Cat# 8690)	1:1000
p-cCbl (Tyr774)	Rabbit	Cell Signalling Technologies (Cat# 3555)	1:700
c-Cbl	Rabbit	Cell Signalling Technologies (Cat# 2747)	1:700
GAPDH	Mouse	Abcam (Cat #ab8245)	1:3000
β-actin	Mouse	Sigma-Aldrich (Cat# A5316)	1:40000
β-tubulin	Mouse	Sigma-Aldrich (Cat# A5317)	1:3000

2.5.4 Co-immunoprecipitation (co-IP) assay

For co-immunoprecipitation studies, $3x10^6$ cells were cultured in 10 cm tissue culture dish (Corning) until they reach 90% confluency. Subsequently, cells were washed with sterile PBS and proteins were solubilised in 500 µl of protein extraction solution (0.5% Brij98-0.5% Triton-X-100-PBS or 0.8% Brij98-0.2% Triton-X-100-PBS) for 4hr on tube rotator at 2 x *g* at 4°C. Insoluble material was pelleted by centrifugation at 16000 x *g* at 4°C and supernatants were incubated with 20 µl of

ANTI-FLAG M2 agarose beads (Sigma-Aldrich) for 4hr on tube rotator at 2 x *g* at 4°C. Then, beads were washed 3x with ice-cold lysis buffer and precipitated proteins were eluted by 30 µl of 2x concentrated Laemmli buffer after incubation at 60°C for 10'. For normalized co-IP blots, proteins were extracted from equal number of cells for each cell line.

2.6 Cellular activity assays

2.6.1 Luciferase TopFlash assay

The experiment was set in a 96-well format using HEK293T cells. Each tested condition was tested in triplicate which served as the technical repeat. Cells were transfected using polyethyleimine (PEI) (Sigma-Aldrich). For each transfected well, a total of 15ng of plasmid DNA was used (Luciferase TopFlash (or FopFlash):Renilla at ration 9:1) and diluted in 7.5µl of DMEM without serum and antibiotics. Separately, 0.75 µg of PEI was diluted in 7.5 µl of FCS. Subsequently, plasmid DNA and PEI solutions were mixed together and incubated for 20 min at room temperature. Meanwhile, cell suspension was prepared in DMEM/10%FCS. For a 96-well plate, $2.5x10^4$ cells/well was required for transfection. Then, cells and plasmid DNA/PEI were mixed together seeded onto the plate. After 24 hours of incubation at 37°C in the CO_2 incubator, medium was replaced with Wnt3a CM/complete growth medium (DMEM/10% FCS) (50:50), or Wnt3a CM/R-Spondin-1 CM/complete growth medium (50:10:40). After 24 hours of treatment, cells were washed twice with PBS and lysed using Passive Lysis Buffer (Promega) for 15min at room temperature on a rocking platform. 20 µl/sample was transferred to a new 96-well opaque plate with clear flat bottom. Firefly (*Photinus pyralis*) and Renilla (*Renilla reniformis*) luminescence signals were measured sequentially from the same sample, using the Dual-Glo

luciferase assay system (Promega). Briefly, the luminescence signal of the firefly luciferase expressed from TopFlash or FopFlash plasmid was quantitatively measured first by the addition of Luciferase Assay Reagent II (LARII). After, the firefly signal was quenched by addition of Stop & Glo® reagent to the same sample, and Renilla luciferase signal was measured and quantified. Luminescence signal was measured using PHERAstar FS microplate reader (BMG Labtech). Firefly luminescence signal values were normalized according to their corresponding Renilla signal values. TOP-flash signal was standardized to the background signal (FOPflash).

2.6.2 Proliferation assay

To evaluate proliferation of Caco-2 in monolayer an Alamar Blue assay was carried out. Caco-2 cells were plated in 96-well plate at concentrations 5000 cells/well, 10000 cells/well, 20000 cells/well and 40000 cells/well. Following 72 hours of incubation in CO_2-incubator 10µl of Alamar Blue (Thermo Scientific) was added to each well and incubated for 4 hours at 37°C. The fluorescence was read using Fluoroskan Ascent™ Microplate Fluorometer. Zero time point was measure after 3 hours of incubation at 37°C in CO_2-incubator to allow cells to attached to the plate prior to addition of Alamar blue to the cells.

2.6.3 Proliferation of Caco-2 in 3D ECM

Caco-2 3D colonies were grown on 100% growth factor reduced BD Matrigel™ (BD Bioscience) supplemented with 2% (v/v) Matrigel™ in complete growth medium or in DMEM supplemented with 10% FCS in 96-well clear bottom black opaque plates (Corning). Each experimental well was coated with 15µl of 100% Matrigel™ and incubated for 15 min in cell incubator at 37°C. Subsequently, $8x10^3$

cells were resuspended in 2% (v/v) Matrigel™/growth media and dispensed into the wells. Cells were incubated at 37°C for 72 hours in humidified incubator in 5% CO_2 atmosphere and cell growth was assayed using CellTiter-Glo (Promega) according to manufacturer's recommendations. The growth rate was expressed as ratio of fluorescence signal on day 3 to fluorescence signal on day of plating.

2.6.4 Growth Inhibition Assay

Inhibitory effects of cetuximab was measured using Alamar Blue assay. Caco-2 cells were plated in 96-well plate at a concentration 3,000 cells/100µl per well. After 24 hours cells were treated with cetuximab antibody (Merck Biopharma) at concentrations 0.1 µg/ml, 0.5 µg/ml, 1 µg/ml, 5 µg/ml, 10 µg/ml, 25µg/ml, and 50µg/ml in complete growth medium or DMEM supplemented with 3% FCS. Following 72 hours of incubation in CO_2-incubator 10µl of Alamar Blue was added to each well and incubated for 4 hours at 37°C. The fluorescence was read using Fluoroskan Ascent™ Microplate Fluorometer. A separate plate was set for each experiment with cell numbers varying from 5000 to 40000 cells/well to allow for accurate control of operating within the linear range of fluorescence/cell density relation in each experiment. Three independent experiments were carried out for each cell line and condition.

2.6.5 Organoid Growth Inhibition Assay

Inhibitory effects of Lapatinib were measured using CellTiter-Glo® 3D Cell Viability Assay (Promega) in a 96-well format. An opaque 96-well plate with clear flat bottom was pre-coated with 15 µl of 100% Matrigel and placed in the incubator. Mouse intestinal organoids from C57Bl/6J-WT and C57Bl/6J-Tspan6 KO mice were mechanically disrupted as described in section 2.2.2. Following the last wash with

PBS-0, a total number of crypts was estimated by counting. Crypts (~25/well) were resuspended in 4% Matrigel/Growth medium and 100 µl of suspension was plated per each well. The plate was incubated for 24 hours at 37°C in CO_2 incubator. After this time period, serial dilutions of an inhibitor (20nM, 50nM, 100nM, 200nM and 400nM) were prepared in complete growth media, and 100µl was added to the test plate. The final concentrations of Lapatinib were: 10nM, 25nM, 100nM, and 200nM. The organoids were cultured for 6 days and the cell viability was measured using CellTiter-Glo® 3D Cell Viability Assay according to the manufacturer's protocol. Briefly, an equal amount of CellTiter-Glo® reagent was added to each well and incubated for 1hr at room temperature. The luminescence was measured using PHERAstar FS microplate reader.

2.6.6 Organoid co-culture assay

For co-culturing C57Bl/6J wild-type or Tspan6 KO organoids, cells were plated together in the same well in two Matrigel™ domes in a 6-well plate and cultured for 7 days in mouse intestinal organoid media without EGF. Two controls were used in this experiment when each type of organoid was plated with Matrigel™ dome (empty) in mouse intestinal organoid media containing 50 ng/ml of EGF (Figure 2-3.A) or in mouse intestinal media without EGF (Figure 2-3.B).

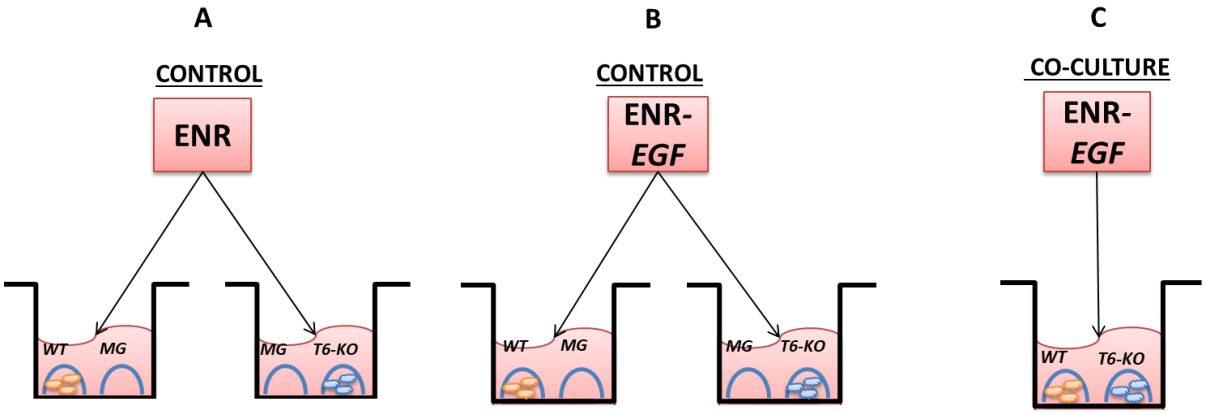

Figure 2-3. Experimental design for organoid co-culture. (A) Viability control of organoid: C57Bl/6J WT or Tspan6 KO organoids were cultured in mouse intestinal organoid media. **(B)** Experimental control of organoids: C57Bl/6J WT or Tspan6 KO organoids were cultured in mouse intestinal organoid media without EGF ligand. **(C)** C57Bl/6J WT and Tspan6 KO organoids were cultured in the same experimental well in mouse intestinal organoid media free of EGF.

2.6.7 EGFR stimulation assay

To evaluate the role of Tspan6 in EGFR-mediated signalling, $3x10^5$ cells were plated into 35mm tissue culture dish in complete growth medium overnight. Subsequently the cells were serum starved for further 24 hours followed by EGF stimulation at 10 ng/ml for fixed periods of time. Cells were subsequently lysed as described in section 2.5.1 and signalling events were assayed using Western blot.

2.6.8 Extracellular vesicle depletion assay

C57Bl/6J Tspan6 KO organoids were cultured in mouse intestinal organoid media without EGF. After three days, conditioned media was collected and divided into two fractions. Extracellular vesicles (EVs) were depleted from one fraction by multi-step centrifugation (Figure 2-4). First, conditioned media was centrifuged at 2000 x *g* for 10 minutes at 4°C, followed by ultracentrifugation at 10000 x *g* for 45 minutes at 4°C, and 70000 x g for 2 hours at 4°C to pellet EVs. The supernatant and

fraction II of conditioned medium were supplemented with 20% (v/v) R-Spondin-1 conditioned medium, 100 ng/ml Noggin (Peprotech), 1x B27 (ThermoFisher Scientific), 1x N2 (ThermoFisher Scientific), 1.25 mM N-Acetyl Cysteine (Sigma-Aldrich), 10 mM Nicotinamide (Sigma-Aldrich) and used to culture C57Bl/6J wild-type or Tspan6 KO organoids. Fresh conditioned media and EVs depleted conditioned medium were prepared for media change each three days of culture. The organoids were cultured in EVs depleted medium for 7 days.

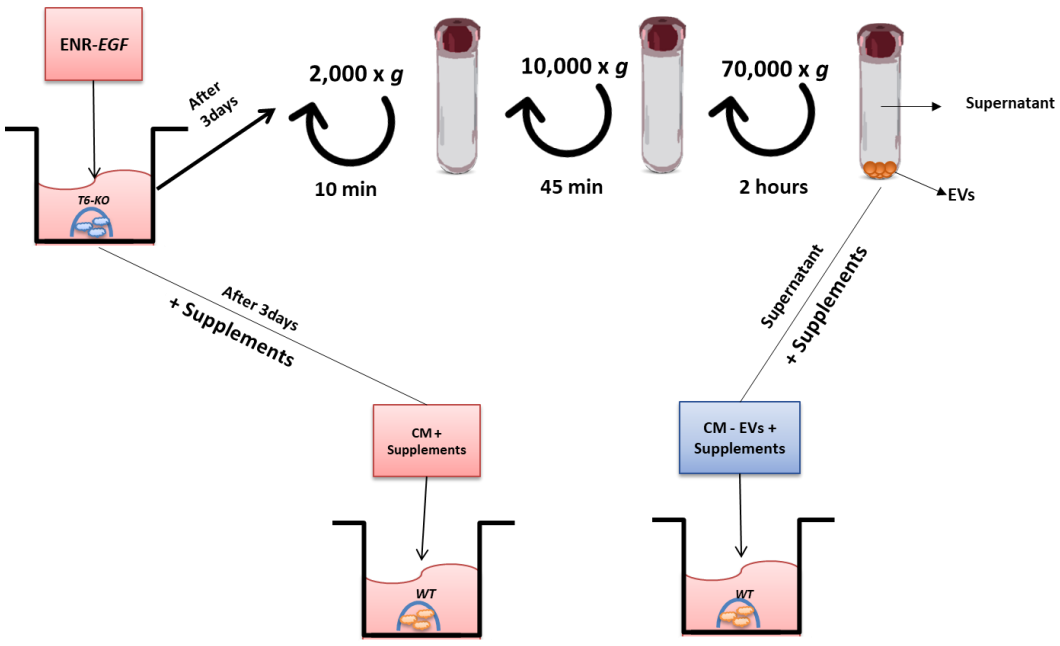

Figure 2-4. Extracellular vesicle depletion by differential centrifugation for functional analysis on organoids. Media conditioned by C57Bl/6J Tspan6 KO organoids in EGF-free conditions was collected after three days of growth. Media was depleted of extracellular vesicles by differential centrifugation in three steps followed by supplementing with essential organoid media components and used to culture C57Bl/6J WT organoids. Non-processed conditioned media was also supplemented with essential organoid media components and used to culture C57Bl/6J WT organoids as control.

2.6.9 Anti-mouse TGF-α ELISA assay

To detect mouse TGF-α in media conditioned by C57Bl/6J wild-type or Tspan6 KO organoids, a sandwich-type ELISA was employed. Organoids were cultured for 3 days in mouse intestinal organoid medium with 16.7 ng/ml of EGF or in the absence of EGF. The conditioned medium was collected and centrifuged at 1000 x *g* for 10 minutes and analysed according to manufacturers' instructions. Briefly, samples and standards were dispensed into ELISA plate wells pre-coated with mouse TGF- α antibody (MyBioSource). Following this, biotinylated detection antibody specific to mouse TGF-α and Avidin-Horseradish-Peroxidase (HRP) conjugates were added consecutively, followed by incubation with substrate solution. The enzyme-substrate reaction was terminated using stop solution and the optical density (OD) was measured spectrophotometrically at a wavelength of 450 nm using PHERAstar plate reader. The concentration of TGF-α was calculated using standard curve. Samples were run in duplicates.

2.6.10 Extracellular vesicle quantification

To identify extracellular vesicles secreted by C57Bl/6J $APC^{min/+}$ and $APC^{min/+}Tspan6^{-/y}$ organoids were cultured for 6 days in mouse intestinal organoids media Intesticult (STEMCell Technologies), in mouse intestinal organoid media without EGF ligands. The conditioned media was collected and filtered using 0.45 µm sterile filters and analysed using Nanosight LM10 v3.3.104 (Malvern Technologies). The experiment principle is depicted in Figure 2-5. Nanoparticle Tracking Analysis (NTA) allows rapid analysis of concentration and size of particles ranging from 10 nm to 1000 nm.

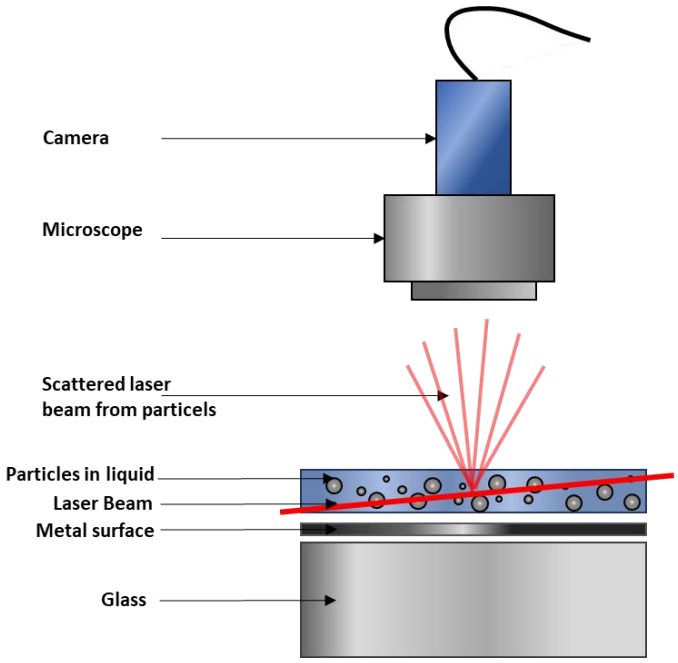

Figure 2-5. Principle of nanoparticle tracking analysis (NTA). Particles or extracellular vesicles in suspension are dispersed into microscope cell. A laser beam is passed through the sample and light scattered from particles can be visualised and recorded in high resolution by camera mounted onto the lens. Vesicles moving under Brownian motion are recorded and video is analysed by NTA software. The software allows tracking of individual particles and calculates their hydrodynamic diameters using the Stokes Einstein equation. The output is presented as histogram representing particle size and concentration distribution.

2.7 Animal studies

2.7.1 Study approval

All animals were treated in accordance with local ethical committee guidelines and the UK Animals (Scientific Procedures) Act 1986, and all procedures were carried out in accordance with Home Office guidelines (United Kingdom) under the project number: 70/8494. All mice were housed with their littermates and maintained on a 12-hour light/dark cycle, with access to food and water *ad libitum.*

2.7.2 Genotyping of Tspan6 KO mice

A constitutive global Tspan6 KO mouse model was generated on C57Bl/6

background by the Deltagen, Inc pharmaceutical company (NY) by the insertion of a Neomycin cassette in exon 2 of the Tspan6 gene. To validate the KO model the DNA purified from ear samples of the 21 days old mice was genotyped in house using KAPA Mouse Genotyping Kit (KAPABiosystems) according to manufacturer's protocol. Briefly, DNA was extracted using KAPA Express Extract enzyme for 10 min at 75°C, and enzymatic activity was terminated at 95°C for 5min. The extracted samples were then amplified by PCR using KAPA2G Fast Genotyping Mix and gene specific primers against exon 2 (forward and reverse) and additional forward primer against the Neomycin cassette (Figure 2-6.A). To detect both wild-type and mutated alleles the multiplex reaction using three primers was performed (Supplementary Table 8-1). PCR conditions for Tspan6 were 7 min at 95°C (initial denaturation) followed by 35 cycles of 10 seconds at 96°C (denaturation), 30 seconds at 60°C (annealing) and 1.5 min at 68°C (elongation). The resulted PCR products were resolved on 1.4% (w/v) agarose gel (Invivogen). The expected PCR product size was 260bp for wild-type and 405bp for Tspan6 KO (targeted) allele (Figure 2-6.B).

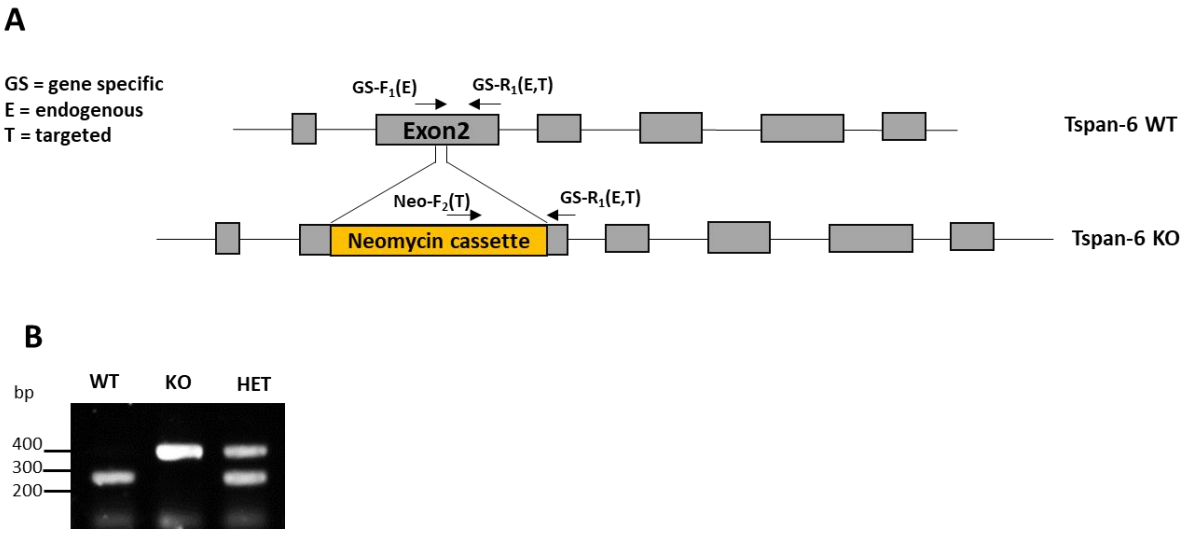

Figure 2-6. The schematic presentation of Tspan-6 KO mouse model generation. (A) The Tspan-6 KO mouse was generated by insertion of Neomycin cassette into exon 2 of Tspan-6 gene. Arrows indicate the set of three primers was used to identify the genotype of mice. Two gene specific (GS) and one neomycin cassette (Neo) primers were used to ensure the correct neomycin cassette insertion and amplify endogenous (E) and targeted (T) alleles. **(B)** A representative agarose gel electrophoresis with the PCR products amplified with specific primers GS-F1, GS-R1, Neo-R2. The PCR product of 260bp corresponds to wild-type (WT) and 405bp corresponds to Tspan-6 knockout (KO) allele; a double band represents a heterozygous (HET) allele.

2.7.3 Mouse models for colorectal carcinogenesis

For *in vivo* tumorigenesis studies an $APC^{min/+}$ C57BL/6 mouse line (Jackson Laboratory) was utilised. To create $APC^{min/+}Tspan6^{-/-}$ animals, Tspan6 $^{-/+}$ female mice were crossed with $APC^{min/+}$ male mice. Genotyping for Tspan6 mutation was carried out as described in Genotyping of Tspan6 KO mice and genotyping of mice for APC mutation was carried out by TransnetYX Inc. All mice were weighed twice a week post weaning and examined for symptoms of disease development, which included weight loss (up to 20%), hunched posture, pale feet, blood in stool, limping. Mice showing these features were culled by cervical dislocation and organs were harvested. The intestine and colon were flushed with ice-cold PBS, opened

longitudinally and fixed in methacarn (6:3:1 methanol absolute : chloroform : acetic acid glacial) for 4 hours at room temperature. The tissue was subsequently rolled and fixed in 10% neutral buffered formalin solution (Sigma-Aldrich) overnight. The rolled intestines were embedded into paraffin blocks in Royal Orthopaedic Hospital NHS Foundation.

2.7.4 Polyp imaging and scoring

To examine polyp burden of C57Bl/6J $APC^{min/+}$ and $APC^{min/+}Tspan6^{-/y}$ mice, intestines were imaged using Brunel BMSF stereomicroscope (Brunel Microscopes Ltd) equipped with 5mpx camera after fixation in methacarn. Polyp counts and size were assessed using ImageJ software. Polyp size was presented as area (mm^2).

2.7.5 Pathological examination

Pathological examination of histological sections (both mouse and human) was performed with the aid of Dr Maha Ibrahim and Dr Rahul Hejmadi. Haematoxylin-eosin stained slides of mouse intestines were assessed for intestinal adenomas. The exclusion criteria were applied during examination.

Table 2-3. Criteria for histopathological examination of mouse intestinal tissue.

Inclusion Criteria	Exclusion Criteria
Intact muscularis mucosae	Epithelium misfolding (due to processing)
Viable mucosa	Degenerated/autolysed
GIT viscera present	Reactive lymphoid follicle underlying the epithelium Tangential sectioning
	Fixation artefact
	Discontinuity of the mucosa of either side of the polyp Fragmented

2.7.6 RNA sequencing

RNA samples were extracted from intestinal polyps of C57Bl/6J $APC^{min/+}$ (n=3) and $APC^{min/+}Tspan6^{-/y}$ (n=5) mice using RNeasy RNA extraction kit (Quiagen). RNA concentrations were determined using Qubit fluorometer (ThermoFisher). The quality of RNAs were checked using Agilent 2200 TapeStation (Agilent Technologies) and RNA 5-100ng RNA in total for each sample with RNA Integrity Number (RIN) of >7.0 was used for library preparation (Supplementary Table 8-3). Poly-adenylated RNA libraries were prepared using the automated Neoprep Library System (Illumina) according to manufacturer's protocol. The libraries were sequenced on an Illumina NextSeq 500/550 (Illumina) using a High out-put flow cell 150 cycle (cat. No. FC-404-2002) using a paired end 75 cycle program. The aim was to achieve approximately 25 million reads per library. The RNAseq reads were aligned to the mouse genome (Mus musculus mm10 Refseq) using the STAR Aligner v.2.5. Library preparation and sequencing was done by Celina Whalley (University of Birmingham). The RNA sequencing data was analysed by Dr Andrew Beggs (University of Birmingham).

2.8 Staining and imaging methods

2.8.1 Human Samples

Human FFPE tissue samples were obtained from Human Biomaterials Resource Centre (HBRC), University of Birmingham under local ethics committee approval (Ref no.16-250). Samples from SCORT and COIN colorectal cancer clinical trials were utilised in this study.

2.8.2 Tissue sectioning

For histopathological analysis and immunohistochemical assay tissue was sectioned to 4µm thickness and mounted on positively charged adhesive-coated

slides (Surgipath™). Slides were kept at 4°C for long term storage.

2.8.3 Immunohistochemistry

To visualise antigens of interest ImmPRESS™ peroxidase detection system (Vector® labs) was used according to manufacturers' recommendations. Briefly, tissue slides were deparaffinised with Xylene (Fisher) and rehydrated with graded ethanol (100%, 95% and 75%); each incubation being 5 minutes in duration. Endogenous peroxidase activity was blocked by incubation of slides in 0.3% hydrogen peroxide solution for 15 minutes. Antigen retrieval in 0.01M citrate buffer (pH 6.0) was performed for detection of Tspan6, p-ERK, Ki67 and β-Catenin in microwave at high power for 20 minutes. For detection of p-EGFR heat mediated EDTA (pH 9.0) antigen retrieval at 65°C overnight (12-16 hours) was used. The sections were blocked with 1x Casein Solution (Vector Labs) for 10min at room temperature following overnight incubation with primary antibody at 4°C. ImmPRESS™ HRP Universal Antibody Polymer Detection Kit (Vector® labs) was then applied for 30 min at room temperature, followed by treatment with substrate/chromogen solution ImmPACT™ Dab (Vector Labs) for 2 min at room temperature. Slides were counterstained with haematoxylin, dehydraded in graded alcohol and mounted with coverslips using DPX resin (Sigma Aldrich). Washes with 1x TBST were performed between each step, three times for 5 minutes.

2.8.4 Tspan6 antibody optimisation

Prior to carrying out immunohistochemical analysis of human tissue samples, Tspan6 antibody (Atlas Antibodies) was validated for specificity and optimised for optimum dilution. Formalin fixed paraffin embedded (FFPE) xenografts of human breast cancer cells MDA-MB-468 pLVx and MDA-MB-468 Tspan6 were stained with

Tspan6 antibody using citrate buffer (pH 6.0) antigen retrieval at concentrations of 1:50, 1:100 and 1:200. A strong membranous staining was detected at concentration 1:100 in cells exogenously expressing Tspan6 (MDA-MB-468 Tspan6), whereas weak staining was detected in cells expressing endogenous Tspan6.

2.9 Immunofluorescence

Mouse intestinal organoids and Caco-2 cells were cultured in 2% Matrigel™ on pre-coated with 100% Matrigel 8-well Nunc® Lab-Tek® Chamber Slide™ system for 5 days. Cells were fixed with 4% paraformaldehyde/3% sucrose/PBS (PFA) supplemented with 1mM $CaCl_2$ and 0.5 mM $MgCl_2$ for 30 min at room temperature and permeabilized with 0.1% (v/v) Triton X-100 for 2 minutes. Organoids were incubated with blocking buffer (10% heat inactivated goat serum/PBS) for 1 hour at room temperature. Subsequently, cells were incubated with primary antibodies overnight at 4°C. On the following day, organoids were incubated with fluorophore-conjugated secondary antibodies and/or Phalloidin Alexa Fluor 568 (Molecular Probes) (diluted 1:40 in 1%BSA/PBS) for 1 hour at room temperature. Cells were then counterstained with Hoechst33342 (1µg/ml in PBS) for 5 min at room temperature. Washes between each step were performed with 1%BSA/PBS (3x 10 min). The images were captured using Zeiss LSM780 confocal system with 40X oil immersion objective.

2.10 Scoring

Scoring of Tspan6 immunohistochemical staining on human colorectal adenocarcinomas and adjacent normal tissues was carried out by histopathologists Dr Maha Ibrahim and Dr Rahul Hejmadi independently and in a blinded fashion. To

evaluate the expression of Tspan6 in human tissues the intensity and percentage (0%-100%) of cells with membranous staining was recorded: 1 - weak or trace; 2 - moderate; 3 – intense. The final H-score was determined by adding the results of multiplication of the percentage of cells with staining intensity ordinal value. In event of any disagreement on scoring an opinion of a third histopathologist was requested.

2.11 Statistical analyses

Statistical analysis of data from all studies was performed using Graph Pad Prism v7.04 (Graphpad Software Inc.) and presented as the mean with standard error mean (SEM) or standard deviation and indicated in figure legends. For box-and-whisker plots, data presented as the median with highest and lowest values. To analyse normally distributed data from two unpaired groups a Student t-test was utilised, for analysis of unpaired non-parametric data a Mann-Whitney U test was used. To compare multiple unmatched groups one-way ANOVA test was used. P value $p< 0.05$ was considered statistically significant. Asterisks indicate levels of significance (* – $p < 0.05$; ** – $p < 0.01$; *** – $p < 0.001$).

3 RESULTS CHAPTER I: EXPRESSION OF TSPAN6 IS DECREASED IN COLORECTAL CANCER

3.1 Introduction

It has been suggested that Tspan6 is a potential diagnostic and prognostic marker for CRC (Sum-Fu, Ming-Hung, Reiping, *et al.* 2014). The expression of Tspan6 in this study was investigated on a small sample size of Taiwanese population (n=30), and no data of Tspan6 protein expression is available for European populations. Recent data indicated that Tspan6 expression correlates with better survival of CRC patients and is positively associated with response to neoadjuvant therapy in locally advanced rectal cancers (Uhlen, Zhang *et al.* 2017). The aim of this chapter was to extend these initial observations by examining the expression of Tspan6 in the cohort of genetically profiled CRC tumours and the adjacent normal tissue, and to evaluate if the expression of Tspan6 is associated with clinicopathological characteristics and mutational profile of CRC tumours. The TCGA data was also interrogated for the methylation status of the *Tspan6* gene.

3.2 The expression of Tspan6 in colorectal adenocarcinoma is greatly reduced compared to adjacent non-cancerous colon epithelium

To examine the expression of Tspan6 in tumours of patients diagnosed with CRC in the UK paired adenocarcinoma and adjacent non-cancerous colon specimens were analysed by IHC. A total of 46 samples were selected in random unbiased fashion from the SCORT clinical trial cohort under local ethics committee approval (Supplementary Table 8-4). Specificity of the antibodies was confirmed by

performing IHC on Tspan6-positive and Tspan6-negative breast cancer xenografts (Figure 3-1).

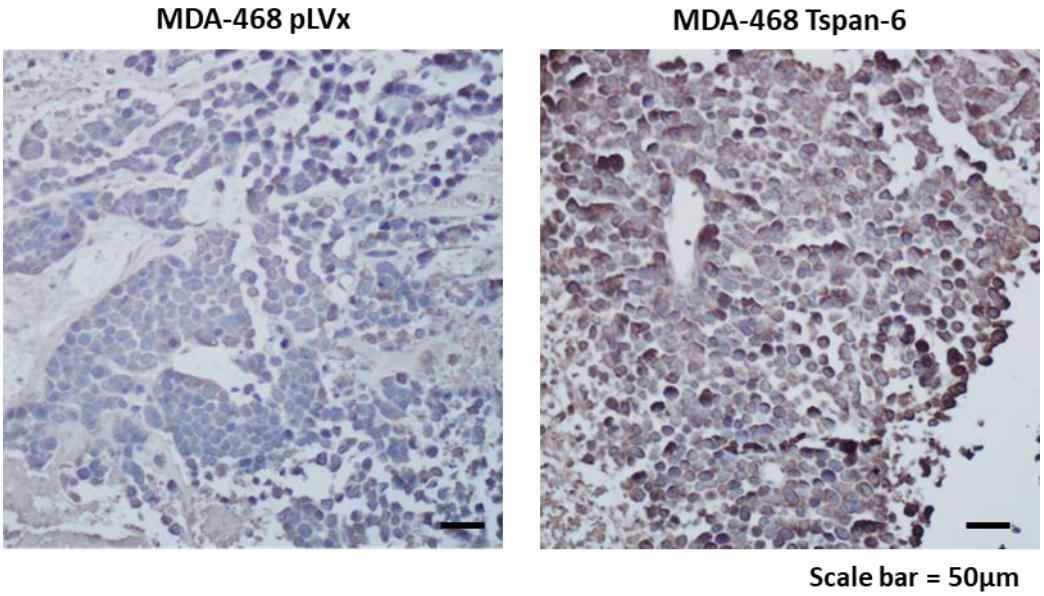

Figure 3-1. Anti-Tspan6 antibody used in immunohistochemical assay is specific to Tspan6 protein. Anti-Tspan6 antibody was tested on paraffin embedded sections of MDA-MB-468 human breast cancer cell line xenografts grown in mouse breast fat pads. Cells expressing endogenous levels of Tspan6 have weak to negative staining (MDA-MB-468 pLVx); cells with exogenously expressed Tspan6 (MDA-MB-468 Tspan6) show intense membranous staining.

In normal tissues Tspan6 was expressed in epithelial cells, and little if any expression was detected in the stromal component of the colonic tissue. A semi-quantitative approach was used to score each sample. In non-cancerous colonic epithelium Tspan6 was predominantly present at the plasma membrane. CRC tumours were highly heterogeneous for Tspan6 expression, and it was noted that intensity of Tspan6 staining at the deeper advancing areas of tumour was higher when compared to the centre of the tumour (data not shown). Furthermore, a significant proportion of tumour cells had decreased or lost the membranous staining of Tspan6, with many tumour cells displaying cytoplasmic distribution (Figure 3-2.A).

Detailed analysis demonstrated that Tspan6 expression was significantly reduced in colorectal adenocarcinomas with a median H-score in normal tissue of 180 vs H-score of 130 in tumours (p=0.0026) (Figure 3-2.B). Interestingly, interrogation of TCGA and methylation data using the MEXPRESS tool revealed negative correlation of Tspan6 expression with methylation (probe cg01473187, Xq22.1, chrX:99891163-99891163) of Tspan6 in colon adenocarcinomas (n=299, p<0.001, r=-0.437) (Figure 3-3). This methylation site is located in the intron 1 of *Tspan6* gene, in the DNase I hypersensitivity cluster, suggesting that this region is a regulatory region of Tspan6 gene transcription.

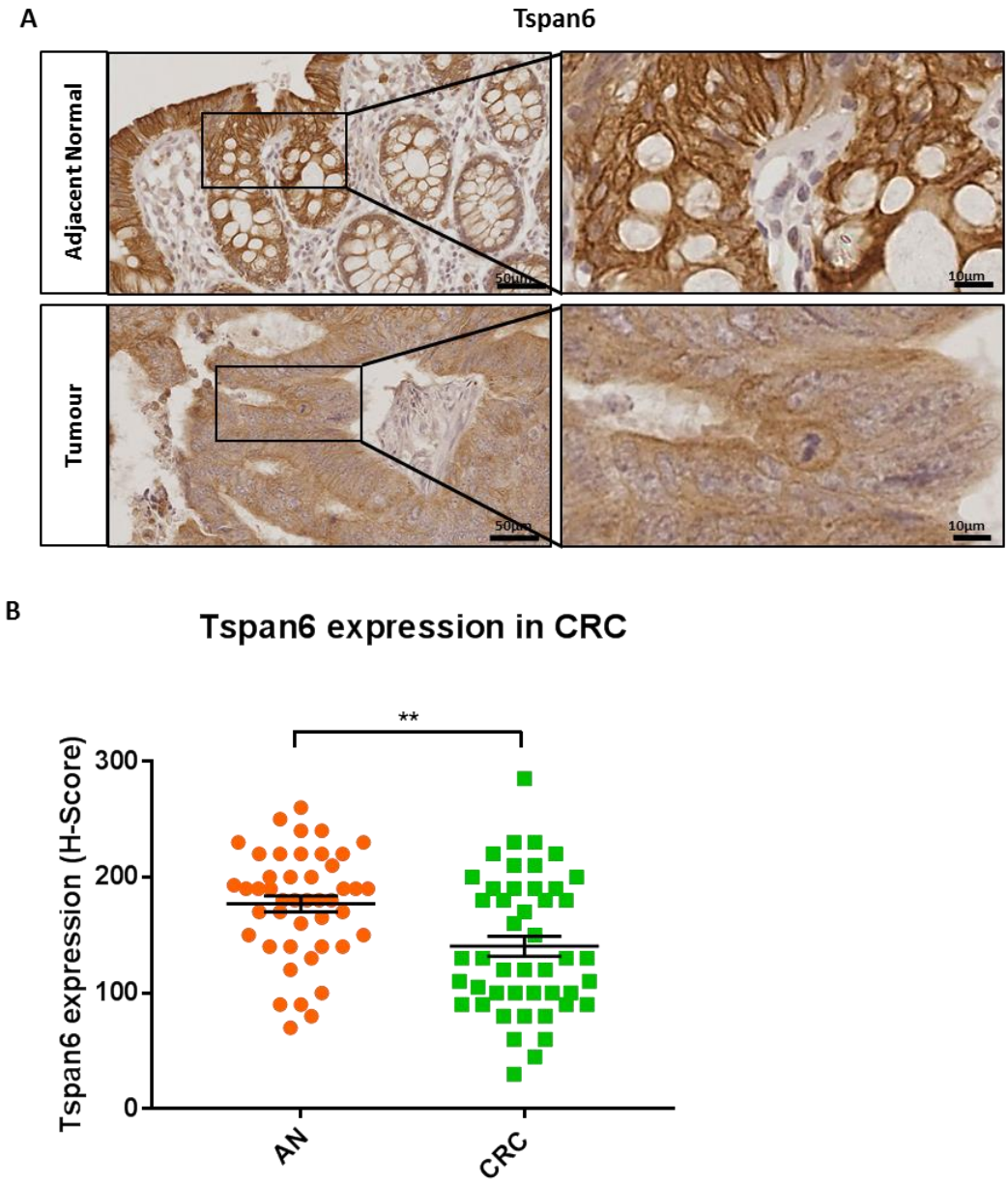

Figure 3-2. Expression of Tspan6 is decreased in colorectal adenocarcinomas. (A) Paraffin embedded sections of tumour and adjacent non-tumour tissue analysed for expression of Tspan6 show strong membranous expression of Tspan6 in normal colon epithelium and weak diffused cytoplasmic staining in tumour tissue. **(B)** Tspan6 expression is significantly decreased in colorectal adenocarcinomas (CRC) compared to adjacent normal (AN) tissues, error bars show mean ± SEM, n=46, **p=0.00258. Wilcoxon matched-pairs signed rank test was used for statistical analysis.

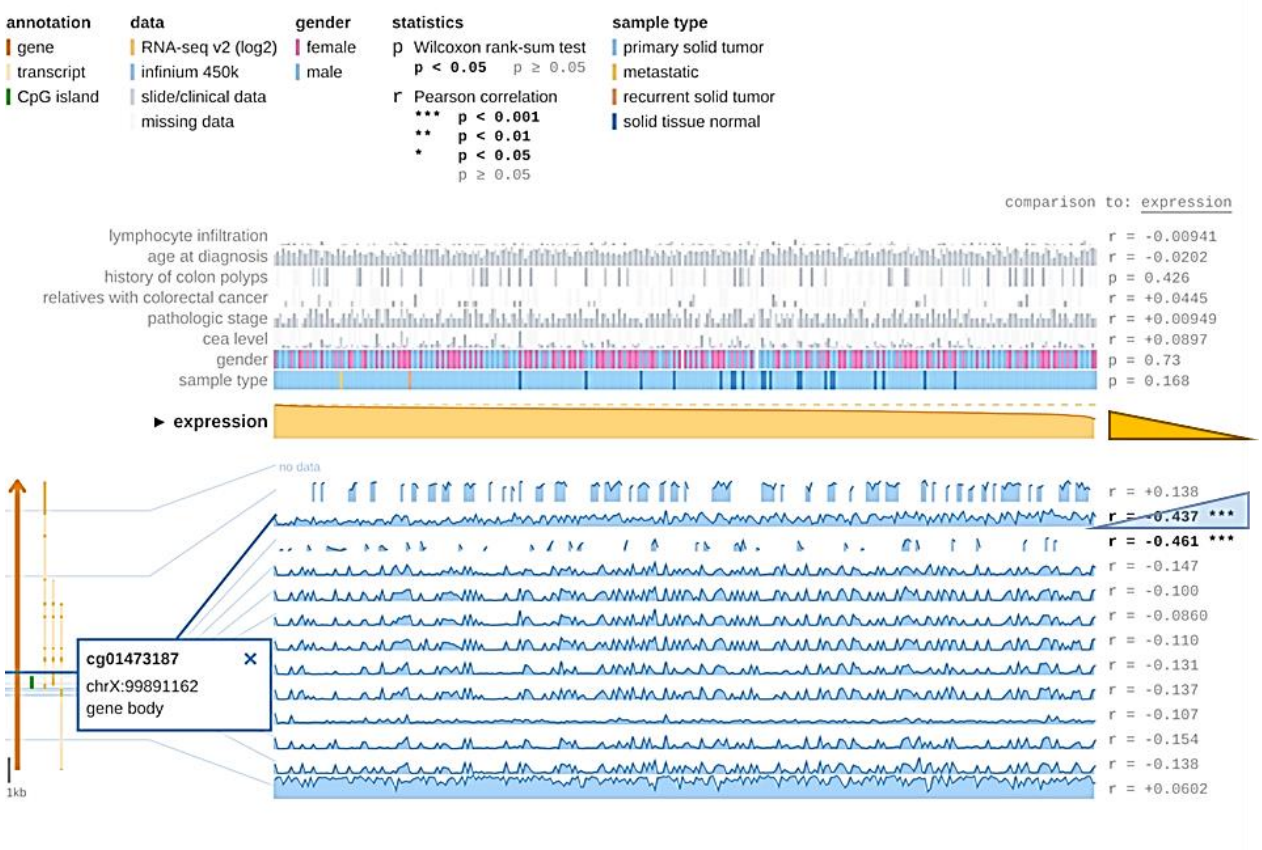

Figure 3-3. Expression of Tspan6 is regulated by DNA methylation. Visualisation of TCGA data for Tspan6 mRNA expression in colon adenocarcinomas using MEXPRESS. Tspan6 expression (yellow) is negatively correlated with increased methylation (cg01473187 probe, blue) in intron 1 at CpG island (green), n=299, p<0.001, Pearson correlation coefficient r=-0.437. Figure is reproduced from (Koch, De Meyer *et al.* 2015).

3.3 Tspan6 expression is not correlated with clinicopathological characteristics of CRC

Next, it was evaluated whether Tspan6 expression is correlated with clinicopathological characteristics of the CRC patients. Specifically, protein expression was analysed in CRC subclassified by various factors such as patient age, gender, tumour stage, extramural vascular invasion (EMVI) status, and tumour site. This analysis demonstrated that Tspan6 expression does not correlate with patient age (r^2=0.0052) (Figure 3-4). In this study, the cohort consisted of 24 males and 13 females (for the rest of the cohort the gender was not recorded). The median Tspan6 H-score in normal tissues was 190 and 175, and in tumours 125 and 120, in males and females respectively. The Tspan6 expression in tumours of the male patients was significantly decreased (p=0.0029), whereas the reduction of the expression in tumours of female patients was not statistically significant (p=0.1406) (Figure 3-5). Of note, there was no difference observed in normal tissue expression (p=0.3462) or tumour (p=0.7352) between the male and female population.

The expression of Tspan6 was compared between CRC tumours at different anatomical sites of the colon: caecum (n=10), sigmoid colon (n=12), rectum (n=7), transverse colon (n=3), ascending (n=4) and descending colon (n=3). It was found that expression of Tspan6 does not differ greatly in normal colon epithelium (p=0.7296) or in CRC tumours (p=0.3952) in different areas of the colon (Figure 3-6).

From the analysed tumours, 12 were positive for EMVI, which is correlated with the poorer prognosis of CRC patients. It was found that median expression of Tspan6 in EMVI+ tumours was non-significantly elevated compared to EMVI- tumours, with median Tspan6 H-score of 135 and 125 correspondingly (Figure 3-7).

In addition, the expression of Tspan6 was analysed in tumours of different stages. In this study, 3 tumours were stage II, 22 stage III and 14 stage IV. It was found that in tumours of stage II and stage III the expression of Tspan6 is decreased (p=0.25, n=3 and p=0.0011, n=22 respectively) (Figure 3-8). However, no difference in Tspan6 expression between normal tissue and tumour was observed for metastasised CRC of stage IV (p=0.7993, n=14), suggesting that Tspan6 expression is downregulated in earlier stages of CRC development and is not affected in advanced adenocarcinomas of stage IV.

In summary, Tspan6 expression does not correlate with age, and tumour site and is likely to play a role in early steps of tumour development as its expression is downregulated in stage II and stage III CRCs.

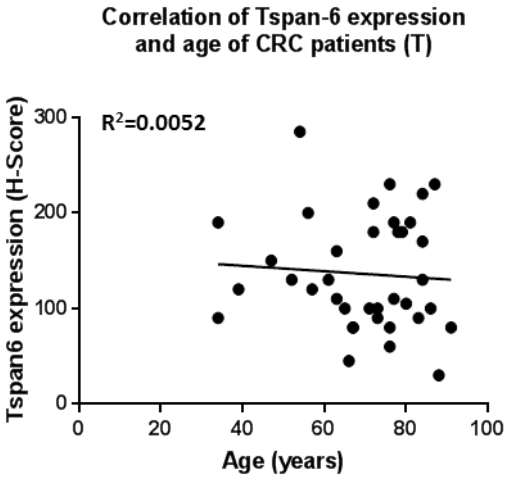

Figure 3-4. Expression of Tspan6 is not correlated with patient age, r^2 represents coefficient of determination (Pearson correlation, n=46, r2=0.0052).

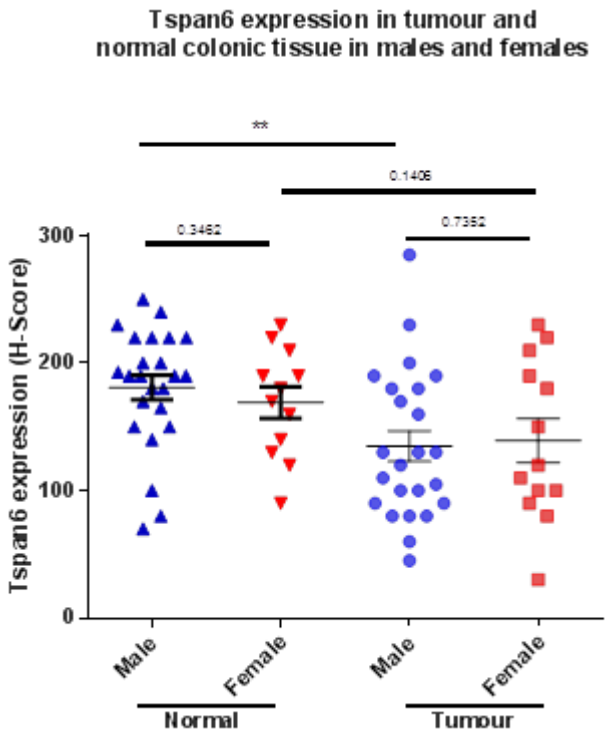

Figure 3-5. Expression of Tspan6 is not correlated with gender of CRC patients. The expression of Tspan6 in adjacent normal and tumour tissues of male (n=24, blue) and female (n=13, red) CRC patients. Tspan6 protein expression is decreased in tumours, **p=0.0029 (males) and p=0.1406 (females). No difference in Tspan6 expression between genders was found in normal (p=0.3462) or tumour (p=0.7352) tissues. Error bars represent mean ±SEM, paired Wilcoxon signed-rank test was used for statistical analysis of Tspan6 expression in normal vs. tumour tissues, and non-parametric Mann-Whitney U test was used for statistical analysis of Tspan6 expression in males and females.

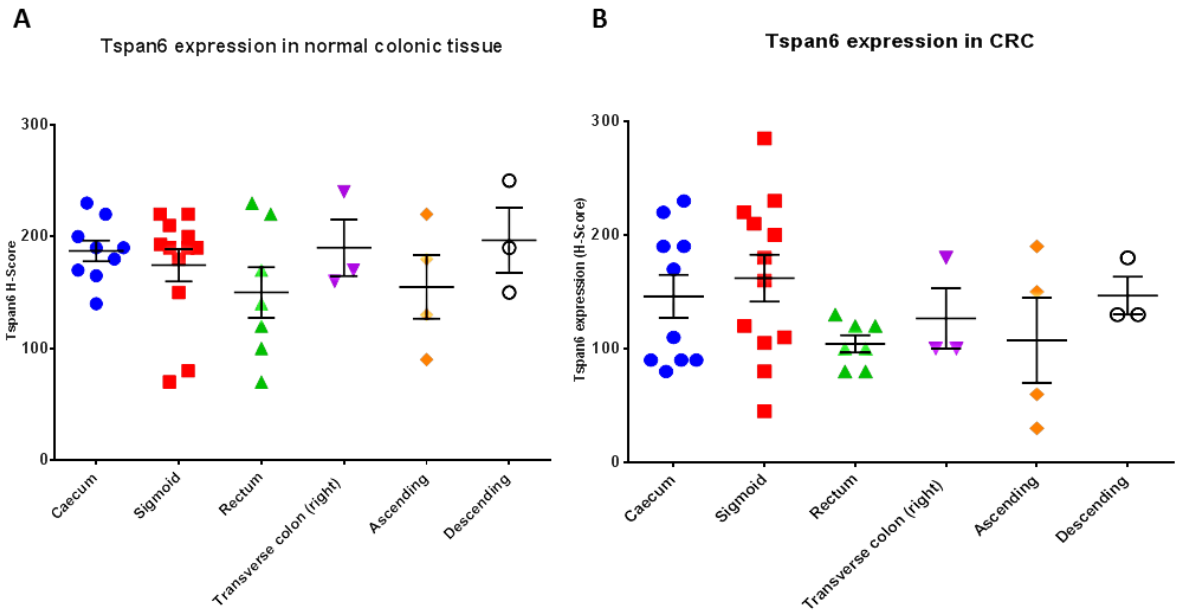

Figure 3-6. Expression of Tspan6 is not linked to tumour site in the colon. Tspan6 expression in adjacent normal colon epithelium **(A)** and colorectal CRC **(B)** at anatomically different sites of the colon. No significant difference in expression of Tspan6 in normal tissues (p=0.7296) or tumour (p=0.3952) was found, error bars represent mean ±SEM, a one-way ANOVA test was used for statistical analysis.

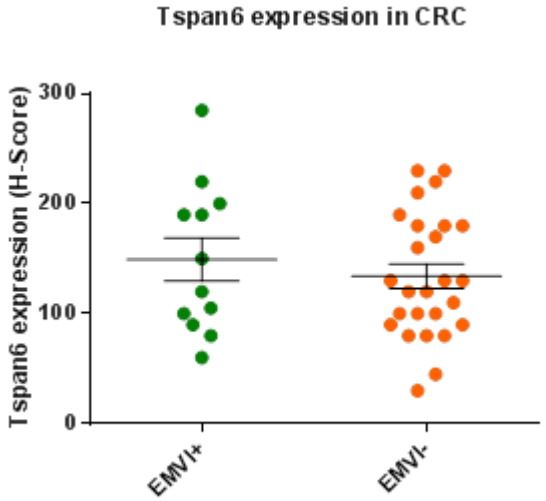

Figure 3-7. Expression of Tspan6 is not correlated with extramural vascular invasion (EMVI) status of CRC. Tspan6 expression in CRC with EMVI+ (green) and EMVI- (orange). No significant difference in protein expression of Tspan6 was found in CRC depending on EMVI status (p=0.6138). Error bars represent mean ±SEM, non-parametric Mann-Whitney U test was used for statistical analysis.

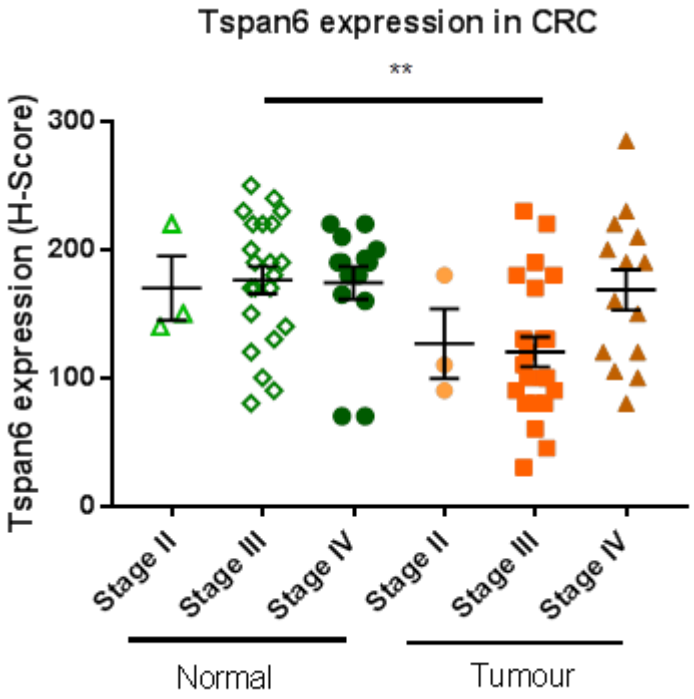

Figure 3-8. Tspan6 is downregulated in stage II and stage III, but not stage IV CRC. The expression of Tspan6 in adjacent normal (green) and tumour tissues (orange) in stage II (n=3), stage III (n=22) and stage IV (n=14) CRC. Tspan6 protein expression is decreased in stage II (p=0.25) and stage III (**p=0.0011) tumours, no significant difference in Tspan6 protein expression was found in stage IV CRC (p=0.7993). Error bars represent mean ±SEM, paired Wilcoxon signed-rank test was used for statistical analysis of Tspan6 expression in normal vs. tumour tissues.

3.4 Tspan6 expression does not correlate with tumour driving mutations

In this study tissues from 46 patients were analysed, of which 36 tumours have been fully sequenced by next generation sequencing (NGS). The expression of Tspan6 in these tumours was analysed in relation to mutations in *KRAS*, *BRAF*, *PIK3CA*, *TP53*, *APC* and *CTNNB1* genes. The data shows that Tspan6 expression does not correlate with mutations in any of these CRC tumour driver genes (Figure 3-9). In addition, copy number of *BRAF*, *PIK3CA*, *PTEN*, and *CTNNB1* genes were increased in some of the analysed tumours. It was found that Tspan6 expression

does not correlate with copy number variation of named genes in these tumours (Figure 3-10). Thus, it was concluded that common cancer driver genes do not regulate expression of Tspan6; however, the results are inconclusive due to the small sample size of cohort study.

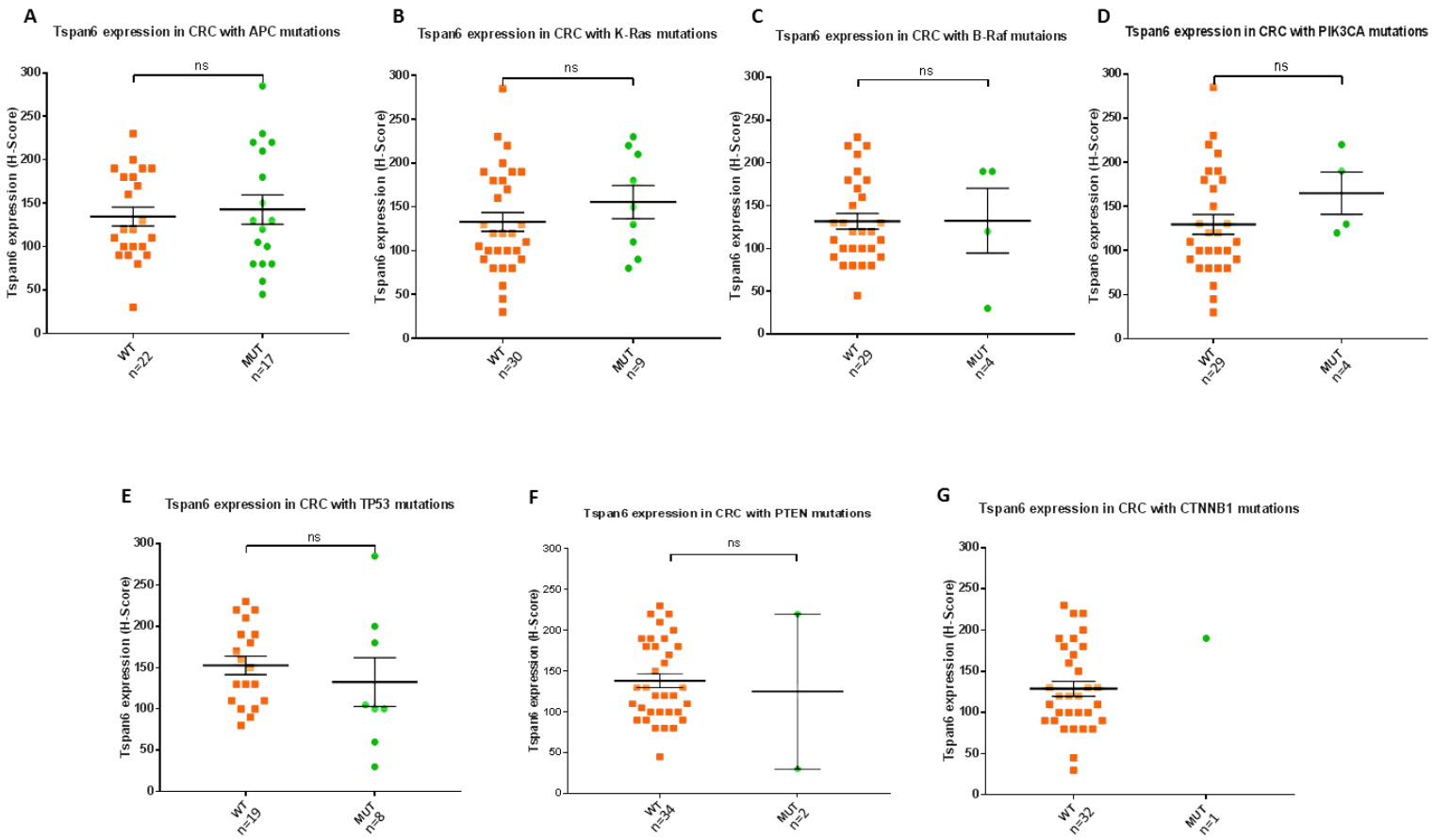

Figure 3-9. Expression of Tspan6 does not correlate with mutations in *APC, KRAS, BRAF, PIK3CA, TP53, PTEN* and *CTNNB1* genes. Tspan6 expression in CRC with wild-type (WT, orange) or mutated (mut, green) genes: *APC* **(A)**, *KRAS* **(B)**, *BRAF* **(C)**, *PIK3CA* **(D)**, *TP53* **(E)**, *PTEN* **(F)** and *CTNNB1* **(G)**. No correlation of Tspan6 expression and mutations in any of the listed genes were found. Error bars represent mean ±SEM, Mann-Whitney U test was used for statistical analysis.

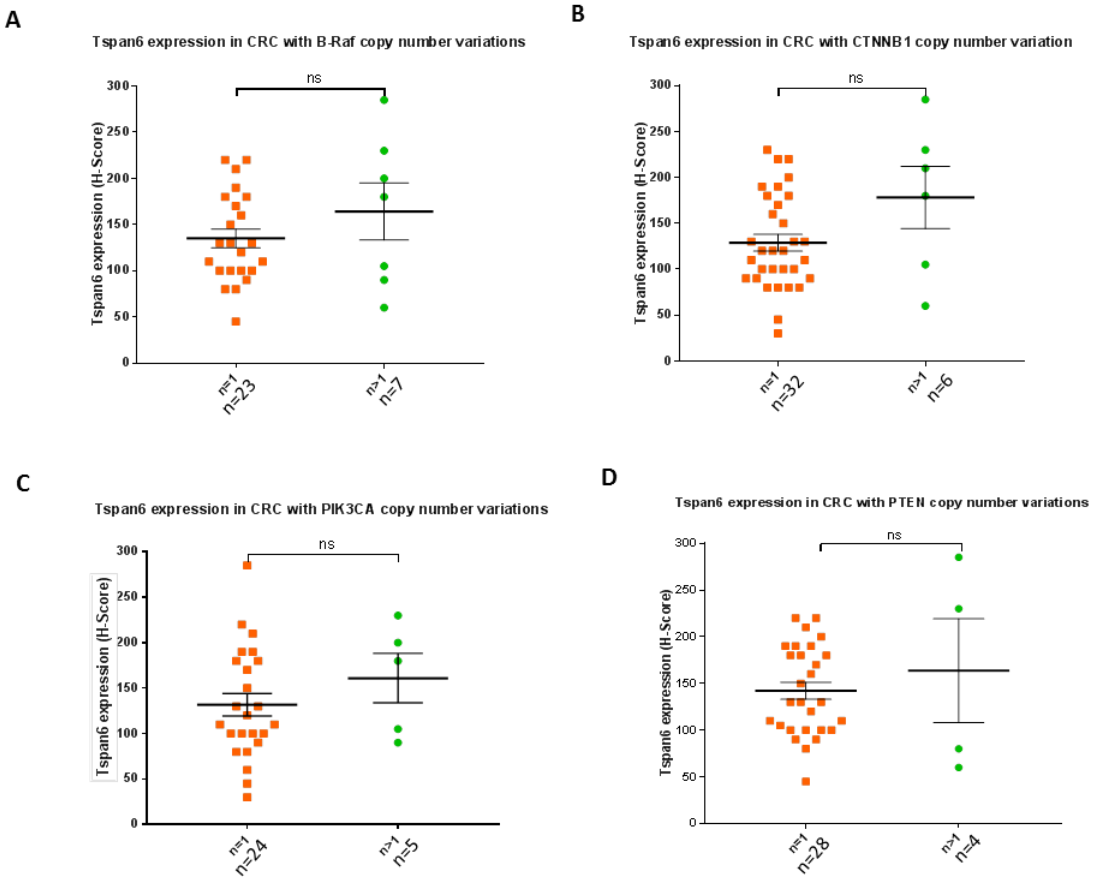

Figure 3-10. Expression of Tspan6 does not correlate with copy number variations of *BRAF, PIK3CA, PTEN* and *CTNNB1* genes. Tspan6 expression in CRC with 1 copy (n=1, orange) or copy number variation (n>1, green) of *BRAF* **(A)**, *CTNNB1* **(B)**, *PIK3CA* **(C)**, and *PTEN* **(D)**. No correlation of Tspan6 expression and mutations in any of the listed genes were found. Error bars represent mean ±SEM, Mann-Whitney U test was used for statistical analysis.

3.5 Discussion

In this chapter the expression of Tspan6 was analysed in the cohort of CRC patients. It was found that Tspan6 protein expression level is decreased in CRC tumours. This data is consistent with mRNA expression data, supporting the hypothesis that Tspan6 is differentially expressed in colorectal cancer (Hlubek, Brabletz *et al.* 2007, Uhlen, Zhang *et al.* 2017). However, this result is in contrast with an earlier report describing the upregulation of Tspan6 in CRC in the Taiwanese population (Sum-Fu, Ming-Hung, Reiping, *et al.* 2014). There are several factors which may account for the discrepancy between these studies. Firstly, there may be age and ethnicity-based differences between two patient cohorts. Secondly, the differences may arise from the variation in the use of immunological reagents: the antibody used for IHC of Tspan6 in Sum-Fu publications was not specified. Finally, relatively small sizes of both cohorts may also account for the observed differences.

Although it was found that Tspan6 protein expression level is decreased in stage II and stage III CRC, but not in stage IV carcinoma, there was no correlation between Tspan6 expression in tumours and clinicopathological parameters, such as age, anatomical site of tumour, or EMVI status. Interestingly, the differences in Tspan6 expression between the tumour and adjacent non-cancerous tissues were more prominent in males than in females. Given that *Tspan6* gene is localised on chromosome X, silencing of the gene during tumour initiation may reflect more dramatically on the male population due to only one copy of the gene. Hence the second copy of functional gene of *Tspan6* in females may partially compensate for the loss of one functional allele of the gene. One cannot exclude the possibility of genetic rearrangements due to chromosomal loss of heterozygosity (LOH) in tumours

resulting in downregulation of Tspan6 in CRC. It has been shown that LOH of X-linked genes is frequent in CRCs and associated with sporadic colon adenocarcinomas (Liu, Kain *et al.* 2012, Ali, Marafie *et al.* 2014, Bottarelli, Azzoni *et al.* 2007). Genes *FLNA*, *TBX22*, *KIAA2022*, *IRS4*, *PCDH11X*, *GPR112* and *F8* are proposed X-linked CRC related genes (Liu, Kain *et al.* 2012). Another study demonstrated downregulation of another X-linked gene, *RPS6KA6,* in 90% of colon carcinomas, 86% of colon adenomas, and 80% of renal cell carcinomas (Lopez-Vicente, Armengol *et al.* 2009). Tspan6 is located at Xq22.1 in the human genome, and loci including Xq22.1–q22.2, Xq21.1, Xq22.1, Xq22.3, Xq22.2 and Xq23 were reported to be susceptible to copy number variation in human CRCs (Ali, Marafie *et al.* 2014). In males, X-linked genes may be silenced by a mutation, gene deletion, or aberrant methylation; in females an additional “skewed” X-inactivation (inactivation of X chromosome with wild-type allele of the gene) is required (Liu, Kain *et al.* 2012). There were no mutations in *Tspan6* gene found to be associated with CRC (Forbes, Beare *et al.* 2017). However, the evidence from methylation and clinical TCGA data suggests that Tspan6 expression is likely to be regulated by epigenetic mechanisms.

There was no correlation identified between the Tspan6 expression and mutations in CRC driver genes, including *KRAS*, *BRAF*, *PIK3CA*, *TP53*, *APC* and *CTNNB1* genes, indicating that the Tspan6 expression is not regulated by aberrant signalling of key signalling pathways implicated in CRC development. Hence, Tspan6 might present a novel tumour-associated gene and downregulation of Tspan6 expression is likely to be an early event in CRC progression. Indeed, the analysis of Tspan6 expression in a cohort of CRC patients suggests that Tspan6 may be considered as a biomarker of non-metastatic (stages I-III) CRC.

4 RESULTS CHAPTER II: TSPAN6 DEFICIENCY ACCENTUATES APC$^{MIN/+}$ PHENOTYPE IN VIVO

4.1 Introduction

The data on Tspan6 expression in patient samples indicated that the expression of Tspan6 is decreased in colorectal cancer. In addition, recent reports linked Tspan6 expression with patient survival as well as response to neoadjuvant therapy in CRCs (Uhlen, Zhang *et al.* 2017, Chauvin, Wang *et al.* 2018). It was, therefore, important to investigate the biological role of Tspan6 in colon epithelium and its possible role in CRC development and progression. The aim of this chapter was to characterise the effects of Tspan6 loss in a mouse model, examine its role in CRC using the APC$^{min/+}$ mouse model and identify the molecular pathways affected by the loss of Tspan6.

4.2 The loss of Tspan6 does not result in spontaneous tumour formation in C57Bl/6J mice

A constitutive global Tspan6 KO mouse model was generated by the Deltagen, Inc pharmaceutical company by the insertion of a Neomycin cassette in exon 2 of the Tspan6 gene. The Tspan6 mice were validated using a PCR genotyping method from the DNA purified from ear samples of the 21 days old littermates and amplified by PCR using gene specific primers. Overall, 23 animals were analysed: eight wild-type, three heterozygous, and 12 knockout mice (Supplementary Table 8-5).

Wild-type and Tspan6 KO mice were culled at 52 weeks of age by cervical dislocation. These mice did not exhibit any obvious symptoms of illness, discomfort

or social anxiety. This was in agreement with previous reports showing that Tspan6 deletion does not affect behaviour patterns in mice (Salas, Callaerts-Vegh *et al.* 2017). Interestingly, Tspan6 KO mice were bigger in size (Figure 4-1.A), which is reflected both in the length of the body and the larger amount of visceral adipose tissue in the abdomen cavity (Figure 4-1.B-C). The data from heterozygote mice were not considered in this study to account for compensation effect from the functional copy of Tspan6 in this model. Although the intestinal epithelium of Tspan6 KO mice appeared normal, it was found that 10 out of 12 Tspan6 KO mice displayed mild to moderate submucosal oedema (Supplementary Table 8-6). In contrast, only two of the wild-type animals presented mild interstitial oedema. Together, these indicate that the loss of Tspan6 results in phenotypic changes of the intestines.

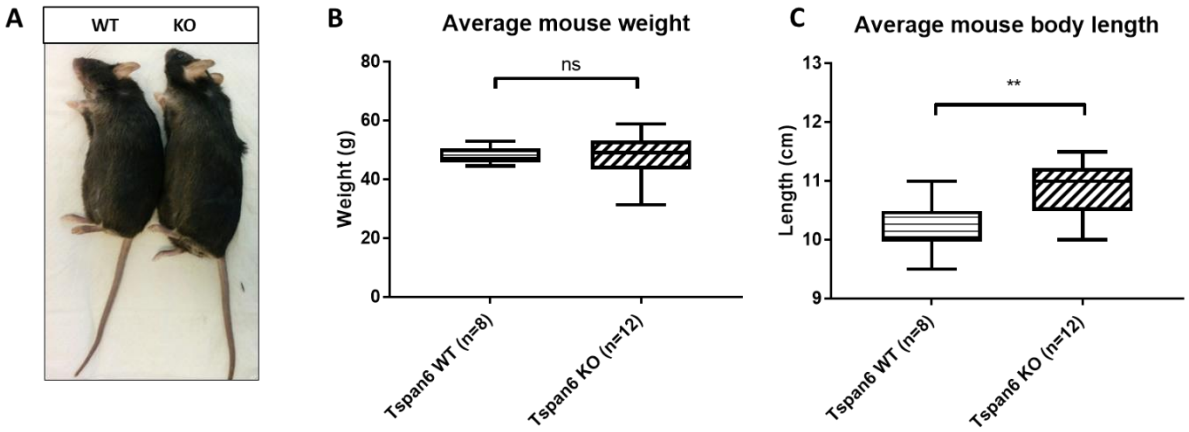

Figure 4-1. The loss of Tspan6 results in enlarged body size of C57Bl/6J mice. (A) The representative image of body size of wild-type (WT) and Tspan6 knockout (KO) mice, n=8 and n=12 respectively. **(B)** The average mouse weight and **(C)** the average body length. The weight of animals was not affected by the expression of Tspan6 and the body length was significantly enlarged (p=0.0081) in Tspan6 KO mice. Mice were weighed immediately after cervical dislocation and the body length was measured from the tip of the nose to the base of the tail of mice. The Student t-test was performed for statistical analysis.

4.3 Tspan6 knockout results in higher polyp burden in intestine and colon of APC$^{min/+}$ mice

To study the role of Tspan6 in colorectal tumorigenesis, Tspan6 KO mice were crossed with APC$^{min/+}$ mice on the C57Bl/6J background. The heterozygous females Tspan6$^{-/+}$ were mated with APC$^{min/+}$ male mice to generate double mutant APC$^{min/+}$Tspan6$^{-/y}$ male mice. The mice were born in expected Mendelian ratios, viable and fertile. In total 7 wild type, 16 Tspan6 KO, 16 APC$^{min/+}$ and 36 APC$^{min/+}$Tspan6$^{-/y}$ mice were analysed in this study. Interestingly, double mutant mice developed symptoms of illness (anaemia, hunched posture, bloody stool and rapid loss of weight) earlier than APC$^{min/+}$ animals, with median 14 weeks postpartum and 16 weeks respectively (Figure 4-2).

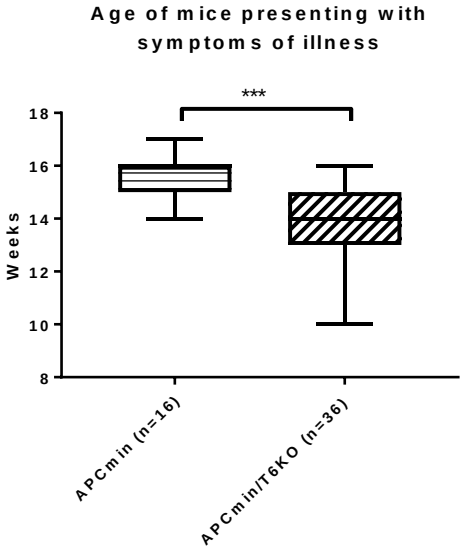

Figure 4-2. The age at which APC$^{min/+}$ and APC$^{min/+}$Tspan6$^{-/y}$ double mutant mice presented with symptoms of illness. The APC$^{min/+}$Tspan6$^{-/y}$ mice developed disease at earlier time points than APC$^{min/+}$ mice, median 14 weeks and 16 weeks correspondingly (p=0.0002). The affected mice were subsequently culled. Error bars are plotted as median plus range. The non-parametric Mann-Whitney test was used for statistical analysis.

Once animals were euthanized, the animal weight and the body length measurements were taken. In accordance to findings with aged animals, Tspan6 KO mice had significantly enlarged body length compared to wild-type (p=0.0033) (Table 4-1). A similar trend was observed in $APC^{min/+}Tspan6^{-/y}$ double mutant mice (p=0.1154). Additionally, the average animal weight was considerably increased with deletion of functional Tspan6 in both normal (WT vs. Tspan6 KO) and colon cancer ($APC^{min/+}$ vs. $APC^{min/+}Tspan6^{-/y}$) models (p=0.0448 and p=0.0491 respectively).

The intestine of animals was cut longitudinally, and polyp number and size were evaluated. A total of 14 $APC^{min/+}$ and 20 $APC^{min/+}Tspan6^{-/y}$ mice were compared. As expected, the intestines of the wild type and Tspan6 KO did not show any visible polyps. The mean number and size of visible polyps was significantly increased in $APC^{min/+}Tspan6^{-/y}$ double mutant mice compared to mice carrying $APC^{min/+}$ mutation alone. The number of polyps among analysed mice doubled upon loss of Tspan6 (p<0.0001), with a mean of 46 and 90 polyps per mouse in $APC^{min/+}$ and $APC^{min/+}Tspan6^{-/y}$ mice respectively (Figure 4-3). The average size of intestinal polyps in $APC^{min/+}Tspan6^{-/y}$ mice increased two-fold compared to $APC^{min/+}$ mice (p=0.0031), 1.96 mm^2 and 0.82 mm^2 respectively. The median size of polyps in $APC^{min/+}$ mice was 0.75 mm^2 and in $APC^{min/+}Tspan6^{-/y}$ mice 1.7 mm^2. These data indicate that the loss of functional Tspan6 increases the incidence of polyp formation in $APC^{min/+}$ mice.

Table 4-1. Summary of average mouse weight and average body length in 16-week-old WT, Tspan6 KO, $APC^{min/+}$ and $APC^{min/+}Tspan6^{-/y}$ mice.

Mouse strain	Average mouse weight(g)	Average body length(cm)
WT (n=7)	30.885	9.671
Tspan6 KO (n=16)	34.481	10.187
p-value (t-test WT vs. KO)	**0.045**	**0.003**
$APC^{min/+}$ (n=16)	22.205	9.000
$APC^{min/+}Tspan6^{-/y}$ (n=36)	24.369	9.231
p-value (t-test $APC^{min/+}$ vs $APC^{min/+}Tspan6^{-/y}$)	**0.049**	**0.115**

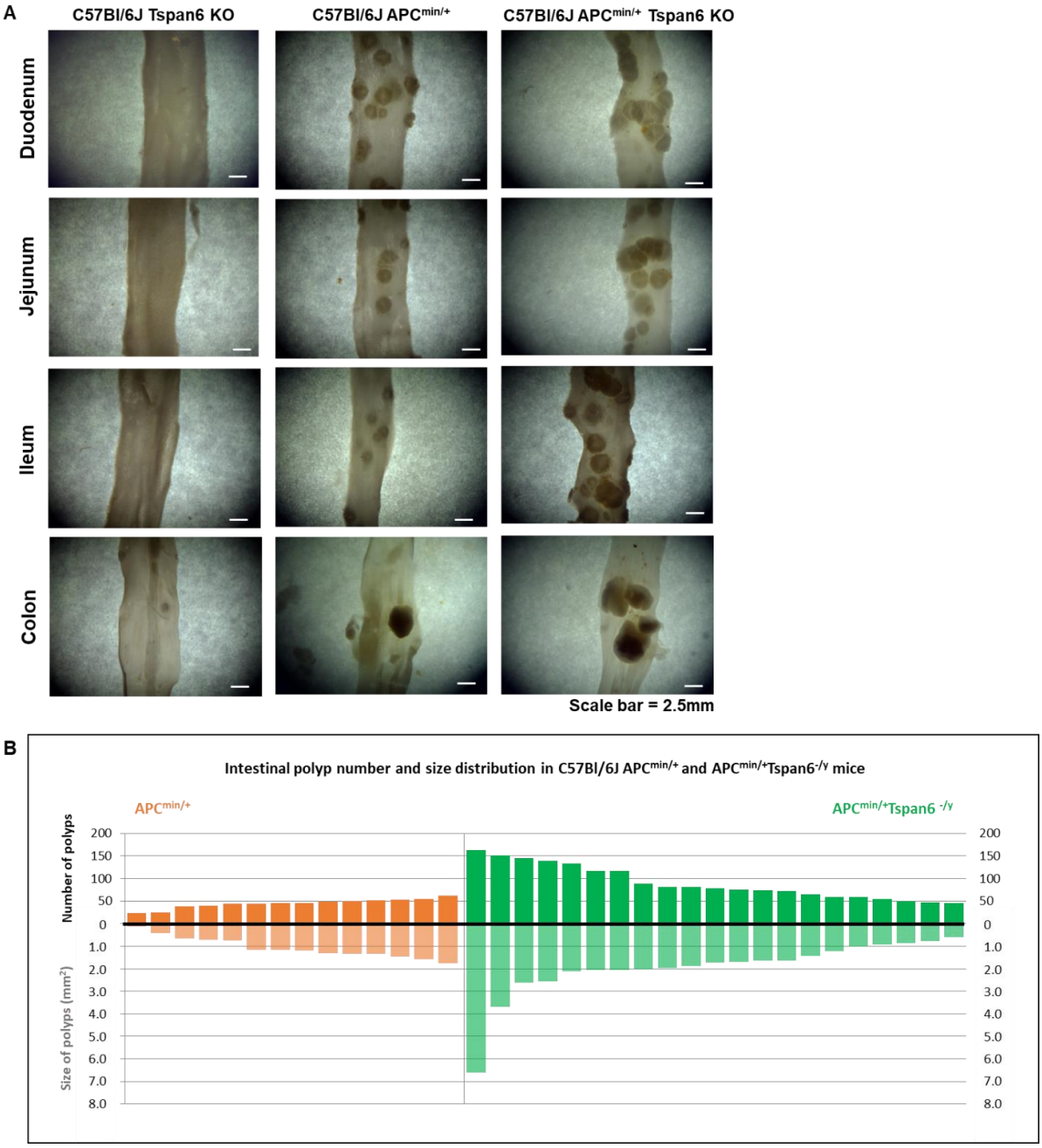

Figure 4-3. Tspan6-deficiency results in increased polyposis in small intestine and colon in C57Bl/6J APC$^{min/+}$ mice. (A) Gross appearance of small intestine and colon from Tspan6 KO, APC$^{min/+}$ and APC$^{min/+}$Tspan6$^{-/y}$ mice. Tspan6 KO mice showed normal mucosa on macroscopic examination. Tspan6 deficient mice showed an increase in tumour numbers and size throughout the intestine compared to APC$^{min/+}$ mice. **(B)** Polyp number and size distribution in intestine of APC$^{min/+}$ and APC$^{min/+}$Tspan6$^{-/y}$ mice. Polyp number was determined across the whole intestine in APC$^{min/+}$ (n=14) and APC$^{min/+}$Tspan6$^{-/y}$ (n=21) mice using stereomicroscopy. APC$^{min/+}$Tspan6$^{-/y}$ mice develop significantly larger number of polyps, $p<0.0001$. The size of polyps was determined by measuring the diameter and presented as area (mm^2). Tspan6 deficiency results in polyps of bigger size, $p=0.0031$. Mann-Whitney non-parametric test was used for statistical analyses.

Interestingly, the incidence of colonic adenoma formation in colon of APC$^{min/+}$ mice has been previously reported to be 35% of the APC$^{min/+}$ population (Moser, Pitot *et al.* 1990, Luongo, Moser *et al.* 1994, Boivin, Washington *et al.* 2003, Xiao, Yin *et al.* 2010, Grill, Neumann *et al.* 2014). In agreement with these studies, it was found that 5 out of 14 APC$^{min/+}$ mice (35.7%) have developed colonic adenomas. Remarkably, the loss of Tspan6 on the APC$^{min/+}$ background enhanced development of colonic polyps to 95.2% with 20 out of 21 of APC$^{min/+}$Tspan6$^{-/y}$ animals presenting with neoplastic lesions in the colon (Figure 4-4). The three-fold difference (p=0.0002) indicates the important role of Tspan6 in modulating tumorigenesis in the colon.

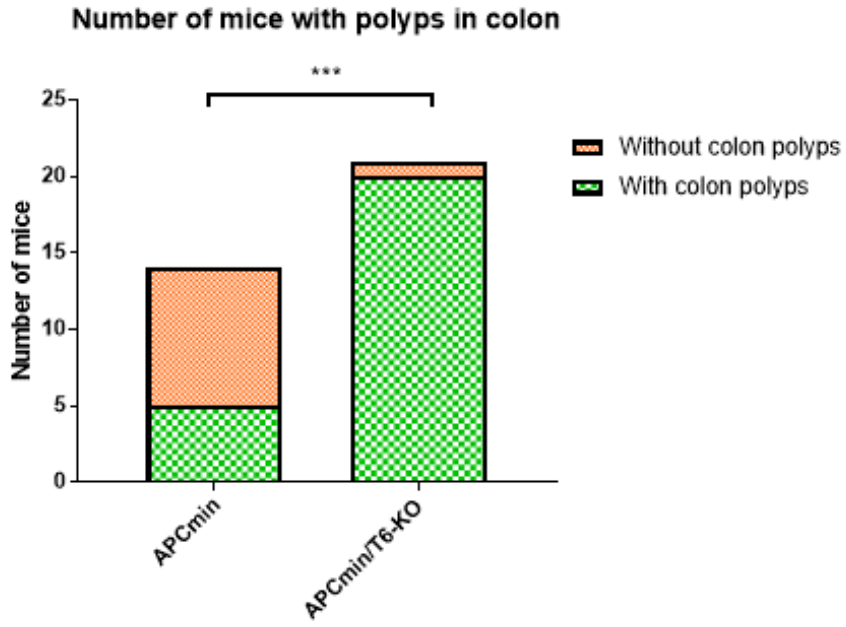

Figure 4-4. The loss of Tspan6 facilitates adenoma formation in colon of C57Bl/6J APC$^{min/+}$ mice. The number and ratio of analysed C57Bl/6J APC$^{min/+}$ and APC$^{min/+}$Tspan6$^{-/y}$ mice that developed adenomatous polyps in the colon. The incidence of colon adenoma formation in APC$^{min/+}$Tspan6$^{-/y}$ mice is significantly higher than in APC$^{min/+}$ mice (p=0.0002). A Fisher's exact test was used for statistical analysis.

4.4 Loss of Tspan6 results in intestinal adenomas with a more severe phenotype

The intestinal 'swiss rolls' from wild-type, Tspan6 KO, $APC^{min/+}$ and double mutant $APC^{min/+}Tspan6^{-/y}$ mice were analysed for the presence of macroscopic and microscopic lesions. The detailed histological analysis of normal intestinal mucosa revealed no foci of cellular transformation or increased proliferation between the $APC^{min/+}$ and double mutant $APC^{min/+}Tspan6^{-/y}$ mice, and complete absence of hyperplastic regions in wild-type and Tspan6 KO (Figure 4-5). The morphology of mucosa in duodenum, jejunum, ileum and colon were comparable: no variations of crypt-to-villi ratio in the small intestine were found. The colonic tissue was also normal. These results indicate that the loss of Tspan6 does not result in morphological changes of mouse normal intestinal mucosa in C57Bl/6J mice. However, in agreement with findings at the macroscopic level, the polyp burden was significantly increased in $APC^{min/+}Tspan6^{-/y}$ mice when compared to $APC^{min/+}$ ($p=0.0172$), with median number of 29 and 17 polyps per histology slide per animal respectively (Figure 4-6). The wild-type and Tspan6 KO mice did not develop any neoplastic lesions.

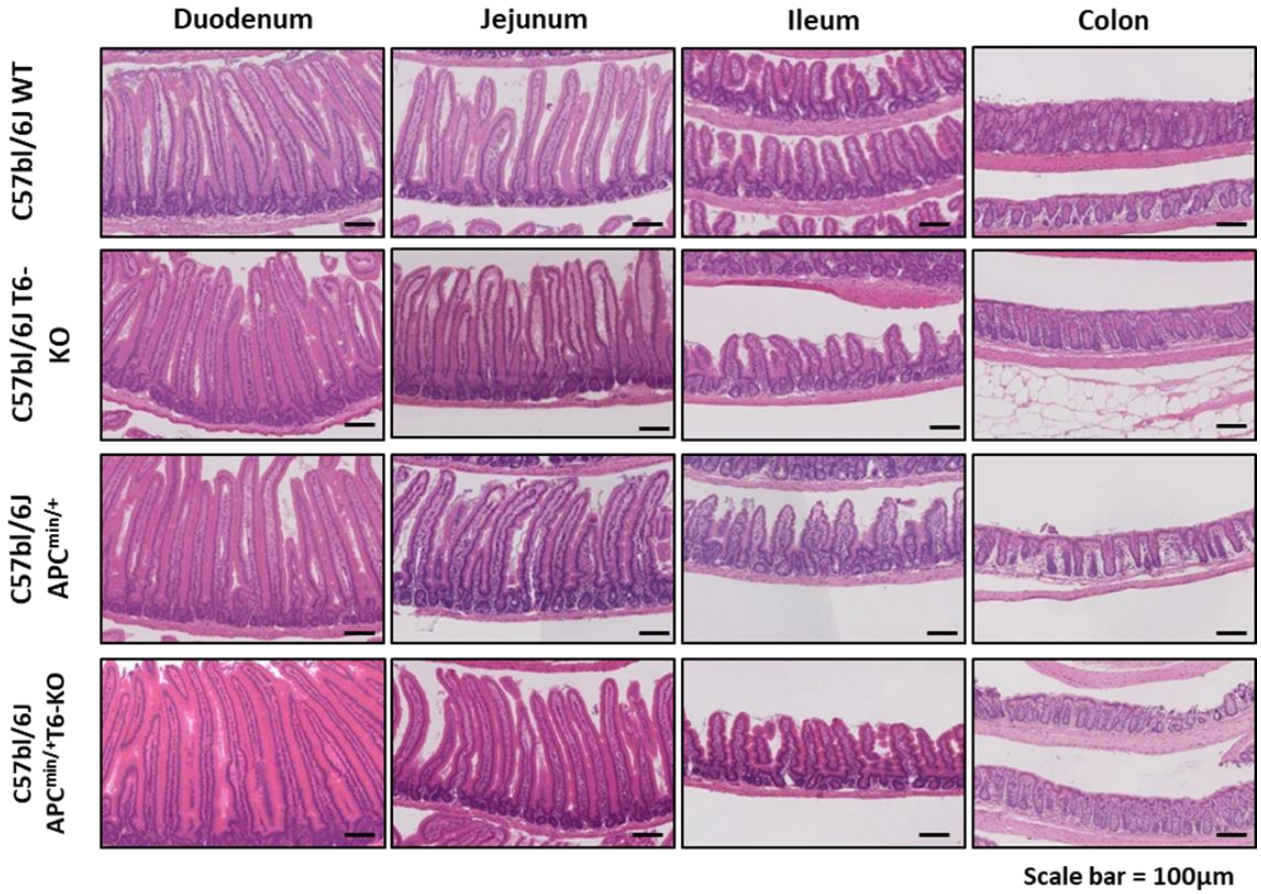

Figure 4-5. The loss of functional Tspan6 does not affect the morphology of normal mucosa in small intestine and colon epithelium in C57Bl/6J mice. The representative images of small intestine and colon tissue sample from wild-type, Tspan6 KO, APCmin$^{/+}$ and APC$^{min/+}$Tspan6$^{-/y}$ mice. The H&E staining revealed that loss of Tspan6 does not result in cellular atypia in intestinal epithelium and with normal villous-to-crypt ratio.

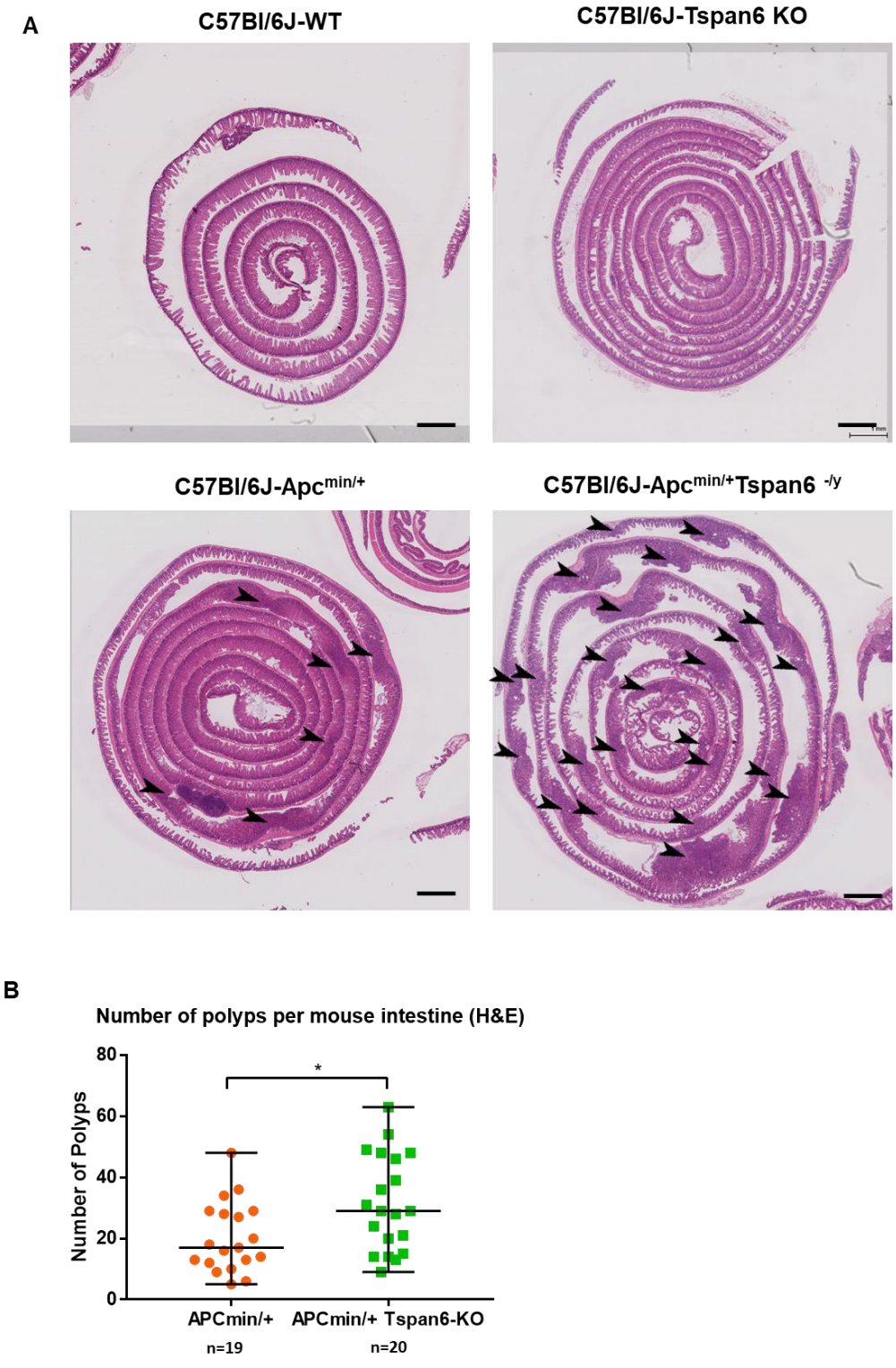

Figure 4-6. The loss of Tspan6 promotes intestinal polyp formation in C57Bl/6J APC$^{min/+}$ mice. **(A)** The representative H&E stained intestinal 'swiss-rolls' of C57Bl/6J WT, Tspan6 KO, APCmin$^{/+}$ and APC$^{min/+}$Tspan6$^{-/y}$ mice. Black arrows indicate intestinal adenomas. **(B)** A number of polyps per histology slide with intestines of APCmin$^{/+}$ and APC$^{min/+}$Tspan6$^{-/y}$ mice. A significantly higher number of polyps was found in APC$^{min/+}$Tspan6$^{-/y}$ mice, p=0.0172. Horizontal bars represent median with range. Mann-Whitney nonparametric test was used for statistical analysis.

To evaluate if the loss of Tspan6 influences morphology of intestinal polyps in $APC^{min/+}$ mice, further histopathological analysis was performed by trained histopathologists in a blinded fashion. Polyps were classified as 1) non-dysplastic, 2) with low-grade dysplasia, and 3) with high grade dysplasia. Low grade dysplastic polyps show elongated crypts with decreased inter-glandular stroma, elongated cell nuclei, decreased number of mucin-producing goblet cells (Figure 4-7.B) (Boivin, Washington *et al.* 2003). High-grade dysplasia was assigned to polyps that had severe disorganization of the glandular architecture, absent stroma between glands, often appearing as cribriform structures usually with intraluminal necrosis and loss of cellular polarity, abnormal nuclear changes such as hyper-chromatism, increased nuclear-cytoplasmic ratio, irregular and pseudostratified nuclei (Figure 4-7.C). In total 19 $APC^{min/+}$ and 23 $APC^{min/+}Tspan6^{-/y}$ mice were analysed. The majority of polyps among both strains appeared to have low grade dysplasia, 95% and 87% of animals respectively. Interestingly, as many as 10 out of 23 $APC^{min/+}Tspan6^{-/y}$ mice (43%) appeared to have low grade dysplastic polyps with foci of high-grade dysplasia, compared to 1 out of 19 in $APC^{min/+}$ mice (5%), indicating that these polyps are progressing to malignant type (Figure 4-7 and Table 4-2). These data suggest that loss of functional Tspan6 accentuates neoplastic features of $APC^{min/+}$ polyps, and, therefore, may contribute to future progression of non-malignant polyps to a more severe phenotype.

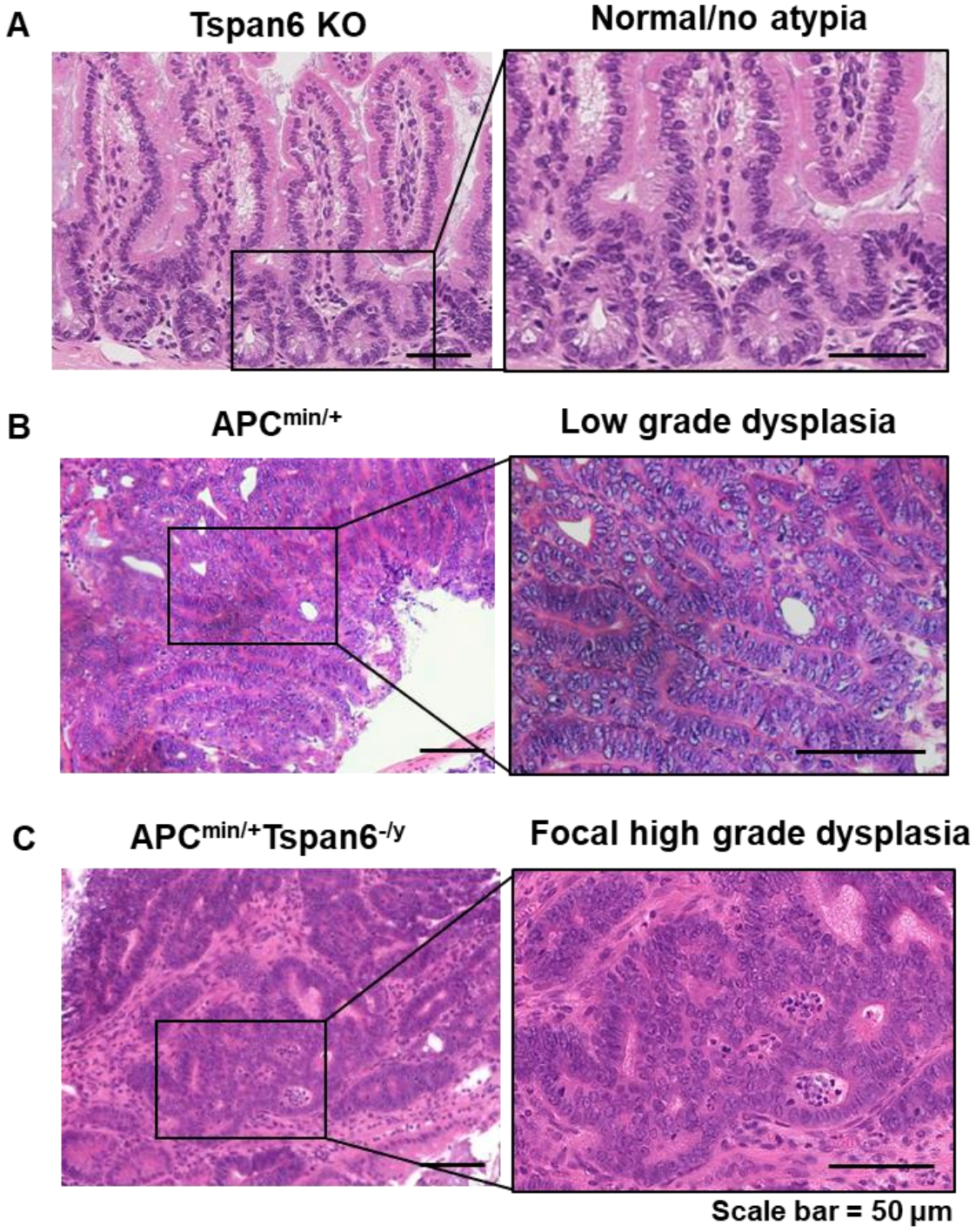

Figure 4-7. The loss of Tspan6 results in more severe histological abnormalities in C57Bl/J6 APCmin/+ mice. Representative images of H&E stained intestinal lesions in APCmin$^{/+}$ and APC$^{min/+}$Tspan6$^{-/y}$ mice. **(A)** Genetic deletion Tspan6 alone does not affect intestinal or colonic epithelia of C57/Bl/J6 mice. **(B)** Polyps of APC$^{min/+}$ present with low grade dysplastic adenomas throughout the small bowel. **(C)** Loss of Tspan6 in APC$^{min/+}$ mice results in the formation of lesions with high incidence of focal high-grade malignant changes of intestinal mucosa.

Table 4-2. The incidence of low grade and focal high-grade adenomas in small intestine and colon of $APC^{min/+}$ and $APC^{min/+}Tspan6^{-/y}$ mice.

	Lesion pathology grade	$APC^{min/+}$	$APC^{min/+}Tspan6^{-/y}$
Small Intestine	Low grade dysplasia	95% (18/19)	87% (20/23)
	High grade dysplasia, focal	5% (01/19)	43% (10/23)
Colon	Low grade dysplasia	13% (03/19)	65% (15/23)
	High grade dysplasia, focal	0% (0/19)	39% (09/23)

4.5 Tspan6 deficiency contributes to upregulation of key signalling pathways in mouse intestinal adenomas

To examine changes in gene expression associated with a loss of Tspan6 in the intestinal epithelium of $APC^{min/+}$ mice, RNA sequencing was performed. Polyadenylated mRNA from intestinal polyps of three $APC^{min/+}$ mice (control) and five $APC^{min/+}Tspan6^{-/y}$ double mutant mice was extracted and sequenced using the Illumina sequencing platform. The whole transcriptome sequencing showed 1238 differentially expressed genes (adjusted p value < 0.05) between the two types of adenomas (Figure 4-8). KEGG analysis revealed a significant enrichment of multiple pathways that are known to enhance tumour progression (Table 4-3). Cell proliferation and growth (MAPK signalling pathway, Wnt signalling pathway, ErbB signalling), focal adhesion, and DNA repair pathways (mismatch repair, nucleotide excision repair) appeared to be upregulated in adenomas of $APC^{min/+}Tspan6^{-/y}$ mice when compared to $APC^{min/+}$ mice.

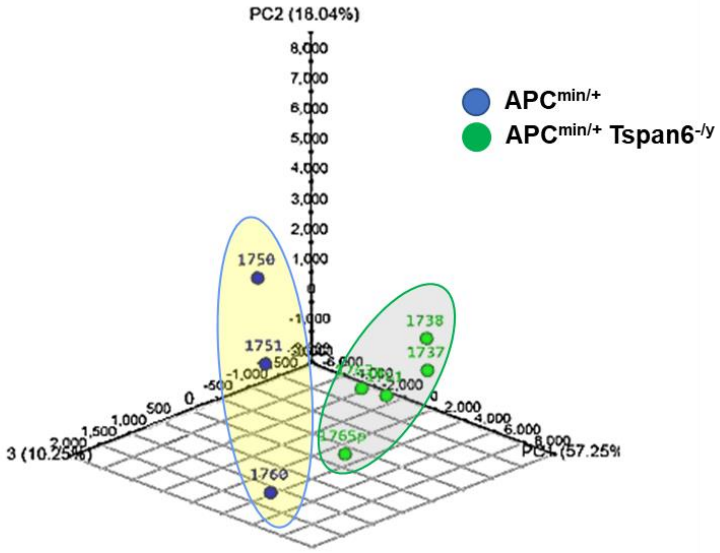

Figure 4-8. The loss of Tspan6 results in differential gene expression in intestinal polyps of APC$^{min/+}$ mice. The principal component analysis plot (PCA) illustrating the differential gene expression between intestinal polyps of APC$^{min/+}$ (blue, n=3) and APC$^{min/+}$Tspan6$^{-/y}$ (green, n=5) mice.

Table 4-3. Summary table of pathway enrichment analysis of RNAseq data

Pathway	p-Value
MAPK signalling pathway	0.003212
Ubiquitin mediated proteolysis	7.81E-07
Endocytosis	0.011859
Focal adhesion	0.019936
Chemokine signalling pathway	0.019289
Wnt signalling pathway	0.016458
Neurotrophin signalling pathway	0.02865
Insulin signalling pathway	0.042612
T cell receptor signalling pathway	0.033175
Phosphatidylinositol signalling system	0.011894
ErbB signalling pathway	0.028932
Nucleotide excision repair	0.019021

Intestinal tumorigenesis is a multistep event commonly described by alterations in Wnt signalling pathways followed by dysregulation of the KRAS-mediated pathway (Fearon, Eric R. 2011). The finding that these pathways appeared to be upregulated in adenomas of $APC^{min/+}Tspan6^{-/y}$ mice are of interest as these imply that the loss of Tspan6 accelerates progression of adenomas to more malignant lesions according to a pattern previously described by Fearon and Vogelstein (Vogelstein, Fearon *et al.* 1988). To confirm if these pathways are indeed hyperactivated in $APC^{min/+}$ and $APC^{min/+}Tspan6^{-/y}$ double mutant mice, the FFPE samples were stained using IHC for p-ERK, p-EGFR and β-catenin. These experiments demonstrated that both MAPK and Wnt pathways are upregulated in polyps of $APC^{min/+}Tspan6^{-/y}$ mice when compared to $APC^{min/+}$ mice (Figure 4-9). In both cases β-catenin staining was predominantly cytoplasmic with a considerable proportion of cells presenting with nuclear staining (Figure 4-9.A). Of note, some membranous staining of β-catenin was observed in polyps of $APC^{min/+}$ mice, and more intensive nuclear staining was seen in polyps of $APC^{min/+}Tspan6^{-/y}$ double mutant mice, indicating the more effective translocation of β-catenin to the nucleus and transcriptional activation of downstream genes. Accordingly, some of the Wnt target genes (i.e. *SFRP1 and AXIN2)* were upregulated in intestinal polyps of $APC^{min/+}Tspan6^{-/y}$ double mutant mice. The abundance of p-ERK in adenomatous polyps of $APC^{min/+}Tspan6^{-/y}$ mice appeared to be markedly increased, supporting the data obtained from RNAseq analysis (Figure 4-9.B). Similarly, stronger staining of p-EGFR (Y1068) was observed in adenomas of $APC^{min/+}Tspan6^{-/y}$ mice when compared to $APC^{min/+}$ mice (Figure 4-9.C). The enhanced activation of EGFR appeared to be particularly interesting, indicating that the dysregulation of MAPK

signalling is not linked to hyperactivation of Ras. In spite of enhanced activation of Wnt and MAPK signalling pathways staining of mouse tissues with anti-Ki-67 demonstrated no difference between $APC^{min/+}$ and $APC^{min/+}Tspan6^{-/y}$ animals (Figure 4-9.D). In addition, the β-catenin, p-ERK and p-EGFR abundance and distribution were analysed in normal mucosa of $APC^{min/+}$ and $APC^{min/+}Tspan6^{-/y}$ mice. As expected, there were no changes in levels of expression of β-catenin, p-ERK, and p-EGFR in normal mucosa (Figure 4-10). Here, the expression of p-EGFR and p-ERK were limited to intestinal crypts and transit amplifying cells and were comparable between the two models. Expression of β-catenin appeared strongly membranous across crypt-villous length with some cytoplasmic and nuclear staining localised to the crypt. These data indicate that *Tspan6* is a modifier gene in colorectal carcinogenesis that augments the effect of tumour driving mutations, such as *APC*.

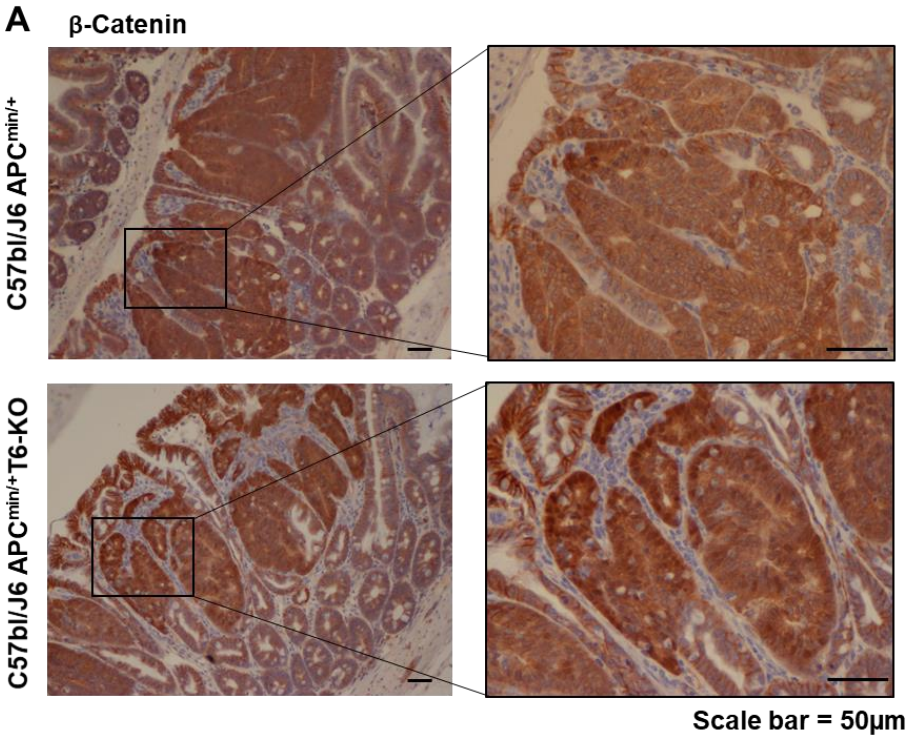
A
β-Catenin
C57bl/J6 APCmin/+
C57bl/J6 APCmin/+T6-KO
Scale bar = 50μm

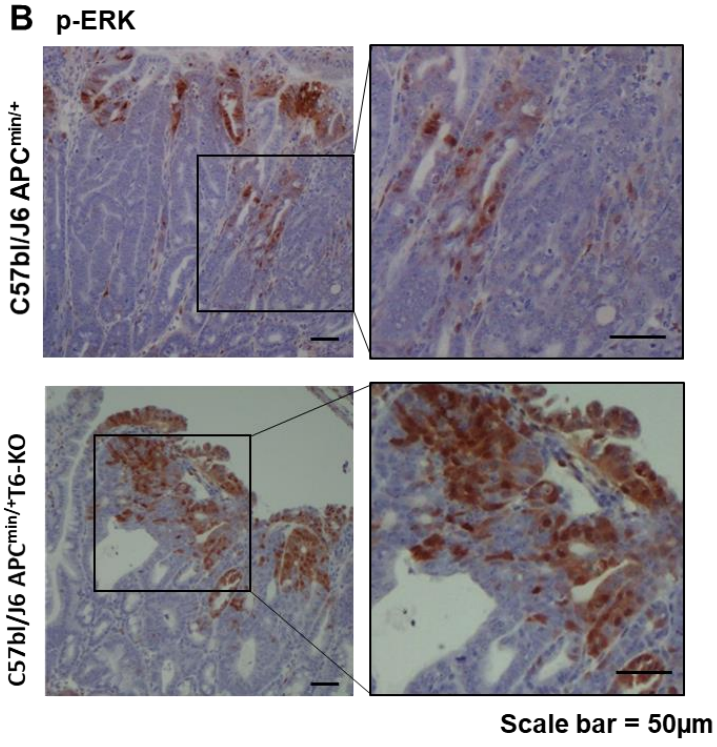
B
p-ERK
C57bl/J6 APCmin/+
C57bl/J6 APCmin/+T6-KO
Scale bar = 50μm

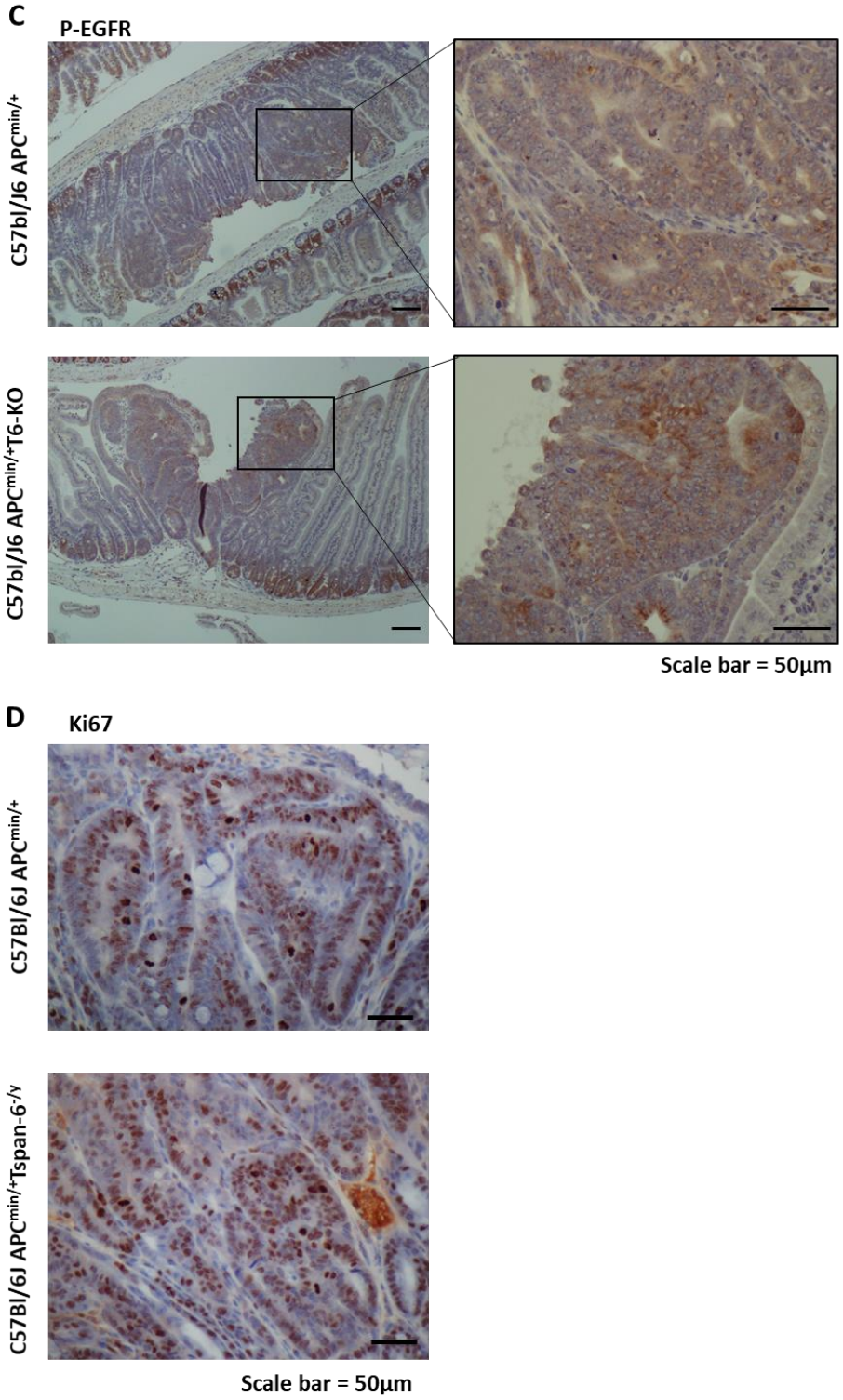

Figure 4-9. The effect of Tspan6-deficiency on expression of β-Catenin, p-ERK, p-EGFR and Ki67 in intestinal polyps of APC$^{min/+}$ mice. (A) A representative image of β-Catenin expression in APC$^{min/+}$ (n=5) and APC$^{min/+}$Tspan6$^{-/y}$ (n=5) polyps. **(B)** A representative image of p-ERK expression in APC$^{min/+}$ (n=5) and APC$^{min/+}$Tspan6$^{-/y}$ (n=5) polyps. **(C)** A representative image of p-EGFR expression in APC$^{min/+}$(n=5) and APC$^{min/+}$Tspan6$^{-/y}$ (n=5) polyps. **(D)** A representative image of Ki67 expression in APC$^{min/+}$ (n=5) and APC$^{min/+}$Tspan6$^{-/y}$ (n=5) polyps.

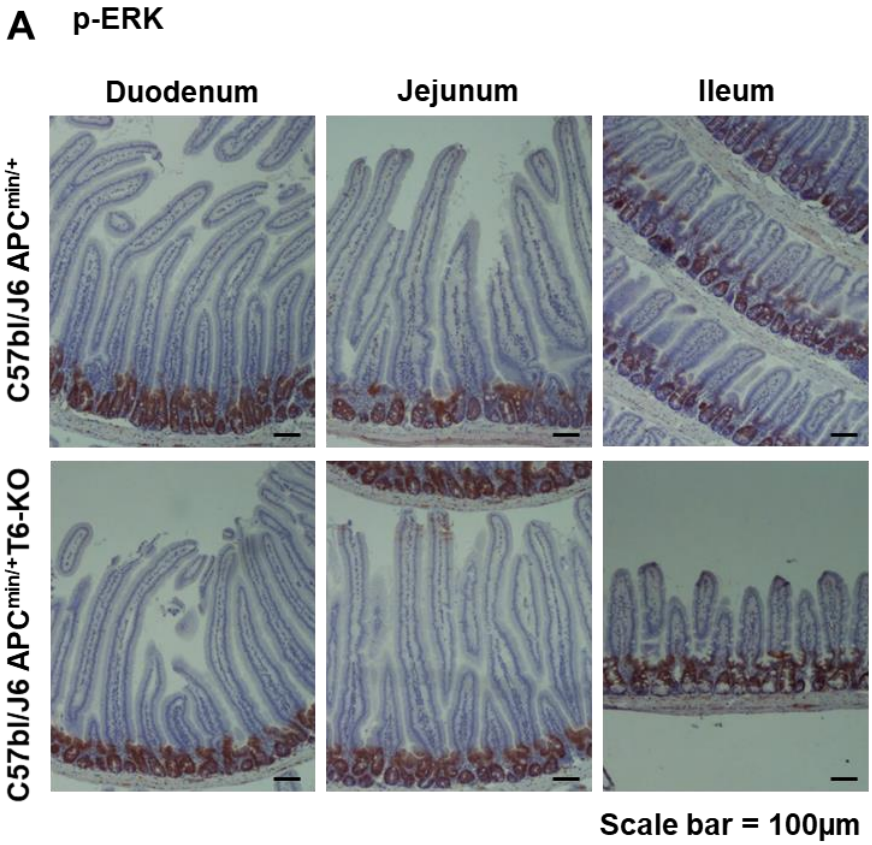
A
p-ERK
Duodenum
Jejunum
Ileum
C57bl/J6 APCmin/+
C57bl/J6 APCmin/+T6-KO
Scale bar = 100µm

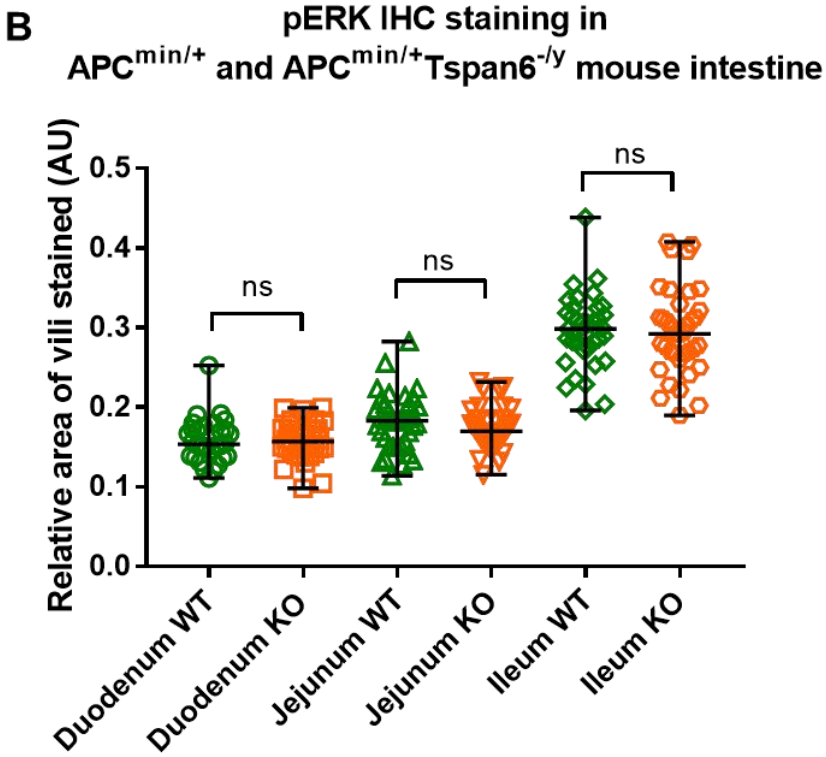
B
pERK IHC staining in
APCmin/+ and APCmin/+Tspan6-/y mouse intestine
Relative area of vili stained (AU)
0.0
0.1
0.2
0.3
0.4
0.5
ns
ns
ns
Duodenum WT
Duodenum KO
Jejunum WT
Jejunum KO
Ileum WT
Ileum KO

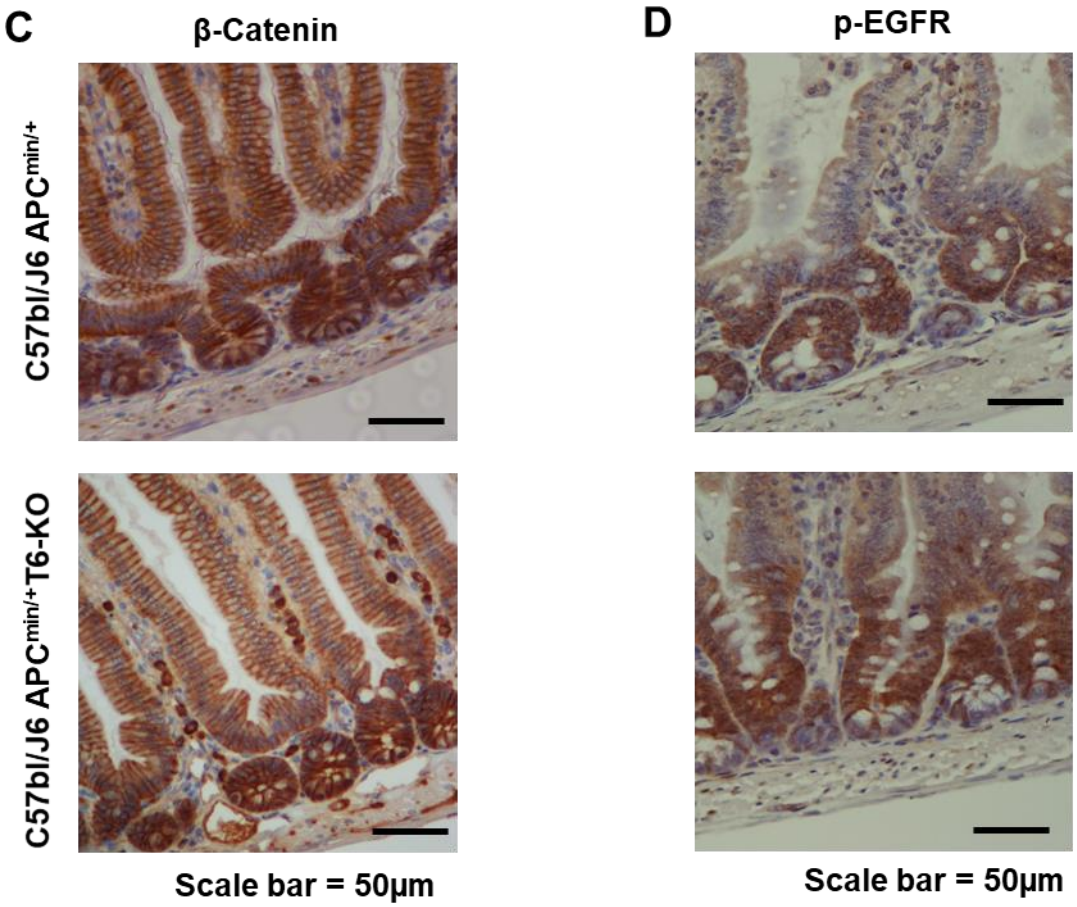

Figure 4-10. The loss of Tspan6 does not affect expression of β-Catenin, p-ERK, and p-EGFR in normal intestinal mucosa intestinal of APC$^{min/+}$ mice. **(A)** A representative image of p-ERK expression in APC$^{min/+}$and APC$^{min/+}$Tspan6$^{-/y}$ normal mucosa. **(B)** A representation of the area of p-ERK staining relative to villi length across the small intestine of APC$^{min/+}$and APC$^{min/+}$Tspan6$^{-/y}$ mice. Horizontal bars represent median with range. Nonparametric Mann-Whitney statistical test was used for analysis. **(C)** A representative image of β-Catenin expression in APC$^{min/+}$and APC$^{min/+}$Tspan6$^{-/y}$ normal mucosa. **(D)** A representative image of p-EGFR expression in normal intestinal epithelium of APC$^{min/+}$and APC$^{min/+}$Tspan6$^{-/y}$ mice.

4.6 Discussion

The role of Tspan6 in CRC initiation and progression *in vivo* has been described in this chapter. The results show that Tspan6 KO mice are viable and fertile with no obvious developmental or pathological defects. Tspan6 deletion did not induce any gross morphological or histopathological abnormalities in adult mice, implying that Tspan6 is largely dispensable for somatic cellular homeostasis. As there are 33 tetraspanins expressed in mammals, there exists a possibility for functional compensation for the loss of Tspan6 by other tetraspanins. For example, a double knockout of tetraspanins CD9 and CD81 resulted in complete infertility in mice due to impaired egg-sperm fusion and spontaneously developed pulmonary emphysema (Rubinstein, Ziyyat *et al.* 2006, Takeda, He *et al.* 2008). The most closely phylogenetically related tetraspanins to Tspan6 are Tspan3 and Tspan7 (Charrin, le Naour *et al.* 2009). While knockout of Tspan7 has not been reported, the phenotype of the animals lacking Tspan3 also appears to be normal (Kwon, Bajaj *et al.* 2015). Interestingly, Tspan3 has been proposed to have a functional relevance in colorectal carcinogenesis through *in silico* analysis of promoter regions in Caco-2 colorectal cell line (Moss, Doran *et al.* 2007). Furthermore, it has been recently demonstrated that Tspan3 is expressed in the endocytic compartment of mammalian cells (Seipold, Damme *et al.* 2017). Therefore, Tspan3 might partly (or fully) compensate for the loss of Tspan6 in regulation of extracellular vesicles secretion, an important functional feature of Tspan6 (see below). Generation of double knockout Tspan6-Tspan3 mice could shed a light on functional redundancy and specificities of these tetraspanins.

It was also found that body length, weight and fat deposition in KO mice is

increased, which could be linked to altered hormone production. Indeed, a significant decrease in thyroid gland weight was noticed in Tspan6 KO animals when compared to wild-type (Supplementary Table 8-7). Moreover, other processes that result in body mass and size changes include insulin-regulated glucose uptake (Rosen, MacDougald 2006) and signalling cascades, including Wnt (Arango, Szotek *et al.* 2005, Kennell, MacDougald 2005), Bone Morphogenic Proteins (BMPs) (Hino, Miyazawa *et al.* 2012, Tseng, He 2007) and Fibroblast Growth Factors (FGFs) (Gesta, Tseng *et al.* 2007, Yamasaki, Emoto *et al.* 1999). In addition to interstitial oedema, it was found that the lungs of Tspan6 KO mice were heavier and often appeared discoloured (darkened) upon *post-mortem* examination. Further investigation will be necessary to identify molecular mechanisms/pathways responsible for these subtle anatomical changes in Tspan6 knockout animals.

Tspan6 KO mice did not show spontaneous tumour formation at 52 weeks of age, indicating that Tspan6 does not function as a tumour suppressor as such. However, our results demonstrate that lack of Tspan6 can accentuate a neoplastic phenotype of $APC^{min/+}$ mouse model. Due to spontaneous loss of heterozygosity (LOH) $APC^{min/+}$ mice develop on average 30 intestinal polyps by 90 days of age (Daniel, L., Liyuan *et al.* 2004, Rene, Sansom Owen 2016). Obstruction caused by polyps, internal bleeding from larger polyps and anaemia results in animal death by 150 days of age (Nalbantoglu, Blanc *et al.* 2016). On average, $APC^{min/+}$ mice in our study presented with severe illness symptoms at 16 weeks of age and $APC^{min/+}Tspan6^{-/y}$ mice at 14 weeks of age, with some animals showing symptoms as early as 11 weeks of age. The loss of Tspan6 significantly increased polyp burden and promoted tumorigenesis, resulting in a substantial increase of focal high-grade

dysplastic adenomas with potential to develop into invasive carcinomas. Similarly to Tspan6, deletion of neural precursor cell expressed developmentally down-regulated protein 4 (Nedd4) and cyclin-dependent kinase 8 (CDK8) exacerbated adenoma formation in $APC^{min/+}$ mice (Lu, Thoeni *et al.* 2016, McCleland, Soukup *et al.* 2015). Thus, Tspan6 can be added to the list of genetic modifiers of APC-driven tumorigenesis *in vivo*.

In the classic adenoma-carcinoma sequence the inactivation of APC was described as the first molecular change in pre-neoplastic colonic tissues (Leslie, Carey *et al.* 2002, Rubinfeld, Albert *et al.* 1997). The RNAseq analysis of intestinal polyps from $APC^{min/+}$ and $APC^{min/+}Tspan6^{-/y}$ mice showed an enrichment of genes associated with Wnt signalling, including Wnt target genes *AXIN2* and *SFRP1*, indicating the hyperactivation of Wnt signalling upon the loss of Tspan6. EGFR signalling pathway dysregulation is associated with progression of tumorigenesis. It was found that MAPK signalling pathway is upregulated in intestinal adenomatous polyps of $APC^{min/+}Tspan6^{-/y}$ when compared to $APC^{min/+}$. EGFR is a known oncogene and is often activated or overexpressed in colorectal cancers (Heinemann, Stintzing *et al.* 2009). Although, due to technical reasons (lack of suitable antibodies), we could not reliably assess the total expression levels of EGFR protein in mice, activation of EGFR was clearly increased in $APC^{min/+}Tspan6^{-/y}$ mice, thus providing an explanation for increased MAPK signalling in these animals. Importantly, the enhancement of Wnt and MAPK signalling in normal mucosa of $APC^{min/+}Tspan6^{-/y}$ mice was not observed, thus indicating that loss of Tspan6 is involved in neoplastic progression only in the context of complete inactivation of the *APC* gene. It has been previously reported that constitutive activation of MAPK signalling pathway results in

polyps with high grade dysplasia in $APC^{min/+}Kras^{G12D}$ mice (Haigis, Kendall *et al.* 2008). These results are consistent with adenoma-carcinoma sequence of colon tumorigenesis. Therefore, one can speculate that Tspan6 plays a regulatory role in EGFR/MAPK signalling in intestinal tissue and its loss contributes to progression of benign adenomas to dysplastic pre-malignant type of lesions.

EGFR hyperactivation occurs in less than 5% of CRC patients due to somatic mutations or gene amplification (Leary, Lin *et al.* 2008, Wood, Parsons *et al.* 2007, Heinemann, Stintzing *et al.* 2009). The mRNA analysis did not allow the evaluation of gene copy number variation or mutations in regulatory regions of DNA. Therefore, possible involvement of genetic mechanisms responsible for excessive EGFR activation in $APC^{min/+}Tspan6^{-/y}$ animals remains unclear.

Interestingly, it was found that Ki67 labelling did not show increase in polyps of double mutant mice, suggesting that the loss of Tspan6 does not affect the cell cycle and proliferation. Thus, it is possible that the EGFR/MAPK activation results in activation of cell survival mechanisms rather than proliferation. It has been previously shown that loss of Ras association domain-containing protein 1 (Rassf1a) in $APC^{min/+}$ mice results in increased intestinal adenoma formation and results in enhanced Wnt signalling during early tumorigenesis. Moreover, proliferation and apoptosis were not affected in Rassf1a-deficient mice (van der Weyden, Arends *et al.* 2008). Alternatively, dysregulation of Tspan6 and APC inactivation may rely on a novel pathway which is important for tumour initiation and early growth of intestinal adenomas. The increased activation of additional signalling pathways in polyps of $APC^{min/+}Tspan6^{-/y}$ mice, such as DNA mismatch repair and focal adhesion, illustrate

later stages of progression to carcinoma and may indicate clonal selection of cancer cells (Fearon, Eric R. 2011).

In this study the incidence of adenoma formation in the colon of Tspan6-deficient $APC^{min/+}$ mice was shown to be significantly higher than in the control group. The anatomy and biology of colon is distinct from small intestine in mice: colon crypts lack the secretory lineage of Paneth cells and the surface of mucosa is flat (Yasuhiro, Hideki 2007). Therefore, tumorigenesis and underlying pathways in the colon is different to that in small intestine (Chen, Hao *et al.* 2004). The mechanisms of adenoma formation and progression have been linked to KRAS activation (Byun, Hung *et al.* 2014), increased expression of cyclooxygenase-2 (COX-2) (Jacoby, Seibert *et al.* 2000, Sonoshita, Takaku *et al.* 2002), and DNA methylation (Hatano, Semi *et al.* 2015, Scarpa, Scarpa *et al.* 2016). In this study the mechanisms of mouse colon tumorigenesis were not explored, however, it became apparent that Tspan6 may regulate a novel uncharacterised pathway of polyp formation in colon of $APC^{min/+}$ mice.

Altogether, results described in this chapter suggest that Tspan6 deficiency facilitates tumorigenesis in synergistic fashion with APC-mutation *in vivo*. The mechanisms of regulation are further discussed in subsequent chapters of this thesis.

5 RESULTS CHAPTER III: TSPAN6 REGULATES AUTOCRINE SECRETION OF EGFR LIGANDS IN MOUSE INTESTINAL ORGANOID MODEL

5.1 Introduction

The consequences of Tspan6 KO *in vivo* indicated that Tspan6 is involved in regulation of several signalling pathways associated with cancer development and progression, including Wnt and MAPK transduction pathways. To address the functional implication of Tspan6 within the intestinal epithelium an *ex vivo* organoid model derived from mouse intestinal tissue was utilised. The aim of this chapter was to characterise mouse intestinal organoids derived from wild-type and Tspan6 KO intestinal tissues and investigate how Tspan6 affects organoid growth.

5.2 Tspan6 does not affect organoid morphology

To determine the molecular function of Tspan6 in the intestinal and colonic tissues an *ex vivo* organoid model was utilised. Organoids were derived from small intestinal tissue of C57Bl/6J WT, Tspan6 KO, $APC^{min/+}$, and $APC^{min/+}Tspan6^{-/y}$ mice. The knockout of Tspan6 in organoid lines was assessed using the PCR genotyping method (Figure 5-1). All types of organoids were cultured using a well-established protocol in media containing EGF, Noggin and R-spondin-1 (Sato, Stange *et al.* 2011). Initially it was evaluated whether the expression of Tspan6 affects the general morphology and size of organoids. Intestinal organoids form structures with the central lumen lined by villus-like epithelium and several surrounding crypt-like domains protruding into the extracellular matrix; apoptotic cells are shed into the

central lumen (Sato, Vries *et al.* 2009). Both wild-type and Tspan6 KO organoids appeared to have a normal phenotype as described above. This phenotype was maintained over 40 passages. In addition, no difference in the plating efficiency between wild-type and Tspan6 KO organoids during their routine passaging was noticed. The populations of $APC^{min/+}$ and $APC^{min/+}Tspan6^{-/y}$ organoids appeared to be heterogeneous: consisting of budded (normal) and spheroid structures. It has been previously reported that due to APC mutation and hyperactivation of Wnt signalling pathway organoids lose the gradient of Wnt signalling from highest at the base of the crypt and lowest at the villous compartment of differentiated cells resulting in symmetrical spheroid structures (Sato, Toshiro, van Es *et al.* 2010). The ratio of budded to spheroid structures did not differ between the $APC^{min/+}$ and $APC^{min/+}Tspan6^{-/y}$ organoids ($p=0.874$) representing approximately half of formed organoids (Figure 5-2.C). Additionally, staining of organoid cultures with phalloidin (marking F-actin) demonstrated that deletion of Tspan6 does not affect polarisation of intestinal organoids. The formation of the F-actin ring on the apical surface of both organoids indicates the appropriate organisation of cytoskeleton and organoid integrity (Figure 5-3). The size of organoids derived from different strains of mice was comparable (Figure 5-2.A, B). These data indicate that the loss of functional Tspan6 does not alter formation and has no obvious effect on the phenotype of intestinal organoids.

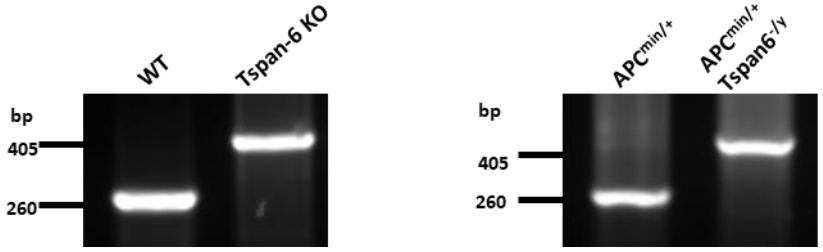

Figure 5-1. A representative agarose gel electrophoresis with the PCR products amplified with specific primers against endogenous and mutated alleles of Tspan6 in wild-type and Tspan6 KO (A) and APC$^{min/+}$ and APC$^{min/+}$Tspan6$^{-/y}$ (B) organoids. The PCR product of 260bp corresponds to wild-type (WT) and 405bp corresponds to Tspan6 KO allele.

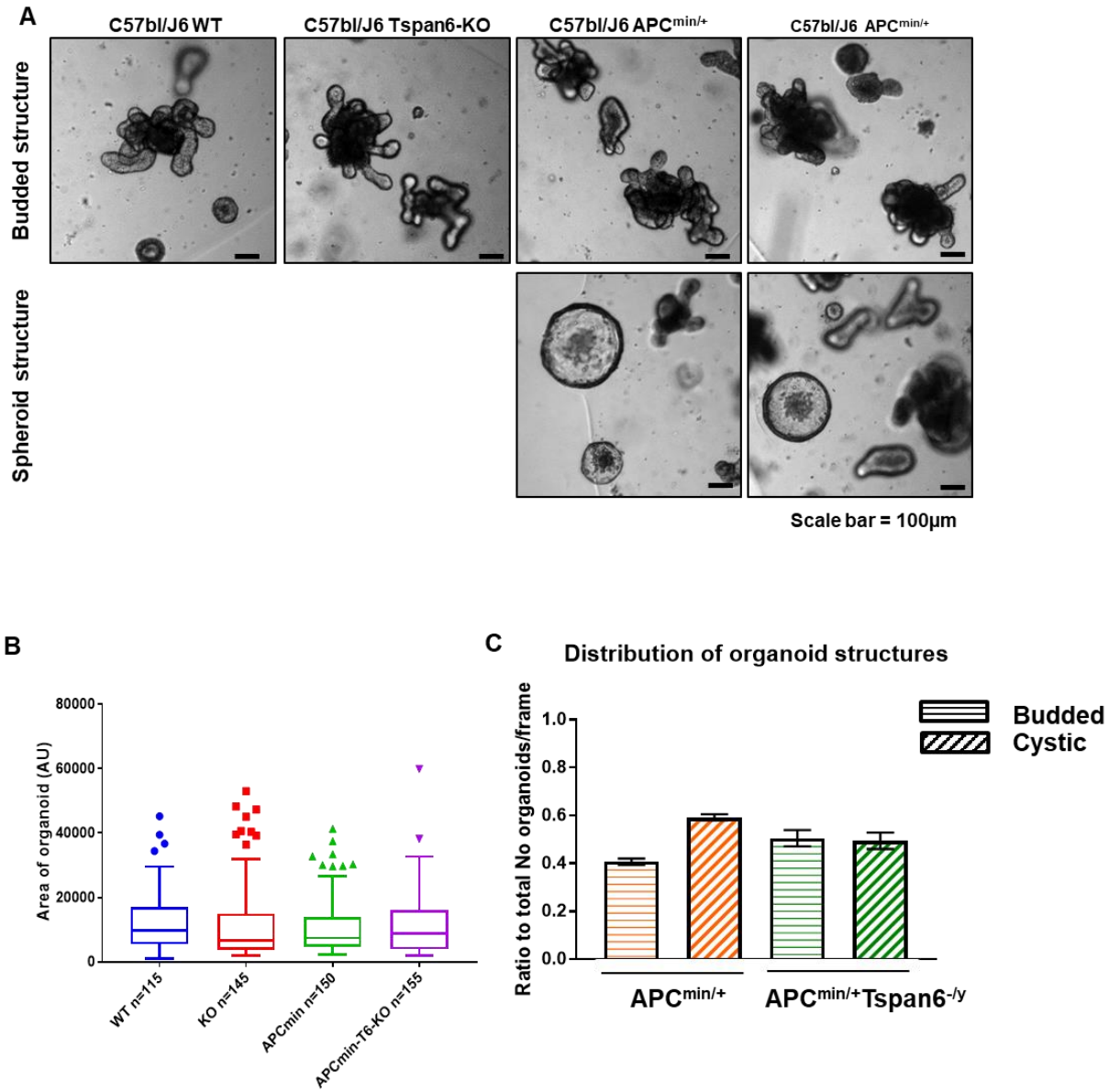

Figure 5-2. Expression of Tspan6 does not affect mouse intestinal organoid morphology. Mouse intestinal organoids were derived from C57bl/6J wild-type, Tspan6 KO, APC$^{min/+}$ and APC$^{min/+}$ Tspan6$^{-/y}$ mice and cultured in mouse intestinal organoid media for 5 days. **(A)** The morphology of organoids was comparable between all four types independent of Tspan6 expression; organoids presented with central lumen lined with villous-like epithelial layer of cells and protruding crypt-like domains. In organoids with aberrant APC activation, APC$^{min/+}$ and APC$^{min/+}$ Tspan6$^{-/y}$ cyst-like organoids were formed due to enhanced Wnt signalling but not the level of Tspan6 expression. **(B)** The size of intestinal organoids derived from C57bl/6J wild-type, Tspan6 KO, APC$^{min/+}$ and APC$^{min/+}$ Tspan6$^{-/y}$ mice. The size of organoids was determined using ImageJ analysis by measuring the area of organoids in the field. For statistical analysis more than 100 organoids were analysed and Student t-test showed non-significant size difference between all types of organoids relative to wild-type. **(C)** Distribution of budded and cystic structures in APC$^{min/+}$ (orange)and APC$^{min/+}$ Tspan6$^{-/y}$ (green) organoid cultures. The appearance of cystic structures in both cultures was at similar frequency (p=0.874). The organoids were imaged on day 5 of culture (analysis of organoid size at later time points proved to be inaccurate due to accumulation of apoptotic cells around organoids) and 10 fields were analysed for each genotype (n=3). Student t-test was used for statistical analysis.

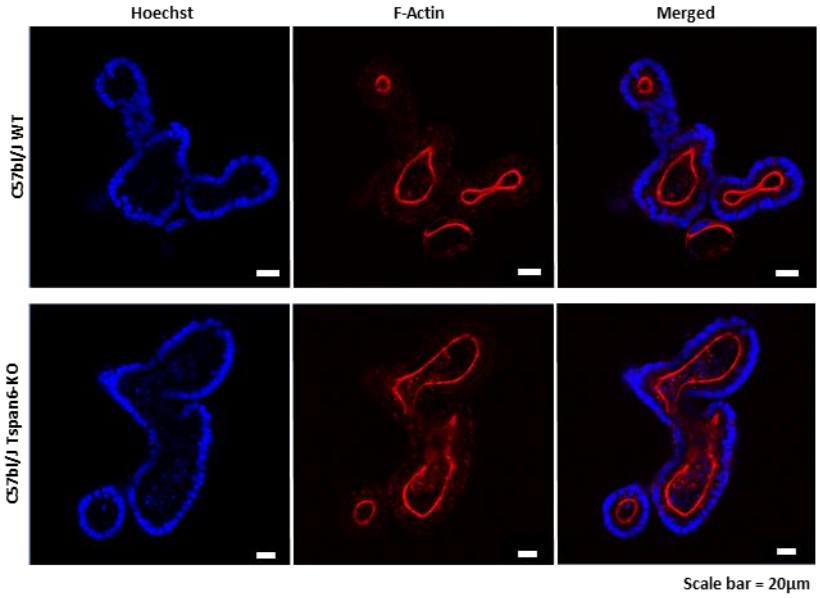

Figure 5-3. Expression of Tspan6 does not affect polarisation of mouse intestinal organoid phenotype. The immunofluorescent image of organoid mid-section shows that cellular polarisation and apical F-actin ring (red) formation are preserved in organoids lacking Tspan6 after five days of culture, Hoechst 33342 was utilised as a nuclear stain (blue).

5.3 Loss of Tspan6 results in increased Wnt and MAPK signalling

To validate the RNAseq data generated using mouse polyps, the expression of β-catenin, pEGFR and pERK was analysed using immunohistochemistry in organoids derived from intestine of WT, Tspan6 KO, $APC^{min/+}$, and $APC^{min/+}Tspan6^{-/y}$ mice. These experiments confirmed that both Wnt and MAPK signalling pathways are hyperactivated in lines lacking Tspan6. In WT organoids a strong nuclear β-catenin expression was localised only in the areas of crypt domains, where the Wnt-mediated signalling is at the highest level (Figure 5-4). In $APC^{min/+}$ organoids, Wnt signalling is moderately enhanced when compared to the WT line. However, in Tspan6 KO and $APC^{min/+}Tspan6^{-/y}$ organoids the level of β-catenin expression appeared to be uniformly high throughout the whole structure of the organoid, including crypt-like structure and villus-like structure, in both membranous and nuclear compartments (Figure 5-4). Likewise, pERK expression in WT and $APC^{min/+}$ organoids was lower than in Tspan6 KO and $APC^{min/+}Tspan6^{-/y}$ organoids, indicating higher levels of MAPK signalling pathway activation in organoids lacking Tspan6 (Figure 5-4). Similar differences were observed when organoids were stained with anti-pEGFR antibody (Figure 5-4). In agreement with the analysis of mouse tissues, there was no apparent difference in Ki67 labelling between WT and Tspan6 KO, and $APC^{min/+}$ and $APC^{min/+}Tspan6^{-/y}$ organoids, indicating that Tspan6 has little if any effect on cellular proliferation under standard culturing conditions. Taken together, these data indicate upregulation of Wnt- and MAPK-signalling pathways represents an intrinsic property of Tspan6-deficient intestinal epithelium.

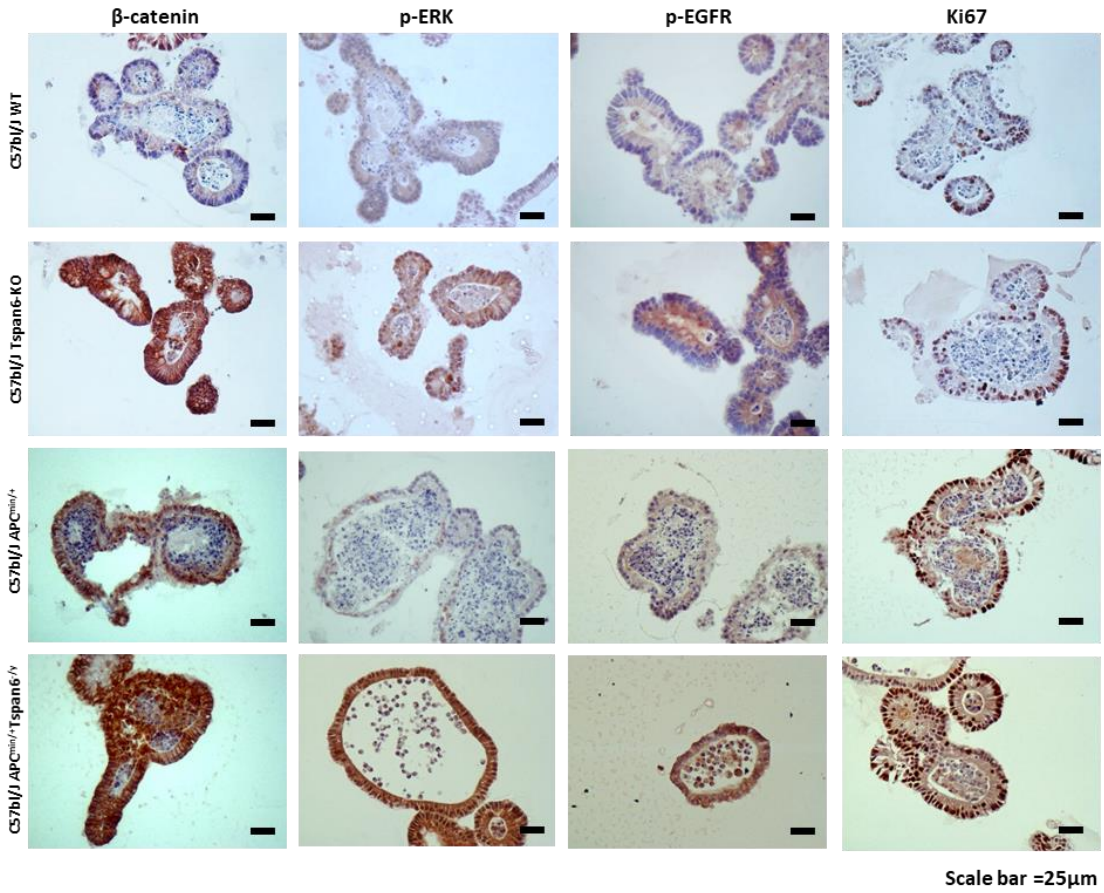

Figure 5-4. IHC characterisation of wild-type, Tspan6 KO, $APC^{min/+}$ and $APC^{min/+}$ $Tspan6^{-/y}$ mouse intestinal organoids. Brightfield images of FFPE sections stained with β-catenin, p-ERK, p-EGFR and Ki67. Sections were counterstained with haematoxylin (blue).

5.4 Tspan6 deficiency results in EGF-independent growth of mouse intestinal organoids

A combination of niche factors, including EGF, is essential for establishment and growth of murine intestinal stem cells (Sato, Stange *et al.* 2011), and as such, a withdrawal of any of these factors results in failure to form organoids and cell death. To further probe functional links of Tspan6 with EGFR mediated signalling, mouse organoids were cultured in EGF-free media. In agreement with previous reports, in

the absence of EGF WT organoids failed to form typically budding structures and underwent cell death (Hisha, Tanaka *et al.* 2013). However, organoids derived from the Tspan6 deficient mice were able to grow, forming budded structures with defined villus- and crypt-like domains (Figure 5-5).

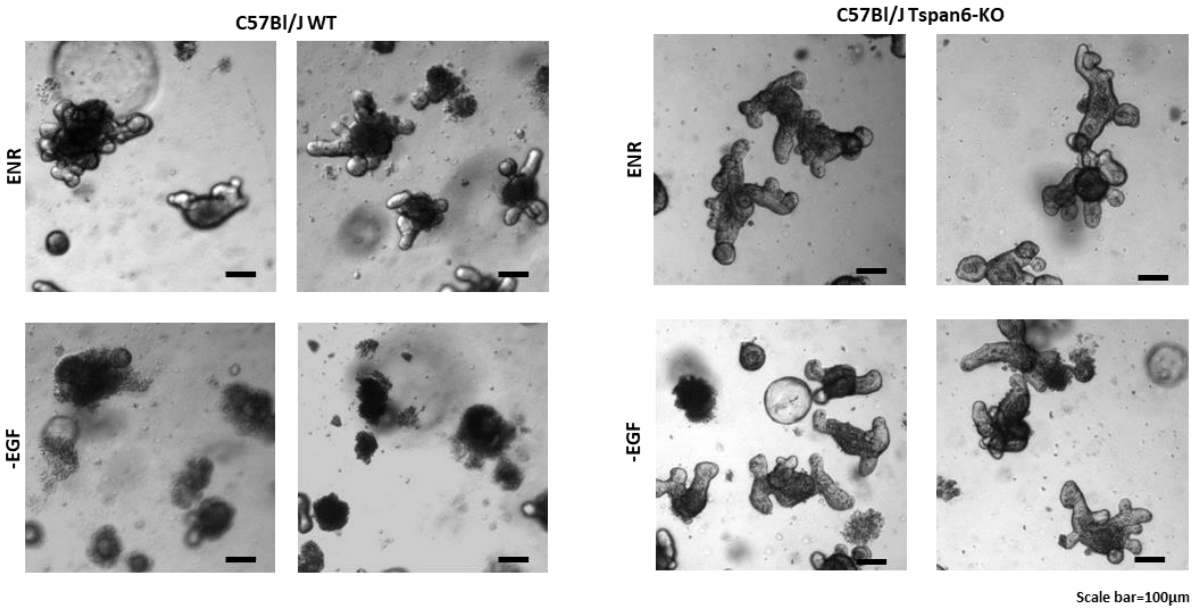

Figure 5-5. Loss of Tspan6 results in EGF-independent growth of mouse intestinal organoids. Wild-type (WT) and Tspan6 KO organoids were cultured in complete organoid growth media containing EGF, Noggin and R-spondin-1 (ENR) and in media lacking EGF (-EGF). In the absence of EGF wild-type organoids undergo cellular death, yet Tspan6 KO organoids grow and differentiate. The organoids were imaged on day 5 of culture and 10 fields were analysed for each genotype (n=4). Student t-test was used for statistical analysis.

To understand the molecular mechanisms underlying this phenomenon, the expression and activation of EGFR as well as changes occurring upon withdrawal of EGF in organoids were examined. As illustrated in Figure 5-6.A, the total levels of EGFR and activation of the receptor were very low when WT and Tspan6 KO

organoids were cultured in standard, EGF-containing media. However, upon EGF withdrawal from the media, the protein level has increased in both organoid lines. Furthermore, the level of activated EGFR (measured using anti-pEGFR Tyr1068 antibodies) was ~3-fold higher in Tspan6 KO organoids when compared to WT organoids (Figure 5-6.B). Accordingly, an increase in ERK phosphorylation was observed in Tspan6 KO organoids when compared to organoids derived from the WT animals. By contrast, there were no differences in the levels of β-catenin phosphorylation on Ser552, a hallmark of in β-catenin activation and translocation to the nucleus. Interestingly, there was a subtle decrease in phosphorylation of β-catenin at Thr41/Ser45 in Tspan6 KO organoids observed in cultures after EGF withdrawal. The increase in Src family activation, Akt phosphorylation and decrease in p38 activation were also noted in Tspan6 KO organoids compared to organoids established from the control animals. These results suggest that Tspan6 KO organoids retain capacity for cellular growth and differentiation through EGFR-mediated MAPK signalling regardless of exogenous extracellular stimuli, namely EGF. In addition, our data suggest that Tspan6 is likely to regulate other signalling pathways which contribute to cell survival and proliferation.

5.5 Tspan6-mediated MAPK activation is EGFR-dependent

The activation of MAPK signalling pathway in Tspan6 KO organoids in the absence of EGF can be mediated by the autocrine secretion of EGFR ligands or by activation of MAPK pathway downstream of the EGFR. To distinguish between these possibilities organoids were grown in the presence of pan-EGFR inhibitor lapatinib. Inhibition of EGFR using lapatinib resulted in growth inhibition of both lines of organoids with no difference in sensitivity to increasing concentration of the inhibitor

(Figure 5-7.A, C). Similarly, both WT and Tspan6 KO organoids were highly sensitive to the MEK inhibitor (Figure 5-7.B). These data strongly suggested that Tspan6 regulates EGF-independent growth of organoid cultures at the level of the receptor activation.

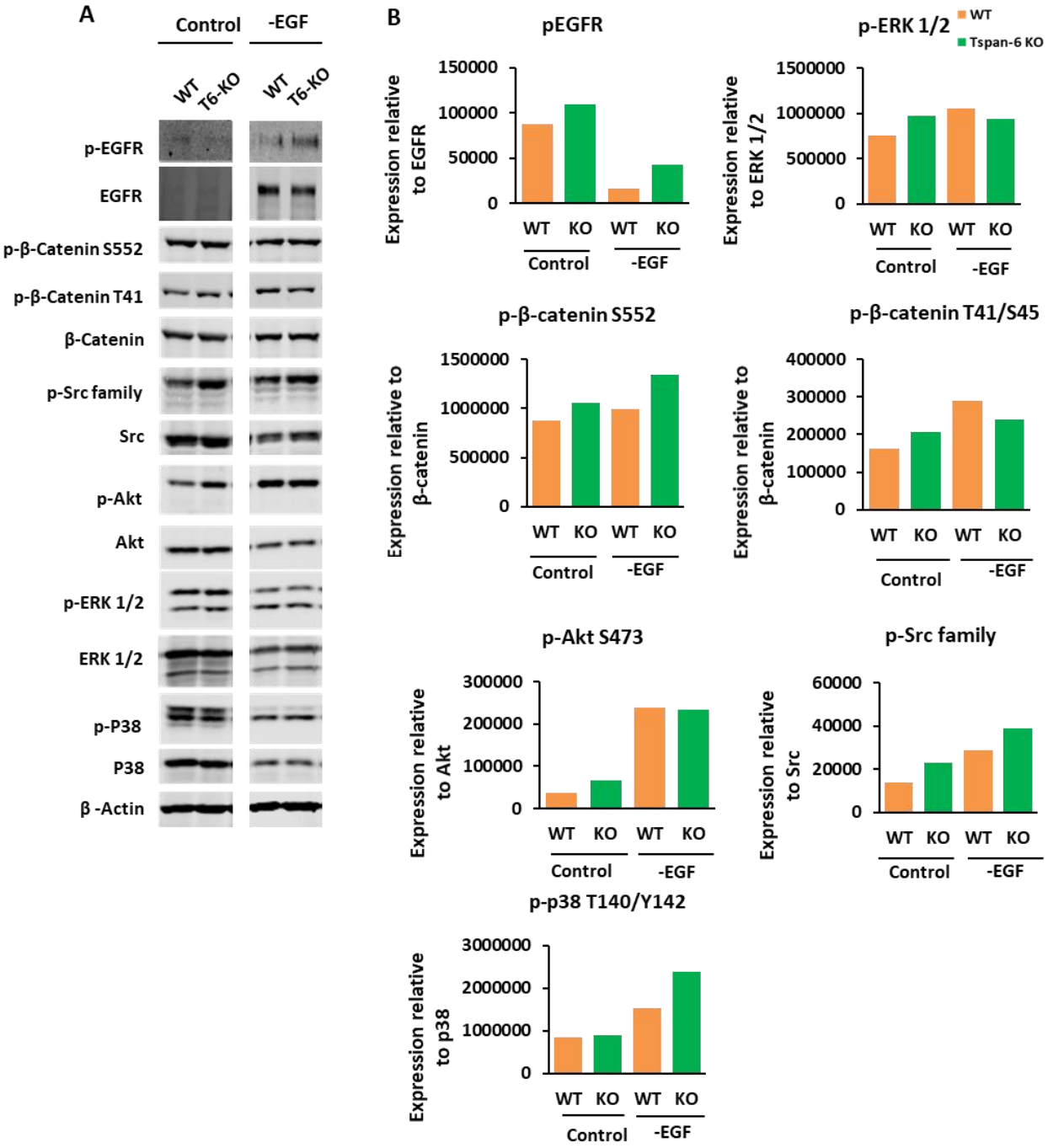

Figure 5-6. The loss of Tspan6 results in differential expression of key signalling molecules in mouse intestinal organoids. (A) Western blot analysis of p-EGFR, p-ERK, p-β-catenin, p-Src family, p-Akt, and p-p38 in WT or Tspan6 KO organoids cultured in complete growth media (control) or in media lacking EGF (-EGF). **(B)** Quantification analysis of phosphorylation level of signalling molecules relative to the total expression of the molecule. Data was normalised to β-actin expression (n=1).

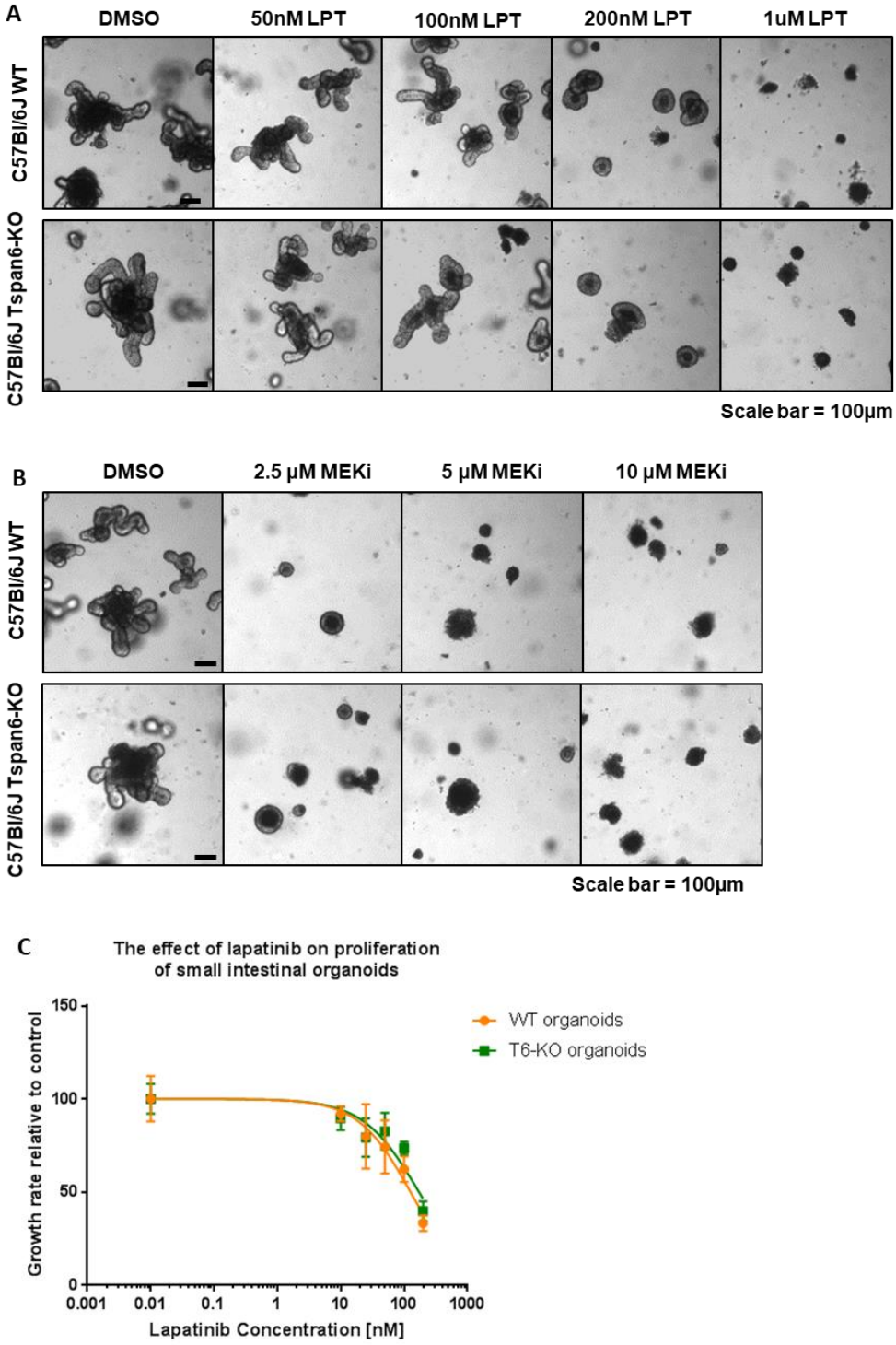

Figure 5-7. Tspan6-mediated MAPK activation is EGFR-dependent. (A) Phase-contrast images of WT and Tspan6 KO organoids in response to increasing concentrations of pan-EGFR inhibitor lapatinib (LPT) after 6 days of culture. **(B)** Phase-contrast images of WT and Tspan6 KO organoids in response to increasing concentrations of MEK inhibitor (MEKi) after 6 days of culture. **(C)** A dose-response curve of WT and Tspan6 KO mouse intestinal organoids treated with lapatinib. Cell viability was measured by CellTiter-Glo3.0 ATP-based assay after 6 days of treatment (n=2). Plots were normalised to DMSO (control) treated organoids.

5.6 Tspan6 regulates secretion of EGFR-ligands

The fact that Tspan6 KO organoids can grow in media without EGF and yet be dependent on signalling via EGF receptor suggests that Tspan6 may regulate autocrine production of EGF ligands. To test this hypothesis the WT and the Tspan6 KO organoids were co-cultured in EGF-free conditions. Remarkably, only when co-cultured with Tspan6 KO organoids did WT organoids form viable structures. Additionally, these organoids were stimulated to proliferate and differentiate, although at a slower rate than in normal conditions, resulting in normal budding structures with formation of crypt-villi substructures (Figure 5-8). These data strongly suggest that growth of Tspan6 KO organoids (and WT organoids in co-culture experiments) in EGF-depleted media is supported by an EGFR-activating autocrine factor.

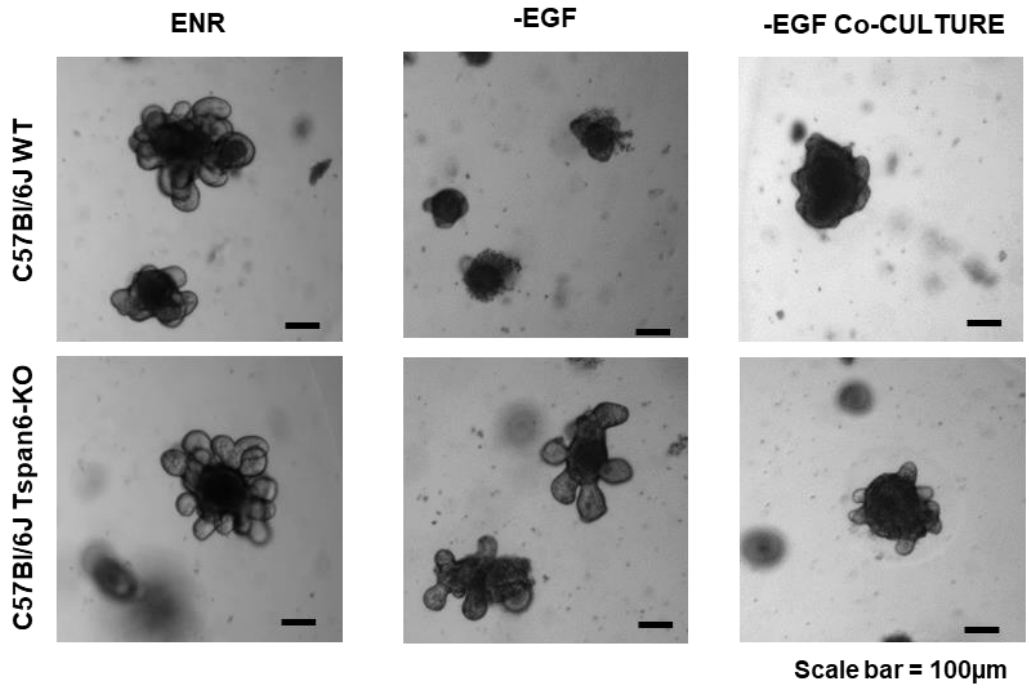

Figure 5-8. Tspan6 regulates secretion of an EGFR-ligand in mouse intestinal organoids. Phase-contrast images of WT and Tspan6 KO intestinal organoids cultured separately in complete growth media containing EGF, Noggin and R-spondin-1 (ENR), and in media lacking EGF (-EGF); and co-cultured together in media lacking EGF (-EGF co-culture). Images were taken on day 7 of culture. Co-culturing with Tspan6 KO organoids rescued WT organoids in –EGF conditions.

5.7 EGFR-ligand is secreted in extracellular vesicles by Tspan6 KO organoids

Tspan6 has been shown to have a role in the formation of multivesicular bodies (MVBs) and secretion of extracellular vehicles (EVs) (Guix, Sannerud *et al.* 2017), which may potentially carry membrane bound EGFR ligands, such as pro-TGFα (transforming growth factor α) and pro-AREG (amphiregulin) (Singh, Carpenter *et al.* 2016). Thus, it was further examined whether a "trans-stimulating proliferative effect" of Tspan6 KO organoids in EGF-free media involves EVs. As expected, media conditioned by the Tspan6 KO organoids grown under the EGF-free conditions

allowed proliferation and differentiation of both Tspan6 KO and WT organoids. Interestingly, after 5 days in culture Tspan6 KO organoids were larger when compared to WT, indicating the knock-in effect of EGFR ligands delivered by EVs to the vesicles secreted in an autocrine fashion (Figure 5-9). Strikingly, when conditioned media was depleted of EVs, WT organoids failed to form viable structures and rapidly underwent cell death (Figure 5-9). Tspan6 KO organoids remained unaffected although of a smaller size when compared to Tspan6 KO organoids grown in the presence of EVs. These data indicate that Tspan6 plays an important role in regulating EV-dependent activation of EGFR-mediated cell signalling.

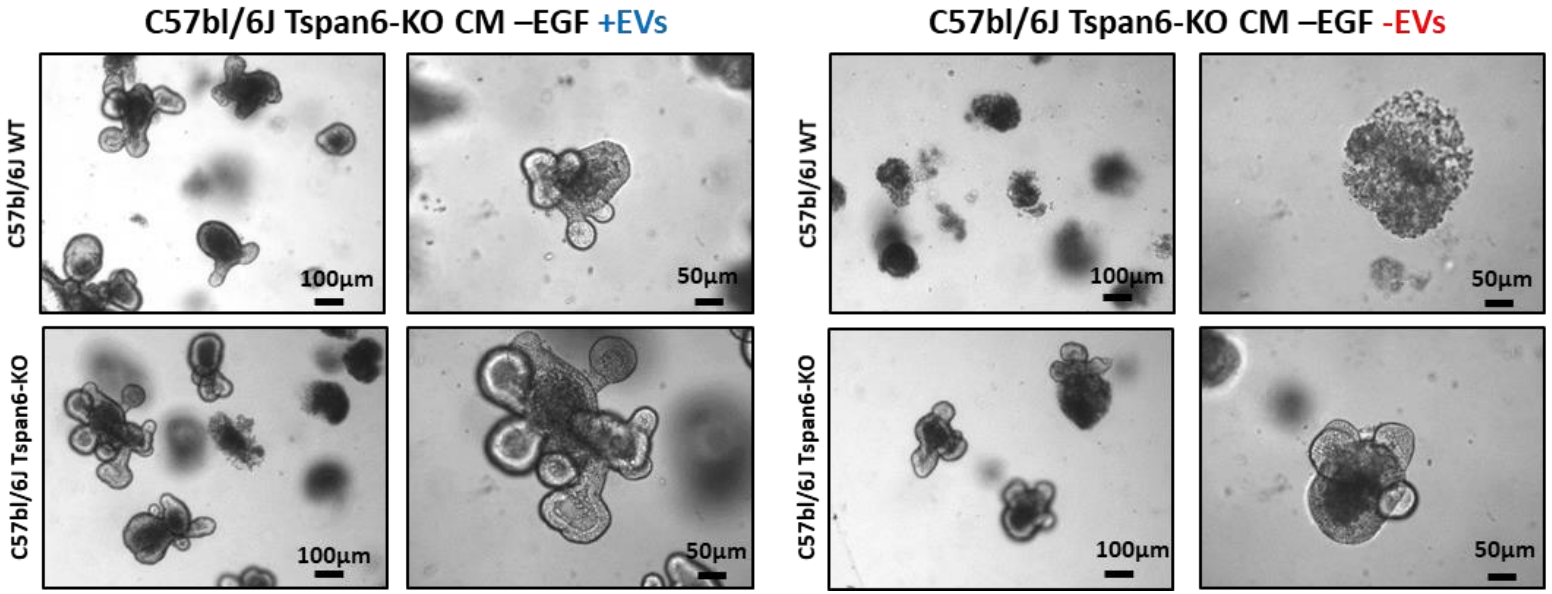

Figure 5-9. Tspan6 regulates secretion of an EGFR-ligand in extracellular vesicles. Phase-contrast images of WT and Tspan6 KO intestinal organoids cultured in the presence (+EVs) or absence (-EVs) of Tspan6 KO-derived extracellular vesicles. The conditioned media from Tspan6 KO organoids cultured for three days in EGF-free media was collected. Half of the conditioned media was depleted from the extracellular vesicles by ultra-centrifugation. Both parts (non-depleted and depleted of EVs) of the condition media were supplemented with essential media components excluding EGF and fed to WT and Tspan6 organoids. Images were taken after 7 days of culture. Tspan6 KO-derived extracellular vesicles facilitated formation and growth of WT organoids in –EGF conditions.

5.8 Tspan6 plays a role in secretion of extracellular vesicles

Extracellular vesicles are a heterogenous group of cell-derived vesicles that range from 30nm to 1µm in size and can be classified into exosomes (30-100 nm) derived from intracellular multivesicular bodies (MVBs) and ectosomes or micro-vesicles (>100nm) that are derived through shedding of the plasma membrane. To evaluate the quantity and the size of secreted vesicles conditioned media from organoids cultured in complete growth media and in media without EGF was analysed using nanoparticle tracking analysis (NTA) that accurately assesses the size and concentration using light-scattering characteristics of the particles. The analysis of the vesicles generated by WT grown under the control conditions revealed six peaks corresponding to 60 nm, 174 nm, 221 nm, 324 nm, 380 nm, and 469 nm, with the mean concentration of $1.27x10^8$ +/- $9.68x10^6$ particles/ml (Figure 5-10. A, C). The size range of vesicles produced by Tspan6 KO organoids was 39 nm, 86 nm, 177 nm, 321 nm, and 456 nm, with the mean concentration of $2.36x10^8$ +/- $2.64x10^7$ particles/ml (Figure 5-10. B, D). The concentration of macro-vesicles (i.e. 320 nm and 450 nm) did not differ between the samples. By contrast, concentration of vesicles of ~175 nm in the media conditioned by Tspan6 KO organoids was ~2-fold higher compared to media conditioned by organoids established from the WT animals (with $2.0x10^6$ and $1.1x10^6$ vesicles/ml respectively) (Figure 5-10. C, D). Moreover, this difference was even more pronounced when vesicles of 50-100 nm (vesicles corresponding to size of exosomes) were analysed: media conditioned by Tspan6 KO organoids contained $1.07x10^5$ +/- $6.9x10^3$ vesicles/ml versus $0.12x10^5$ +/- $2.6x10^3$ vesicles/ml in media conditioned by the WT organoids (Figure 5-10. E, F). Vesicles generated by WT and Tspan6 KO organoids

in EGF-free conditions were analysed in parallel. The distribution of vesicle size was different when compared to that seen for organoids grown under the control conditions, with three major peaks detected corresponding to the vesicles of ~220 nm, 540 nm, and 720 nm. An additional peak was recorded for WT organoids vesicles of 329 nm that was not seen in Tspan6 KO vesicle profile (Figure 5-10. G, J). The mean concentration of vesicles did not differ greatly between the samples, with $1.49x10^9$ +/- $3.23x10^7$ vesicles/ml and $1.13x10^9$ +/- $5.58x10^7$ vesicles/ml found in the media conditioned by WT and Tspan6 KO organoids respectively. Notably, examination of exosome-size vesicles (50 nm-100 nm) revealed that Tspan6 KO organoids produced ~900-fold more vesicles than the WT organoids (554.7 +/- 198 vesicles/ml vs. $4.5x10^4$ +/- 9.2 10^3 vesicles/ml) (Figure 5-10. K, L). These data indicate that Tspan6 participates in vesicle production and negatively regulates production of vesicles up to 100 nm size, namely exosomes, *ex vivo* in control and EGF-free conditions.

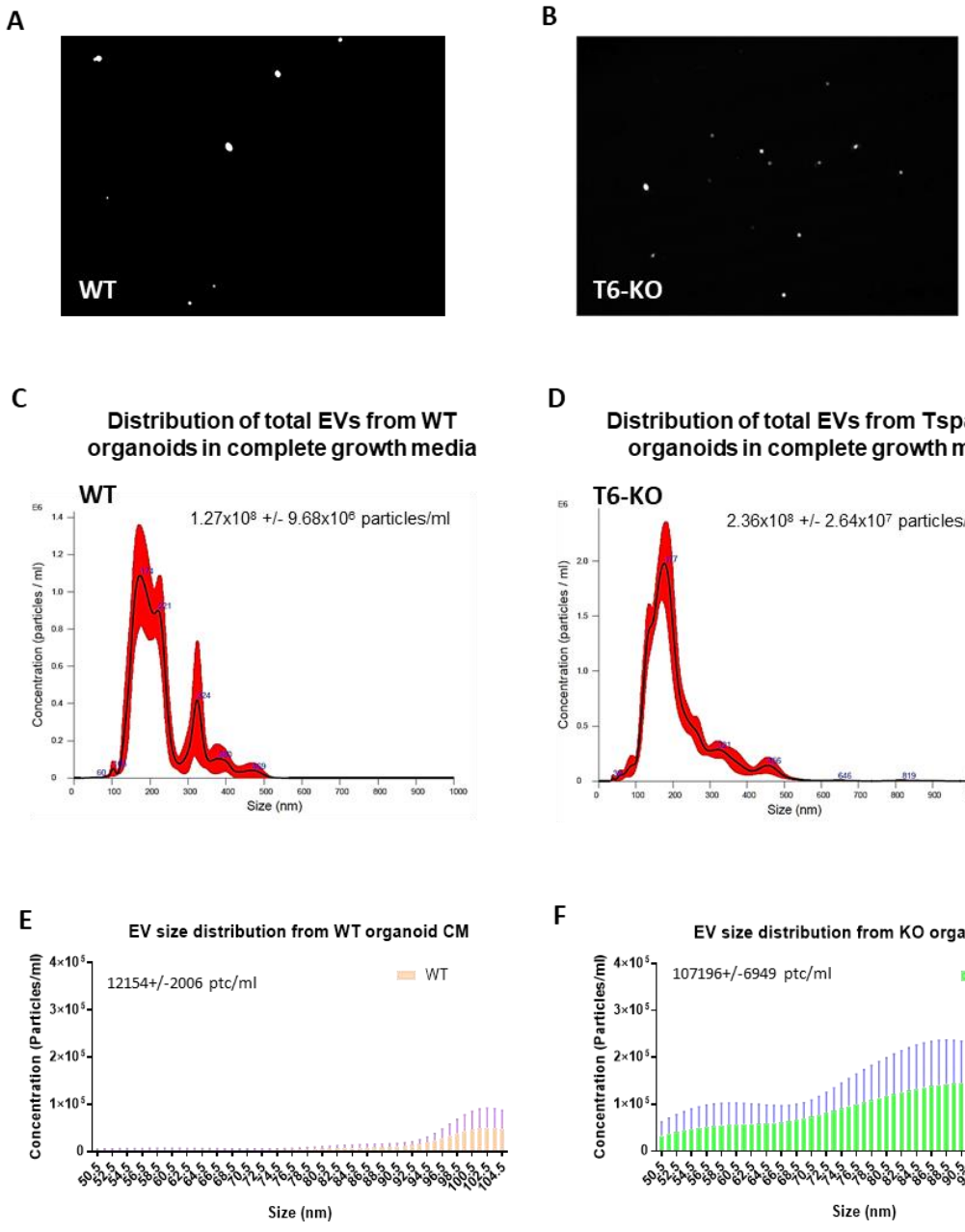
A
WT
B
T6-KO
C
Distribution of total EVs from WT organoids in complete growth media
WT
1.27x10⁸ +/- 9.68x10⁶ particles/ml
Concentration (particles / ml)
Size (nm)
D
Distribution of total EVs from Tspan6 KO organoids in complete growth media
T6-KO
2.36x10⁸ +/- 2.64x10⁷ particles/ml
Concentration (particles / ml)
Size (nm)
E
EV size distribution from WT organoid CM
12154+/-2006 ptc/ml
WT
Concentration (Particles/ml)
Size (nm)
F
EV size distribution from KO organoid CM
107196+/-6949 ptc/ml
KO
Concentration (Particles/ml)
Size (nm)

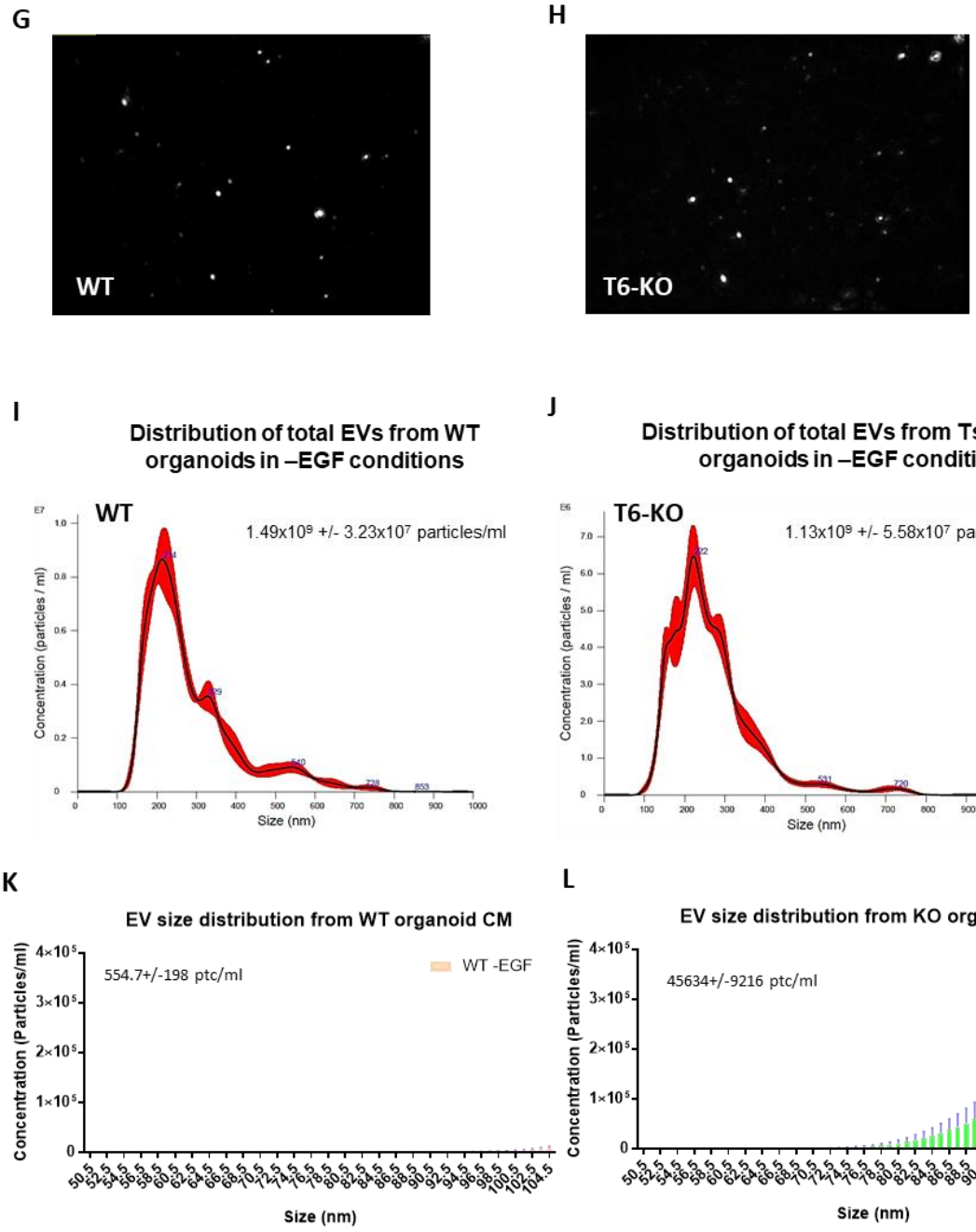
G
WT
H
T6-KO
I
Distribution of total EVs from WT organoids in –EGF conditions
WT
1.49x10⁹ +/- 3.23x10⁷ particles/ml
Concentration (particles / ml)
Size (nm)
J
Distribution of total EVs from Tspan6 KO organoids in –EGF conditions
T6-KO
1.13x10⁹ +/- 5.58x10⁷ particles/ml
Concentration (particles / ml)
Size (nm)
K
EV size distribution from WT organoid CM
554.7+/-198 ptc/ml
WT -EGF
Concentration (Particles/ml)
Size (nm)
L
EV size distribution from KO organoid CM
45634+/-9216 ptc/ml
T6-KO -EGF
Concentration (Particles/ml)
Size (nm)

Figure 5-10. Loss of Tspan6 results in higher production of extracellular vesicles. (A-B) NTA video screenshot of EVs derived from wild-type (WT) and Tspan6 KO organoids respectively cultured in complete organoid growth media. **(C-D)** Representative NTA profiles of total EVs derived from WT and Tspan6 KO organoids respectively cultured in complete organoid growth media. Total concentration of exosomes and ±SEM (red) are also indicated on the graph. **(E-F)** Exosomal fraction of EVs derived from WT and Tspan6 KO organoids respectively cultured in complete organoid growth media. Total concentration of exosomes and ±SEM (red) are also indicated on the graph. **(G-H)** NTA video screenshot of EVs derived from WT and Tspan6 KO organoids respectively cultured for 5 days in media lacking EGF. Total concentration of exosomes and ±SEM (red) are also indicated on the graph. **(I-J)** Representative NTA profiles of total EVs derived from WT and Tspan6 KO organoids respectively cultured for 5 days in media lacking EGF, presented as concentration vs. size histogram. Total concentration of exosomes and ±SEM (red) are also indicated on the graph. **(K-L)** Exosomal fraction of EVs derived from WT and Tspan6 KO organoids respectively cultured in complete organoid growth media. Total concentration of exosomes and ±SEM (red) are also indicated on the graph (n=1).

5.9 Tspan6 facilitates production of TGF-α

Extracellular vesicles and exosomes released by cells carry molecules and genetic material that are utilised for autocrine-dependent growth and for paracrine intercellular communications in normal and cancerous tissues (Abak, Abhari *et al.* 2018, Rashed, Bayraktar *et al.* 2017, Bobrie, Colombo *et al.* 2011). In this study Tspan6 has been shown to regulate the release of EGFR ligands in the form of extracellular vesicles that contribute to integrity and survival of intestinal organoids under EGF-free culturing conditions. It has been shown that TGF-α is secreted by the intestinal epithelium and an increase in its expression directly associates with development of sporadic colorectal neoplasms (Tu, Ahearn *et al.* 2015). Thus, it was examined whether TGF-α secretion is affected by Tspan6 expression by intestinal organoids. Specifically, ELISA was carried out on media conditioned by wild-type and Tspan6 KO organoids cultured in complete growth media or in media free of EGF. The analysis revealed that in both conditions WT organoids release approximately 6.55-fold less TGF-α than Tspan6 KO organoids, 47.1 +/- 5.91 pg/ml and 308.7 +/- 5.4 pg/ml respectively (Figure 5-11). These data indicate that extracellular vesicles released by Tspan6 KO organoids carry EGFR ligand, namely TGF-α.

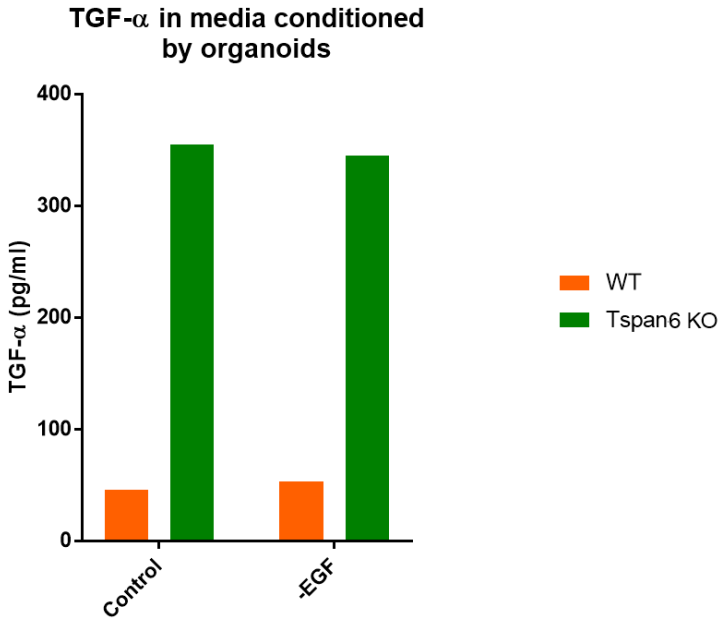

Figure 5-11. Loss of Tspan6 results in higher production of TGF-α. WT and Tspan6 KO intestinal organoids were cultured in complete growth media (control) and in the absence of EGF (-EGF) for 3 days and conditioned media was analysed by ELISA. The results were normalised to β-actin level measured by Western blot (n=1).

5.10 Loss of Tspan6 results in an increased number of Paneth cells in mouse intestinal organoids

In the intestinal stem cell crypt niche, Paneth cells produce EGF and TGF-α and are playing a major role in maintaining stem cells in the intestinal crypts (Clevers, Bevins 2013). To evaluate the role of Tspan6 on Paneth cell population the WT and Tspan6 KO organoids were stained for the Paneth cell marker Lysozyme using an immunofluorescence technique. Strikingly, the increased population of Paneth cells in the crypt domain of Tspan6 KO organoids was observed when compared to wild-type, with the mean of 2.7 +/- 0.28 and 4.6 +/- 0.54 Paneth cells per crypt (Figure 5-12). These data demonstrate that Tspan6 is involved in promoting the commitment to Paneth cell lineage in *ex vivo* organoid model.

5.11 Tspan6 deficiency results in Wnt-independent growth of mouse colon organoids

In mice, colon crypts lack Paneth cells; therefore, stem cells can regulate Wnt, MAPK and Notch pathways in autocrine fashion or with assistance of other cells, namely fibroblasts (Date, Sato 2015, Kabiri, Greicius *et al.* 2014). For the maintenance of the colonic organoid cultures, the addition of Wnt ligands are required, and Wnt3a – a potent canonical β-catenin dependent Wnt signalling pathway activator. To evaluate if the lack of Paneth cells in colonic crypts affects the ability of Tspan6 KO organoids to maintain their population and expansion, the organoids were derived from the colon of wild-type and Tspan6 KO mice and cultured in the media lacking Wnt3a and EGF. In agreement with previous reports, upon withdrawal of Wnt3a from the media, the wild-type organoids underwent cell-death after three days of culture. By contrast, Tspan6 KO colonic organoids were able to expand in this media and formed a heterogenous population of cystic and differentiated structures (Figure 5-13). In additional experiments both growth factors, Wnt3a and EGF, were withdrawn from the culture media. As predicted, wild-type colonic organoids failed to form viable structures resulting in cell death (Figure 5-13). However, colonic organoids lacking the functional Tspan6 were able to grow, proliferate and differentiate. Furthermore, the ability to modulate Wnt signalling was observed by both intestinal and colon organoids lacking functional Tspan6 (Figure 5-14). These data indicate that Tspan6 regulates MAPK and Wnt signalling pathways in organoids derived from intestinal and colonic tissue.

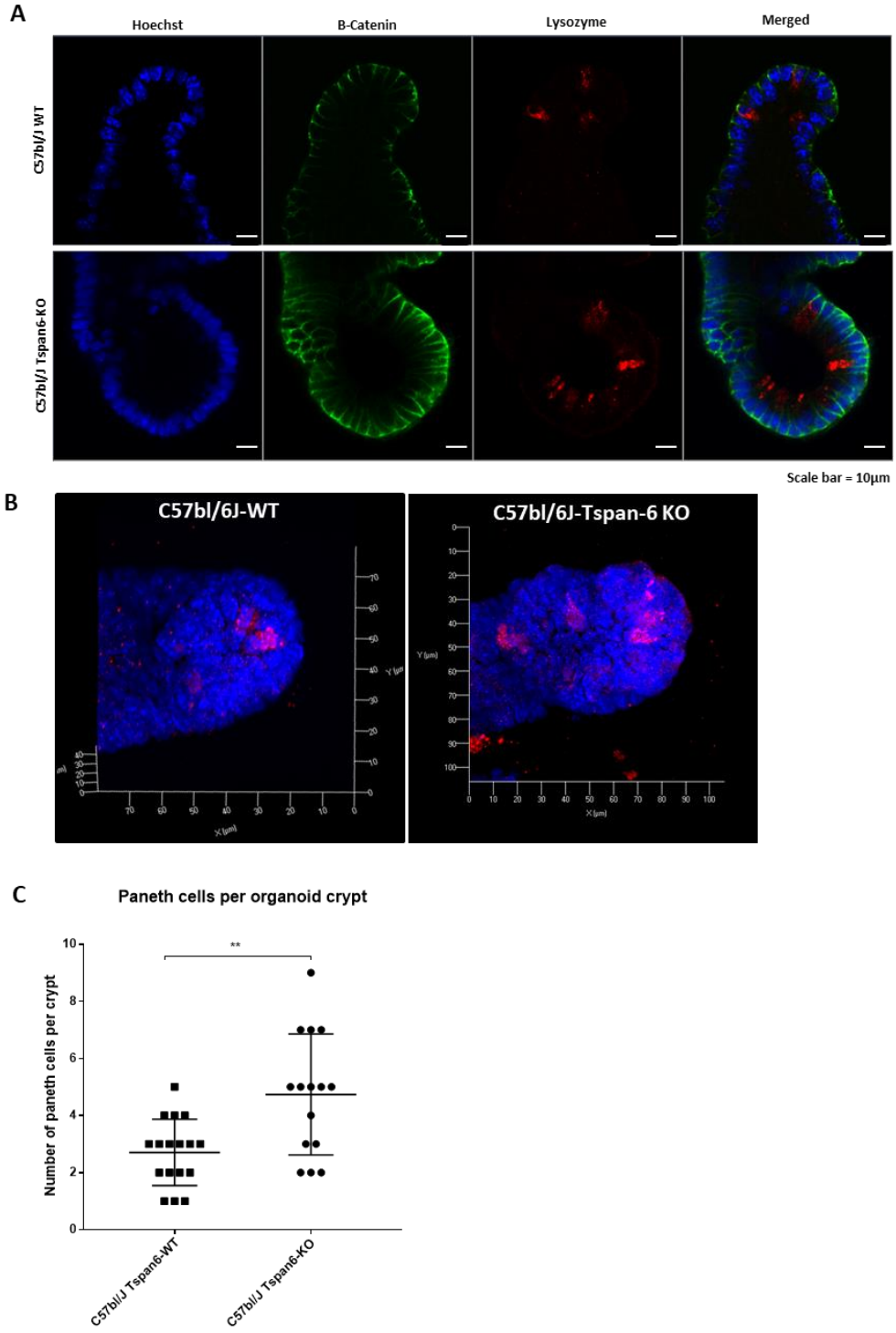

Figure 5-12. Loss of Tspan6 promotes Paneth cell expansion in mouse intestinal organoids. (A) A whole-mount immunostaining of WT and Tspan6 KO organoids after 5 days of culture. β-catenin (green) staining is more intense, and number of Paneth cells marked with lysozyme (red) is increased in Tspan6 KO organoids. Nuclei (blue) were counterstained with Hoechst 33342. **(B)** Maximum projection image showing distribution of Paneth cell is the intestinal organoid crypt. **(C)** Quantification of number of Paneth cells per organoid crypt in WT (n=15) and Tspan6 KO (n=14) organoids. Student t-test was performed for statistical analysis.

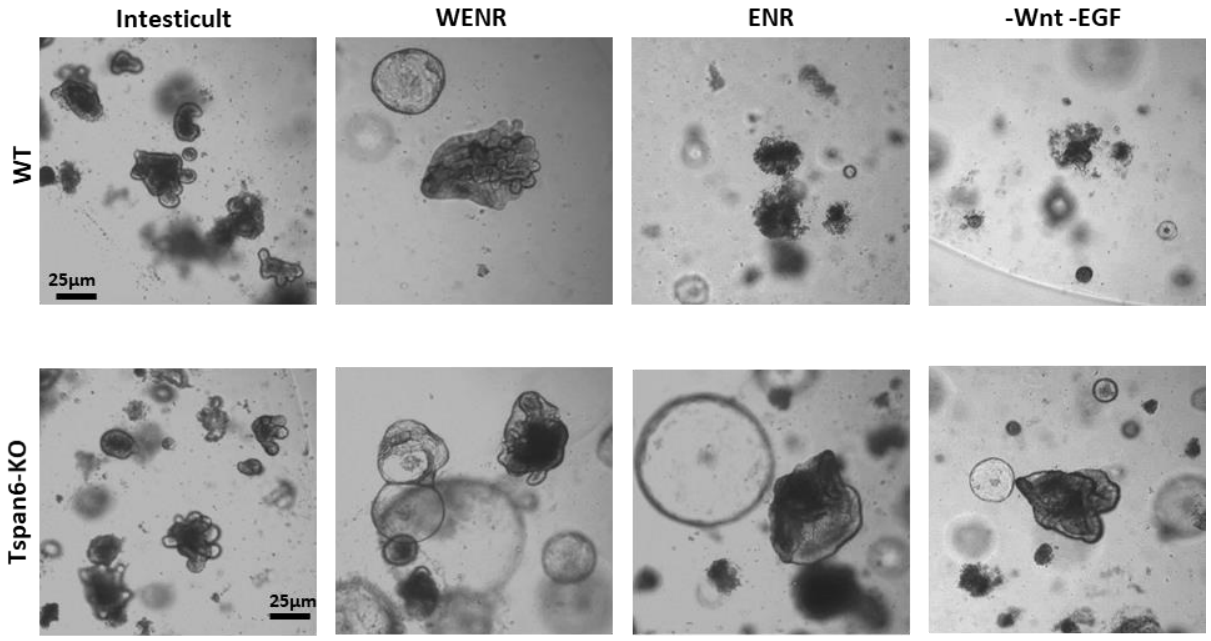

Figure 5-13. Loss of Tspan6 results in EGF- and Wnt-independent growth of mouse colonic organoids. Wild-type and Tspan6 KO colonic organoids were cultured in commercially available mouse intestinal organoid media (Intesticult), complete colon organoid growth media containing Wnt3a, EGF, Noggin and R-spondin-1 (WENR), organoid growth media lacking Wnt3a (ENR)and in media lacking both Wnt3a and EGF (-Wnt -EGF). In the absence of Wnt3a and both growth factors (Wnt3a and EGF) wild-type organoids undergo cellular death, and Tspan6 KO colon organoids preserve ability to grow and differentiate (n=3).

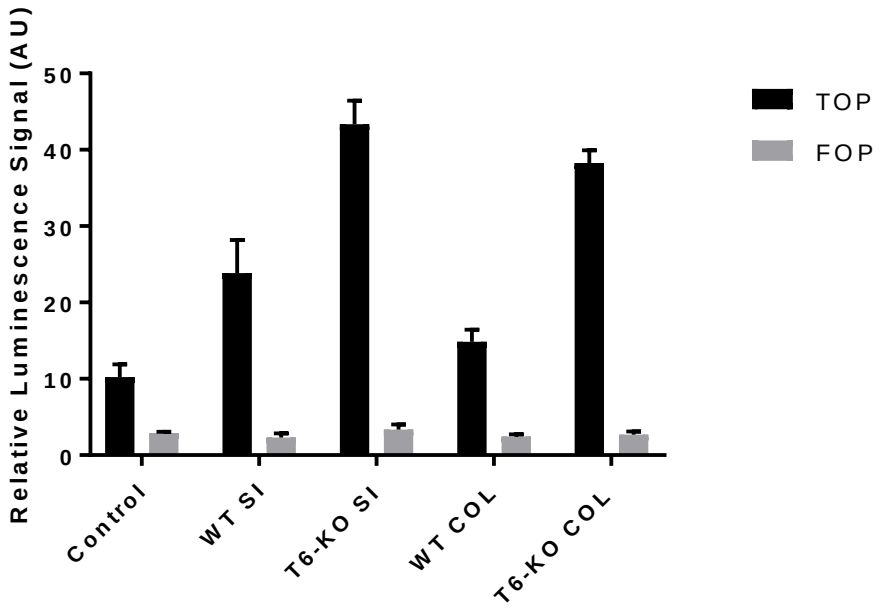

Figure 5-14. The loss of Tspan6 results in enhanced Wnt activity in mouse intestinal and colon organoids. The TOP/FOP analysis of HEK293 T cells stimulated with DMEM/F-12 media (control), or media conditioned by WT and Tspan6 KO intestinal (SI) and colonic (COL) organoids for 24 hours (n=1).

5.12 Discussion

The results described in this chapter demonstrate that loss of functional Tspan6 results in EGF-independent growth of mouse intestinal organoids. Further, the upregulation in activation of EGFR and ERK was observed by IHC. EGF and EGFR dependent signalling play an important role in intestinal cell homeostasis and regulate cell migration and proliferation (Date, Sato 2015, Suzuki, Sekiya *et al.* 2010). Accordingly, EGF withdrawal results in attenuation of intestinal organoid growth and decreased survival (Drost, van Jaarsveld *et al.* 2015, Matano, Date *et al.* 2015). Further support for the essential role of EGFR-dependent signalling in maintaining growth of intestinal organoids was provided by Sato and colleagues who demonstrated that organoid cultures with mutations in KRAS or PI3KCA, downstream effectors of the EGFR signalling cascade, can grow in EGF-free media (Sato, Stange *et al.* 2011, Matano, Date *et al.* 2015). Interestingly, the total level of EGFR in EGF-free conditions was elevated, suggesting upregulation of receptor in response to limiting ligand availability.

It was noticed that activation of p38 is induced in Tspan6 KO organoids in response to EGF withdrawal from the culture. While the biological significance of this observation in the context of Tspan6 KO animals requires further investigation, recent study demonstrated that p38 activation is associated with crypt formation and differentiation of intestinal organoids (Rodriguez-Colman, Schewe *et al.* 2017). Moreover, conditional deletion of p38α was also shown to affect differentiation of the secretory lineage of cells of the mouse intestinal epithelium (Otsuka, Kang *et al.* 2010). It is therefore possible that EGF-dependent regulation of p38 contributes to the phenotypic changes associated with deletion of Tspan6 in $APC^{min+/-}$ animals.

The growth inhibition by lapatinib, a highly specific EGFR inhibitor, demonstrated the essential role of EGFR-dependent signalling in growth of Tspan6 KO organoids. This data strongly suggested that survival of Tspan6 KO organoids in EGF-free media is dependent on the autocrine secretion of an EGFR-ligand, a notion, which was further supported by the rescue of WT organoid growth in EGF-free conditions in co-culture with Tspan6 KO organoids. Interestingly, a similar mechanism has been previously proposed in studies using mouse intestinal organoids deficient of negative EGFR regulators Lrig-1 and TRPV1 (Wong, Stange *et al.* 2012, de Jong, Takahashi *et al.* 2014).

In this study Tspan6 KO organoids were demonstrated to secrete TGF-α regardless of EGF presence in the culturing media, indicating that TGF-α release is not mediated by limiting exogenous EGFR ligand. TGF-α is ubiquitously expressed and binds to EGFR with a high affinity (Singh, Carpenter *et al.* 2016). In addition, TGF-α has been shown to play a role in intestinal homeostasis (Troyer, Luetteke *et al.* 2001). It has also been demonstrated that TGF-α expression is increased in HCT116 human colorectal cancer cell line in response to growth factor deficiency in culture, providing a mechanism of escape from growth factor dependency (Awwad, Sergina *et al.* 2003). The analysis of media conditioned by the wild-type and Tspan6 KO organoids revealed increased production of extracellular vesicles by Tspan6 KO organoids, specifically the significant increase in exosomes was observed in both control and EGF-free conditions. These data suggest that autocrine-dependent growth of Tspan6 KO organoids in EGF-depleted media is linked to EV-dependent increased production of TGF-α.

Extracellular vesicles are a class of cell-derived membrane coated particles that are secreted by various types of cells and implicated in mediating cell-cell communication (Abak, Abhari *et al.* 2018, Rashed, Bayraktar *et al.* 2017). Extracellular vesicles comprise of micro-vesicles, exosomes, exosome-like particles and apoptotic bodies (van Niel, Guillaume, D'Angelo *et al.* 2018, Mathivanan, Ji *et al.* 2010). Interestingly, a recent study demonstrated secretion of exosomes from organoid-like 3D cultures of 67 human cancer cell lines (Eguchi, Sogawa *et al.* 2017). Exosomes have been reported to contain lipids, membrane receptors, mRNA, microRNA, transcriptional factors, splicing factors, infectious particles, and growth factors, including EGFR-ligands HB-EGF, AREG and TGF-α (Quesenberry, Aliotta *et al.* 2015, Mathivanan, Fahner *et al.* 2012, Tauro, Greening *et al.* 2012, Balaj, Lessard *et al.* 2011, Bobrie, Colombo *et al.* 2011, Thery 2011, Al-Nedawi, Meehan *et al.* 2009, Simpson, Lim *et al.* 2009). Various studies demonstrated the ability of EVs and exosomes to mediate EGFR-mediated signalling. As such, expression of epidermal growth factor seven-transmembrane subfamily CD97 on exosomes was shown to affect proliferation and invasion of gastric cancer cells via exosome-mediated MAPK signalling pathway (Li, Liu *et al.* 2015). Another study demonstrated the capability of cancer-derived exosomes expressing a mutant epidermal growth factor receptor (EGFRvIII) to promote anti-apoptotic cellular responses and promote cell growth (Al-Nedawi, Meehan *et al.* 2008). Furthermore, the EGFR ligand amphiregulin (AREG) was shown to be expressed on exosomes derived from *KRAS* mutant DLD-1 colon cancer cells and induce cell invasiveness (Higginbotham, Demory Beckler *et al.* 2011). Interestingly, authors demonstrated that exosomal AREG is more potent in EGFR activation and augmenting invasiveness of recipient cells than its soluble

counterpart. Although the EVs in this experiment were not molecularly characterised, the inability of wild-type mouse intestinal organoids to grow in co-culture experiments with Tspan6 KO organoids suggests that TGF-α is present on EVs and serves as a strong mitogenic activator of EGFR in the intestinal epithelium.

What could the mechanisms underlying the role of Tspan6 in vesicle-associated production of TGF-α be? Tspan6 has been previously shown to participate in biogenesis of exosomal vesicles *in vitro* through the interaction with syntenin-1 (Guix, Sannerud *et al.* 2017). Interestingly, pro-TGF-α is able to directly bind to the PDZ2 domain of syntein-1 and is expressed on exosomes (Fernandez-Larrea, Merlos-Suarez *et al.* 1999). In another study it has been demonstrated that the N-terminus of TGF-α is expressed on the surface of exosomes, prompting effective binding to EGFR once released (Higginbotham, Demory Beckler *et al.* 2011). Unpublished data from Berditchevski's lab shows the direct interaction of syntenin-1 with Tspan6 via PDZ1 and TGF-α via PDZ2 domain *in vitro* (unpublished). These data strongly support the role of the Tspan6-syntenin-1 complex in biogenesis of TGF-α containing exosomes. Furthermore, syntenin-1 has been shown to associate with Src and such interaction is implicated in syntenin-1 mediated exosome biogenesis (Imjeti, Menck *et al.* 2017). Therefore, one can speculate that Tspan6 regulates exosomal production via interaction with syntenin-1.

Production of growth factors essential for stem cell maintenance (EGF, TGF-α, Wnt3a and Notch ligands) is executed by Paneth cells (Sasaki, Sachs *et al.* 2016). Paneth cells terminally reside at the bottom of intestinal crypt interspersed between stem cells (Date, Sato 2015, Clevers, Bevins 2013). Interestingly, it was found that

the number of Paneth cells in crypts of Tspan6 KO organoids is increased. To note, it has been shown that Wnt signalling is essential for Paneth cell terminal differentiation (Farin, Van Es *et al.* 2012, van Es, Jay *et al.* 2005, Andreu, Colnot *et al.* 2005). As such, the increased activation of Wnt signalling in Tspan6 KO organoids was demonstrated using TCF/LEF luciferase reporter assay. Importantly, Tspan6 KO colonic organoids exhibited Wnt3a and EGF independency in culture (Figure 5-13). These data indicate that Tspan6 additionally regulates Wnt signalling in the intestinal and colonic epithelium. Paneth cells are absent in colonic epithelium, therefore, there is a requirement for exogenous Wnt addition to the culture medium of mouse colonic organoids (Date, Sato 2015, Sato, Stange *et al.* 2011). It has been shown that colonic deep secretory cells (DSCs) that are intermingled between colonic stem cells are supporting stem cell homeostasis and promote organoid growth in the similar fashion to Paneth cells (Sasaki, Sachs *et al.* 2016). Tspan6 was previously shown to be expressed in Lgr5+ and Olfm4+ intestinal stem cells (Dalerba, Kalisky *et al.* 2011). Perhaps, the loss of Tspan6 in stem cells promotes Wnt activation, resulting in differentiation to Paneth cells in intestinal crypts and possibly DSCs in colonic crypts and regulates their secretory function facilitating bi-directional Wnt activation in mouse colonic organoids. The enhanced Wnt signalling in Tspan6 KO organoids can occur by one of the following mechanisms: 1) Tspan6 regulates Wnt ligand secretion (indeed, Wnt ligands have been previously shown to be expressed on exosomes (Zhang, L., Wrana 2014, Gross, Chaudhary *et al.* 2012, Koles, Budnik 2012)); 2) Tspan6 mediated EGFR activation results in robust crosstalk between Wnt and EGFR pathways. In this regard, it has been previously reported that KRAS synergistically enhances Wnt signalling in intestinal tumour cells (Janssen, Alberici *et*

al. 2006). Furthermore, Akt was shown to be hyperactivated in Tspan6 KO organoids and was previously reported to negatively regulate GSK3β, a kinase that mediates β-catenin proteasomal degradation, resulting in enhanced Wnt signalling as demonstrated by increased level of p-β-catenin at Thr41/Ser45 (He, Yin *et al.* 2007, Holmberg, Seidelin *et al.* 2017). Additionally, it was found that p38 MAPK is hyperactivated in Tspan6 KO organoids cultured in EGF-free conditions, which may negatively regulate GSK3β (Thornton, Pedraza-Alva *et al.* 2008), thus providing Tspan6 KO cells with an alternative mechanism for Wnt signalling upregulation in organoid cultures. EGFR has also been shown to directly interact with β-catenin: EGFR phosphorylates β-catenin at Tyr654, destabilising E-cadherin-β-catenin complex and releasing β-catenin for nuclear translocation (Georgopoulos, Kirkwood *et al.* 2014). Finally, in organoids lacking Tspan6 enhanced activation of Src family kinases was observed. Src may represent another point of Wnt and EGFR signalling convergence, as in study by Piedra and colleagues Src was shown to phosphorylate β-catenin at Tyr654, whereas Fer or Fyn phosphorylate β-catenin at Tyr142, resulting in disruption of β-catenin-α-catenin interaction at the adherent junctions and subsequent release of β-catenin into the cytoplasm (Piedra, Miravet *et al.* 2003).

In summary, the results described in this chapter demonstrate that Tspan6 negatively regulates Wnt and EGFR-mediated signalling via production of extracellular vesicles, which are likely to contain EGFR-ligand TGF-α. Furthermore, one can hypothesise that Tspan6 negatively regulates EVs production via association with syntenin-1.

6 RESULTS CHAPTER IV: TSPAN6 EXPRESSION REGULATES LUMENOGENESIS IN CACO-2 3D CYSTS

6.1 Introduction

The expression of Tspan6 was shown to regulate the EGFR-dependent signalling in mouse intestinal organoids, and Tspan6 knockout resulted in acquired EGF-independency in culture. To extend these observations the role of Tspan6 EGFR-dependent signalling using Caco-2 human colon epithelial cells was examined. Specifically, it was investigated whether expression of Tspan6 changes growth characteristics of Caco-2 in 2D and 3D cultures, and whether Tspan6 expression affects EGFR signalling and cellular response to the inhibitory effect of cetuximab, an EGFR inhibitor used in CRC treatment.

6.2 Caco-2 as a colorectal cancer model

To investigate the role of Tspan6 in CRC further Caco-2 cells were employed. These cells express relatively low levels of endogenous Tspan6 protein (Figure 6-1.C) and harbour only a small number of cancer-driving mutations including stop-gain mutation in APC (Q1367*) (Table 6-1). Importantly, Caco-2 cells are KRAS/BRAF wild-type and express EGFR protein (Figure 6-7). Therefore, the Caco-2 cell line is a good model for the study of Tspan6 role in EGFR-mediated signalling.

Table 6-1. Mutation profile of Caco-2 cell line. (Catalogue of Somatic Mutations in Cancer (COSMIC), accessed in May 2016).

Caco-2 Mutation Profile			
Gene (name)	**CDS syntax**	**AA syntax**	**Mutation type**
CTNNB1	c. 734G>C	p. G245A	Substitution - Missense (pathogenic)
SMAD4	c. 1051G>C	p. D351H	Substitution - Missense
APC	c. 4099C>T	p. Q1367*	Substitution - Missense

6.3 Tspan6 expression facilitates lumen formation in Caco-2 cultured in 3D ECM

Stable expression of FLAG-tagged Tspan6 in Caco-2 cells was established by lentiviral transduction to generate Caco-2-Tspan6 cell line (Figure 6-1.A-B). A control cell line Caco-2-pLVx was also established by transducing Caco-2 cells with viral particles carrying an empty pLVx-puro (puromycin resistant) plasmid. As indicated in Figure 6-1.C the level of expression of Flag-tagged Tspan6 protein in a pool of transfected Caco-2-Tspan6 cells was 14-fold higher than in Caco-2-pLVx cells. Subsequently, the effect of Tspan6 expression on cellular behaviour of Caco-2 cells was analysed. The expression of Tspan6 did not change the morphology of Caco-2 cells when cultured under standard 2D conditions (Figure 6-1.D). Furthermore, cell proliferation under standard culturing conditions on plastic in the complete growth medium was not affected either (Figure 6-2). Assessing cell characteristics in the three-dimensional extracellular matrix (Matrigel™) revealed that Caco-2 cells display certain characteristics of differentiating enterocytes and form organised polarised

colonies with a central lumen, often referred to as cysts (Ivanov, Hopkins *et al.* 2008, Jaffe, Kaji *et al.* 2008). It was found that Caco-2-Tspan6 colonies form a well-developed central lumen at a faster rate than the control Caco-2-pLVx cells ($p<0.0001$) (Figure 6-3.A). Specifically, at day five ~82% of Caco-2-Tspan6 colonies and ~ 34% of Caco-2-pLVx colonies have a discernible lumen (Figure 6-3.B). To examine if expression of Tspan6 results in higher cell proliferation and, therefore, enhanced maturation of Caco-2 3D cysts, the growth rate of colonies was analysed using CellTiter Glo-3D (Promega). It was found that proliferation of Caco-2 cells in 3D ECM is not affected by expression of Tspan6 (Figure 6-3.C). Therefore, enhanced lumen formation of Caco-2-Tspan6 colonies is a result of other cellular processes affected by the expression of Tspan6.

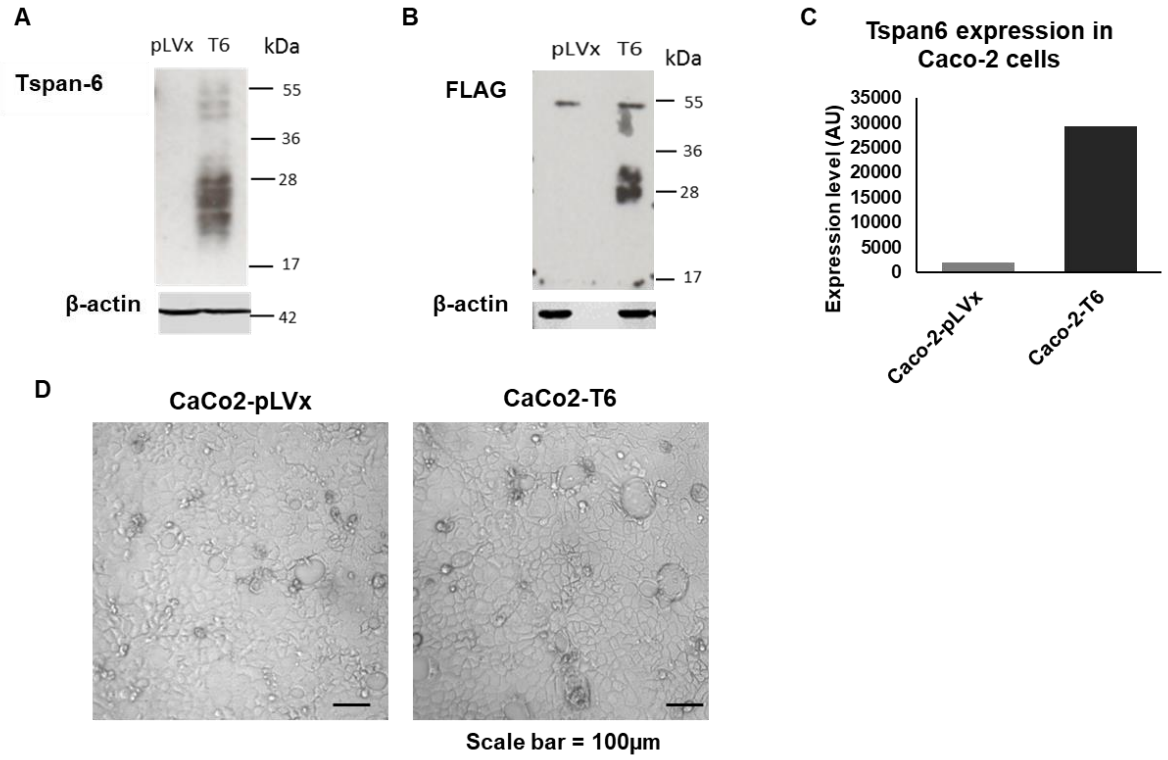

Figure 6-1. Expression of human TSPAN6 in Caco-2 colorectal cancer cell line. Caco-2 cells were transduced with control (pLVx) or human Tspan6 (T6) packaged lentivirus and stable cell lines were established using puromycin (2.5 µg/ml) selection for 7 days. Expression of FLAG-TSPAN6 in Caco-2 (expected size 28kDa) detected by **(A**) anti-Tspan6 antibody and **(B)** anti-FLAG antibody**. (C)** Expression level of Tspan6 in a stably transfected pool of Caco-2-pLVX and Caco-2-Tspan6 (T6) cells. The expression was normalised to β-actin expression. **(D)** Phase-contrast images of Caco-2 cells expressing pLVx and Tspan6 vectors.

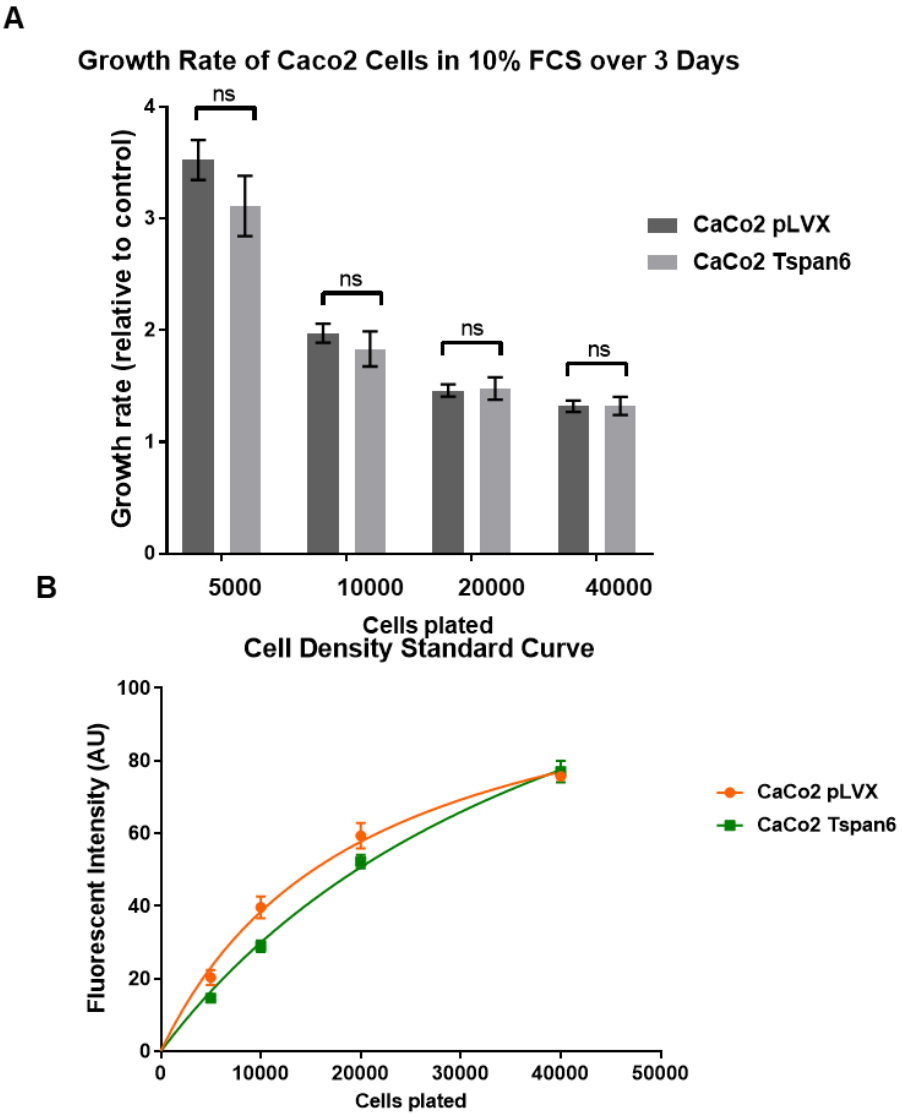

Figure 6-2. Tspan6 does not affect proliferation of Caco-2 cells. (A) Effect of Tspan6 on cell proliferation in high serum (10% FCS) conditions. For high serum conditions no significant difference was found between Caco-2 pLVX and Caco-2 Tspan6 cell proliferation, p=0.2146, p=0.4326, p=0.8725, p>0.9999 for cells plated at densities 5000, 10000, 20000, and 40000 cells/well correspondingly. **(B)** Cell density standard curve. Caco-2 cells were plated at densities 5000, 10000, 20000, and 40000 cells/well in 96-well plate and the fluorescence intensity was measured using Alamar Blue assay. The high cell density (40000 cells) reaches the saturation of fluorescent intensity indicated by the plateauing of the standard curve. All results are expressed as ratio of experimental to control (day 0) fluorescent intensities. Vertical bars represent the mean of triplicate assays and error bars are plotted as ± SEM. Non-parametric two-tailed unpaired Student T-test was used for statistical analyses (n=3).

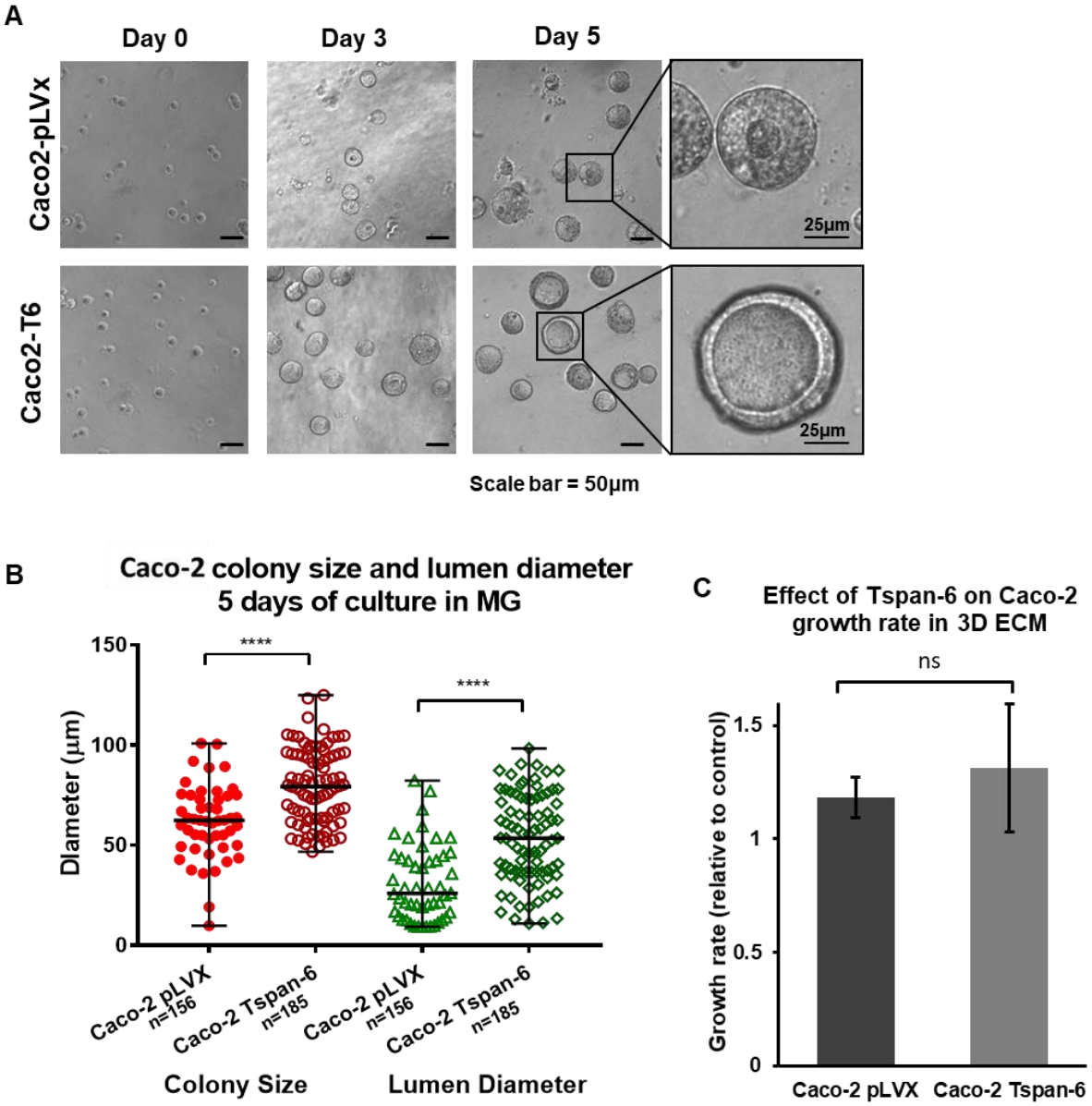

Figure 6-3. Tspan6 promotes single lumen formation at a higher rate in colonies of Caco-2 cells grown in three-dimensional ECM. (A) Representation of the development of Caco-2 cysts throughout five days of culturing in 3D ECM. Caco-2 cells expressing Tspan6 form larger lumen at an earlier stage than control cells (day 5) when cultured in 3D ECM**. (B)** Tspan6 expressing cells formed colonies of bigger size ($p<0.0001$) with median colony size of 79.3 µm and 62.4 µm in control cells; Tspan6 expressing colonies develop larger lumens than control cells ($p<0.0001$) after five days of culture in 3D ECM with median lumen diameter of 53.5 µm and 25.9 µm respectively. Images were acquired by phase contrast microscopy and images of 25 fields were taken for subsequent analysis. Lumen formation was examined by measuring colony and lumen diameter in ImageJ. Error bars represent median with range. Mann-Whitney non-parametric t-test was used for statistical analyses. **(C)** Effect of Tspan6 on cell proliferation in 3D ECM. Cell viability was measured using CellTiter Glo-3D viability assay. Results are shown as growth rate relative to day 0 measurement and expressed as the mean of triplicate assays, error bars are plotted as ± SEM (n=3).

6.4 Tspan6 does not affect polarisation of Caco-2 cells

Lumen formation in Caco-2 3D cysts occurs due to cellular polarisation as early as the first cell division (Taniguchi, Shao *et al.* 2015, Rodriguez-Boulan, Macara 2014, Jaffe, Kaji *et al.* 2008, Martin-Belmonte, Mostov 2008). First, the localisation of Tspan6 in Caco-2 cells was assessed. It was found that Tspan6 is strongly expressed at the basal membrane of 3D cysts, and weaker enrichment at lateral and apical surfaces (Figure 6-4). Secondly, the markers of cellular polarity were examined in confluent 2D and 3D Caco-2 cultures. Caco-2 two-dimensional monolayers are intensively used for studies of intestinal polarity due to the ability to spontaneously polarise in a tight monolayer (Schneeberger, Roth *et al.* 2018). The expression of Tspan6 did not result in altered polarisation of 2D cell monolayer (Figure 6-5). Both cell lines exhibited polarity as early as 10 days of culture, showing formed tight junctions at the apical surface (ZO-1), Na^+/K^+-ATPase at the basolateral surface and integrin-α6 at the basal surface of polarised Caco-2 monolayer. In agreement with the results of 2D culture experiments, it was found that Tspan6 does not affect cellular polarity in Caco-2 3D cysts (Figure 6-6). In both cell lines enhanced F-actin accumulation at the apical surface facing a central lumen was observed. Moreover, no apparent differences were seen when colonies were stained with antibodies recognising tight junctions (ZO-1) or adherens junctions (E-cadherin). A characteristic punctate pattern of distribution of ZO-1 at the apical surface and marked localisation of E-cadherin at the basolateral surface were seen irrespectively of the expression of Tspan6.

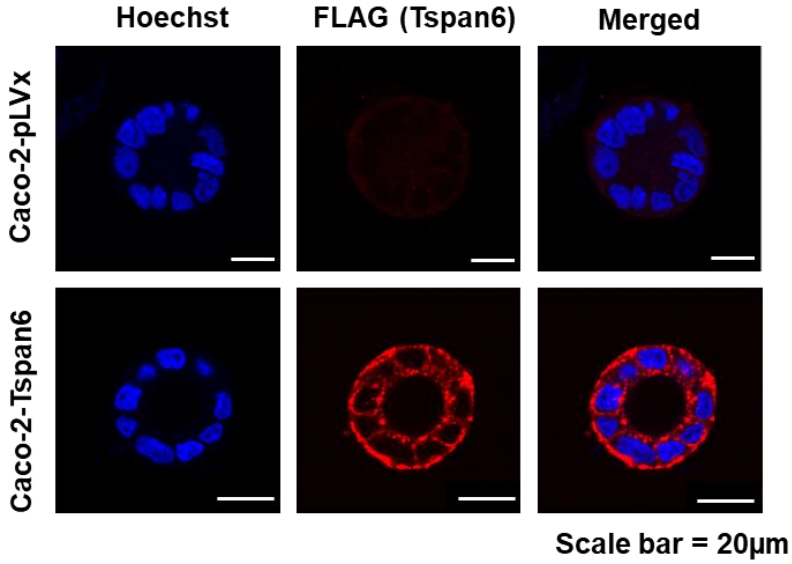

Figure 6-4. Localisation of Tspan6 in Caco-2 3D cysts. Single confocal section through the middle of Caco-2 cysts stained for DNA (blue) and FLAG (red).

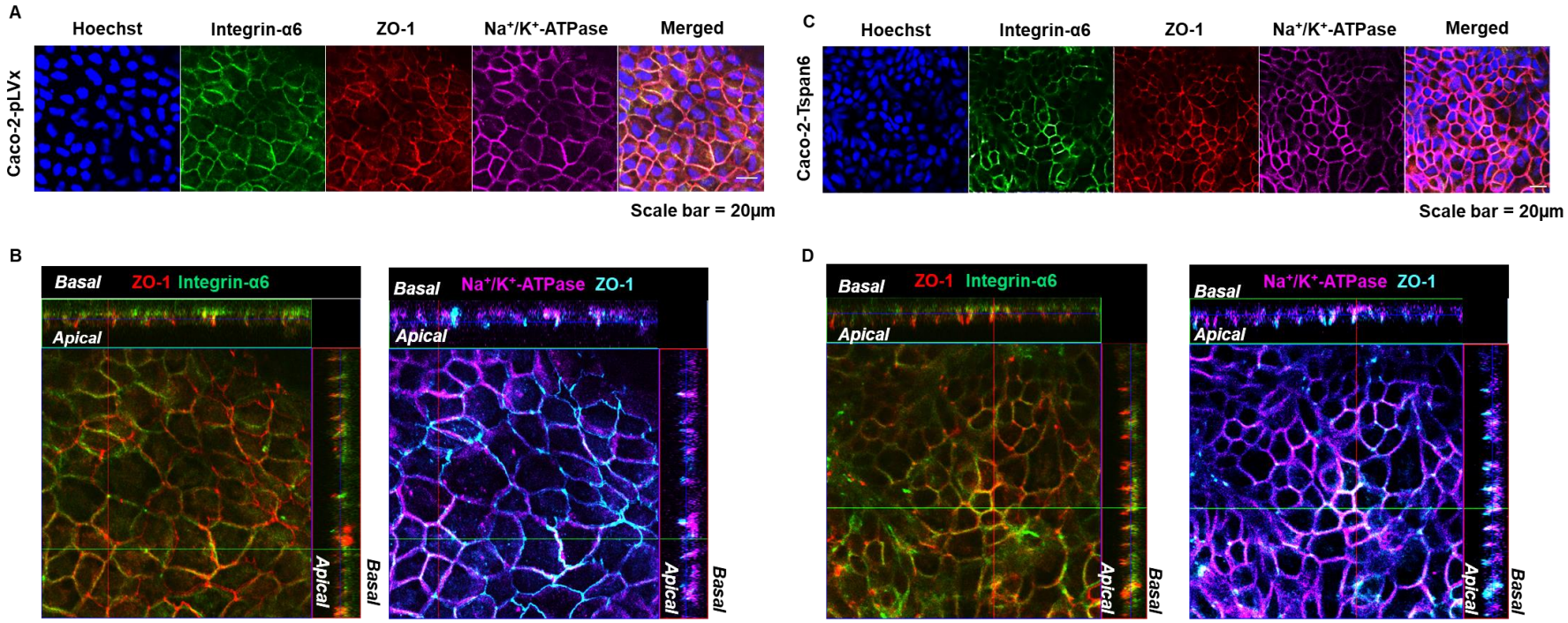

Figure 6-5. Expression of Tspan6 does not affect polarisation of Caco-2 2D monolayer. The immunofluorescent image of Caco-2 pLVx **(A)** and Caco-2 Tspan6 **(C)** polarised monolayer stained for DNA (blue), integrin-α6 (green), ZO-1 (red), and Na^+/K^+-ATPase (magenta). **(B, D)** Z-stack image analysis of protein spatial organisation in Caco-2 polarised 2D monolayer expressing pLVx **(B)** and Tspan6 **(D).** The red and green lines in the xy plane indicates the site from which the xz image was constructed.

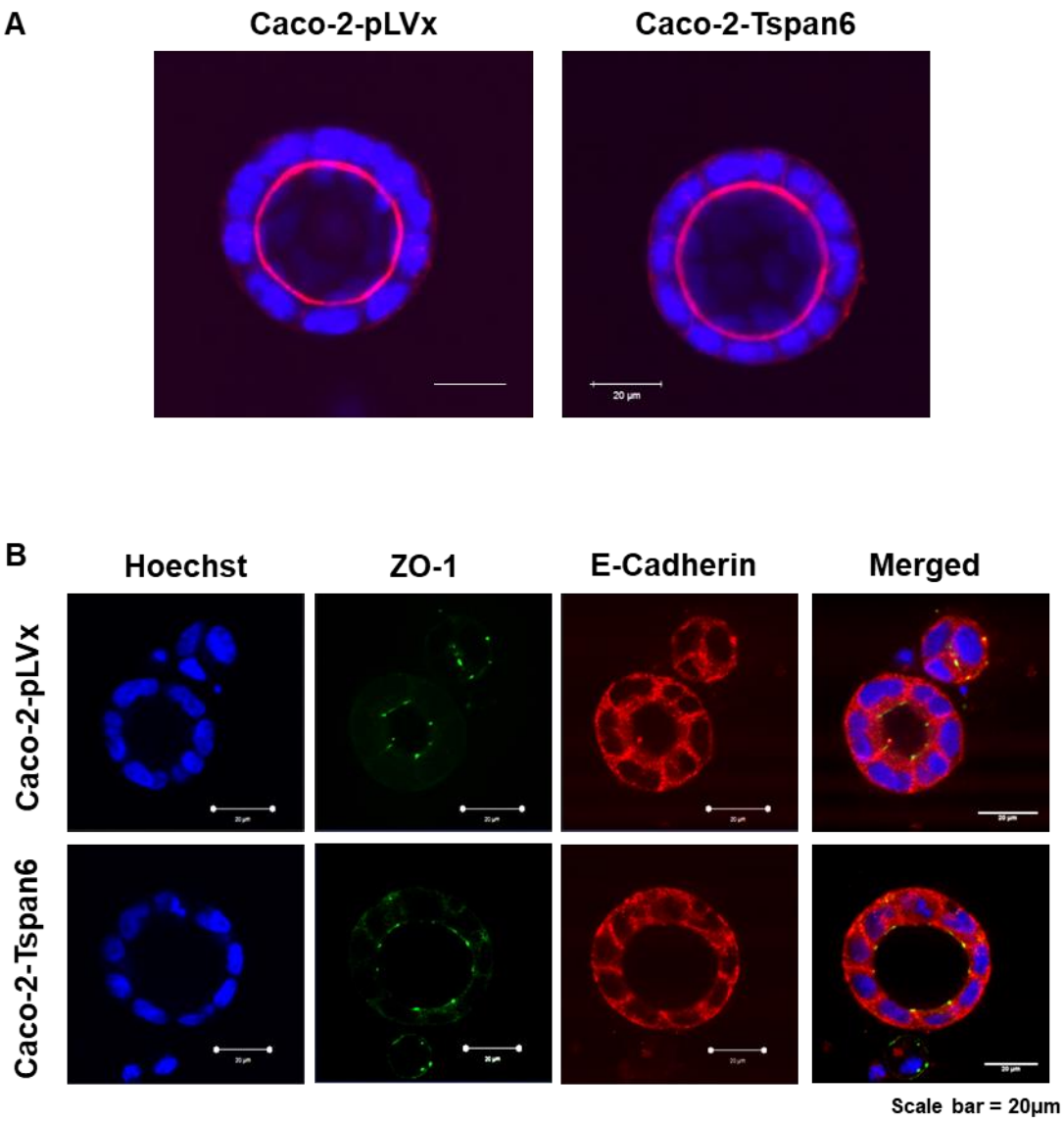

Figure 6-6. Expression of Tspan6 does not affect polarisation of Caco-2 3D cysts. (A) The immunofluorescent image of single confocal section shows that cellular polarisation and apical F-actin ring (red) formation is preserved in Caco-2 cells expressing Tspan6; Hoechst 33342 marks nuclei (blue). **(B)** Single confocal section through the middle of Caco-2 cysts stained for DNA (blue), ZO-1 (green), and E-Cadherin (red).

6.5 Tspan6 facilitates lumen formation in EGFR-dependent manner

The RNAseq data analysis of the mouse intestinal polyps derived from $APC^{min/+}$ and $APC^{min/+}Tspan6^{-/y}$ double mutant mice, as well as the evidence of acquired EGF-independent growth of Tspan6 KO mouse intestinal organoids prompted us to investigate if expression of Tspan6 regulates cell signalling via EGFR in Caco-2 cells. The expression levels of the receptor and ligand-induced phosphorylation at Tyr1068 were examined. The total levels of EGFR was consistently higher (by ~1.5-fold) in Caco-2-Tspan6 cells when compared to the control Caco-2-pLVx cells. In spite of this, the relative level of activation (i.e. ratio of pEGFR to the total EGFR) appeared to be higher in Caco-2-pLVx cells (Figure 6-7.A-B). Strikingly, these differences were even more pronounced when cells were cultured in 3D ECM: here the expression of EGFR was ~9-fold higher in Tspan6–expressing cells when compared to the control, and conversely, a greater level of activation (approximately 4-fold) was seen in the control, Caco-2-pLVx cells (Figure 6-7.D). In addition, EGFR appeared to localise to lateral and basal surfaces of 3D Caco-2 cysts similarly to Tspan6 expression pattern (Figure 6-7.E).

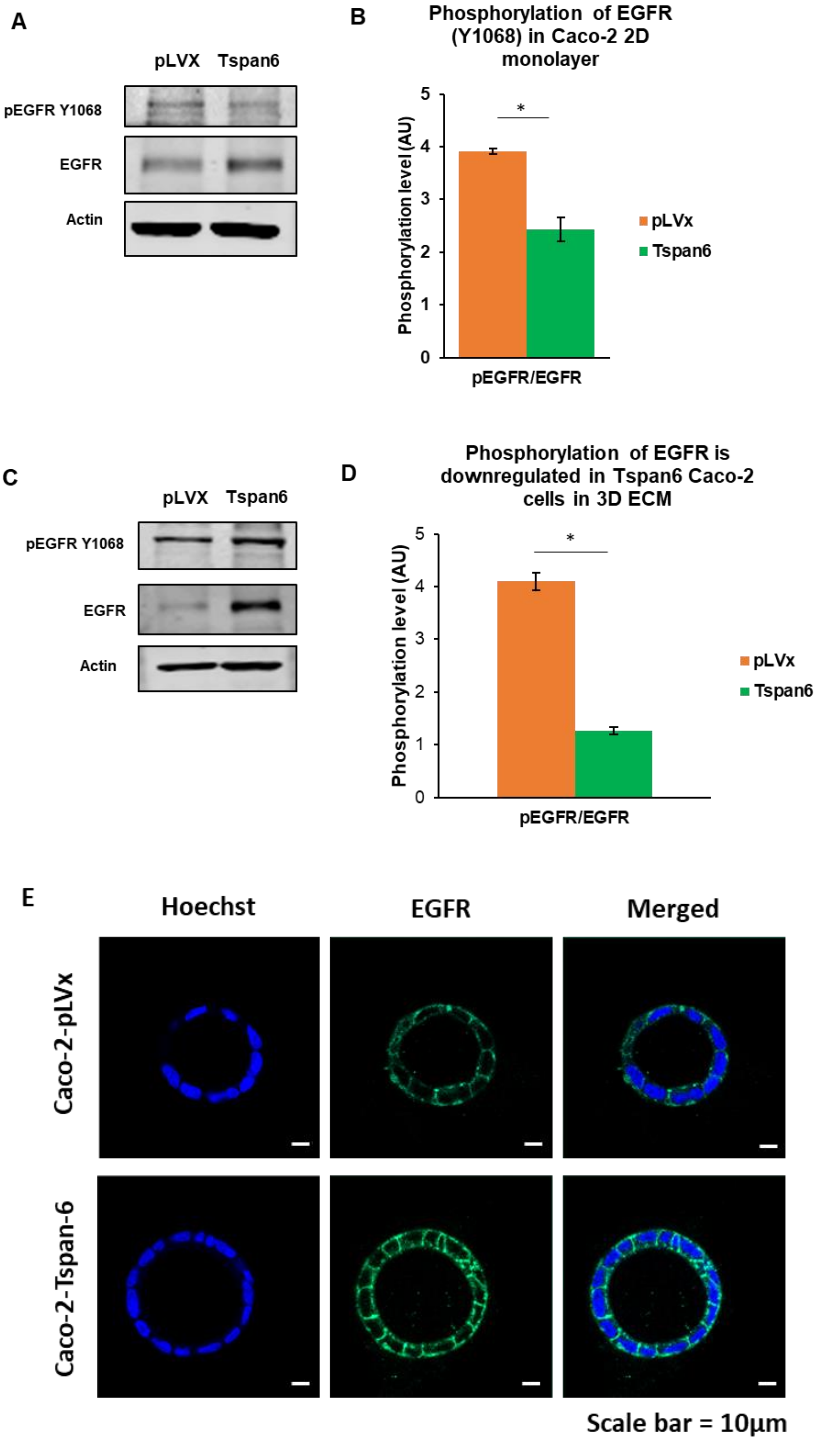

Figure 6-7. The analysis of EGFR expression in Caco-2 cells. (A, C) Western blot representing expression and activation of EGFR (by phosphorylation at Tyr1068) in Caco-2 two-dimensional monolayer **(A)** and three-dimensional cysts cultured in Matrigel™ for 5 days **(C). (B, D)** The level of EGFR activation in Caco-2 pLVx and Tspan6-expressing cells cultured in 2D **(B)** and 3D ECM **(D).** EGFR is hyperactivated in 2D cultures (n=3, p=0.0066) and in 3D cultures (n=2. P=0.0079). The resuls are expressed as a ratio of signal intensities to total level of EGFR in cells normalised to β-actin. Bar chart represents a mean of triplicate (for 2D) and duplicate (for 3D) assays and error bars are plotted as ±SEM. **(E)** Single confocal section through the middle of Caco-2 cysts stained for DNA (blue) and EGFR (green).

Further, to examine if attenuation of EGFR activation in the presence of Tspan6 correlates with lumen formation in Caco-2 cysts, the effect of EGFR stimulation with EGF and inhibition with cetuximab was assessed. Cetuximab is a monoclonal antibody against EGFR, which recognises the extracellular portion of the receptor and inhibits the receptor-ligand interaction. Firstly, Caco-2 cells were cultured in 3D Matrigel™ in the presence of EGF (10 ng/ml) or a vehicle (control). The stimulation of Caco-2-pLVx with EGF resulted only in slight changes to the number of lumen-forming colonies: 28% of lumen bearing colonies in EGF-treated cells versus 34% in control conditions (Figure 6-8.A-D). The lumen formation of Caco-2-Tspan6 cells, however, was greatly impaired upon stimulation with EGF, resulting in reduction from 82% to 43% of lumen-bearing colonies (Figure 6-8.A-D). This observation indicated that EGFR activation is linked to lumen formation and suggested EGFR-dependent signalling pathways are negatively regulated by Tspan6 under normal growth conditions. In the converse experiments, Caco-2 cells were cultured in 3D Matrigel™ in the presence or absence of cetuximab at different concentrations (10 µg/ml, 25 µg/ml and 100 µg/ml). Little if any difference in cell growth and lumen formation was observed when 10 µg/ml of cetuximab was administered on cells when compared to control conditions (data not shown). Culturing cells with 100 µg/ml cetuximab resulted in near complete growth inhibition of Caco-2 cells. By contrast, inhibition of EGFR with 25 µg/ml cetuximab led to enhanced lumen formation in control cell line (Caco-2-pLVx) and did not affect lumen-formation in Caco-2-Tspan6: 62% and 70% of analysed colonies in the control cell line and cells expressing Tspan6, respectively, were presented with the lumen (Figure 6-8.E-F). Taken together, these data demonstrate that the expression of

Tspan6 negatively regulates EGFR activation that in turn facilitates lumen formation in Caco-2 3D cysts and this process is likely to be mediated by ligand binding to EGFR.

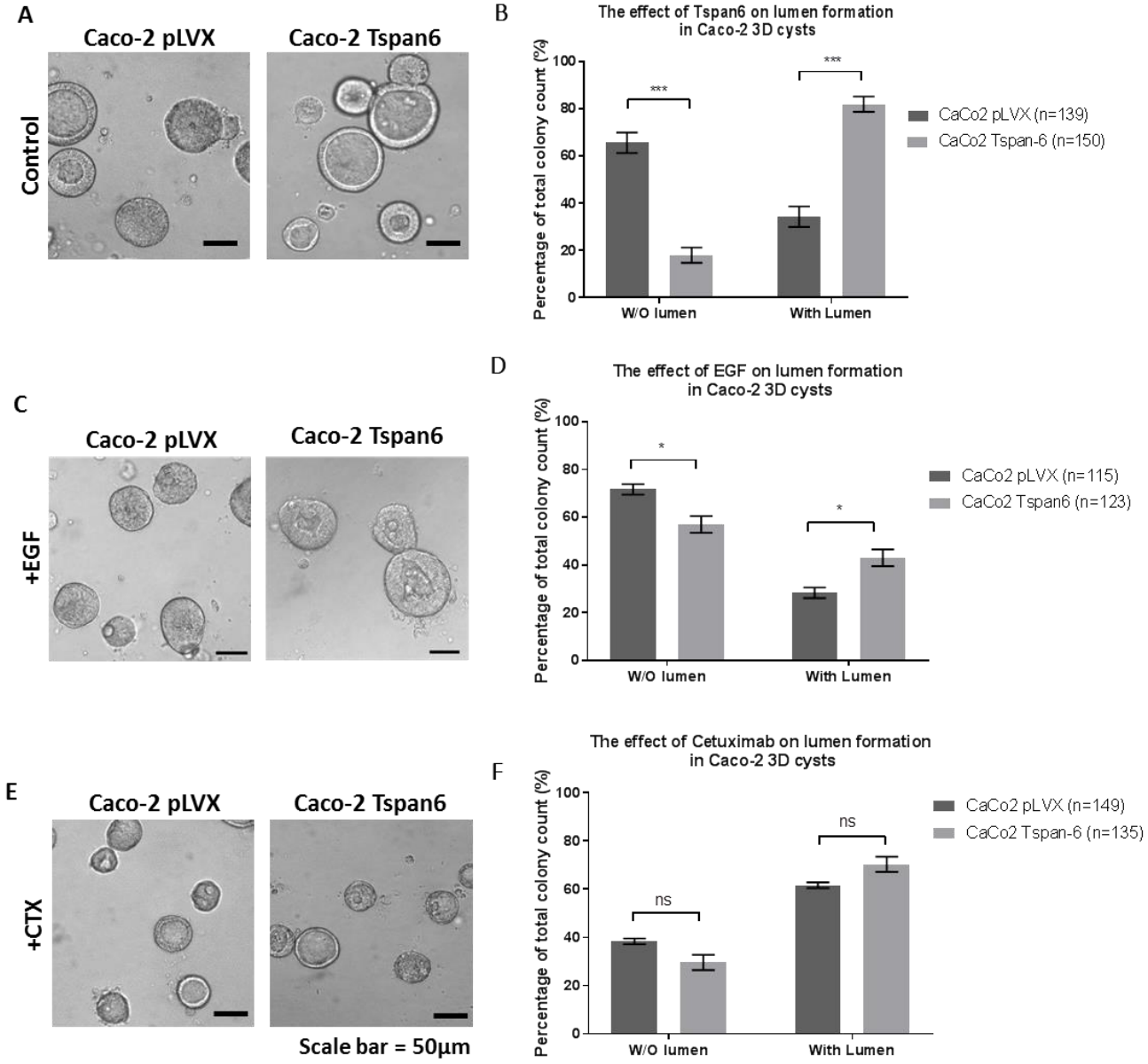

Figure 6-8. Tspan6 regulates EGFR-dependent growth of Caco-2 cells in 3D ECM. (A) Caco-2 cells expressing Tspan6 form a well-developed central lumen at a faster rate than control cells in 3D ECM colonies. **(B)** Tspan6 expression results in more colonies forming central lumen after five days of culture (p=0.00090). Number of colonies with and without lumen formed by pLVx and Tspan6 expressing Caco-2 cell line and expressed as percentage of total colonies counted. Quantification was carried out after 5 days of culturing. **(C)** Activation of EGFR with EGF results in slower development of central lumen in Caco-2 Tspan6 3D cysts. **(D)** EGFR hyperactivation by EGF results in reduction of Caco-2-Tspan6 lumen-bearing colonies; Tspan6 expressing cells formed more colonies with lumens than control cells (p=0.0239). **(E)** Inhibition of autocrine activation of EGFR with cetuximab (25µg/ml) led to enhanced lumen formation in control cell line and did not affect lumen-formation in Caco-2-Tspan6**. (F)** The lumen formation has increased in Caco-2-pLVx 3D cysts upon EGFR inhibition with cetuximab and no difference in lumen formation between pLVx and Tspan6 cells was detected (p=0.0633). Bar charts represent mean of triplicate assays and error bars are plotted as ± SEM.

6.6 Tspan6 regulates EGFR-dependent signalling in Caco-2 cells

To investigate the role of Tspan6 in EGFR-mediated cell responses, the signalling profile of Caco-2 cells in response to EGFR activation by EGF was evaluated in more detail. Control and Tspan6 expressing Caco-2 cells were stimulated with 10 ng/ml EGF for 10 min, 20 min, 40 min and 60 min and the phosphorylation of EGFR, ERK 1/2, Akt, and p38 was analysed by Western blot (Figure 6-9). In addition, β-catenin-mediated signalling was also examined. Upon EGF administration a rapid activation of EGFR (as indicated by phosphorylation at Tyr1068) is taking place in both Caco-2-pLVx and Caco-2-Tspan6 cells. During the time course of EGF stimulation, a trend in low levels of phosphorylation of EGFR in Caco-2-Tspan6 cells was observed at all time points when compared to Caco-2-pLVx. A similar trend was noticed when phosphorylation of ERK 1/2 and Akt, well-established downstream effectors of EGFR, was examined.

Upon ligand-binding, EGFR is phosphorylated at multiple residues that in turn recruit cytoplasmic molecules to regulate EGFR-mediated cellular responses (Wee, Wang 2017). Phosphorylation at Tyr1045 results in the recruitment of cCbl to EGFR (via Grb2) and subsequent ubiquitin-mediated receptor degradation (Sigismund, Algisi *et al.* 2013). In this regard, the phosphorylation of EGFR at Tyr1045 and cCbl at Tyr774 were higher in Tspan6 expressing cells following EGF stimulation. Interestingly, a significantly higher increase in cCbl phosphorylation ($p=0.0092$) in Caco-2-pLVx cells in control conditions was also observed. It can be speculated that Tspan6 negatively regulates secretion of EGFR ligands, therefore, the increase in receptor activation and subsequent degradation by cCbl-mediated ubiquitination in Caco-2-pLVx cells under basal growth conditions are expected. An additional

mechanism of EGFR-mediated signalling regulation is phosphorylation of Thr654 by protein kinase C (PKC) that blocks EGF-induced internalisation and downregulation of the receptor (Lund, Lazar *et al.* 1990). Accordingly, our data indicated that in the presence of Tspan6 phosphorylated EGFR at Thr654 was lower than in control cells during EGF stimulation, indicating a more effective negative feedback loop of EGFR-mediated signalling takes place in cells expressing functional Tspan6.

In agreement with results seen with organoids, it was found that low expression of Tspan6 in Caco-2-pLVx cells correlated with the increased activation of p38 MAPK. Although the implications of p38 activation and Tspan6 expression are currently unknown, it is possible that p38 activation has an inhibitory effect on GSK3β, and subsequently affects β-catenin dependent pathways. As such, it was found that β-catenin phosphorylation (regulated by GSK3β) at Ser552 is increased by ~2-fold in Caco-2-pLVx cells upon stimulation with EGF but remains unaffected in Caco-2-Tspan6 cells. Furthermore, these changes were accompanied by relatively low phosphorylation levels of β-catenin Thr41 and Ser45 in Caco-2-pLVx cells when compared to Tspan6-expressing cells.

In summary, these data presented here further indicate that Tspan6 expression modifies the EGFR-mediated signalling *in vitro*.

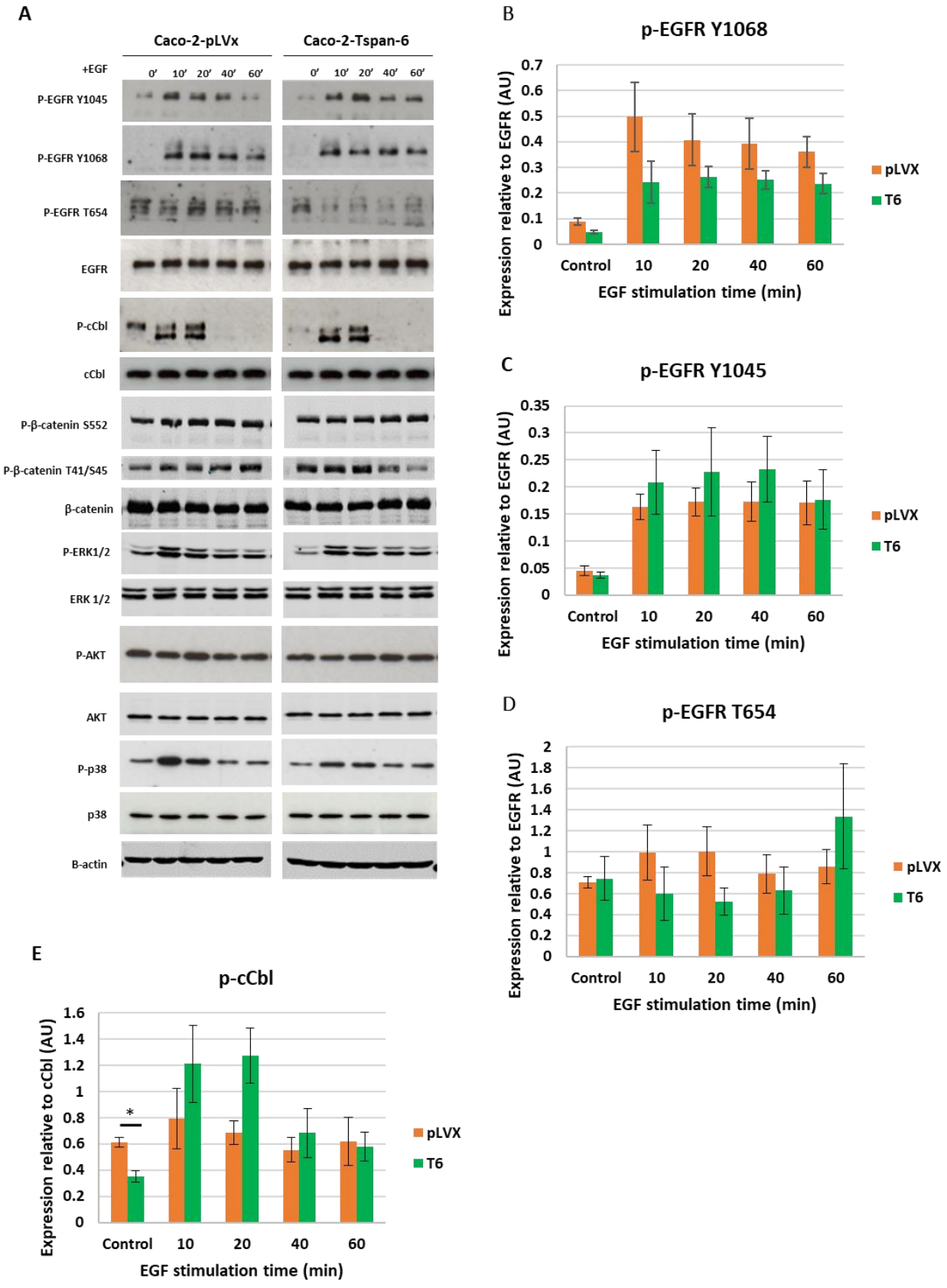
A
Caco-2-pLVx
Caco-2-Tspan-6
+EGF
0′ 10′ 20′ 40′ 60′
P-EGFR Y1045
P-EGFR Y1068
P-EGFR T654
EGFR
P-cCbl
cCbl
P-β-catenin S552
P-β-catenin T41/S45
β-catenin
P-ERK1/2
ERK 1/2
P-AKT
AKT
P-p38
p38
B-actin
B
p-EGFR Y1068
Expression relative to EGFR (AU)
0.7
0.6
0.5
0.4
0.3
0.2
0.1
0
Control 10 20 40 60
EGF stimulation time (min)
pLVX
T6
C
p-EGFR Y1045
Expression relative to EGFR (AU)
0.35
0.3
0.25
0.2
0.15
0.1
0.05
0
Control 10 20 40 60
EGF stimulation time (min)
pLVX
T6
D
p-EGFR T654
Expression relative to EGFR (AU)
2
1.8
1.6
1.4
1.2
1
0.8
0.6
0.4
0.2
0
Control 10 20 40 60
EGF stimulation time (min)
pLVX
T6
E
p-cCbl
Expression relative to cCbl (AU)
1.6
1.4
1.2
1
0.8
0.6
0.4
0.2
0
*
Control 10 20 40 60
EGF stimulation time (min)
pLVX
T6

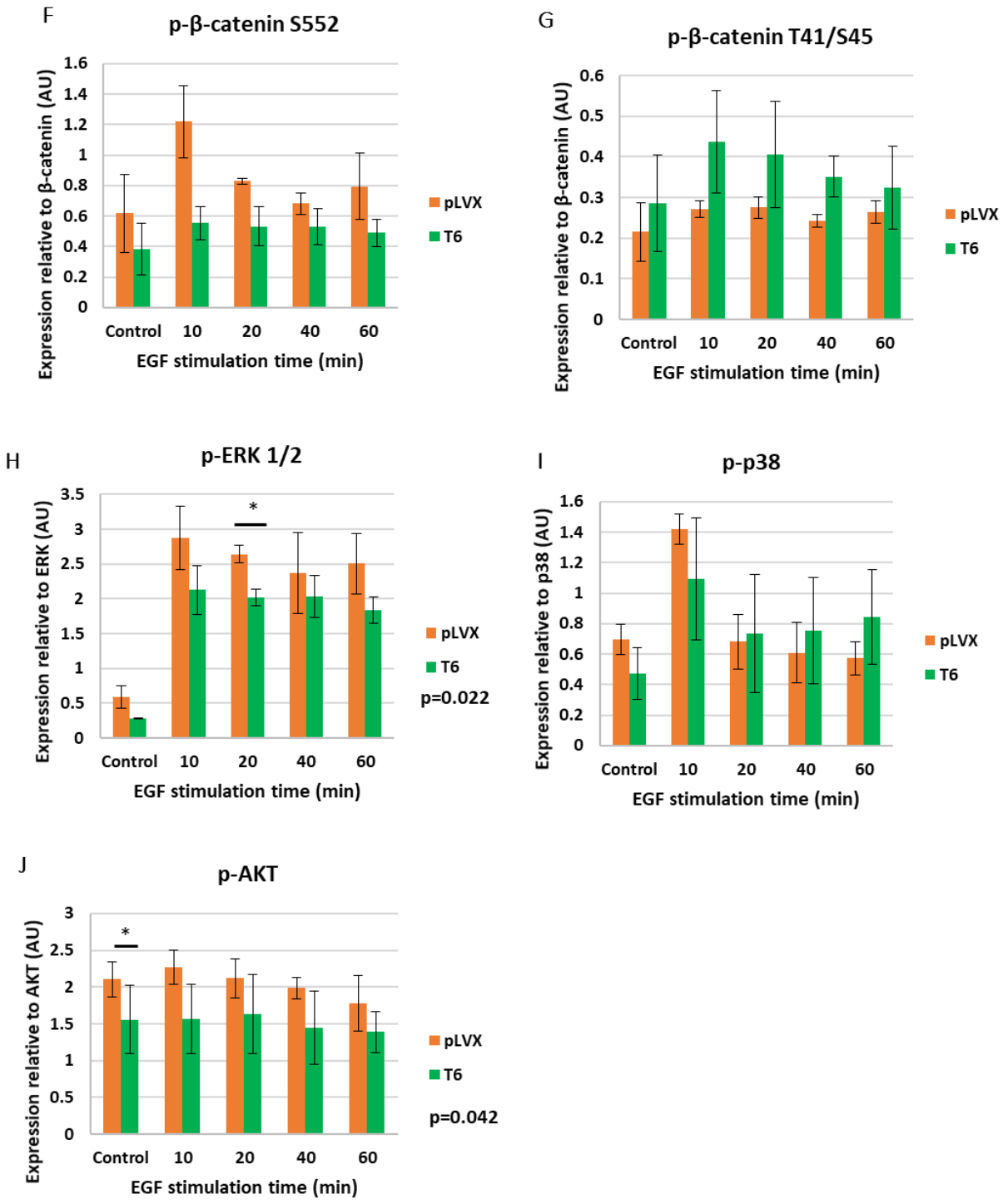

Figure 6-9. Tspan6 regulates EGFR-dependent signalling in Caco-2 cells. **(A)** Western blot analysis of p-EGFR, p-ERK, p-β-catenin, p-Akt, and p-p38 in pLVx and Tspan6 expressing Caco-2 cells in response to timecourse of EGF stimulation (10 ng/ml). **(B-J)** Quantification analysis of phosphorylation level of signalling molecules relative to the total expression of the unphosphorylated molecule expressed as mean signal ±SEM of triplicate experiments. Data was normalised to β-actin expression.

6.7 Expression of Tspan6 correlates with better response to EGFR inhibitor cetuximab

The emerged role of Tspan6 in regulation of EGFR-mediated signalling instigated the rationale to determine whether Tspan6 affects cell proliferation and cellular responses to an EGFR inhibitor, namely cetuximab. The effect of cetuximab at different concentrations (ranging from 0.1 µg/ml to 50 µg/ml) were assessed using Alamar Blue assay. The inhibition of proliferation induced by cetuximab on Caco-2 cells was determined as percentage viability in comparison with the untreated control. Of note, the anti-proliferative effect of cetuximab was observed at concentration as low as 0.1 µg/ml ($p<0.0001$) (Figure 6-10). The level of growth inhibition observed in control cells (Caco-2-pLVx) was approximately 10% compared to untreated cells at 0.5 µg/ml, reaching 25% of inhibition at 50 µg/ml of cetuximab, which is in agreement with previously published studies (Song, Liu *et al.* 2014, Herreros-Villanueva, Muniz *et al.* 2010, Brandi, Tavolari *et al.* 2012). However, the anti-proliferative effect of cetuximab in cells expressing Tspan6 appeared to be significantly more dramatic at concentrations of cetuximab as low as 0.5 µg/ml showing 18% of inhibition compared to 12% in Caco-2-pLVx cells ($p=0.0128$). The strongest effect was seen at high concentrations of cetuximab (50 µg/ml), reaching approximately 32% of growth inhibition. Thus, these results demonstrate that Tspan6 expression can potentiate sensitivity to the inhibitory effect of cetuximab. This data confirms the role of Tspan6 in regulation of EGFR-mediated cellular responses.

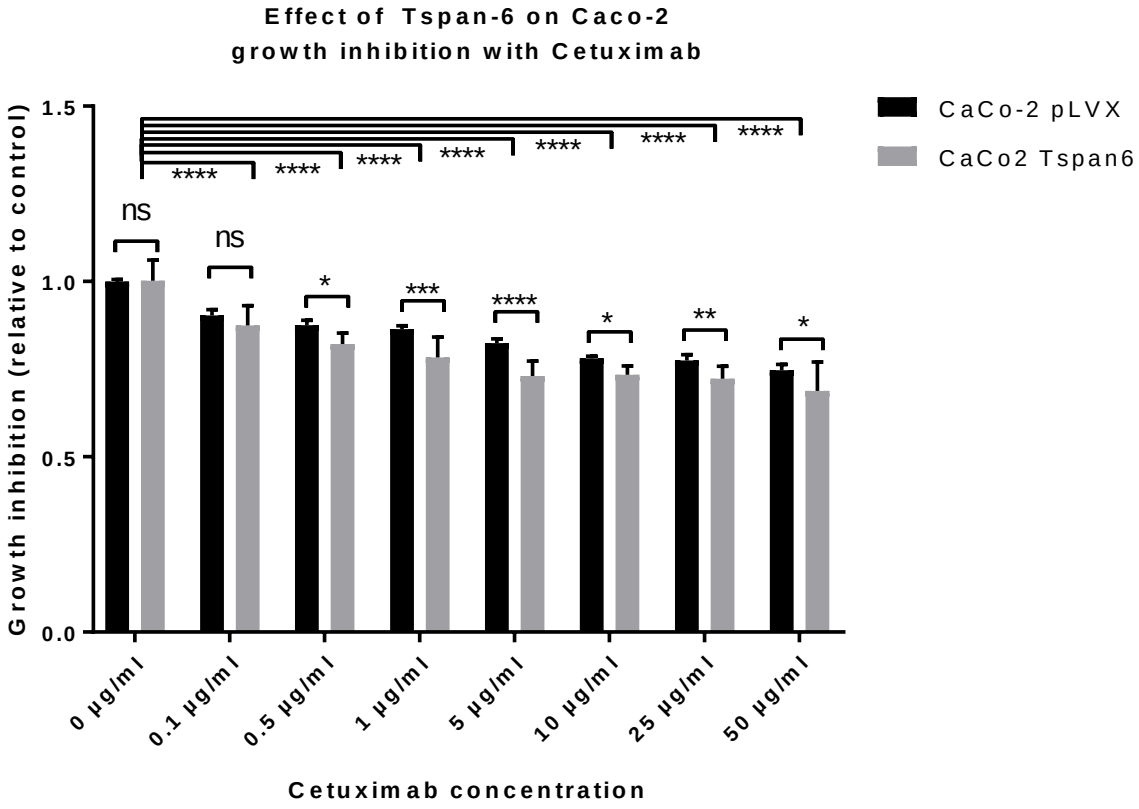

Figure 6-10. Tspan6 affect response of Caco-2 cells to cetuximab after 72-hour treatment in 2D. Effect of cetuximab on Tspan6 expressing and control Caco-2 cells. Results expressed as percentage of control with 100% representing untreated control cells. Vertical bars ± SEM of triplicate assays. P < 0.05 versus control values of untreated cells (Two-tailed Student t-test).

6.8 Tspan6-Syntenin-1 complex regulates lumen production in Caco-2 three-dimensional polarised cysts

The results presented in this thesis strongly suggest that Tspan6 plays a role in EGFR-dependent signalling via autocrine ligand secretion. It was recently reported that Tspan6 regulates exosome secretion *in vitro* via its cytoplasmic partner syntenin-1, an adaptor protein implicated in biogenesis of exosomes (Guix, Sannerud *et al.* 2017). The possibility of direct association of Tspan6 with syntenin-1 and EGFR in Caco-2 cells was further addressed. Indeed, syntenin-1 can be co-precipitated with

Tspan6 in stringent conditions known to disrupt the association of tetraspanins with most of their transmembrane partners (0.5% Brij98 - 0.5% Triton-X-100) (Figure 6-11.B). By contrast, EGFR co-immunoprecipitated with Tspan6 only under low stringency conditions (0.8% Brij98 - 0.2% Triton-X-100) suggesting an indirect association of the tetraspanin with the receptor (possibly via other proteins in the tetraspanin-enriched microdomain (TEM/TERM)) (Figure 6-11.C). Following this observation, we investigated if EGFR-mediated lumen formation in Caco-2 cells is regulated by syntenin-1 expression. Syntenin-1 was depleted using small interfering RNA in the control and Tspan6-expressing cells cultured in 3D-Matrigel™ for 5 days after transfection. A reduction in number of spheroids presented with visible lumen was noted in both cell lines (Figure 6-12.C-D). Specifically, only 5% and 3% of colonies formed central lumen in Caco-2-pLVx and Caco-2-Tspan6 respectively. Importantly, the expression of syntenin-1 remained downregulated after 5 days of culture (Figure 6-12.A-B). These data indicate that syntenin-1 may play a role in lumen formation in Caco-2 cells, thus supporting the hypothesis that Tspan6 regulated EGFR-mediated cell responses in the complex with syntenin-1.

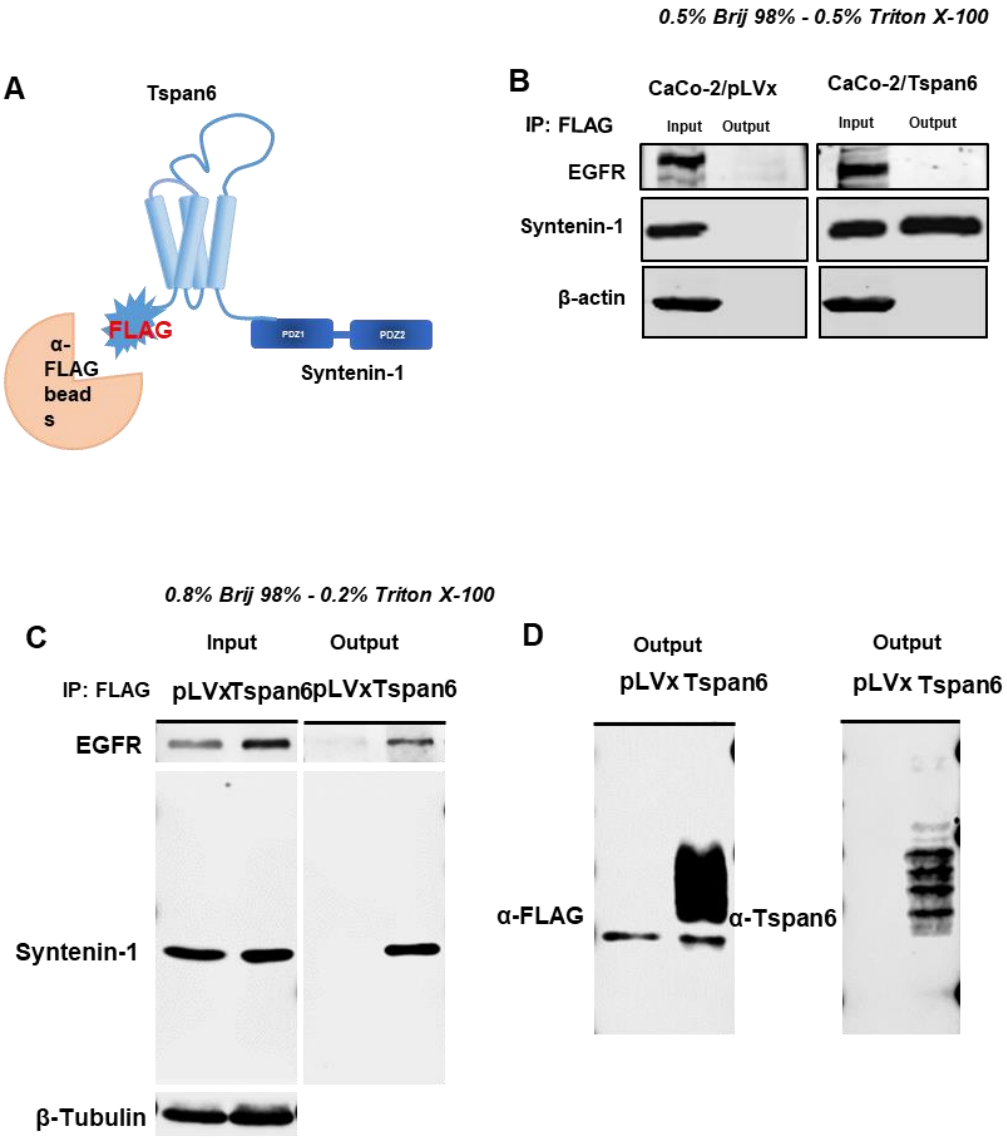

Figure 6-11. Tspan6 is associated with syntenin-1 and EGFR in Caco-2 cells. (A) Schematic presentation of FLAG-tagged Tspan6 and syntenin-1 in the co-immunoprecipitation assay. FLAG is expressed on the N-terminus of Tspan6 and syntenin-1 binds C-terminus of Tspan6. **(B-D)** Analysis of proteins in Tspan6 immunoprecipitates in buffer containing 0.5% Brij-0.5% Triton X-100 **(B)** or 0.8% Brij-0.2% Triton X-100 **(C, D).** Immunoprecipitation control using anti-FLAG and Tspan6 antibody **(D).**

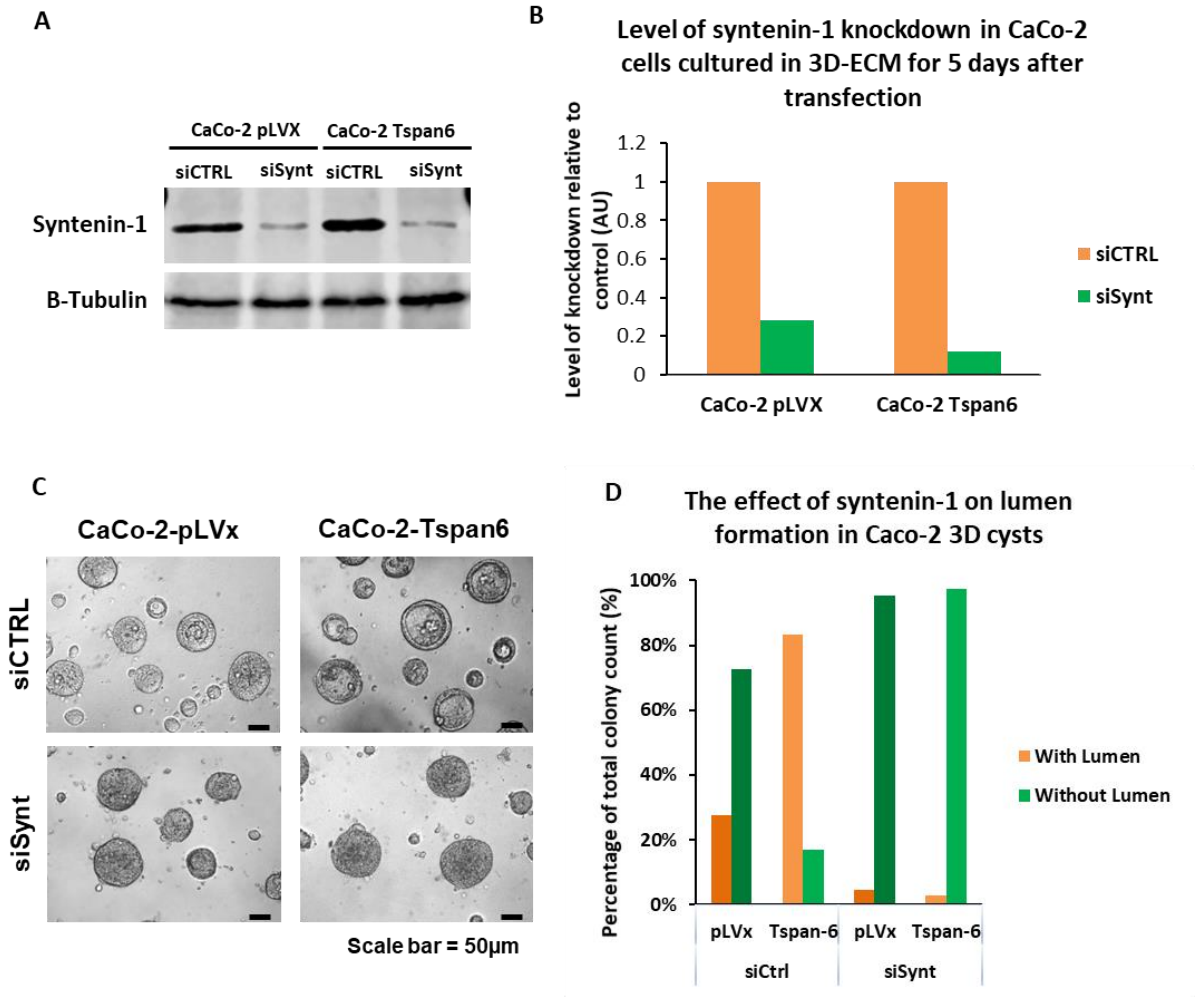

Figure 6-12. Knockdown of syntenin-1 results in significant reduction of lumen formation in colonies of Caco-2 cells in three-dimensional ECM. (A) Western blot showing level of syntenin-1 expression in Caco-2 cells treated with control siRNA and syntenin-1 siRNA for 5 days. **(B)** Bar chart representing level of syntenin-1 knockdown by siRNA in Caco-2 3D cysts after five days of culture. **(C)** A phase-contrast image of Caco-2 cells transfected with siRNA (control or syntenin-1) and cultured for 5 days in 3D ECM after 24 hours of transfection. **(D)** The percentage of Caco-2 colonies that formed the lumen (orange) or appeared without lumen (green) when treated with control (left) and syntenin-1 siRNA (right) (n=1).

6.9 Discussion

When cultured in three-dimensional ECM Caco-2 cells exhibit characteristics of enterocytic differentiation and form organised polarised colonies with a central lumen, often referred to as cysts (Ivanov, Hopkins *et al.* 2008, Jaffe, Kaji *et al.* 2008). The expression of Tspan6 was shown to facilitate lumen formation at a faster rate than control cells without affecting cellular polarisation. The lumen formation in Caco-2 cells is linked to polarised spindle orientation during mitosis, and dysregulation of Rho GTPase Cdc42-dependent signalling (or changes in the expression or function of other proteins, including cancer-promoting phosphatase PRL-3 and PTEN) were shown to disrupt lumenogenesis, promoting formation of multiple lumens in culture (Bray, Brakebusch *et al.* 2011, Lujan, Varsano *et al.* 2016, Jagan, Fatehullah *et al.* 2013).

The expression of Tspan6 does not seem to affect proliferation and cellular polarity nor does this lead to the formation of multiple lumens when Caco-2 cells are cultured in 3D ECM. These results suggest that Tspan6 may be involved in pathways which control lumen expansion. It has been previously reported that lumen formation by Caco-2 cells in 3D ECM is driven by polarised fluid secretion mediated by Na^+/K^+-ATPase and the cystic fibrosis transmembrane receptor (CFTR) localised at the basolateral and apical surfaces respectively (Jaffe, Kaji *et al.* 2008). Interestingly, it was found that Tspan6 can be co-immunoprecipitated with Na^+/K^+-ATPase and two proteins are co-localised at the basolateral surface of Caco-2 3D cysts by immunofluorescence (Supplementary Figure 8-2 and Supplementary Figure 8-3). This data points towards a potentially new mechanism of regulation of Na^+/K^+-ATPase in the context of lumen formation by Tspan6. However, more work will be

required to understand the biological significance of this interaction and whether the activity of the Tspan6-Na^+/K^+-ATPase complex is linked to the modulatory effect of Tspan6 on signalling via EGFR. In this regard, it is interesting that inhibition of Na^+/K^+-ATPase using ouabain, resulted in the increased activation of EGFR (Rajamanickam, Kastelic *et al.* 2017), thus suggesting an alternative pathway whereby Tspan6 is regulating the activity of EGFR via Na^+/K^+-ATPase. Conversely, one can speculate that Tspan6-dependent regulation of EGFR signalling would regulate activity of the Na^+/K^+-ATPase pump and control the rate of fluid secretion into the central lumen during the formation of Caco-2 cysts. Indeed, it has been shown that inhibition of MAPK activity in HT29 colorectal cells promoted lumen formation (Herr, Kohler *et al.* 2015). Furthermore, p38 and ERK were found to inhibit the Na^+/K^+-ATPase pump in Caco-2 cells (El Moussawi, Chakkour *et al.* 2018).

It was found that Tspan6 is directly associated with syntenin-1 in Caco-2 cells. Remarkably, similar to the effect of EGFR hyperactivation by EGF, knockdown of syntenin-1 resulted in near complete ablation of lumen formation by Caco-2 in 3D. Therefore, it is possible that syntenin-1 is a key factor that mediates the effect of Tspan6 on activation of EGFR. In this regard, syntenin-1 is known to interact with syndecans, a family of transmembrane proteoglycans, that are able to capture EGFR and ErbB2 with their ectodomain and control autophosphorylation of the receptor (Ramani, Purushothaman *et al.* 2013, Baietti, Zhang *et al.* 2012, Wang, H., Jin *et al.* 2015). Therefore, one can speculate that depletion of syntenin-1 (or Tspan6-dependent re-localisation of the protein in cells) will affect the mode of syndecans-EGFR and prolong EGFR autophosphorylation leading to the suppression of lumen formation. Alternatively, ablation of the lumen formation in Caco-2 cells following

syntenin-1 depletion may be a result of impaired growth, resulting in immature cyst formation, as silencing of syntenin-1 demonstrated the reduced growth and proliferation of the human colon cancer cell line HT29 and the human breast cancer cell line MCF7 (Kashyap, Roucourt *et al.* 2015).

Tspan6 was found to bind to the first PDZ domain of syntenin-1 (Guix, Sannerud *et al.* 2017). Interestingly, unpublished data from our lab showed that syntenin-1 binds to pro-TGF-α via PDZ2 domain and is able to bind Tspan6 and pro-TGF-α simultaneously. Thus, it is feasible that Tspan6 acting via syntenin-1 affects intracellular trafficking of pro-TGF-α (for example, by preventing effective recruitment of the protein to exosomes) (Figure 6-13). Consequently, suppressed autocrine activation of EGFR and its downstream targets (e.g. MAPKs) would leave Na^+/K^+-ATPase more active (see above) and, therefore, result in a quicker expansion of the lumen. Alternatively, Tspan6 may use syntenin-1 for activation of other pathways that are known to regulate Na^+/K^+-ATPase function. Src kinase may represent one such molecule. Na^+/K^+-ATPase has been shown to inhibit activity of Src in multiple studies (Weigand, Swarts *et al.* 2012, Banerjee, Cui *et al.* 2018, Zhang, Aalkjaer *et al.* 2018). On the other hand, Src was implicated in exosome biogenesis through interaction with syntenin-1 (Imjeti, Menck *et al.* 2017). Therefore, one cannot exclude a possibility of Tspan6 controlling the balance of Src-Na^+/K^+-ATPase and Src-syntenin-1 associations, which may have important consequences for Src activation and, subsequently, exosomal production.

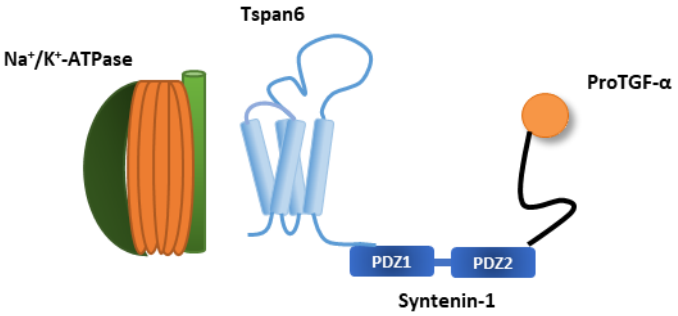

Figure 6-13. Schematic representation of Tspan6 interaction in Caco-2 cells.

In summary, results of this chapter further suggest that Tspan6 may be considered as a new modulatory molecule that regulates EGFR-mediated responses in colon epithelial cells. Moreover, the interaction with syntenin-1 may represent a key factor in regulation of the biological activity of Tspan6 (particularly in the context of exosome-dependent production of TGF-α). Further studies will be necessary to examine whether or not changes in the expression of Tspan6 in CRC tissue and associated modulations of EGFR-dependent signalling could be used as a novel biomarker for anti-EGFR therapy response in patients with KRAS/BRAF wild-type colon adenocarcinomas.

7 DISCUSSION AND FUTURE DIRECTIONS

7.1 Tspan6 as a biomarker in CRC

The data presented in this thesis demonstrated that Tspan6 protein expression is reduced in CRC when compared to adjacent normal tissue in humans, specifically in early stages of CRC (stage II and stage III). It remains unclear whether decreased Tspan6 expression results from malignant transformation of cells or drives tumorigenesis following tumour initiation by aberrant Wnt signalling as was demonstrated in $APC^{min/+}$ mice. In this regard, in the small cohort of CRC patients analysed, there was no correlation found between Tspan6 expression and cancer driver gene mutations, suggesting that Tspan6 regulation occurs independently of these signalling pathways, possibly as an alternative mechanism of selection pressure acquired by tumour cells.

The analysis of Tspan6 KO revealed that although *Tspan6* is not a tumour suppressor gene it has a role in APC-driven neoplastic transformation of epithelial cells. This suggests that changes in Tspan6 expression may represent an early event in tumorigenesis contributing to the development of polyps in the intestine and colon and may be indicative of cancer development. Indeed, it has been recently reported that the expression of Tspan6 in polyps adjacent to cancer was lower as compared to cancer-free polyps (Druliner, Wang *et al.* 2018). These findings support the important role of Tspan6 in colon tumorigenesis and implicate Tspan6 as a possible marker for progression of adenomatous polyps to malignant carcinomas. Further analysis of Tspan6 expression along with examination of EGFR activation in the cohort of adenoma samples, including sporadic cases and polyps from FAP patients should

clarify the involvement of Tspan6 in early events of carcinogenesis. It is important to note that only 5% of adenomatous polyps give rise to cancer in humans and yet it remains unclear why some polyps transform to malignant type and others do not, raising the question if Tspan6 dysregulation favours the malignant transformation of adenomatous polyps (Druliner, Rashtak *et al.* 2016, Heitman, Ronksley *et al.* 2009, Saini, Kim *et al.* 2006, Church 2004).

The specific reduction of Tspan6 in the stage II localised tumours and stage III invasive carcinomas (lymph node metastases present), but not in metastatic stage IV CRCs, is a further indication that Tspan6 may play a critical role in early steps of carcinogenesis. Importantly, approximately 20-30% of stage II and ~15% of stage III CRC patients relapse after treatment (a combination of surgery and chemotherapy) (Paspala, Machairas *et al.* 2018, Labianca, Nordlinger *et al.* 2013, de Wit, Fijneman *et al.* 2013). Thus, further experiments will be required to examine whether Tspan6 expression correlates with patients' resistance to chemotherapy. This will be particularly important in the context of the treatment regimens targeting EGFR. Indeed, our results indicate that Tspan6 regulates cellular responses to cetuximab. To address if Tspan6 expression correlates with response to anti-EGFR treatment, the cohort of CRC samples from the COIN clinical trial is currently being investigated. Of note, this trial includes patients with no mutation in *Kras*, who were treated intermittently with chemotherapy plus continuous (or intermittent) treatment with cetuximab. The analysis of Tspan6 methylation profiles in tumours resistant to cetuximab therapy will also be examined. In addition, samples from the FOxTROT clinical trial, in which CRC patients underwent neo-adjuvant chemotherapy ± panitumumab (anti-EGFR monoclonal antibody) independently of tumour stage, will

be analysed for Tspan6 expression to evaluate if its expression is linked to patient responses to the treatment. Analysis of this cohort will also allow examining if Tspan6 expression correlates with disease recurrence.

7.2 Tspan6-EGFR axis in CRC

This study strongly suggests that Tspan6 affects neoplastic transformation of intestinal and colonic epithelial cells by regulating the EGFR-mediated signalling via mechanisms involving autocrine secretion of EGFR ligand TGF-α. Although there is no evidence indicating that TGF-α is directly involved in the CRC development and progression, previous studies demonstrated that the high levels of TGF-α expression in normal colonic mucosa can be considered as a potential biomarker for the development adenoma and CRC (Daniel, Bostick *et al.* 2009). Furthermore, the increased levels of TGF-α in the blood of CRC patients and in cancerous tissues may be an informative indicator for designing the optimal treatment targeting EGFR (Zhao, Wang *et al.* 2017, Troiani, Martinelli *et al.* 2013). Therefore, it will be important to extend our study further and analyse a possible link between the expression of Tspan6 and TGF-α in CRC patients and its relevance to patient's responses to EGFR-targeting therapies (see above).

Although the data presented in this thesis suggests that Tspan6 acts via regulated secretion of TGF-α, other pathways exist which may link EGFR and Tspan6 (via TGF-α) that should be considered and explored in the future studies. For example, it is possible that Tspan6 regulates the exit of TGF-α from the ER. In this regard, it has been demonstrated that syntenin-1, the only known cytoplasmic partner of Tspan6, is important for surface delivery of TGF-α (Fernandez-Larrea, Merlos-

Suarez *et al.* 1999). Alternatively, Tspan6 may act via syntenin-1 to regulate TGF-α shedding by ADAM17 as syntenin-1 is known to directly associate with Src kinase that in turn regulates ADAM17 sheddase function in cleaving pro-TGF-α at the cell membrane (Imjeti, Menck *et al.* 2017, Van Schaeybroeck, Kelly *et al.* 2008). The association with syntenin-1 and the formation of the tri-partite Tspan6-syntenin-TGF-α complex (preliminary data from Berditchevski's laboratory) on one hand and observed co-immunoprecipitation with EGFR on the other (this study), suggest that Tspan6 may regulate the dynamics of EGFR-TGF-α binding by controlling spatial localisation of the ligand and/or receptor on the cell surface.

Tetraspanins have been previously implicated in regulation of EGFR/ErbB2 dependent signalling by affecting various pathways (Berditchevski, Odintsova 2016). In cells expressing Tspan6 the increased amount of EGFR seems to indicate that pathways that regulate trafficking or/and degradation of the receptor are most affected. The receptor internalisation and degradation are dependent on ubiquitination of the protein, which is mediated by cCbl ubiquitin ligase and is activated by ligand-induced autophosphorylation of EGFR (at Tyr1045) (Sorkin, Goh 2009, Thien, Langdon 2001, Carraway 2010). Our results demonstrate decreased phosphorylation of cCbl in Tspan6 expressing cells under steady state conditions which points towards a yet unidentified intracellular pathways that control activation of this protein. Further analysis will be necessary to establish whether this change in the phosphorylation status of cCbl would have functional consequences for Tspan6-dependent regulation of EGFR expression.

7.3 Tspan6-syntenin-1 complex in EVs biogenesis

Our data suggest that Tspan6-dependent regulation of EGFR-mediated signalling involves production of EVs (Figure 7-1). Intriguingly, whereas there was no obvious difference in the total number of EVs produced by organoids derived from the WT or Tspan6 KO animals, there was ~9-fold increase in the production of smaller vesicles (50-100nm) by organoids established from the knockout animals. Although technical challenges (i.e. small quantities of conditioned media) did not allow us to establish the identity of these vesicles (i.e. exosomes or small ectosomes), these results further support the notion that Tspan6 plays an important role in exocytic (or/and ectocytic) release of vesicles by cells. The mechanisms of exosome formation and secretion has been extensively investigated over the last few years (Juan, Furthauer 2018, Toh, Lai *et al.* 2018, Colombo, Moita *et al.* 2013, Ramani, Purushothaman *et al.* 2013) and our recent data indicate that Tspan6 may control the production of exosomes by neuronal cells (Guix, Sannerud *et al.* 2017). Thus, finding a direct mechanistic link between Tspan6 and established pathways underlying formation of MVBs and production of exosomes is critical. One of the potential candidates is syntenin-1. Syntenin-1 is known to be a key molecule in biogenesis of exosomes which functions as a part of the complex containing syndecans (Baietti, Zhang *et al.* 2012).

Thus, it will be important to investigate the relationship between Tspan6-syntenin-1 and syndecan-syntenin-1 complexes and establish molecular pathways that control their assembly. The role of Src kinase may be particularly important. It has been recently demonstrated that Src impacts endocytosis of syndecans from the plasma membrane, and recruits syntenin-1 to the endocytic compartments,

promoting budding and biogenesis of syntenin-1-syndecan enriched exosomes (Imjeti, Menck *et al.* 2017). Interestingly, it was noticed that Src phosphorylation is increased in cells and organoids expressing low levels of Tspan6, supporting a possible involvement of Src in Tspan6-dependent pathway linked to exosomal biogenesis.

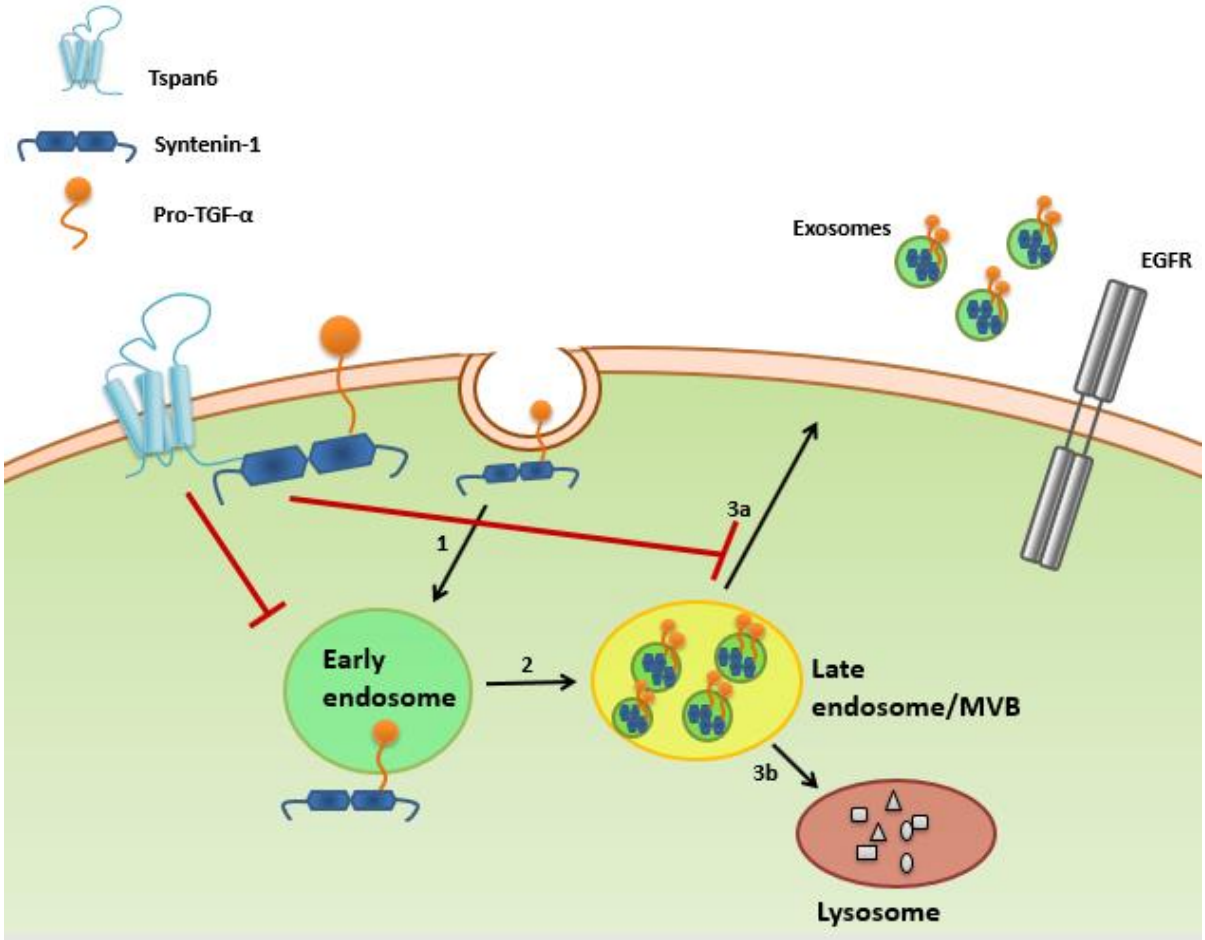

Figure 7-1. Schematic model of Tspan6 regulation of autocrine secretion of EGFR ligands. Association of syntenin-1 with Tspan6 (via PDZ-1) and proTGF-α (via PDZ-2) can inhibit **(1)** endocytosis, **(2)** endosome maturation and production of ILVs, **(3)** skewing late endosome fate from **(3a)** fusion with plasma membrane and exosomal release to **(3b)** fusion with lysosomes and cargo degradation.

In the context of Alzheimer's disease and degradation of amyloid precursor protein (APP) high levels of Tspan6 were shown to inhibit fusion of late endocytic vesicles with autophagosomes and lysosomes, favouring exosomal release over lysosomal degradation (Guix, Sannerud *et al.* 2017). Our data suggest that the endo-lysosomal trafficking pathways linking Tspan6 and polarised production/secretion of exosomes may be tissue specific, making this a very interesting topic for further investigation. Interestingly, Tspan6 was found to be expressed on exosomes derived from the apical membrane of polarised LIM1863 colon carcinoma cell line (Tauro, Greening *et al.* 2012). Moreover, syntenin-1 was also detected in apical endocytic compartments in polarised Madin-Darby canine kidney (MDCK) cells (Fialka, Steinlein *et al.* 1999). In this study due to three-dimensional organisation of organoids, the vesicles/exosomes derived only from the basolateral surface of organoids were analysed. This poses an important question for future investigation: whether quantitative differences in production of small vesicles (associated with Tspan6 deficiency) are due to changes in the formation of MVBs or, in fact, reflective of more general alterations in intracellular secretory apparatus.

In addition to exosomes, loss of Tspan6 influenced the secretion of extracellular macrovesicles (up to 1 μm in diameter). The reliable, unequivocal method to isolate and characterise different EV subtypes has not been established to date. The protein profile of EVs is similar due to enrichment in transmembrane proteins and no unique protein marker for each subtype of EVs has been reported (Yanez-Mo, Siljander *et al.* 2015). The best studied EVs are exosomes that are typically isolated by size exclusion chromatography, differential centrifugation or sucrose/iodixanol density gradient centrifugation. However, there is no evidence that

EVs produced by different pathways (e.g. exocytosis or ectocytosis) do greatly differ in size. Therefore, it is also important to consider the possible contribution of Tspan6 to production of ectosomes, 100 nm-1 μm vesicles derived from outward budding of the cell membrane. Although the signalling potential of ectosomes has not been studied extensively, the elevated number of ectosomes in plasma and tumour biopsies is positively correlated with tumour progression in pancreatic cancer patients (Kalra, Drummen *et al.* 2015, Minciacchi, You *et al.* 2015). Tetraspanins have been reported to induce membrane curvature (Bari, Guo *et al.* 2011, Wrigley, Ahmed *et al.* 2000), and, therefore, may be considered as potential regulators of the ectosome production as well. For example, Tspan6 in this study and some other tetraspanins in previous reports were shown to regulate activation of ERK 1/2, a key component of the ARF6-dependent pathway leading to the formation of membrane-derived vesicles by a human melanoma cell line (Muralidharan-Chari, Clancy *et al.* 2009).

7.4 Tspan6 and CRC: extracellular vesicles, immunity and microbiota

Exosomes are known to transfer genetic material between cells. In total, 764 miRNAs and 1639 mRNAs have been characterised in extracellular vesicles (Abak, Abhari *et al.* 2018). The mRNA, miRNA, lncRNA profile was not examined in this study; however, it is important to note that the exosome-derived RNAs were demonstrated to play an important role in tumorigenesis and modulation of the EGFR-mediated signalling. For example, miR-221/222 (transcriptional targets of EGFR) promotes migration and metastasis of gastric cancer cells (Wang, Zhao *et al.* 2014). In addition, miR-24 expression promotes EGFR signalling in breast cancer tumours (Du, Fang *et al.* 2013) and miR-148a enhances EGFR activation in

glioblastoma (Kim, Zhang *et al.* 2014). Conversely, miR-155 and miR-133a suppress EGFR in breast cancer and non-small cell lung carcinoma (NSCLC) respectively (Neilsen, Noll *et al.* 2013, Wang, Hsiao *et al.* 2014). Therefore, it is important to investigate the molecular composition of extracellular vesicles derived from Tspan6-low expressing cells to identify additional onco-drivers that can be secreted by EVs in Tspan6 dependent manner.

Exosomes have been also shown to modify the tumour microenvironment (Abak, Abhari *et al.* 2018). As such, tumour-derived exosomes expressing TGF-β1 were shown to induce T-regulatory (Treg) lymphocytes and inhibit cytotoxic cells in favour of tumour immune response escape (Clayton, Mitchell *et al.* 2007). In addition, tumour-derived exosomes from the mouse colon carcinoma CT26 cells, lymphoma EL4, embryo fibroblast NIH/3T3 cells, and human lung adenocarcinoma H23 cells, as well as from human extranodal natural killer (NK)/T cell lymphoma (ENKL) primary cells were shown to suppress immune response through production of interleukin-6 (IL-6) (Nagarajah 2016, Zhang, Li *et al.* 2015, Chalmin, Ladoire *et al.* 2010). Of note, AREG-induced EGFR signalling was shown to affect T-cell suppressive function. The unpublished data from our lab suggests the regulatory role of Tspan6 in modulation of the immune-microenvironment in colon adenomas and CRC through recruitment of T lymphocytes. The regulation of syntenin-1 by Tspan6 may explain this effect, as syntenin-1 was shown to negatively regulate immunoglobulin production *in vivo* (Tamura, Ikutani *et al.* 2015). Furthermore, the increase in Paneth cells observed in organoid cultures upon Tspan6 KO raise the question whether Tspan6 expression regulates microbiome interaction with the colon epithelium as Paneth cells are the main source of antimicrobial peptides and microbial disbalance modulates

susceptibility to CRC (Clevers, Bevins 2013, Tilg, Adolph *et al.* 2018, Chen 2018). Tspan6 may simply affect the number of Paneth cells in the colon epithelium, regulate the secretion of antimicrobial peptides or affect bacterial adherence to the epithelium, which has been demonstrated for CD9 and *Staphylococcus aureus* adherence to keratinocytes; CD9, CD63 and CD151 in adherence of *Neisseria meningitidis* to human pharynx carcinoma cell line (Ventress, Partridge *et al.* 2016, Green, Monk *et al.* 2011). Altogether, there are numerous possibilities for Tspan6 to regulate not only colon epithelium but also stromal component and microbiota, which have implications in CRC development and should be investigated further.

In summary, the work presented in this thesis demonstrates that Tspan6 is an effective regulator of CRC development though modulation of the EGFR signalling, and it potentially represents an additional link to anti-EGFR therapy resistance. Work presented in this thesis unravelled numerous aspects of Tspan6 in CRC development that require investigation. Here I propose that Tspan6 may present as a new avenue for CRC management and improved therapy regimen for patients with KRAS wt CRC. Finally, understanding the molecular functions of Tspan6 in CRCs and other tumours will aid the development of novel targeted therapies.

8 SUPPLEMENTARY DATA

Table 8-1. Tspan6 genotyping primer sequences.

Primers	Sequence
Reverse common WT and KO (GS (E, T))	5'- CTTACTCACCAGTTTCAGCATCCAG-3'
Forward WT-specific (GS (E))	5'- TGTGATCAAGGACTCAAGCTTGTAC-3'
Forward KO-specific (Neo (T))	5'- GGGTGGGATTAGATAAATGCCTGCTCT -3'

Table 8-2. Concentrations of RNAs extracted from mouse intestinal polyps.

Sample	RNA concentration (ng/ul)
$APC^{min/+}$ (1)	222
$APC^{min/+}$ (2)	1120
$APC^{min/+}$ (3)	448
$APC^{min/+}$ $Tspan6^{-/y}$ (1)	348
$APC^{min/+}$ $Tspan6^{-/y}$ (2)	412
$APC^{min/+}$ $Tspan6^{-/y}$ (3)	856
$APC^{min/+}$ $Tspan6^{-/y}$ (4)	204
$APC^{min/+}$ $Tspan6^{-/y}$ (5)	450

Table 8-3. RIN values and concentration of RNA libraries generated.

Sample	Concentration (ng/ul)	RIN
$APC^{min/+}$ (1)	4160	8
$APC^{min/+}$ (2)	9300	8.8
$APC^{min/+}$ (3)	1880	8.5
$APC^{min/+}$ $Tspan6^{-/y}$ (1)	4300	9.2
$APC^{min/+}$ $Tspan6^{-/y}$ (2)	4900	8.9
$APC^{min/+}$ $Tspan6^{-/y}$ (3)	8780	9.6
$APC^{min/+}$ $Tspan6^{-/y}$ (4)	3500	9.9
$APC^{min/+}$ $Tspan6^{-/y}$ (5)	18700	9.3

Table 8-4. Summary of clinicopathological characteristics of SCORT clinical samples used in the study.

Patient No	Age	Gender	Tumour site	Histology	TNM Stage			EMVI	Operation	Dead	Tspan6 H-Score	
					T	N	M				Tumour	Normal
1	83	Male	Caecum	Adenocarcinoma	3	1	0	N	Right hemicolectomy	Yes	90	220
2	76	Male	Sigmoid	Adenocarcinoma	4	0	0	N	Anterior resection	No	230	190
3	39	Male	Sigmoid	Adenocarcinoma	4	0	0	N	Anterior resection	No	120	70
4	67	Male	Sigmoid	Adenocarcinoma	3	1	0	N	Anterior resection	No	80	190
5			Rectum	Adenocarcinoma	4	0	0	Y	Anterior resection	No	120	70
6	91	Female	Caecum	Adenocarcinoma	4	0	0	N	Right hemicolectomy	No	80	190
7	66	Male	Sigmoid	Adenocarcinoma	3	0	0	N	Sigmoid colectomy	No	45	80
8	34	Female	Caecum	Adenocarcinoma with neuroendocrine differentiation	2	2	0	N	Pan-proctocolectomy	No	90	140
9	72	Male	Transverse colon (right)	Adenocarcinoma	3	0	0	N	Right hemicolectomy	No	180	240
10	67	Male	Rectum	Adenocarcinoma	3	0	0	N	Anterior resection	No	80	170
11	57	Female	Rectum	Adenocarcinoma	3	0	0	N	Anterior resection	No	120	120
12	81	Female	Ascending	Adenocarcinoma	3	0	0	N	Right hemicolectomy	No	190	90
13	77	Male	Caecum	Adenocarcinoma	4	2	0	Y	Right hemicolectomy	No	190	180
14	86	Female	Transverse colon (right)	Adenocarcinoma	3	0	0	N	Right hemicolectomy	No	100	170

15	84	Female	Sigmoid	Adenocarcinoma	4	1	0	Y	Left hemicolectomy	No	220	180
16	76	Male	Rectum	Adenocarcinoma	3	1	0	Y	Hartman's procedure	No	80	230
17	56	Male	Sigmoid	Adenocarcinoma	4	0	0	Y	Anterior resection	No	200	220
18	54	Male	Sigmoid & hepatic flexure	Adenocarcinoma	4	2	0	Y	Total colectomy	No	285	200
19	80	Male	Sigmoid	Adenocarcinoma	4	2	1	Y	Sigmoid colectomy	No	105	190
21	34	Male	Caecum	Adenocarcinoma	4	2	0	Y	Right hemicolectomy	No	190	165
22			Caecum	Adenocarcinoma	3	2	0	N	Right hemicolectomy	No	220	170
23	87	Female	Caecum	Adenocarcinoma	3	0	0	N	Right hemicolectomy	No	230	230
24	72	Female	Sigmoid	Adenocarcinoma	4	1	0	N	Sigmoid colectomy	No	210	210
25	71	Female	Transverse	Adenocarcinoma	4	0	0	N	Right hemicolectomy	No	100	160
26	84	Male	Descending	Adenocarcinoma	3	0	0	N	Left hemicolectomy	No	130	250
27	84	Male	Caecum	Adenocarcinoma	3	0	0	N	Right hemicolectomy	No	170	200
28	63	Male	Sigmoid	Adenocarcinoma	2	1	0	N	Anterior resection	No	110	150
29	73	Male	Caecum	Adenocarcinoma	3	1	0	Y	Right hemicolectomy	No	90	190
30	76	Male	Ascending	Adenocarcinoma	3	1	0	Y	Right hemicolectomy	No	60	180
31	65	Male	Rectum	Adenocarcinoma	3	1	0	Y	Anterior resection	No	100	140
32	88	Female	Ascending	Adenocarcinoma	3	1	0	N	Right hemicolectomy	No	30	130
33	52	Male	Rectum	Adenocarcinoma	3	0	0	N	Anterior resection	No	130	100
34	47	Female	Ascending	Adenocarcinoma	4	2	0	Y	Right hemicolectomy	No	150	220
35	61	Male	Descending	Adenocarcinoma	3	0	0	N	Left hemicolectomy	No	130	150
36	73	Male	Rectum	Adenocarcinoma	3	2	0	N	Anterior resection	No	100	220

37	63	Male	Sigmoid	Adenocarcinoma	4	0	0	N	Sigmoid colectomy	No	160	193
44	79	Female	Descending	Adenocarcinoma	3	1	0	N	Left hemicolectomy	No	180	190
45	77	Female	Caecum	Adenocarcinoma	3	0	0	N	Right hemicolectomy	No	110	N/A
46	78	Male	Sigmoid	Adenocarcinoma	2	0	0	N	Sigmoid colectomy	No	180	220

Table 8-5. The genotype of analysed mice.

Animal ID	Gender	Strain
1601	Male	Tspan6 KO
1602	Male	Tspan6 KO
1603	Male	Tspan6 WT
1604	Male	Tspan6 KO
1605	Male	Tspan6 WT
1606	Male	Tspan6 WT
1607	Male	Tspan6 WT
1608	Male	Tspan6 WT
1609	Male	Tspan6 KO
1610	Male	Tspan6 KO
1611	Male	Tspan6 KO
1612	Male	Tspan6 WT
1613	Male	Tspan6 WT
1614	Male	Tspan6 WT
1615	Male	Tspan6 KO
1616	Male	Tspan6 KO
1617	Male	Tspan6 KO
1618	Female	Tspan6 KO
1619	Female	Tspan6 KO
1620	Female	Tspan6 HET
1621	Female	Tspan6 HET
1622	Female	Tspan6 KO
1623	Female	Tspan6 HET

Table 8-6. Summary of histological analysis of oedema in Tspan6 WT and Tspan6 KO mice.

Mouse ID	Genotype	Histology
1601	Tspan6 KO	Mild interstitial oedema
1602	Tspan6 KO	Mild interstitial oedema
1604	Tspan6 KO	Moderate interstitial oedema
1609	Tspan6 KO	Mild interstitial oedema
1610	Tspan6 KO	Moderate interstitial oedema
1611	Tspan6 KO	Mild interstitial oedema
1613	Tspan6 WT	Mild interstitial oedema
1614	Tspan6 WT	Moderate interstitial oedema
1616	Tspan6 KO	Mild interstitial oedema
1617	Tspan6 KO	Mild interstitial oedema
1618	Tspan6 KO	Mild interstitial oedema
1622	Tspan6 KO	Mild interstitial oedema

Table 8-7. Summary of average weight of collected organs from wild-type and Tspan6 KO mice (WT n=8, Tspan6 KO n=12). At large no differences were observed in organ weight between the two strains of the animals; lungs and thyroid gland were significantly heavier in Tspan6 KO mice. The organs were weighed immediately after removal from cadavers and Student t-test was used for statistical analysis

	Heart(g)	Lungs(g)	Liver(g)	Spleen(g)	Kidneys(g)	Pancreas(g)	Thyroid(g)
Tspan6 WT (n=8)	0.23	0.22	0.10	0.10	0.66	0.26	0.37
Tspan6 KO (n=12)	0.23	0.29	0.11	0.11	0.66	0.29	0.28
p-value	**0.89**	**0.02**	**0.07**	**0.24**	**0.87**	**0.31**	**0.03**

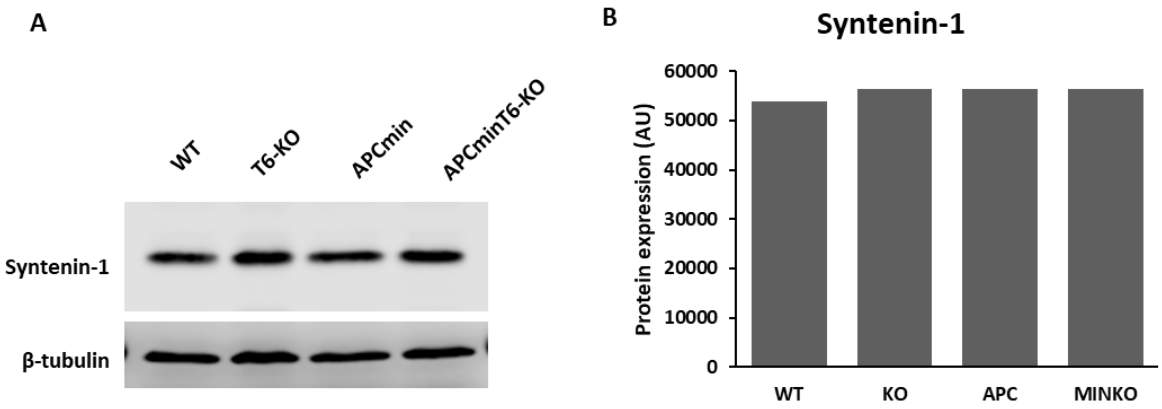

Figure 8-1. Mouse intestinal organoids express syntenin-1 at the same level independently of APC mutation or Tspan6 expression. (A) Western blot analysis of syntenin-1 in WT or Tspan6 KO organoids cultured in complete growth media. **(B)** Quantification analysis of syntenin-1 normalised to β-tubulin expression.

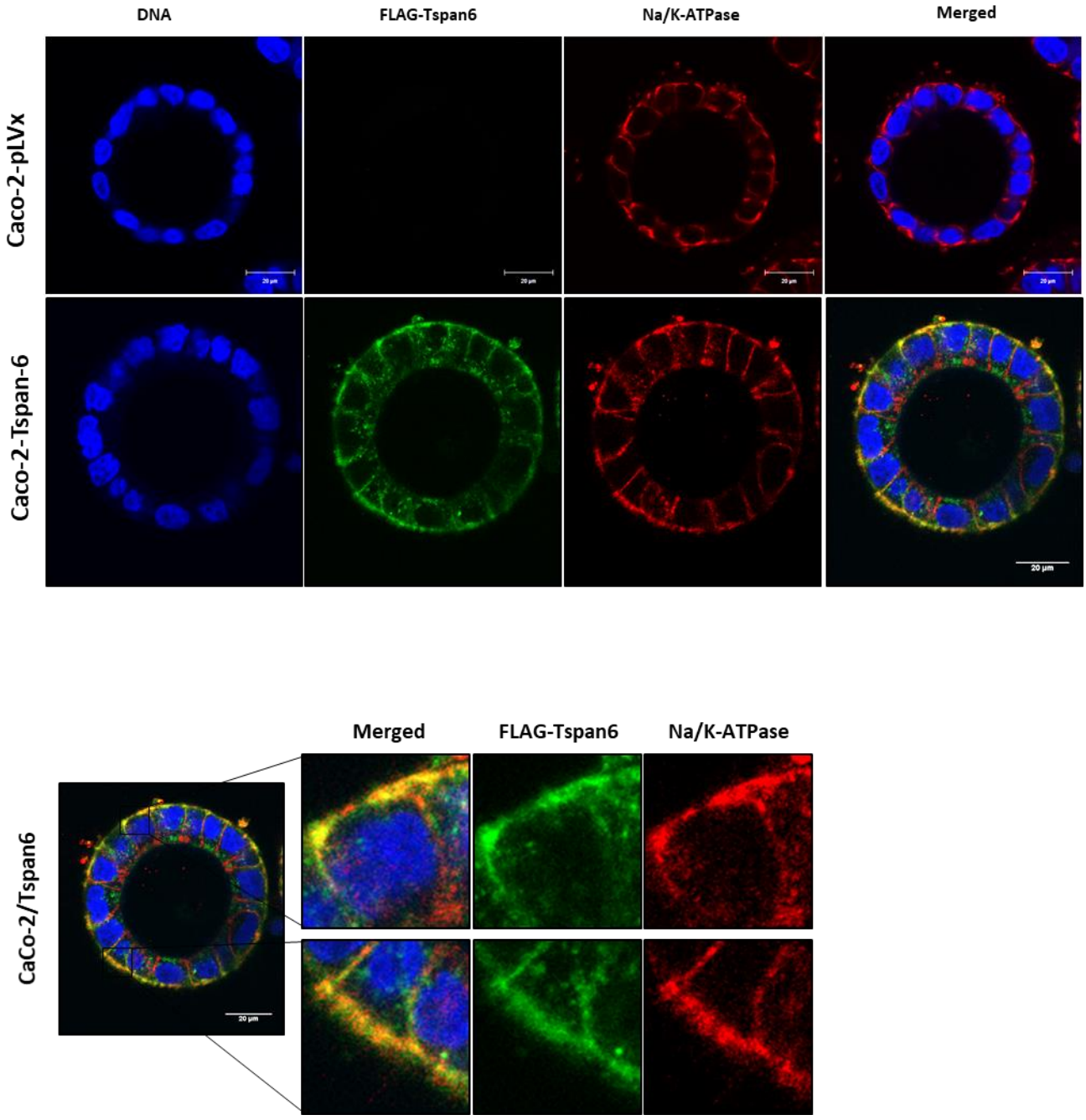

Figure 8-2. Na^+/K^+-ATPase co-localises with Tspan6 in Caco-2 3D cysts. Single confocal section through the middle of Caco-2 cysts stained for DNA (blue), FLAG (green), and Na^+/K^+-ATPase (red).

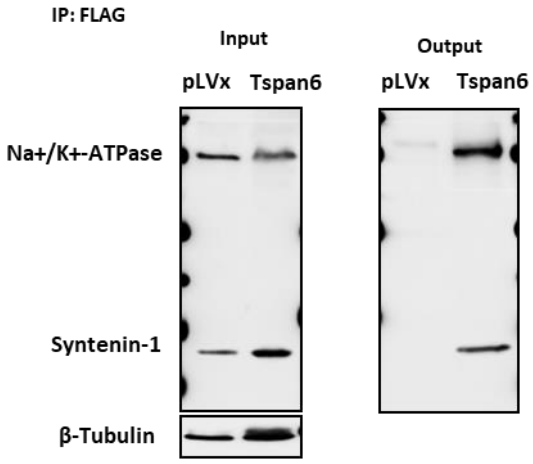

Figure 8-3. Na^+/K^+-ATPase is associated with tetraspanin-enriched microdomain in Caco-2 cells. Analysis of proteins in Tspan6 immunoprecipitates in buffer containing 0.8% Brij-0.2% Triton X-100.

9 REFERENCES

AABERG-JESSEN, C., SORENSEN, M.D., MATOS, A.L.S.A., MOREIRA, J.M., BRUNNER, N., KNUDSEN, A. and KRISTENSEN, B.W., 2018. Co-expression of TIMP-1 and its cell surface binding partner CD63 in glioblastomas. *BMC cancer,* **18**(1), pp. 270-018-4179-y.

ABAK, A., ABHARI, A. and RAHIMZADEH, S., 2018. Exosomes in cancer: small vesicular transporters for cancer progression and metastasis, biomarkers in cancer therapeutics. *PeerJ,* **6**, pp. e4763.

ABE, M., SUGIURA, T., TAKAHASHI, M., ISHII, K., SHIMODA, M. and SHIRASUNA, K., 2008. A novel function of CD82/KAI-1 on E-cadherin-mediated homophilic cellular adhesion of cancer cells. *Cancer letters,* **266**(2), pp. 163-170.

ACS, A.C.S., 2018-last update, *Types of cancer in the colon and rectum*. Available: https://www.cancer.org/cancer/colon-rectal-cancer/about/what-is-colorectal-cancer.html [08/25, 2018].

ADVANI, S.M., ADVANI, P., DESANTIS, S.M., BROWN, D., VONVILLE, H.M., LAM, M., LOREE, J.M., SARSHEKEH, A.M., BRESSLER, J., LOPEZ, D.S., DANIEL, C.R., SWARTZ, M.D. and KOPETZ, S., 2018. Clinical, Pathological, and Molecular Characteristics of CpG Island Methylator Phenotype in Colorectal Cancer: A Systematic Review and Meta-analysis. *Translational oncology,* **11**(5), pp. 1188-1201.

ALENQUER, M. and AMORIM, M.J., 2015. Exosome Biogenesis, Regulation, and Function in Viral Infection. *Viruses,* **7**(9), pp. 5066-5083.

ALI, R.H., MARAFIE, M.J., BITAR, M.S., AL-DOUSARI, F., ISMAEL, S., BIN HAIDER, H., AL-ALI, W., JACOB, S.P. and AL-MULLA, F., 2014. Gender-Associated Genomic Differences in Colorectal Cancer: Clinical Insight from Feminization of Male Cancer Cells. *International Journal of Molecular Sciences,* **15**(10), pp. 17344-17365.

AL-NEDAWI, K., MEEHAN, B., MICALLEF, J., LHOTAK, V., MAY, L., GUHA, A. and RAK, J., 2008. Intercellular transfer of the oncogenic receptor EGFRvIII by microvesicles derived from tumour cells. *Nature cell biology,* **10**(5), pp. 619-624.

AL-NEDAWI, K., MEEHAN, B. and RAK, J., 2009. Microvesicles: messengers and mediators of tumor progression. *Cell cycle (Georgetown, Tex.),* **8**(13), pp. 2014-2018.

AMIT, S., HATZUBAI, A., BIRMAN, Y., ANDERSEN, J.S., BEN-SHUSHAN, E., MANN, M., BEN-NERIAH, Y. and ALKALAY, I., 2002. Axin-mediated CKI phosphorylation of beta-catenin at Ser 45: a molecular switch for the Wnt pathway. *Genes & development,* **16**(9), pp. 1066-1076.

ANDREU, P., COLNOT, S., GODARD, C., GAD, S., CHAFEY, P., NIWA-KAWAKITA, M., LAURENT-PUIG, P., KAHN, A., ROBINE, S., PERRET, C. and ROMAGNOLO, B., 2005. Crypt-restricted proliferation and commitment to the Paneth cell lineage following Apc loss in the mouse intestine. *Development (Cambridge, England),* **132**(6), pp. 1443-1451.

ARANGO, N.A., SZOTEK, P.P., MANGANARO, T.F., OLIVA, E., DONAHOE, P.K. and TEIXEIRA, J., 2005. *Conditional deletion of β-catenin in the mesenchyme of the developing mouse uterus results in a switch to adipogenesis in the myometrium.*

ARENA, S., BELLOSILLO, B., SIRAVEGNA, G., MARTINEZ, A., CANADAS, I., LAZZARI, L., FERRUZ, N., RUSSO, M., MISALE, S., GONZALEZ, I., IGLESIAS, M., GAVILAN, E., CORTI, G.,

HOBOR, S., CRISAFULLI, G., SALIDO, M., SANCHEZ, J., DALMASES, A., BELLMUNT, J., DE FABRITIIS, G., ROVIRA, A., DI NICOLANTONIO, F., ALBANELL, J., BARDELLI, A. and MONTAGUT, C., 2015. Emergence of Multiple EGFR Extracellular Mutations during Cetuximab Treatment in Colorectal Cancer. *Clinical cancer research : an official journal of the American Association for Cancer Research,* **21**(9), pp. 2157-2166.

ARENDS, M.J., 2013. Pathways of colorectal carcinogenesis. *Applied immunohistochemistry & molecular morphology : AIMM,* **21**(2), pp. 97-102.

ARMELAO, F. and DE PRETIS, G., 2014. Familial colorectal cancer: a review. *World journal of gastroenterology,* **20**(28), pp. 9292-9298.

ASHTON, G.H., SORELLI, P., MELLERIO, J.E., KEANE, F.M., EADY, R.A. and MCGRATH, J.A., 2001. Alpha 6 beta 4 integrin abnormalities in junctional epidermolysis bullosa with pyloric atresia. *The British journal of dermatology,* **144**(2), pp. 408-414.

ASSIE, G., LETOUZE, E., FASSNACHT, M., JOUINOT, A., LUSCAP, W., BARREAU, O., OMEIRI, H., RODRIGUEZ, S., PERLEMOINE, K., RENE-CORAIL, F., ELAROUCI, N., SBIERA, S., KROISS, M., ALLOLIO, B., WALDMANN, J., QUINKLER, M., MANNELLI, M., MANTERO, F., PAPATHOMAS, T., DE KRIJGER, R., TABARIN, A., KERLAN, V., BAUDIN, E., TISSIER, F., DOUSSET, B., GROUSSIN, L., AMAR, L., CLAUSER, E., BERTAGNA, X., RAGAZZON, B., BEUSCHLEIN, F., LIBE, R., DE REYNIES, A. and BERTHERAT, J., 2014. Integrated genomic characterization of adrenocortical carcinoma. *Nature genetics,* **46**(6), pp. 607-612.

AUNE, D., CHAN, D.S.M., LAU, R., VIEIRA, R., GREENWOOD, D.C., KAMPMAN, E. and NORAT, T., 2011. Dietary fibre, whole grains, and risk of colorectal cancer: systematic review and dose-response meta-analysis of prospective studies. *BMJ,* **343**.

AWWAD, R.A., SERGINA, N., YANG, H., ZIOBER, B., WILLSON, J.K., ZBOROWSKA, E., HUMPHREY, L.E., FAN, R., KO, T.C., BRATTAIN, M.G. and HOWELL, G.M., 2003. The role of transforming growth factor alpha in determining growth factor independence. *Cancer research,* **63**(15), pp. 4731-4738.

BAARSMA, H.A., KONIGSHOFF, M. and GOSENS, R., 2013. The WNT signaling pathway from ligand secretion to gene transcription: molecular mechanisms and pharmacological targets. *Pharmacology & therapeutics,* **138**(1), pp. 66-83.

BABAEI-JADIDI, R., LI, N., SAADEDDIN, A., SPENCER-DENE, B., JANDKE, A., MUHAMMAD, B., IBRAHIM, E.E., MURALEEDHARAN, R., ABUZINADAH, M., DAVIS, H., LEWIS, A., WATSON, S., BEHRENS, A., TOMLINSON, I. and NATERI, A.S., 2011. FBXW7 influences murine intestinal homeostasis and cancer, targeting Notch, Jun, and DEK for degradation. *The Journal of experimental medicine,* **208**(2), pp. 295-312.

BAIETTI, M.F., ZHANG, Z., MORTIER, E., MELCHIOR, A., DEGEEST, G., GEERAERTS, A., IVARSSON, Y., DEPOORTERE, F., COOMANS, C., VERMEIREN, E., ZIMMERMANN, P. and DAVID, G., 2012. Syndecan-syntenin-ALIX regulates the biogenesis of exosomes. *Nature cell biology,* **14**(7), pp. 677-685.

BALAJ, L., LESSARD, R., DAI, L., CHO, Y.J., POMEROY, S.L., BREAKEFIELD, X.O. and SKOG, J., 2011. Tumour microvesicles contain retrotransposon elements and amplified oncogene sequences. *Nature communications,* **2**, pp. 180.

BALEATO, R.M., GUTHRIE, P.L., GUBLER, M.C., ASHMAN, L.K. and ROSELLI, S., 2008. Deletion of CD151 results in a strain-dependent glomerular disease due to severe alterations of the glomerular basement membrane. *The American journal of pathology,* **173**(4), pp. 927-937.

BANERJEE, M., CUI, X., LI, Z., YU, H., CAI, L., JIA, X., HE, D., WANG, C., GAO, T. and XIE, Z., 2018. Na/K-ATPase Y260 Phosphorylation-mediated Src Regulation in Control of Aerobic Glycolysis and Tumor Growth. *Scientific reports,* **8**(1), pp. 12322-018-29995-2.

BANG, I., KIM, H.R., BEAVEN, A.H., KIM, J., KO, S.B., LEE, G.R., KAN, W., LEE, H., IM, W., SEOK, C., CHUNG, K.Y. and CHOI, H.J., 2018. Biophysical and functional characterization of Norrin signaling through Frizzled4. *Proceedings of the National Academy of Sciences of the United States of America,* **115**(35), pp. 8787-8792.

BARI, R., GUO, Q., XIA, B., ZHANG, Y.H., GIESERT, E.E., LEVY, S., ZHENG, J.J. and ZHANG, X.A., 2011. Tetraspanins regulate the protrusive activities of cell membrane. *Biochemical and biophysical research communications,* **415**(4), pp. 619-626.

BARKER, N., RIDGWAY, R.A., VAN ES, J.H., VAN DE WETERING, M., BEGTHEL, H., VAN DEN BORN, M., DANENBERG, E., CLARKE, A.R., SANSOM, O.J. and CLEVERS, H., 2009. Crypt stem cells as the cells-of-origin of intestinal cancer. *Nature,* **457**(7229), pp. 608-611.

BASTOS, N., RUIVO, C.F., DA SILVA, S. and MELO, S.A., 2018. Exosomes in cancer: Use them or target them? *Seminars in cell & developmental biology; The cancer secretome and secreted biomarkers; The vertebrate habenula,* **78**, pp. 13-21.

BEHRENS, J., 2005. The role of the Wnt signalling pathway in colorectal tumorigenesis. *Biochemical Society transactions,* **33**(Pt 4), pp. 672-675.

BELKIN, A.M. and STEPP, M.A., 2000. Integrins as receptors for laminins. *Microscopy research and technique,* **51**(3), pp. 280-301.

BERDITCHEVSKI, F., 2001. Complexes of tetraspanins with integrins: more than meets the eye. *Journal of cell science,* **114**(Pt 23), pp. 4143-4151.

BERDITCHEVSKI, F. and ODINTSOVA, E., 2016. ErbB receptors and tetraspanins: Casting the net wider. *The international journal of biochemistry & cell biology,* **77**(Pt A), pp. 68-71.

BERDITCHEVSKI, F. and ODINTSOVA, E., 2007. Tetraspanins as regulators of protein trafficking. *Traffic (Copenhagen, Denmark),* **8**(2), pp. 89-96.

BERDITCHEVSKI, F., ODINTSOVA, E., SAWADA, S. and GILBERT, E., 2002. Expression of the palmitoylation-deficient CD151 weakens the association of alpha 3 beta 1 integrin with the tetraspanin-enriched microdomains and affects integrin-dependent signaling. *The Journal of biological chemistry,* **277**(40), pp. 36991-37000.

BIGAGLI, E., LUCERI, C., GUASTI, D. and CINCI, L., 2016. Exosomes secreted from human colon cancer cells influence the adhesion of neighboring metastatic cells: Role of microRNA-210. *Cancer biology & therapy,* , pp. 1-8.

BILGER, A., SULLIVAN, R., PRUNUSKE, A.J., CLIPSON, L., DRINKWATER, N.R. and DOVE, W.F., 2008. Widespread hyperplasia induced by transgenic TGFalpha in ApcMin mice is associated with only regional effects on tumorigenesis. *Carcinogenesis,* **29**(9), pp. 1825-1830.

BOAVIDA, L.C., QIN, P., BROZ, M., BECKER, J.D. and MCCORMICK, S., 2013. Arabidopsis tetraspanins are confined to discrete expression domains and cell types in reproductive tissues and form homo- and heterodimers when expressed in yeast. *Plant Physiology,* **163**(2), pp. 696-712.

BOBRIE, A., COLOMBO, M., RAPOSO, G. and THERY, C., 2011. Exosome secretion: molecular mechanisms and roles in immune responses. *Traffic (Copenhagen, Denmark),* **12**(12), pp.

1659-1668.

BOIVIN, G.P., WASHINGTON, K., YANG, K., WARD, J.M., PRETLOW, T.P., RUSSELL, R., BESSELSEN, D.G., GODFREY, V.L., DOETSCHMAN, T., DOVE, W.F., PITOT, H.C., HALBERG, R.B., ITZKOWITZ, S.H., GRODEN, J. and COFFEY, R.J., 2003. Pathology of mouse models of intestinal cancer: consensus report and recommendations. *Gastroenterology,* **124**(3), pp. 762-777.

BONGERS, G., MUNIZ, L.R., PACER, M.E., IUGA, A.C., THIRUNARAYANAN, N., SLINGER, E., SMIT, M.J., REDDY, E.P., MAYER, L., FURTADO, G.C., HARPAZ, N. and LIRA, S.A., 2012. A role for the epidermal growth factor receptor signaling in development of intestinal serrated polyps in mice and humans. *Gastroenterology,* **143**(3), pp. 730-740.

BOTTARELLI, L., AZZONI, C., NECCHI, F., LAGRASTA, C., TAMBURINI, E., D'ADDA, T., PIZZI, S., SARLI, L., RINDI, G. and BORDI, C., 2007. Sex chromosome alterations associate with tumor progression in sporadic colorectal carcinomas. *Clinical cancer research : an official journal of the American Association for Cancer Research,* **13**(15 Pt 1), pp. 4365-4370.

BOYLE, P. and LANGMAN, J.S., 2000. ABC of colorectal cancer: Epidemiology. *BMJ (Clinical research ed.),* **321**(7264), pp. 805-808.

BRANDI, G., TAVOLARI, S., DE ROSA, F., DI GIROLAMO, S., AGOSTINI, V., BARBERA, M.A., FREGA, G. and BIASCO, G., 2012. Antitumoral efficacy of the protease inhibitor gabexate mesilate in colon cancer cells harbouring KRAS, BRAF and PIK3CA mutations. *PloS one,* **7**(7), pp. e41347.

BRAY, K., BRAKEBUSCH, C. and VARGO-GOGOLA, T., 2011. The Rho GTPase Cdc42 is required for primary mammary epithelial cell morphogenesis in vitro. *Small GTPases,* **2**(5), pp. 247-258.

BRENNER, H., KLOOR, M. and POX, C.P., 2014. Colorectal cancer. *Lancet (London, England),* **383**(9927), pp. 1490-1502.

BYUN, A.J., HUNG, K.E., FLEET, J.C., BRONSON, R.T., MASON, J.B., GARCIA, P.E. and CROTT, J.W., 2014. Colon-specific tumorigenesis in mice driven by Cre-mediated inactivation of *Apc* and activation of mutant *Kras*. *Cancer letters,* **347**(2), pp. 191-195.

CAMPS, J., GRADE, M., NGUYEN, Q.T., HÃ¶RMANN, P., BECKER, S., HUMMON, A.B., RODRIGUEZ, V., CHANDRASEKHARAPPA, S., CHEN, Y., DIFILIPPANTONIO, M.J., BECKER, H., GHADIMI, B.M. and RIED, T., 2008. Chromosomal Breakpoints in Primary Colon Cancer Cluster at Sites of Structural Variants in the Genome. *Cancer research,* **68**(5), pp. 1284-1295.

CANCER RESEARCH UK, 2015-last update, **Bowel cancer incidence statistics, Cancer Research UK**. Available: https://www.cancerresearchuk.org/health-professional/cancer-statistics/statistics-by-cancer-type/bowel-cancer [August/2018, 2018].

CANNON, K.S. and CRESSWELL, P., 2001. Quality control of transmembrane domain assembly in the tetraspanin CD82. *The EMBO journal,* **20**(10), pp. 2443-2453.

CARRAWAY, K.L., 2010. E3 Ubiquitin Ligases in ErbB Receptor Quantity Control. *Seminars in cell & developmental biology,* **21**(9), pp. 936-943.

CASTELLANO, E. and DOWNWARD, J., 2010. Role of RAS in the regulation of PI 3-kinase. *Current topics in microbiology and immunology,* **346**, pp. 143-169.

CHAIROUNGDUA, A., SMITH, D.L., POCHARD, P., HULL, M. and CAPLAN, M.J., 2010.

Exosome release of beta-catenin: a novel mechanism that antagonizes Wnt signaling. *The Journal of cell biology,* **190**(6), pp. 1079-1091.

CHALMIN, F., LADOIRE, S., MIGNOT, G., VINCENT, J., BRUCHARD, M., REMY-MARTIN, J.P., BOIREAU, W., ROULEAU, A., SIMON, B., LANNEAU, D., DE THONEL, A., MULTHOFF, G., HAMMAN, A., MARTIN, F., CHAUFFERT, B., SOLARY, E., ZITVOGEL, L., GARRIDO, C., RYFFEL, B., BORG, C., APETOH, L., REBE, C. and GHIRINGHELLI, F., 2010. Membrane-associated Hsp72 from tumor-derived exosomes mediates STAT3-dependent immunosuppressive function of mouse and human myeloid-derived suppressor cells. *The Journal of clinical investigation,* **120**(2), pp. 457-471.

CHAN, T.L., ZHAO, W., , LEUNG, S.Y. and YUEN, S.T., 2003. ***BRAF*** and ***KRAS*** Mutations in Colorectal Hyperplastic Polyps and Serrated Adenomas. *Cancer Res,* **63**(16), pp. 4878.

CHANG, L., CHANG, M., CHANG, H.M. and CHANG, F., 2017. Expending Role of Microsatellite Instability in Diagnosis and Treatment of Colorectal Cancers. *Journal of Gastrointestinal Cancer,* **48**(4), pp. 305-313.

CHARRIN, S., JOUANNET, S., BOUCHEIX, C. and RUBINSTEIN, E., 2014. Tetraspanins at a glance. *Journal of cell science,* **127**(Pt 17), pp. 3641-3648.

CHARRIN, S., LE NAOUR, F., SILVIE, O., MILHIET, P.E., BOUCHEIX, C. and RUBINSTEIN, E., 2009. Lateral organization of membrane proteins: tetraspanins spin their web. *The Biochemical journal,* **420**(2), pp. 133-154.

CHARRIN, S., MANIE, S., BILLARD, M., ASHMAN, L., GERLIER, D., BOUCHEIX, C. and RUBINSTEIN, E., 2003. Multiple levels of interactions within the tetraspanin web. *Biochemical and biophysical research communications,* **304**(1), pp. 107-112.

CHARRIN, S., MANIE, S., OUALID, M., BILLARD, M., BOUCHEIX, C. and RUBINSTEIN, E., 2002. Differential stability of tetraspanin/tetraspanin interactions: role of palmitoylation. *FEBS letters,* **516**(1-3), pp. 139-144.

CHAUVIN, A., WANG, C.S., GEHA, S., GARDE-GRANGER, P., MATHIEU, A.A., LACASSE, V. and BOISVERT, F.M., 2018. The response to neoadjuvant chemoradiotherapy with 5-fluorouracil in locally advanced rectal cancer patients: a predictive proteomic signature. *Clinical proteomics,* **15**, pp. 16-018-9192-2. eCollection 2018.

CHEN, G.Y., 2018. The Role of the Gut Microbiome in Colorectal Cancer. *Clinics in colon and rectal surgery,* **31**(3), pp. 192-198.

CHEN, L., ZHU, Y.Y., ZHANG, X.J., WANG, G.L., LI, X.Y., HE, S., ZHANG, J.B. and ZHU, J.W., 2009. TSPAN1 protein expression: a significant prognostic indicator for patients with colorectal adenocarcinoma. *World journal of gastroenterology,* **15**(18), pp. 2270-2276.

CHEN, L.C., HAO, C.Y., CHIU, Y.S., WONG, P., MELNICK, J.S., BROTMAN, M., MORETTO, J., MENDES, F., SMITH, A.P., BENNINGTON, J.L., MOORE, D. and LEE, N.M., 2004. Alteration of gene expression in normal-appearing colon mucosa of APC(min) mice and human cancer patients. *Cancer research,* **64**(10), pp. 3694-3700.

CHEN, X., HALBERG, R.B., BURCH, R.P. and DOVE, W.F., 2008. Intestinal adenomagenesis involves core molecular signatures of the epithelial-mesenchymal transition. *Journal of molecular histology,* **39**(3), pp. 283-294.

CHERUKURI, A., SHOHAM, T., SOHN, H.W., LEVY, S., BROOKS, S., CARTER, R. and

PIERCE, S.K., 2004. The tetraspanin CD81 is necessary for partitioning of coligated CD19/CD21-B cell antigen receptor complexes into signaling-active lipid rafts. *Journal of immunology (Baltimore, Md.: 1950),* **172**(1), pp. 370-380.

CHIANG SUM-FU, TSAI MING-HUNG, TANG REIPING, *ET AL.*, 2014. Membrane Proteins as Potential Colon Cancer Biomarkers: Verification of 4 Candidates from a Secretome Dataset. *Surgical Science,* **5**(10), pp. 418-438.

CHIGITA, S., SUGIURA, T., ABE, M., KOBAYASHI, Y., SHIMODA, M., ONODA, M. and SHIRASUNA, K., 2012. CD82 inhibits canonical Wnt signalling by controlling the cellular distribution of beta-catenin in carcinoma cells. *International journal of oncology,* **41**(6), pp. 2021-2028.

CHRISTIANSON, H.C., SVENSSON, K.J., VAN KUPPEVELT, T.H., LI, J.P. and BELTING, M., 2013. Cancer cell exosomes depend on cell-surface heparan sulfate proteoglycans for their internalization and functional activity. *Proceedings of the National Academy of Sciences of the United States of America,* **110**(43), pp. 17380-17385.

CHURCH, J.M., 2004. Clinical significance of small colorectal polyps. *Diseases of the colon and rectum,* **47**(4), pp. 481-485.

CLARKE, A.R., CUMMINGS, M.C. and HARRISON, D.J., 1995. Interaction between murine germline mutations in p53 and APC predisposes to pancreatic neoplasia but not to increased intestinal malignancy. *Oncogene,* **11**(9), pp. 1913-1920.

CLAYTON, A., MITCHELL, J.P., COURT, J., MASON, M.D. and TABI, Z., 2007. Human tumor-derived exosomes selectively impair lymphocyte responses to interleukin-2. *Cancer research,* **67**(15), pp. 7458-7466.

CLEVERS, H.C. and BEVINS, C.L., 2013. Paneth cells: maestros of the small intestinal crypts. *Annual Review of Physiology,* **75**, pp. 289-311.

COLNOT, S., NIWA-KAWAKITA, M., HAMARD, G., GODARD, C., LE PLENIER, S., HOUBRON, C., ROMAGNOLO, B., BERREBI, D., GIOVANNINI, M. and PERRET, C., 2004. Colorectal cancers in a new mouse model of familial adenomatous polyposis: influence of genetic and environmental modifiers. *Laboratory investigation; a journal of technical methods and pathology,* **84**(12), pp. 1619-1630.

COLOMBO, M., MOITA, C., VAN NIEL, G., KOWAL, J., VIGNERON, J., BENAROCH, P., MANEL, N., MOITA, L.F., THERY, C. and RAPOSO, G., 2013. Analysis of ESCRT functions in exosome biogenesis, composition and secretion highlights the heterogeneity of extracellular vesicles. *Journal of cell science,* **126**(Pt 24), pp. 5553-5565.

COLUSSI, D., BRANDI, G., BAZZOLI, F. and RICCIARDIELLO, L., 2013. Molecular pathways involved in colorectal cancer: implications for disease behavior and prevention. *International journal of molecular sciences,* **14**(8), pp. 16365-16385.

COSTA-SILVA, B., AIELLO, N.M., OCEAN, A.J., SINGH, S., ZHANG, H., THAKUR, B.K., BECKER, A., HOSHINO, A., MARK, M.T., MOLINA, H., XIANG, J., ZHANG, T., THEILEN, T.M., GARCIA-SANTOS, G., WILLIAMS, C., ARARSO, Y., HUANG, Y., RODRIGUES, G., SHEN, T.L., LABORI, K.J., LOTHE, I.M., KURE, E.H., HERNANDEZ, J., DOUSSOT, A., EBBESEN, S.H., GRANDGENETT, P.M., HOLLINGSWORTH, M.A., JAIN, M., MALLYA, K., BATRA, S.K., JARNAGIN, W.R., SCHWARTZ, R.E., MATEI, I., PEINADO, H., STANGER, B.Z., BROMBERG, J. and LYDEN, D., 2015. Pancreatic cancer exosomes initiate pre-metastatic niche formation in the liver. *Nature cell biology,* **17**(6), pp. 816-826.

CREAMER, B., SHORTER, R.G. and BAMFORTH, J., 1961. The turnover and shedding of epithelial cells. I. The turnover in the gastro-intestinal tract. *Gut,* **2**, pp. 110-118.

DAHLHOFF, M., HORST, D., GERHARD, M., KOLLIGS, F.T., WOLF, E. and SCHNEIDER, M.R., 2008. Betacellulin stimulates growth of the mouse intestinal epithelium and increases adenoma multiplicity in Apc+/Min mice. *FEBS letters,* **582**(19), pp. 2911-2915.

DALERBA, P., KALISKY, T., SAHOO, D., RAJENDRAN, P.S., ROTHENBERG, M.E., LEYRAT, A.A., SIM, S., OKAMOTO, J., JOHNSTON, D.M., QIAN, D., ZABALA, M., BUENO, J., NEFF, N.F., WANG, J., SHELTON, A.A., VISSER, B., HISAMORI, S., SHIMONO, Y., VAN DE WETERING, M., CLEVERS, H., CLARKE, M.F. and QUAKE, S.R., 2011. Single-cell dissection of transcriptional heterogeneity in human colon tumors. *Nature biotechnology,* **29**(12), pp. 1120-1127.

DANGLOT, L., CHAINEAU, M., DAHAN, M., GENDRON, M.C., BOGGETTO, N., PEREZ, F. and GALLI, T., 2010. Role of TI-VAMP and CD82 in EGFR cell-surface dynamics and signaling. *Journal of cell science,* **123**(Pt 5), pp. 723-735.

DANIEL, C.R., BOSTICK, R.M., FLANDERS, W.D., LONG, Q., FEDIRKO, V., SIDELNIKOV, E. and SEABROOK, M.E., 2009. TGF-alpha expression as a potential biomarker of risk within the normal-appearing colorectal mucosa of patients with and without incident sporadic adenoma. *Cancer epidemiology, biomarkers & prevention : a publication of the American Association for Cancer Research, cosponsored by the American Society of Preventive Oncology,* **18**(1), pp. 65-73.

DANIEL, L., LIYUAN, D., JACQUETTA, T. and RIMA, R., 2004. ApcMin/+ mouse model of colon cancer: Gene expression profiling in tumors. *Journal of cellular biochemistry,* **93**(6), pp. 1242-1254.

DATE, S. and SATO, T., 2015. Mini-gut organoids: reconstitution of the stem cell niche. *Annual Review of Cell and Developmental Biology,* **31**, pp. 269-289.

DE JONG, P.,R., TAKAHASHI, N., HARRIS, A.R., LEE, J., BERTIN, S., JEFFRIES, J., JUNG, M., DUONG, J., TRIANO, A.I., LEE, J., NIV, Y., HERDMAN, D.S., TANIGUCHI, K., KIM, C., DONG, H., ECKMANN, L., STANFORD, S.M., BOTTINI, N., CORR, M. and RAZ, E., 2014. Ion channel TRPV1-dependent activation of PTP1B suppresses EGFR-associated intestinal tumorigenesis. *The Journal of clinical investigation,* **124**(9), pp. 3793-3806.

DOWTY, J.G., WIN, A.K., BUCHANAN, D.D., LINDOR, N.M., MACRAE, F.A., CLENDENNING, M., ANTILL, Y.C., THIBODEAU, S.N., CASEY, G., GALLINGER, S., LE MARCHAND, L., NEWCOMB, P.A., HAILE, R.W., YOUNG, G.P., JAMES, P.A., GILES, G.G., GUNAWARDENA, S.R., LEGGETT, B.A., GATTAS, M., BOUSSIOUTAS, A., AHNEN, D.J., BARON, J.A., PARRY, S., GOLDBLATT, J., YOUNG, J.P., HOPPER, J.L. and JENKINS, M.A., 2013. Cancer risks for MLH1 and MSH2 mutation carriers. *Human mutation,* **34**(3), pp. 10.1002/humu.22262.

DROST, J., VAN JAARSVELD, R.H., PONSIOEN, B., ZIMBERLIN, C., VAN BOXTEL, R., BUIJS, A., SACHS, N., OVERMEER, R.M., OFFERHAUS, G.J., BEGTHEL, H., KORVING, J., VAN DE WETERING, M., SCHWANK, G., LOGTENBERG, M., CUPPEN, E., SNIPPERT, H.J., MEDEMA, J.P., KOPS, G.J. and CLEVERS, H., 2015. Sequential cancer mutations in cultured human intestinal stem cells. *Nature,* **521**(7550), pp. 43-47.

DRULINER, B.R., RASHTAK, S., RUAN, X., BAE, T., VASMATZIS, N., O'BRIEN, D., JOHNSON, R., FELMLEE-DEVINE, D., WASHECHEK-ALETTO, J., BASU, N., LIU, H., SMYRK, T., ABYZOV, A. and BOARDMAN, L.A., 2016. Colorectal Cancer with Residual Polyp of Origin: A Model of Malignant Transformation. *Translational oncology,* **9**(4), pp. 280-286.

DRULINER, B.R., WANG, P., BAE, T., BAHETI, S., SLETTEDAHL, S., MAHONEY, D., VASMATZIS, N., XU, H., KIM, M., BOCKOL, M., O'BRIEN, D., GRILL, D., WARNER, N., MUNOZ-

GOMEZ, M., KOSSICK, K., JOHNSON, R., MOUCHLI, M., FELMLEE-DEVINE, D., WASHECHEK-ALETTO, J., SMYRK, T., OBERG, A., WANG, J., CHIA, N., ABYZOV, A., AHLQUIST, D. and BOARDMAN, L.A., 2018. Molecular characterization of colorectal adenomas with and without malignancy reveals distinguishing genome, transcriptome and methylome alterations. *Scientific reports,* **8**(1), pp. 3161-018-21525-4.

DRUMMER, H.E., WILSON, K.A. and POUMBOURIOS, P., 2002. Identification of the hepatitis C virus E2 glycoprotein binding site on the large extracellular loop of CD81. *Journal of virology,* **76**(21), pp. 11143-11147.

DU, W.W., FANG, L., LI, M., YANG, X., LIANG, Y., PENG, C., QIAN, W., O'MALLEY, Y.Q., ASKELAND, R.W., SUGG, S.L., QIAN, J., LIN, J., JIANG, Z., YEE, A.J., SEFTON, M., DENG, Z., SHAN, S.W., WANG, C.H. and YANG, B.B., 2013. MicroRNA miR-24 enhances tumor invasion and metastasis by targeting PTPN9 and PTPRF to promote EGF signaling. *Journal of cell science,* **126**(Pt 6), pp. 1440-1453.

EGUCHI, T., SOGAWA, C., OKUSHA, Y., UCHIBE, K., IINUMA, R., ONO, K., NAKANO, K., MURAKAMI, J., ITOH, M., ARAI, K., FUJIWARA, T., NAMBA, Y., MURATA, Y., OHYAMA, K., SHIMOMURA, M., OKAMURA, H., TAKIGAWA, M., NAKATSURA, T., KOZAKI, K., OKAMOTO, K. and CALDERWOOD, S.K., 2017. Organoids with cancer stem cell-like properties secrete exosomes and HSP90 in a 3D nanoenvironment. *PLoS ONE,* **13**(2), pp. e0191109.

EKSTROM, E.J., BERGENFELZ, C., VON BULOW, V., SERIFLER, F., CARLEMALM, E., JONSSON, G., ANDERSSON, T. and LEANDERSSON, K., 2014. WNT5A induces release of exosomes containing pro-angiogenic and immunosuppressive factors from malignant melanoma cells. *Molecular cancer,* **13**, pp. 88-4598-13-88.

EL MOUSSAWI, L., CHAKKOUR, M. and KREYDIYYEH, S.I., 2018. Epinephrine modulates Na+/K+ ATPase activity in Caco-2 cells via Src, p38MAPK, ERK and PGE2. *PloS one,* **13**(2), pp. e0193139.

ETTRICH, T.J. and SEUFFERLEIN, T., 2018. Regorafenib. *Recent results in cancer research.Fortschritte der Krebsforschung.Progres dans les recherches sur le cancer,* **211**, pp. 45-56.

FAIR, K.L., COLQUHOUN, J. and HANNAN, N.R.F., 2018. Intestinal organoids for modelling intestinal development and disease. *Philosophical transactions of the Royal Society of London.Series B, Biological sciences,* **373**(1750), pp. 10.1098/rstb.2017.0217.

FARES, J., KASHYAP, R. and ZIMMERMANN, P., 2016. Syntenin: Key player in cancer exosome biogenesis and uptake? *Cell Adhesion & Migration,* **11**(2), pp. 124-126.

FARIN, H.F., VAN ES, J.H. and CLEVERS, H., 2012. Redundant Sources of Wnt Regulate Intestinal Stem Cells and Promote Formation of Paneth Cells. *Gastroenterology,* **143**(6), pp. 1518-1529.e7.

FEARON, E.R. and VOGELSTEIN, B., 1990. A genetic model for colorectal tumorigenesis. *Cell,* **61**(5), pp. 759-767.

FEARON, E.R., 2011. Molecular Genetics of Colorectal Cancer. *Annual Review of Pathology: Mechanisms of Disease,* **6**(1), pp. 479-507.

FERLAY J, SOERJOMATARAM I, ERVIK M, DIKSHIT R, ESER S, MATHERS C, REBELO M, PARKIN DM, FORMAN D and BRAY, F., 2013-last update, GLOBOCAN 2012 v1.0, Cancer Incidence and Mortality Worldwide: IARC CancerBase No. 11. Available: http://globocan.iarc.fr [08/21, 2018].

FERLAY, J., SOERJOMATARAM, I., DIKSHIT, R., ESER, S., MATHERS, C., REBELO, M., PARKIN, D.M., FORMAN, D. and BRAY, F., 2015. Cancer incidence and mortality worldwide: sources, methods and major patterns in GLOBOCAN 2012. *International journal of cancer,* **136**(5), pp. E359-86.

FERNANDEZ-LARREA, J., MERLOS-SUAREZ, A., URENA, J.M., BASELGA, J. and ARRIBAS, J., 1999. A role for a PDZ protein in the early secretory pathway for the targeting of proTGF-alpha to the cell surface. *Molecular cell,* **3**(4), pp. 423-433.

FIALKA, I., STEINLEIN, P., AHORN, H., BOCK, G., BURBELO, P.D., HABERFELLNER, M., LOTTSPEICH, F., PAIHA, K., PASQUALI, C. and HUBER, L.A., 1999. Identification of syntenin as a protein of the apical early endocytic compartment in Madin-Darby canine kidney cells. *The Journal of biological chemistry,* **274**(37), pp. 26233-26239.

FLEMING, N.I., JORISSEN, R.N., MOURADOV, D., CHRISTIE, M., SAKTHIANANDESWAREN, A., PALMIERI, M., DAY, F., LI, S., TSUI, C., LIPTON, L., DESAI, J., JONES, I.T., MCLAUGHLIN, S., WARD, R.L., HAWKINS, N.J., RUSZKIEWICZ, A.R., MOORE, J., ZHU, H.J., MARIADASON, J.M., BURGESS, A.W., BUSAM, D., ZHAO, Q., STRAUSBERG, R.L., GIBBS, P. and SIEBER, O.M., 2013. SMAD2, SMAD3 and SMAD4 mutations in colorectal cancer. *Cancer research,* **73**(2), pp. 725-735.

FONSECA-NUNES, A., JAKSZYN, P. and AGUDO, A., 2013. Iron and Cancer Riskâ€"A Systematic Review and Meta-analysis of the Epidemiological Evidence. *Cancer Epidemiol Biomarkers Prev,* .

FORBES, S.A., BEARE, D., BOUTSELAKIS, H., BAMFORD, S., BINDAL, N., TATE, J., COLE, C.G., WARD, S., DAWSON, E., PONTING, L., STEFANCSIK, R., HARSHA, B., KOK, C.Y., JIA, M., JUBB, H., SONDKA, Z., THOMPSON, S., DE, T. and CAMPBELL, P.J., 2017. COSMIC: somatic cancer genetics at high-resolution. *Nucleic acids research,* **45**, pp. D777-D783.

FRANCIES, H.E., BARTHORPE, A., MCLAREN-DOUGLAS, A., BARENDT, W.J. and GARNETT, M.J., 2016. Drug Sensitivity Assays of Human Cancer Organoid Cultures. *Methods in molecular biology (Clifton, N.J.),* .

FREDERICKS E, DEALTRY G, *ET AL.*, 2015. Fredericks E, Dealtry G, Roux S (2015) Molecular aspects of Colorectal Carcinogenesis: A Review. *J Cancer Biol Res,* **3(1)**, pp. 1057.

FUERER, C., NUSSE, R. and TEN BERGE, D., 2008. Wnt signalling in development and disease. Max Delbruck Center for Molecular Medicine meeting on Wnt signaling in Development and Disease. *EMBO reports,* **9**(2), pp. 134-138.

GEORGOPOULOS, N.T., KIRKWOOD, L.A. and SOUTHGATE, J., 2014. A novel bidirectional positive-feedback loop between Wntâ€"Î²-catenin and EGFRâ€"ERK plays a role in context-specific modulation of epithelial tissue regeneration. *Journal of cell science,* **127**(13), pp. 2967.

GESTA, S., TSENG, Y. and KAHN, C.R., 2007. *Developmental Origin of Fat: Tracking Obesity to Its Source.*

GHOSSOUB, R., LEMBO, F., RUBIO, A., GAILLARD, C.B., BOUCHET, J., VITALE, N., SLAVIK, J., MACHALA, M. and ZIMMERMANN, P., 2014. Syntenin-ALIX exosome biogenesis and budding into multivesicular bodies are controlled by ARF6 and PLD2. *Nature communications,* **5**, pp. 3477.

GOMEZ-ORTE, E., SAENZ-NARCISO, B., MORENO, S. and CABELLO, J., 2013. Multiple functions of the noncanonical Wnt pathway. *Trends in genetics : TIG,* **29**(9), pp. 545-553.

GONG, J., CHEHRAZI-RAFFLE, A., REDDI, S. and SALGIA, R., 2018. Development of PD-1 and PD-L1 inhibitors as a form of cancer immunotherapy: a comprehensive review of registration trials and future considerations. *Journal for immunotherapy of cancer,* **6**(1), pp. 8-018-0316-z.

GONZALEZ, R.S., WASHINGTON, K. and SHI, C., 2017. Current applications of molecular pathology in colorectal carcinoma. *Applied Cancer Research,* **37**(1), pp. 13.

GRECO, C., BRALET, M.P., AILANE, N., DUBART-KUPPERSCHMITT, A., RUBINSTEIN, E., LE NAOUR, F. and BOUCHEIX, C., 2010. E-cadherin/p120-catenin and tetraspanin Co-029 cooperate for cell motility control in human colon carcinoma. *Cancer research,* **70**(19), pp. 7674-7683.

GREEN, L.R., MONK, P.N., PARTRIDGE, L.J., MORRIS, P., GORRINGE, A.R. and READ, R.C., 2011. Cooperative role for tetraspanins in adhesin-mediated attachment of bacterial species to human epithelial cells. *Infection and immunity,* **79**(6), pp. 2241-2249.

GRILL, J.I., NEUMANN, J., HERBST, A., HILTWEIN, F., OFNER, A., MARSCHALL, M.K., WOLF, E., KIRCHNER, T., GOKE, B., SCHNEIDER, M.R. and KOLLIGS, F.T., 2014. DRO1 inactivation drives colorectal carcinogenesis in ApcMin/+ mice. *Molecular cancer research : MCR,* **12**(11), pp. 1655-1662.

GROSS, J.C., CHAUDHARY, V., BARTSCHERER, K. and BOUTROS, M., 2012. Active Wnt proteins are secreted on exosomes. *Nature cell biology,* **14**(10), pp. 1036-1045.

GUIX, F.X., SANNERUD, R., BERDITCHEVSKI, F., ARRANZ, A.M., HORRE, K., SNELLINX, A., THATHIAH, A., SAIDO, T., SAITO, T., RAJESH, S., OVERDUIN, M., KUMAR-SINGH, S., RADAELLI, E., CORTHOUT, N., COLOMBELLI, J., TOSI, S., MUNCK, S., SALAS, I.H., ANNAERT, W. and DE STROOPER, B., 2017. Tetraspanin 6: a pivotal protein of the multiple vesicular body determining exosome release and lysosomal degradation of amyloid precursor protein fragments. *Molecular neurodegeneration,* **12**(1), pp. 25-017-0165-0.

GUO, Q., XIA, B., ZHANG, F., RICHARDSON, M.M., LI, M., ZHANG, J.S., CHEN, F. and ZHANG, X.A., 2012. Tetraspanin CO-029 inhibits colorectal cancer cell movement by deregulating cell-matrix and cell-cell adhesions. *PloS one,* **7**(6), pp. e38464.

HAEUW, J.F., GOETSCH, L., BAILLY, C. and CORVAIA, N., 2011. Tetraspanin CD151 as a target for antibody-based cancer immunotherapy. *Biochemical Society transactions,* **39**(2), pp. 553-558.

HAGGAR, F.A. and BOUSHEY, R.P., 2009. Colorectal cancer epidemiology: incidence, mortality, survival, and risk factors. *Clinics in colon and rectal surgery,* **22**(4), pp. 191-197.

HAIGIS, K.M., KENDALL, K.R., WANG, Y., CHEUNG, A., HAIGIS, M.C., GLICKMAN, J.N., NIWA-KAWAKITA, M., SWEET-CORDERO, A., SEBOLT-LEOPOLD, J., SHANNON, K.M., SETTLEMAN, J., GIOVANNINI, M. and JACKS, T., 2008. Differential effects of oncogenic K-Ras and N-Ras on proliferation, differentiation and tumor progression in the colon. *Nature genetics,* **40**(5), pp. 600-608.

HAINING, E.J., YANG, J., BAILEY, R.L., KHAN, K., COLLIER, R., TSAI, S., WATSON, S.P., FRAMPTON, J., GARCIA, P. and TOMLINSON, M.G., 2012. The TspanC8 subgroup of tetraspanins interacts with A disintegrin and metalloprotease 10 (ADAM10) and regulates its maturation and cell surface expression. *The Journal of biological chemistry,* **287**(47), pp. 39753-39765.

HALBERG, R.B., WAGGONER, J., RASMUSSEN, K., WHITE, A., CLIPSON, L., PRUNUSKE, A.J., BACHER, J.W., SULLIVAN, R., WASHINGTON, M.K., PITOT, H.C., PETRINI, J.H., ALBERTSON, D.G. and DOVE, W.F., 2009. Long-lived Min mice develop advanced intestinal cancers

through a genetically conservative pathway. *Cancer research,* **69**(14), pp. 5768-5775.

HALF, E., BERCOVICH, D. and ROZEN, P., 2009. Familial adenomatous polyposis. *Orphanet journal of rare diseases,* **4**, pp. 22-1172-4-22.

HAMAMOTO, T., BEPPU, H., OKADA, H., KAWABATA, M., KITAMURA, T., MIYAZONO, K. and KATO, M., 2002. Compound disruption of smad2 accelerates malignant progression of intestinal tumors in apc knockout mice. *Cancer research,* **62**(20), pp. 5955-5961.

HAO, H.X., JIANG, X. and CONG, F., 2016. Control of Wnt Receptor Turnover by R-spondin-ZNRF3/RNF43 Signaling Module and Its Dysregulation in Cancer. *Cancers,* **8**(6), pp. 10.3390/cancers8060054.

HAPAK, S.M., ROTHLIN, C.V. and GHOSH, S., 2018. PAR3-PAR6-atypical PKC polarity complex proteins in neuronal polarization. *Cellular and molecular life sciences : CMLS,* **75**(15), pp. 2735-2761.

HASHIDA, H., TAKABAYASHI, A., TOKUHARA, T., HATTORI, N., TAKI, T., HASEGAWA, H., SATOH, S., KOBAYASHI, N., YAMAOKA, Y. and MIYAKE, M., 2003. Clinical significance of transmembrane 4 superfamily in colon cancer. *British journal of cancer,* **89**(1), pp. 158-167.

HATANO, Y., SEMI, K., HASHIMOTO, K., LEE, M.S., HIRATA, A., TOMITA, H., KUNO, T., TAKAMATSU, M., AOKI, K., TAKETO, M.M., KIM, Y., HARA, A. and YAMADA, Y., 2015. Reducing DNA methylation suppresses colon carcinogenesis by inducing tumor cell differentiation. *Carcinogenesis,* **36**(7), pp. 719-729.

HE, X.C., YIN, T., GRINDLEY, J.C., TIAN, Q., SATO, T., TAO, W.A., DIRISINA, R., PORTER-WESTPFAHL, K., HEMBREE, M., JOHNSON, T., WIEDEMANN, L.M., BARRETT, T.A., HOOD, L., WU, H. and LI, L., 2007. PTEN-deficient intestinal stem cells initiate intestinal polyposis. *Nature genetics,* **39**(2), pp. 189-198.

HE, Y., KONG, F., DU, H. and WU, M., 2014. Decreased expression of uroplakin Ia is associated with colorectal cancer progression and poor survival of patients. *International journal of clinical and experimental pathology,* **7**(8), pp. 5031-5037.

HEINEMANN, V., STINTZING, S., KIRCHNER, T., BOECK, S. and JUNG, A., 2009. Clinical relevance of EGFR- and KRAS-status in colorectal cancer patients treated with monoclonal antibodies directed against the EGFR. *Cancer treatment reviews,* **35**(3), pp. 262-271.

HEITMAN, S.J., RONKSLEY, P.E., HILSDEN, R.J., MANNS, B.J., ROSTOM, A. and HEMMELGARN, B.R., 2009. Prevalence of adenomas and colorectal cancer in average risk individuals: a systematic review and meta-analysis. *Clinical gastroenterology and hepatology : the official clinical practice journal of the American Gastroenterological Association,* **7**(12), pp. 1272-1278.

HEMLER, M.E., 2014. Tetraspanin proteins promote multiple cancer stages. *Nature reviews.Cancer,* **14**(1), pp. 49-60.

HEMLER, M.E., 2005. Tetraspanin functions and associated microdomains. *Nature reviews.Molecular cell biology,* **6**(10), pp. 801-811.

HERR, R., KOHLER, M., ANDRLOVA, H., WEINBERG, F., MOLLER, Y., HALBACH, S., LUTZ, L., MASTROIANNI, J., KLOSE, M., BITTERMANN, N., KOWAR, S., ZEISER, R., OLAYIOYE, M.A., LASSMANN, S., BUSCH, H., BOERRIES, M. and BRUMMER, T., 2015. B-Raf inhibitors induce epithelial differentiation in BRAF-mutant colorectal cancer cells. *Cancer research,* **75**(1), pp. 216-229.

HERREROS-VILLANUEVA, M., MUNIZ, P., GARCIA-GIRON, C., CAVIA-SAIZ, M. and DEL CORRAL, M.J., 2010. TAp73 is one of the genes responsible for the lack of response to chemotherapy depending on B-Raf mutational status. *Journal of translational medicine,* **8**, pp. 15-5876-8-15.

HIGGINBOTHAM, J.N., DEMORY BECKLER, M., GEPHART, J.D., FRANKLIN, J.L., BOGATCHEVA, G., KREMERS, G.J., PISTON, D.W., AYERS, G.D., MCCONNELL, R.E., TYSKA, M.J. and COFFEY, R.J., 2011. Amphiregulin exosomes increase cancer cell invasion. *Current biology : CB,* **21**(9), pp. 779-786.

HINO, J., MIYAZAWA, T., MIYAZATO, M. and KANGAWA, K., 2012. Bone morphogenetic protein-3b (BMP-3b) is expressed in adipocytes and inhibits adipogenesis as a unique complex. *International journal of obesity (2005),* **36**(5), pp. 725-734.

HISHA, H., TANAKA, T., KANNO, S., TOKUYAMA, Y., KOMAI, Y., OHE, S., YANAI, H., OMACHI, T. and UENO, H., 2013. Establishment of a novel lingual organoid culture system: generation of organoids having mature keratinized epithelium from adult epithelial stem cells. *Scientific reports,* **3**, pp. 3224.

HLUBEK, F., BRABLETZ, T., BUDCZIES, J., PFEIFFER, S., JUNG, A. and KIRCHNER, T., 2007. Heterogeneous expression of Wnt/beta-catenin target genes within colorectal cancer. *International journal of cancer,* **121**(9), pp. 1941-1948.

HOLMBERG, F.E.O., SEIDELIN, J.B., YIN, X., MEAD, B.E., TONG, Z., LI, Y., KARP, J.M. and NIELSEN, O.H., 2017. Culturing human intestinal stem cells for regenerative applications in the treatment of inflammatory bowel disease. *EMBO Molecular Medicine,* **9**(5), pp. 558-570.

HOPF, T.A., COLWELL, L.J., SHERIDAN, R., ROST, B., SANDER, C. and MARKS, D.S., 2012. Three-dimensional structures of membrane proteins from genomic sequencing. *Cell,* **149**(7), pp. 1607-1621.

HOSHINO, A., COSTA-SILVA, B., SHEN, T.L., RODRIGUES, G., HASHIMOTO, A., TESIC MARK, M., MOLINA, H., KOHSAKA, S., DI GIANNATALE, A., CEDER, S., SINGH, S., WILLIAMS, C., SOPLOP, N., URYU, K., PHARMER, L., KING, T., BOJMAR, L., DAVIES, A.E., ARARSO, Y., ZHANG, T., ZHANG, H., HERNANDEZ, J., WEISS, J.M., DUMONT-COLE, V.D., KRAMER, K., WEXLER, L.H., NARENDRAN, A., SCHWARTZ, G.K., HEALEY, J.H., SANDSTROM, P., LABORI, K.J., KURE, E.H., GRANDGENETT, P.M., HOLLINGSWORTH, M.A., DE SOUSA, M., KAUR, S., JAIN, M., MALLYA, K., BATRA, S.K., JARNAGIN, W.R., BRADY, M.S., FODSTAD, O., MULLER, V., PANTEL, K., MINN, A.J., BISSELL, M.J., GARCIA, B.A., KANG, Y., RAJASEKHAR, V.K., GHAJAR, C.M., MATEI, I., PEINADO, H., BROMBERG, J. and LYDEN, D., 2015. Tumour exosome integrins determine organotropic metastasis. *Nature,* **527**(7578), pp. 329-335.

HOUGARDY, B.M., MADURO, J.H., VAN DER ZEE, A.G., WILLEMSE, P.H., DE JONG, S. and DE VRIES, E.G., 2005. Clinical potential of inhibitors of survival pathways and activators of apoptotic pathways in treatment of cervical cancer: changing the apoptotic balance. *The Lancet.Oncology,* **6**(8), pp. 589-598.

HUANG, D. and DU, X., 2008. Crosstalk between tumor cells and microenvironment via Wnt pathway in colorectal cancer dissemination. *World journal of gastroenterology,* **14**(12), pp. 1823-1827.

HUANG, S., YUAN, S., DONG, M., SU, J., YU, C., SHEN, Y., XIE, X., YU, Y., YU, X., CHEN, S., ZHANG, S., PONTAROTTI, P. and XU, A., 2005. The phylogenetic analysis of tetraspanins projects the evolution of cell-cell interactions from unicellular to multicellular organisms. *Genomics,* **86**(6), pp. 674-684.

HUMAN PROTEIN ATLAS, 2017, 2017-last update, **A pathology atlas of the human cancer**

transcriptome. . Available: https://www.proteinatlas.org/ENSG00000000003-TSPAN6/pathology/tissue/colorectal+cancer#Location [08/21, 2018].

HUNG, K.E., MARICEVICH, M.A., RICHARD, L.G., CHEN, W.Y., RICHARDSON, M.P., KUNIN, A., BRONSON, R.T., MAHMOOD, U. and KUCHERLAPATI, R., 2010. Development of a mouse model for sporadic and metastatic colon tumors and its use in assessing drug treatment. *Proceedings of the National Academy of Sciences of the United States of America,* **107**(4), pp. 1565-1570.

HUR, J., CHOI, J.I., LEE, H., NHAM, P., KIM, T.W., CHAE, C.W., YUN, J.Y., KANG, J.A., KANG, J., LEE, S.E., YOON, C.H., BOO, K., HAM, S., ROH, T.Y., JUN, J.K., LEE, H., BAEK, S.H. and KIM, H.S., 2016. CD82/KAI1 Maintains the Dormancy of Long-Term Hematopoietic Stem Cells through Interaction with DARC-Expressing Macrophages. *Cell stem cell,* **18**(4), pp. 508-521.

IMHOF, I., GASPER, W.J. and DERYNCK, R., 2008. Association of tetraspanin CD9 with transmembrane TGF{alpha} confers alterations in cell-surface presentation of TGF{alpha} and cytoskeletal organization. *Journal of cell science,* **121**(Pt 13), pp. 2265-2274.

IMJETI, N.S., MENCK, K., EGEA-JIMENEZ, A., LECOINTRE, C., LEMBO, F., BOUGUENINA, H., BADACHE, A., GHOSSOUB, R., DAVID, G., ROCHE, S. and ZIMMERMANN, P., 2017. Syntenin mediates SRC function in exosomal cell-to-cell communication. *Proc Natl Acad Sci USA,* **114**(47), pp. 12495.

IVANOV, A.I., HOPKINS, A.M., BROWN, G.T., GERNER-SMIDT, K., BABBIN, B.A., PARKOS, C.A. and NUSRAT, A., 2008. Myosin II regulates the shape of three-dimensional intestinal epithelial cysts. *Journal of cell science,* **121**(11), pp. 1803-1814.

JACKSTADT, R. and SANSOM, O.J., 2015. Mouse models of intestinal cancer. *The Journal of pathology,* **238**(2), pp. 141-151.

JACOBY, R.F., SEIBERT, K., COLE, C.E., KELLOFF, G. and LUBET, R.A., 2000. The Cyclooxygenase-2 Inhibitor Celecoxib Is a Potent Preventive and Therapeutic Agent in the Min Mouse Model of Adenomatous Polyposis. *Cancer research,* **60**(18), pp. 5040-5044.

JAFFE, A.B., KAJI, N., DURGAN, J. and HALL, A., 2008. Cdc42 controls spindle orientation to position the apical surface during epithelial morphogenesis. *The Journal of cell biology,* **183**(4), pp. 625-633.

JAGAN, I., FATEHULLAH, A., DEEVI, R.K., BINGHAM, V. and CAMPBELL, F.C., 2013. Rescue of glandular dysmorphogenesis in PTEN-deficient colorectal cancer epithelium by PPARgamma-targeted therapy. *Oncogene,* **32**(10), pp. 1305-1315.

JAGER, D., HALAMA, N., ZORNIG, I., KLUG, P., KRAUSS, J. and HAAG, G.M., 2016. Immunotherapy of Colorectal Cancer. *Oncology research and treatment,* **39**(6), pp. 346-350.

JANSSEN, K.P., ALBERICI, P., FSIHI, H., GASPAR, C., BREUKEL, C., FRANKEN, P., ROSTY, C., ABAL, M., EL MARJOU, F., SMITS, R., LOUVARD, D., FODDE, R. and ROBINE, S., 2006. APC and oncogenic KRAS are synergistic in enhancing Wnt signaling in intestinal tumor formation and progression. *Gastroenterology,* **131**(4), pp. 1096-1109.

JESS, T., RUNGOE, C. and PEYRIN-BIROULET, L., 2012. Risk of colorectal cancer in patients with ulcerative colitis: a meta-analysis of population-based cohort studies. *Clinical gastroenterology and hepatology : the official clinical practice journal of the American Gastroenterological Association,* **10**(6), pp. 639-645.

JOUANNET, S., SAINT-POL, J., FERNANDEZ, L., NGUYEN, V., CHARRIN, S., BOUCHEIX, C., BROU, C., MILHIET, P.E. and RUBINSTEIN, E., 2016. TspanC8 tetraspanins differentially regulate the cleavage of ADAM10 substrates, Notch activation and ADAM10 membrane compartmentalization. *Cellular and molecular life sciences : CMLS,* **73**(9), pp. 1895-1915.

JUAN, T. and FURTHAUER, M., 2018. Biogenesis and function of ESCRT-dependent extracellular vesicles. *Seminars in cell & developmental biology,* **74**, pp. 66-77.

JUNG, P., SATO, T., MERLOS-SUAREZ, A., BARRIGA, F.M., IGLESIAS, M., ROSSELL, D., AUER, H., GALLARDO, M., BLASCO, M.A., SANCHO, E., CLEVERS, H. and BATLLE, E., 2011. Isolation and in vitro expansion of human colonic stem cells. *Nature medicine,* **17**(10), pp. 1225-1227.

JUNGE, H.J., YANG, S., BURTON, J.B., PAES, K., SHU, X., FRENCH, D.M., COSTA, M., RICE, D.S. and YE, W., 2009. TSPAN12 regulates retinal vascular development by promoting Norrin- but not Wnt-induced FZD4/beta-catenin signaling. *Cell,* **139**(2), pp. 299-311.

KABAT, G.C., MILLER, A.B., JAIN, M. and ROHAN, T.E., 2007. A cohort study of dietary iron and heme iron intake and risk of colorectal cancer in women. *British journal of cancer,* **97**(1), pp. 118-122.

KABIRI, Z., GREICIUS, G., MADAN, B., BIECHELE, S., ZHONG, Z., ZARIBAFZADEH, H., EDISON, ALIYEV, J., WU, Y., BUNTE, R., WILLIAMS, B.O., ROSSANT, J. and VIRSHUP, D.M., 2014. Stroma provides an intestinal stem cell niche in the absence of epithelial Wnts. *Development (Cambridge, England),* **141**(11), pp. 2206-2215.

KALRA, H., DRUMMEN, G.P.C. and MATHIVANAN, S., 2015. Focus on Extracellular Vesicles: Introducing the Next Small Big Thing. *International Journal of Molecular Sciences,* **17**(2), pp. 170.

KARAMATIC CREW, V., BURTON, N., KAGAN, A., GREEN, C.A., LEVENE, C., FLINTER, F., BRADY, R.L., DANIELS, G. and ANSTEE, D.J., 2004. CD151, the first member of the tetraspanin (TM4) superfamily detected on erythrocytes, is essential for the correct assembly of human basement membranes in kidney and skin. *Blood,* **104**(8), pp. 2217-2223.

KASHYAP, R., ROUCOURT, B., LEMBO, F., FARES, J., CARCAVILLA, A.M., RESTOUIN, A., ZIMMERMANN, P. and GHOSSOUB, R., 2015. Syntenin controls migration, growth, proliferation, and cell cycle progression in cancer cells. *Frontiers in Pharmacology,* **6**, pp. 241.

KATOH, M., 2017. Canonical and non-canonical WNT signaling in cancer stem cells and their niches: Cellular heterogeneity, omics reprogramming, targeted therapy and tumor plasticity (Review). *International journal of oncology,* **51**(5), pp. 1357-1369.

KAZAROV, A.R., YANG, X., STIPP, C.S., SEHGAL, B. and HEMLER, M.E., 2002. An extracellular site on tetraspanin CD151 determines alpha 3 and alpha 6 integrin-dependent cellular morphology. *The Journal of cell biology,* **158**(7), pp. 1299-1309.

KEDRIN, D. and GALA, M.K., 2015. Genetics of the serrated pathway to colorectal cancer. *Clinical and translational gastroenterology,* **6**, pp. e84.

KEGELMAN, T.P., DAS, S.K., EMDAD, L., HU, B., MENEZES, M.E., BHOOPATHI, P., WANG, X.Y., PELLECCHIA, M., SARKAR, D. and FISHER, P.B., 2015. Targeting tumor invasion: the roles of MDA-9/Syntenin. *Expert opinion on therapeutic targets,* **19**(1), pp. 97-112.

KENNELL, J.A. and MACDOUGALD, O.A., 2005. Wnt Signaling Inhibits Adipogenesis through ß-Catenin-dependent and -independent Mechanisms. *Journal of Biological Chemistry,* **280**(25), pp.

24004-24010.

KETTUNEN, H.L., KETTUNEN, A.S.L. and RAUTONEN, N.E., 2003. Intestinal Immune Responses in Wild-Type and ***Apc***$^{Min/+}$ Mouse, a Model for Colon Cancer. *Cancer Res,* **63**(16), pp. 5136.

KHELWATTY, S., ESSAPEN, S., BAGWAN, I., GREEN, M., SEDDON, A. and MODJTAHEDI, H., 2017. The impact of co-expression of wild-type EGFR and its ligands determined by immunohistochemistry for response to treatment with cetuximab in patients with metastatic colorectal cancer. *Oncotarget,* **8**(5), pp. 7666-7677.

KIM, J., ZHANG, Y., SKALSKI, M., HAYES, J., KEFAS, B., SCHIFF, D., PUROW, B., PARSONS, S., LAWLER, S. and ABOUNADER, R., 2014. microRNA-148a is a prognostic oncomiR that targets MIG6 and BIM to regulate EGFR and apoptosis in glioblastoma. *Cancer research,* **74**(5), pp. 1541-1553.

KIM, S.Y. and KIM, T.I., 2018. Serrated neoplasia pathway as an alternative route of colorectal cancer carcinogenesis. *Intestinal research,* **16**(3), pp. 358-365.

KINZLER, K.W. and VOGELSTEIN, B., 1996. Lessons from hereditary colorectal cancer. *Cell,* **87**(2), pp. 159-170.

KITADOKORO, K., BORDO, D., GALLI, G., PETRACCA, R., FALUGI, F., ABRIGNANI, S., GRANDI, G. and BOLOGNESI, M., 2001. CD81 extracellular domain 3D structure: insight into the tetraspanin superfamily structural motifs. *The EMBO journal,* **20**(1-2), pp. 12-18.

KNOBLICH, K., WANG, H.X., SHARMA, C., FLETCHER, A.L., TURLEY, S.J. and HEMLER, M.E., 2014. Tetraspanin TSPAN12 regulates tumor growth and metastasis and inhibits beta-catenin degradation. *Cellular and molecular life sciences : CMLS,* **71**(7), pp. 1305-1314.

KNUDSON, A.G., 1971. Mutation and Cancer: Statistical Study of Retinoblastoma. *Proceedings of the National Academy of Sciences of the United States of America,* **68**(4), pp. 820-823.

KOCH, A., DE MEYER, T., JESCHKE, J. and VAN CRIEKINGE, W., 2015. MEXPRESS: visualizing expression, DNA methylation and clinical TCGA data. *BMC Genomics,* **16**(1), pp. 636.

KOHNO, M., HASEGAWA, H., MIYAKE, M., YAMAMOTO, T. and FUJITA, S., 2002. CD151 enhances cell motility and metastasis of cancer cells in the presence of focal adhesion kinase. *International journal of cancer,* **97**(3), pp. 336-343.

KOLES, K. and BUDNIK, V., 2012. Exosomes go with the Wnt. *Cellular logistics,* **2**(3), pp. 169-173.

KOMIYA, Y. and HABAS, R., 2008. Wnt signal transduction pathways. *Organogenesis,* **4**(2), pp. 68-75.

KOO, B.K., SPIT, M., JORDENS, I., LOW, T.Y., STANGE, D.E., VAN DE WETERING, M., VAN ES, J.H., MOHAMMED, S., HECK, A.J., MAURICE, M.M. and CLEVERS, H., 2012. Tumour suppressor RNF43 is a stem-cell E3 ligase that induces endocytosis of Wnt receptors. *Nature,* **488**(7413), pp. 665-669.

KRASINSKAS, A.M., 2011. EGFR Signaling in Colorectal Carcinoma. *Pathology research international,* **2011**, pp. 932932.

KRAUSOVA, M. and KORINEK, V., 2014. Wnt signaling in adult intestinal stem cells and cancer. *Cellular signalling,* **26**(3), pp. 570-579.

KUCHERLAPATI, M.H., LEE, K., NGUYEN, A.A., CLARK, A.B., HOU, H.,Jr, ROSULEK, A., LI, H., YANG, K., FAN, K., LIPKIN, M., BRONSON, R.T., JELICKS, L., KUNKEL, T.A., KUCHERLAPATI, R. and EDELMANN, W., 2010. An Msh2 conditional knockout mouse for studying intestinal cancer and testing anticancer agents. *Gastroenterology,* **138**(3), pp. 993-1002.e1.

KUIPERS, E.J., GRADY, W.M., LIEBERMAN, D., SEUFFERLEIN, T., SUNG, J.J., BOELENS, P.G., VAN DE VELDE, C.,J.H. and WATANABE, T., 2015. COLORECTAL CANCER. *Nature reviews.Disease primers,* **1**, pp. 15065-15065.

KURAGUCHI, M., WANG, X.P., BRONSON, R.T., ROTHENBERG, R., OHENE-BAAH, N.Y., LUND, J.J., KUCHERLAPATI, M., MAAS, R.L. and KUCHERLAPATI, R., 2006. Adenomatous polyposis coli (APC) is required for normal development of skin and thymus. *PLoS genetics,* **2**(9), pp. e146.

KWON, H.Y., BAJAJ, J., ITO, T., BLEVINS, A., KONUMA, T., WEEKS, J., LYTLE, N.K., KOECHLEIN, C.S., RIZZIERI, D., CHUAH, C., OEHLER, V.G., SASIK, R., HARDIMAN, G. and REYA, T., 2015. Tetraspanin 3 Is Required for the Development and Propagation of Acute Myelogenous Leukemia. *Cell stem cell,* **17**(2), pp. 152-164.

LABIANCA, R., NORDLINGER, B., BERETTA, G.D., MOSCONI, S., MANDALA, M., CERVANTES, A., ARNOLD, D. and ESMO GUIDELINES WORKING GROUP, 2013. Early colon cancer: ESMO Clinical Practice Guidelines for diagnosis, treatment and follow-up. *Annals of oncology : official journal of the European Society for Medical Oncology,* **24 Suppl 6**, pp. vi64-72.

LAI, M.B., ZHANG, C., SHI, J., JOHNSON, V., KHANDAN, L., MCVEY, J., KLYMKOWSKY, M.W., CHEN, Z. and JUNGE, H.J., 2017. TSPAN12 Is a Norrin Co-receptor that Amplifies Frizzled4 Ligand Selectivity and Signaling. *Cell reports,* **19**(13), pp. 2809-2822.

LARKI, P., GHARIB, E., YAGHOOB TALEGHANI, M., KHORSHIDI, F., NAZEMALHOSSEINI-MOJARAD, E. and ASADZADEH AGHDAEI, H., 2017. Coexistence of KRAS and BRAF Mutations in Colorectal Cancer: A Case Report Supporting The Concept of Tumoral Heterogeneity. *Cell Journal (Yakhteh),* **19**, pp. 113-117.

LARSSON, S.C. and WOLK, A., 2006. Meat consumption and risk of colorectal cancer: a meta-analysis of prospective studies. *International journal of cancer,* **119**(11), pp. 2657-2664.

LATYSHEVA, N., MURATOV, G., RAJESH, S., PADGETT, M., HOTCHIN, N.A., OVERDUIN, M. and BERDITCHEVSKI, F., 2006. Syntenin-1 is a new component of tetraspanin-enriched microdomains: mechanisms and consequences of the interaction of syntenin-1 with CD63. *Molecular and cellular biology,* **26**(20), pp. 7707-7718.

LE NAOUR, F., RUBINSTEIN, E., JASMIN, C., PRENANT, M. and BOUCHEIX, C., 2000. Severely reduced female fertility in CD9-deficient mice. *Science (New York, N.Y.),* **287**(5451), pp. 319-321.

LE, D.T., URAM, J.N., WANG, H., BARTLETT, B.R., KEMBERLING, H., EYRING, A.D., SKORA, A.D., LUBER, B.S., AZAD, N.S., LAHERU, D., BIEDRZYCKI, B., DONEHOWER, R.C., ZAHEER, A., FISHER, G.A., CROCENZI, T.S., LEE, J.J., DUFFY, S.M., GOLDBERG, R.M., DE LA CHAPELLE, A., KOSHIJI, M., BHAIJEE, F., HUEBNER, T., HRUBAN, R.H., WOOD, L.D., CUKA, N., PARDOLL, D.M., PAPADOPOULOS, N., KINZLER, K.W., ZHOU, S., CORNISH, T.C., TAUBE, J.M., ANDERS, R.A., ESHLEMAN, J.R., VOGELSTEIN, B. and DIAZ, L.A.,Jr, 2015. PD-1 Blockade in Tumors with Mismatch-Repair Deficiency. *The New England journal of medicine,* **372**(26), pp. 2509-2520.

LE, S., ANSARI, U., MUMTAZ, A., MALIK, K., PATEL, P., DOYLE, A. and KHACHEMOUNE, A., 2017. Lynch Syndrome and Muir-Torre Syndrome: An update and review on the genetics, epidemiology, and management of two related disorders. *Dermatology online journal,* **23**(11),.

LEARY, R.J., LIN, J.C., CUMMINS, J., BOCA, S., WOOD, L.D., PARSONS, D.W., JONES, S., SJÖBLOM, T., PARK, B., PARSONS, R., WILLIS, J., DAWSON, D., WILLSON, J.K.V., NIKOLSKAYA, T., NIKOLSKY, Y., KOPELOVICH, L., PAPADOPOULOS, N., PENNACCHIO, L.A., WANG, T., MARKOWITZ, S.D., PARMIGIANI, G., KINZLER, K.W., VOGELSTEIN, B. and VELCULESCU, V.E., 2008. Integrated analysis of homozygous deletions, focal amplifications, and sequence alterations in breast and colorectal cancers. *Proceedings of the National Academy of Sciences,* **105**(42), pp. 16224-16229.

LESLIE, A., CAREY, F.A., PRATT, N.R. and STEELE, R.J., 2002. The colorectal adenoma-carcinoma sequence. *The British journal of surgery,* **89**(7), pp. 845-860.

LEVY, S., 2014. Function of the tetraspanin molecule CD81 in B and T cells. *Immunologic research,* **58**(2-3), pp. 179-185.

LEVY, S. and SHOHAM, T., 2005. Protein-protein interactions in the tetraspanin web. *Physiology (Bethesda, Md.),* **20**, pp. 218-224.

LI, C., LIU, D.R., LI, G.G., WANG, H.H., LI, X.W., ZHANG, W., WU, Y.L. and CHEN, L., 2015. CD97 promotes gastric cancer cell proliferation and invasion through exosome-mediated MAPK signaling pathway. *World journal of gastroenterology,* **21**(20), pp. 6215-6228.

LIEBMANN, C., 2001. Regulation of MAP kinase activity by peptide receptor signalling pathway: paradigms of multiplicity. *Cellular signalling,* **13**(11), pp. 777-785.

LIU, C., ENG, C., SHEN, J., LU, Y., TAKATA, Y., MEHDIZADEH, A., CHANG, G.J., RODRIGUEZ-BIGAS, M.A., LI, Y., CHANG, P., MAO, Y., HASSAN, M.M., WANG, F. and LI, D., 2016. Serum exosomal miR-4772-3p is a predictor of tumor recurrence in stage II and III colon cancer. *Oncotarget,* **7**(46), pp. 76250-76260.

LIU, C., LI, Y., SEMENOV, M., HAN, C., BAEG, G.H., TAN, Y., ZHANG, Z., LIN, X. and HE, X., 2002. Control of beta-catenin phosphorylation/degradation by a dual-kinase mechanism. *Cell,* **108**(6), pp. 837-847.

LIU, J., CHEN, C., LI, G., CHEN, D. and ZHOU, Q., 2017. Upregulation of TSPAN12 is associated with the colorectal cancer growth and metastasis. *American journal of translational research,* **9**(2), pp. 812-822.

LIU, R., KAIN, M. and WANG, L., 2012. Inactivation of X-linked tumor suppressor genes in human cancer. *Future oncology (London, England),* **8**(4), pp. 463-481.

LIU, X., JAKUBOWSKI, M. and HUNT, J.L., 2011. KRAS gene mutation in colorectal cancer is correlated with increased proliferation and spontaneous apoptosis. *American Journal of Clinical Pathology,* **135**(2), pp. 245-252.

LONGATI, P., JIA, X., EIMER, J., WAGMAN, A., WITT, M.R., REHNMARK, S., VERBEKE, C., TOFTGARD, R., LOHR, M. and HEUCHEL, R.L., 2013. 3D pancreatic carcinoma spheroids induce a matrix-rich, chemoresistant phenotype offering a better model for drug testing. *BMC cancer,* **13**, pp. 95-2407-13-95.

LOPEZ-VICENTE, L., ARMENGOL, G., PONS, B., COCH, L., ARGELAGUET, E., LLEONART, M., HERNANDEZ-LOSA, J., DE TORRES, I. and RAMON Y CAJAL, S., 2009.

Regulation of replicative and stress-induced senescence by RSK4, which is down-regulated in human tumors. *Clinical cancer research : an official journal of the American Association for Cancer Research,* **15**(14), pp. 4546-4553.

LU, C., THOENI, C., CONNOR, A., KAWABE, H., GALLINGER, S. and ROTIN, D., 2016. Intestinal knockout of Nedd4 enhances growth of Apc(min) tumors. *Oncogene,* **35**(45), pp. 5839-5849.

LU, J., LI, J., LIU, S., WANG, T., IANNI, A., BOBER, E., BRAUN, T., XIANG, R. and YUE, S., 2017. Exosomal tetraspanins mediate cancer metastasis by altering host microenvironment. *Oncotarget,* **8**(37), pp. 62803-62815.

LUGA, V., ZHANG, L., VILORIA-PETIT, A.M., OGUNJIMI, A.A., INANLOU, M.R., CHIU, E., BUCHANAN, M., HOSEIN, A.N., BASIK, M. and WRANA, J.L., 2012. Exosomes mediate stromal mobilization of autocrine Wnt-PCP signaling in breast cancer cell migration. *Cell,* **151**(7), pp. 1542-1556.

LUJAN, P., VARSANO, G., RUBIO, T., HENNRICH, M.L., SACHSENHEIMER, T., GALVEZ-SANTISTEBAN, M., MARTIN-BELMONTE, F., GAVIN, A.C., BRUGGER, B. and KOHN, M., 2016. PRL-3 disrupts epithelial architecture by altering the post-mitotic midbody position. *Journal of cell science,* **129**(21), pp. 4130-4142.

LUND, K.A., LAZAR, C.S., CHEN, W.S., WALSH, B.J., WELSH, J.B., HERBST, J.J., WALTON, G.M., ROSENFELD, M.G., GILL, G.N. and WILEY, H.S., 1990. Phosphorylation of the epidermal growth factor receptor at threonine 654 inhibits ligand-induced internalization and down-regulation. *The Journal of biological chemistry,* **265**(33), pp. 20517-20523.

LUONGO, C., MOSER, A.R., GLEDHILL, S. and DOVE, W.F., 1994. Loss of Apc+ in intestinal adenomas from Min mice. *Cancer research,* **54**(22), pp. 5947-5952.

MACDONALD, B.T., TAMAI, K. and HE, X., 2009. Wnt/beta-catenin signaling: components, mechanisms, and diseases. *Developmental cell,* **17**(1), pp. 9-26.

MAECKER, H.T. and LEVY, S., 1997. Normal lymphocyte development but delayed humoral immune response in CD81-null mice. *The Journal of experimental medicine,* **185**(8), pp. 1505-1510.

MAISONIAL-BESSET, A., WITKOWSKI, T., NAVARRO-TEULON, I., BERTHIER-VERGNES, O., FOIS, G., ZHU, Y., BESSE, S., BAWA, O., BRIAT, A., QUINTANA, M., PICHARD, A., BONNET, M., RUBINSTEIN, E., POUGET, J.P., OPOLON, P., MAIGNE, L., MIOT-NOIRAULT, E., CHEZAL, J.M., BOUCHEIX, C. and DEGOUL, F., 2017. Tetraspanin 8 (TSPAN 8) as a potential target for radio-immunotherapy of colorectal cancer. *Oncotarget,* **8**(13), pp. 22034-22047.

MALLA, R.R., PANDRANGI, S., KUMARI, S., GAVARA, M.M. and BADANA, A.K., 2018. Exosomal tetraspanins as regulators of cancer progression and metastasis and novel diagnostic markers. *Asia-Pacific journal of clinical oncology,* .

MARKOWITZ, S.D. and BERTAGNOLLI, M.M., 2009. Molecular origins of cancer: Molecular basis of colorectal cancer. *The New England journal of medicine,* **361**(25), pp. 2449-2460.

MARMOL, I., SANCHEZ-DE-DIEGO, C., PRADILLA DIESTE, A., CERRADA, E. and RODRIGUEZ YOLDI, M.J., 2017. Colorectal Carcinoma: A General Overview and Future Perspectives in Colorectal Cancer. *International journal of molecular sciences,* **18**(1), pp. 10.3390/ijms18010197.

MARTIN-BELMONTE, F. and MOSTOV, K., 2008. Regulation of cell polarity during epithelial morphogenesis. *Current opinion in cell biology,* **20**(2), pp. 227-234.

MATANO, M., DATE, S., SHIMOKAWA, M., TAKANO, A., FUJII, M., OHTA, Y., WATANABE, T., KANAI, T. and SATO, T., 2015. Modeling colorectal cancer using CRISPR-Cas9-mediated engineering of human intestinal organoids. *Nature medicine,* **21**(3), pp. 256-262.

MATHIVANAN, S., FAHNER, C.J., REID, G.E. and SIMPSON, R.J., 2012. ExoCarta 2012: database of exosomal proteins, RNA and lipids. *Nucleic acids research,* **40**(Database issue), pp. D1241-4.

MATHIVANAN, S., JI, H. and SIMPSON, R.J., 2010. Exosomes: extracellular organelles important in intercellular communication. *Journal of proteomics,* **73**(10), pp. 1907-1920.

MATTHEWS, A.L., KOO, C.Z., SZYROKA, J., HARRISON, N., KANHERE, A. and TOMLINSON, M.G., 2018. Regulation of Leukocytes by TspanC8 Tetraspanins and the "Molecular Scissor" ADAM10. *Frontiers in immunology,* **9**, pp. 1451.

MATTHEWS, A.L., SZYROKA, J., COLLIER, R., NOY, P.J. and TOMLINSON, M.G., 2017. Scissor sisters: regulation of ADAM10 by the TspanC8 tetraspanins. *Biochemical Society transactions,* **45**(3), pp. 719-730.

MAZUROV, D., BARBASHOVA, L. and FILATOV, A., 2013. Tetraspanin protein CD9 interacts with metalloprotease CD10 and enhances its release via exosomes. *The FEBS journal,* **280**(5), pp. 1200-1213.

MAZZOTTA, S., NEVES, C., BONNER, R.J., BERNARDO, A.S., DOCHERTY, K. and HOPPLER, S., 2016. Distinctive Roles of Canonical and Noncanonical Wnt Signaling in Human Embryonic Cardiomyocyte Development. *Stem cell reports,* **7**(4), pp. 764-776.

MCCLELAND, M.L., SOUKUP, T.M., LIU, S.D., ESENSTEN, J.H., DE SOUSA E MELO, F., YAYLAOGLU, M., WARMING, S., ROOSE-GIRMA, M. and FIRESTEIN, R., 2015. Cdk8 deletion in the Apc(Min) murine tumour model represses EZH2 activity and accelerates tumourigenesis. *The Journal of pathology,* **237**(4), pp. 508-519.

MCGOUGH, I.J. and VINCENT, J., 2016. Exosomes in developmental signalling. *Development,* **143**(14), pp. 2482.

MCINTYRE, R.E., BUCZACKI, S.J.A., ARENDS, M.J. and ADAMS, D.J., 2015. Mouse models of colorectal cancer as preclinical models. *Bioessays,* **37**(8), pp. 909-920.

MEHDAWI, L.M., PRASAD, C.P., EHRNSTROM, R., ANDERSSON, T. and SJOLANDER, A., 2016. Non-canonical WNT5A signaling up-regulates the expression of the tumor suppressor 15-PGDH and induces differentiation of colon cancer cells. *Molecular oncology,* **10**(9), pp. 1415-1429.

MIDDENDORP, S., SCHNEEBERGER, K., WIEGERINCK, C.L., MOKRY, M., AKKERMAN, R.D., VAN WIJNGAARDEN, S., CLEVERS, H. and NIEUWENHUIS, E.E., 2014. Adult stem cells in the small intestine are intrinsically programmed with their location-specific function. *Stem cells (Dayton, Ohio),* **32**(5), pp. 1083-1091.

MILLER, J.R., 2002. The Wnts. *Genome biology,* **3**(1), pp. REVIEWS3001.

MIN, G., WANG, H., SUN, T.T. and KONG, X.P., 2006. Structural basis for tetraspanin functions as revealed by the cryo-EM structure of uroplakin complexes at 6-A resolution. *The Journal of cell biology,* **173**(6), pp. 975-983.

MINCHEVA-NILSSON, L. and BARANOV, V., 2014. Cancer exosomes and NKG2D receptor-ligand interactions: impairing NKG2D-mediated cytotoxicity and anti-tumour immune surveillance.

Seminars in cancer biology, **28**, pp. 24-30.

MINCIACCHI, V.R., YOU, S., SPINELLI, C., MORLEY, S., ZANDIAN, M., ASPURIA, P.J., CAVALLINI, L., CIARDIELLO, C., REIS SOBREIRO, M., MORELLO, M., KHARMATE, G., JANG, S.C., KIM, D.K., HOSSEINI-BEHESHTI, E., TOMLINSON GUNS, E., GLEAVE, M., GHO, Y.S., MATHIVANAN, S., YANG, W., FREEMAN, M.R. and DI VIZIO, D., 2015. Large oncosomes contain distinct protein cargo and represent a separate functional class of tumor-derived extracellular vesicles. *Oncotarget,* **6**(13), pp. 11327-11341.

MITCHELL, R.A., LUWOR, R.B. and BURGESS, A.W., 2018. The Epidermal Growth Factor Receptor: Structure-Function Informing the Design of Anticancer Therapeutics. *Experimental cell research,* .

MIYAZAKI, T., MULLER, U. and CAMPBELL, K.S., 1997. Normal development but differentially altered proliferative responses of lymphocytes in mice lacking CD81. *The EMBO journal,* **16**(14), pp. 4217-4225.

MOORE, T. and DVEKSLER, G.S., 2014. Pregnancy-specific glycoproteins: complex gene families regulating maternal-fetal interactions. *The International journal of developmental biology,* **58**(2-4), pp. 273-280.

MORAN, A., ORTEGA, P., DE JUAN, C., FERNANDEZ-MARCELO, T., FRIAS, C., SANCHEZ-PERNAUTE, A., TORRES, A.J., DIAZ-RUBIO, E., INIESTA, P. and BENITO, M., 2010. Differential colorectal carcinogenesis: Molecular basis and clinical relevance. *World journal of gastrointestinal oncology,* **2**(3), pp. 151-158.

MOSER, A.R., PITOT, H.C. and DOVE, W.F., 1990. A dominant mutation that predisposes to multiple intestinal neoplasia in the mouse. *Science (New York, N.Y.),* **247**(4940), pp. 322-324.

MOSS, A.C., DORAN, P.P. and MACMATHUNA, P., 2007. In Silico Promoter Analysis can Predict Genes of Functional Relevance in Cell Proliferation: Validation in a Colon Cancer Model. *Translational oncogenomics,* **2**, pp. 1-16.

MUNOZ, N.M., UPTON, M., ROJAS, A., WASHINGTON, M.K., LIN, L., CHYTIL, A., SOZMEN, E.G., MADISON, B.B., POZZI, A., MOON, R.T., MOSES, H.L. and GRADY, W.M., 2006. Transforming growth factor beta receptor type II inactivation induces the malignant transformation of intestinal neoplasms initiated by Apc mutation. *Cancer research,* **66**(20), pp. 9837-9844.

MURALIDHARAN-CHARI, V., CLANCY, J., PLOU, C., ROMAO, M., CHAVRIER, P., RAPOSO, G. and D'SOUZA-SCHOREY, C., 2009. ARF6-regulated shedding of tumor cell-derived plasma membrane microvesicles. *Current biology : CB,* **19**(22), pp. 1875-1885.

MURAYAMA, Y., SHINOMURA, Y., ORITANI, K., MIYAGAWA, J., YOSHIDA, H., NISHIDA, M., KATSUBE, F., SHIRAGA, M., MIYAZAKI, T., NAKAMOTO, T., TSUTSUI, S., TAMURA, S., HIGASHIYAMA, S., SHIMOMURA, I. and HAYASHI, N., 2008. The tetraspanin CD9 modulates epidermal growth factor receptor signaling in cancer cells. *Journal of cellular physiology,* **216**(1), pp. 135-143.

NAGARAJAH, S., 2016. Exosome Secretion â€" More Than Simple Waste Disposal? Implications for Physiology, Diagnostics and Therapeutics. *Journal of Circulating Biomarkers,* **5**, pp. 7.

NALBANTOGLU, I., BLANC, V. and DAVIDSON, N.O., 2016. Characterization of Colorectal Cancer Development in Apc(min/+) Mice. *Methods in molecular biology (Clifton, N.J.),* **1422**, pp. 309-327.

NAYAK, L., BHATTACHARYYA, N.P. and DE, R.K., 2016. Wnt signal transduction pathways: modules, development and evolution. *BMC systems biology,* **10 Suppl 2**, pp. 44-016-0299-7.

NAZARENKO, I., RANA, S., BAUMANN, A., MCALEAR, J., HELLWIG, A., TRENDELENBURG, M., LOCHNIT, G., PREISSNER, K.T. and ZOLLER, M., 2010. Cell surface tetraspanin Tspan8 contributes to molecular pathways of exosome-induced endothelial cell activation. *Cancer research,* **70**(4), pp. 1668-1678.

NEILSEN, P.M., NOLL, J.E., MATTISKE, S., BRACKEN, C.P., GREGORY, P.A., SCHULZ, R.B., LIM, S.P., KUMAR, R., SUETANI, R.J., GOODALL, G.J. and CALLEN, D.F., 2013. Mutant p53 drives invasion in breast tumors through up-regulation of miR-155. *Oncogene,* **32**(24), pp. 2992-3000.

NIKOPOULOS, K., VENSELAAR, H., COLLIN, R.W., RIVEIRO-ALVAREZ, R., BOONSTRA, F.N., HOOYMANS, J.M., MUKHOPADHYAY, A., SHEARS, D., VAN BERS, M., DE WIJS, I.J., VAN ESSEN, A.J., SIJMONS, R.H., TILANUS, M.A., VAN NOUHUYS, C.E., AYUSO, C., HOEFSLOOT, L.H. and CREMERS, F.P., 2010. Overview of the mutation spectrum in familial exudative vitreoretinopathy and Norrie disease with identification of 21 novel variants in FZD4, LRP5, and NDP. *Human mutation,* **31**(6), pp. 656-666.

NISHIUCHI, R., SANZEN, N., NADA, S., SUMIDA, Y., WADA, Y., OKADA, M., TAKAGI, J., HASEGAWA, H. and SEKIGUCHI, K., 2005. Potentiation of the ligand-binding activity of integrin alpha3beta1 via association with tetraspanin CD151. *Proceedings of the National Academy of Sciences of the United States of America,* **102**(6), pp. 1939-1944.

NOONE AM, HOWLADER N, *ET AL.*, 2018. SEER Cancer Statistics Review, 1975-2015, National Cancer Institute. Bethesda, MD, https://seer.cancer.gov/csr/1975_2015/, based on November 2017 SEER data submission, posted to the SEER web site, April 2018.

NOY, P.J., YANG, J., REYAT, J.S., MATTHEWS, A.L., CHARLTON, A.E., FURMSTON, J., ROGERS, D.A., RAINGER, G.E. and TOMLINSON, M.G., 2016. TspanC8 Tetraspanins and A Disintegrin and Metalloprotease 10 (ADAM10) Interact via Their Extracellular Regions: EVIDENCE FOR DISTINCT BINDING MECHANISMS FOR DIFFERENT TspanC8 PROTEINS. *The Journal of biological chemistry,* **291**(7), pp. 3145-3157.

NUSSE, R. and CLEVERS, H., 2017. Wnt/beta-Catenin Signaling, Disease, and Emerging Therapeutic Modalities. *Cell,* **169**(6), pp. 985-999.

ODINTSOVA, E., VOORTMAN, J., GILBERT, E. and BERDITCHEVSKI, F., 2003. Tetraspanin CD82 regulates compartmentalisation and ligand-induced dimerization of EGFR. *Journal of cell science,* **116**(Pt 22), pp. 4557-4566.

OGATA-KAWATA, H., IZUMIYA, M., KURIOKA, D., HONMA, Y., YAMADA, Y., FURUTA, K., GUNJI, T., OHTA, H., OKAMOTO, H., SONODA, H., WATANABE, M., NAKAGAMA, H., YOKOTA, J., KOHNO, T. and TSUCHIYA, N., 2014. Circulating exosomal microRNAs as biomarkers of colon cancer. *PloS one,* **9**(4), pp. e92921.

OSHIMA, M., OSHIMA, H., KITAGAWA, K., KOBAYASHI, M., ITAKURA, C. and TAKETO, M., 1995. Loss of Apc heterozygosity and abnormal tissue building in nascent intestinal polyps in mice carrying a truncated Apc gene. *Proceedings of the National Academy of Sciences of the United States of America,* **92**(10), pp. 4482-4486.

OTSUKA, M., KANG, Y.J., REN, J., JIANG, H., WANG, Y., OMATA, M. and HAN, J., 2010. Distinct effects of p38alpha deletion in myeloid lineage and gut epithelia in mouse models of inflammatory bowel disease. *Gastroenterology,* **138**(4), pp. 1255-65, 1265.e1-9.

PARKIN, D.M. and BOYD, L., 2011. 6. Cancers attributable to dietary factors in the UK in 2010: III. Low consumption of fibre. *British journal of cancer,* **105**, pp. S27-S30.

PATAI, A.V., MOLNAR, B., TULASSAY, Z. and SIPOS, F., 2013. Serrated pathway: alternative route to colorectal cancer. *World journal of gastroenterology,* **19**(5), pp. 607-615.

PEREZ-HERNANDEZ, D., GUTIERREZ-VAZQUEZ, C., JORGE, I., LOPEZ-MARTIN, S., URSA, A., SANCHEZ-MADRID, F., VAZQUEZ, J. and YANEZ-MO, M., 2013. The intracellular interactome of tetraspanin-enriched microdomains reveals their function as sorting machineries toward exosomes. *The Journal of biological chemistry,* **288**(17), pp. 11649-11661.

PIEDRA, J., MIRAVET, S., CASTAÃ±O, J., PÃ¡LMER, H.,G., HEISTERKAMP, N., GARCÃA, D.H. and DUÃ±ACH, M., 2003. p120 Catenin-Associated Fer and Fyn Tyrosine Kinases Regulate Î²-Catenin Tyr-142 Phosphorylation and Î²-Catenin-Î±-Catenin Interaction. *Molecular and cellular biology,* **23**(7), pp. 2287-2297.

POLAKIS, P., 2012. Wnt signaling in cancer. *Cold Spring Harbor perspectives in biology,* **4**(5), pp. 10.1101/cshperspect.a008052.

POLLARD, P., DEHERAGODA, M., SEGDITSAS, S., LEWIS, A., ROWAN, A., HOWARTH, K., WILLIS, L., NYE, E., MCCART, A., MANDIR, N., SILVER, A., GOODLAD, R., STAMP, G., COCKMAN, M., EAST, P., SPENCER-DENE, B., POULSOM, R., WRIGHT, N. and TOMLINSON, I., 2009. The Apc 1322T mouse develops severe polyposis associated with submaximal nuclear beta-catenin expression. *Gastroenterology,* **136**(7), pp. 2204-2213.e1-13.

POULTER, J.A., ALI, M., GILMOUR, D.F., RICE, A., KONDO, H., HAYASHI, K., MACKEY, D.A., KEARNS, L.S., RUDDLE, J.B., CRAIG, J.E., PIERCE, E.A., DOWNEY, L.M., MOHAMED, M.D., MARKHAM, A.F., INGLEHEARN, C.F. and TOOMES, C., 2010. Mutations in TSPAN12 cause autosomal-dominant familial exudative vitreoretinopathy. *American Journal of Human Genetics,* **86**(2), pp. 248-253.

PRETLOW, T.P., EDELMANN, W., KUCHERLAPATI, R., PRETLOW, T.G. and AUGENLICHT, L.H., 2003. Spontaneous aberrant crypt foci in Apc1638N mice with a mutant Apc allele. *The American journal of pathology,* **163**(5), pp. 1757-1763.

PROX, J., WILLENBROCK, M., WEBER, S., LEHMANN, T., SCHMIDT-ARRAS, D., SCHWANBECK, R., SAFTIG, P. and SCHWAKE, M., 2012. Tetraspanin15 regulates cellular trafficking and activity of the ectodomain sheddase ADAM10. *Cellular and molecular life sciences : CMLS,* **69**(17), pp. 2919-2932.

QU, X., SANDMANN, T., FRIERSON, H.,Jr, FU, L., FUENTES, E., WALTER, K., OKRAH, K., RUMPEL, C., MOSKALUK, C., LU, S., WANG, Y., BOURGON, R., PENUEL, E., PIRZKALL, A., AMLER, L., LACKNER, M.R., TABERNERO, J., HAMPTON, G.M. and KABBARAH, O., 2016. Integrated genomic analysis of colorectal cancer progression reveals activation of EGFR through demethylation of the EREG promoter. *Oncogene,* **35**(50), pp. 6403-6415.

QUESADA, C.F., KIMATA, H., MORI, M., NISHIMURA, M., TSUNEYOSHI, T. and BABA, S., 1998. Piroxicam and acarbose as chemopreventive agents for spontaneous intestinal adenomas in APC gene 1309 knockout mice. *Japanese journal of cancer research : Gann,* **89**(4), pp. 392-396.

QUESENBERRY, P.J., ALIOTTA, J., CAMUSSI, G., ABDEL-MAGEED, A., WEN, S., GOLDBERG, L., ZHANG, H., TETTA, C., FRANKLIN, J., COFFEY, R.J., DANIELSON, K., SUBRAMANYA, V., GHIRAN, I., DAS, S., CHEN, C.C., PUSIC, K.M., PUSIC, A.D., CHATTERJEE, D., KRAIG, R.P., BALAJ, L. and DOONER, M., 2015. Potential functional applications of extracellular vesicles: a report by the NIH Common Fund Extracellular RNA Communication Consortium. *Journal of Extracellular Vesicles,* **4**, pp. 10.3402/jev.v4.27575.

RAJAMANICKAM, G.D., KASTELIC, J.P. and THUNDATHIL, J.C., 2017. The ubiquitous isoform of Na/K-ATPase (ATP1A1) regulates junctional proteins, connexin 43 and claudin 11 via Src-EGFR-ERK1/2-CREB pathway in rat Sertoli cells. *Biology of reproduction,* **96**(2), pp. 456-468.

RAMANI, V.C., PURUSHOTHAMAN, A., STEWART, M.D., THOMPSON, C.A., VLODAVSKY, I., AU, J.L. and SANDERSON, R.D., 2013. The heparanase/syndecan-1 axis in cancer: mechanisms and therapies. *The FEBS journal,* **280**(10), pp. 2294-2306.

RAO, T.P. and KUHL, M., 2010. An updated overview on Wnt signaling pathways: a prelude for more. *Circulation research,* **106**(12), pp. 1798-1806.

RASHED, M.,H., BAYRAKTAR, E., HELAL, G.,K., ABD-ELLAH, M., AMERO, P., CHAVEZ-REYES, A. and RODRIGUEZ-AGUAYO, C., 2017. Exosomes: From Garbage Bins to Promising Therapeutic Targets. *International Journal of Molecular Sciences,* **18**(3), pp. 538.

REITMAIR, A.H., SCHMITS, R., EWEL, A., BAPAT, B., REDSTON, M., MITRI, A., WATERHOUSE, P., MITTRUCKER, H.W., WAKEHAM, A. and LIU, B., 1995. MSH2 deficient mice are viable and susceptible to lymphoid tumours. *Nature genetics,* **11**(1), pp. 64-70.

RENE, J. and SANSOM OWEN, J., 2016. Mouse models of intestinal cancer. *The Journal of pathology,* **238**(2), pp. 141-151.

REYA, T. and CLEVERS, H., 2005. Wnt signalling in stem cells and cancer. *Nature,* **434**(7035), pp. 843-850.

RHEE, Y., KIM, K. and KANG, G.H., 2016. CpG Island Methylator Phenotype-High Colorectal Cancers and Their Prognostic Implications and Relationships with the Serrated Neoplasia Pathway. *Gut and Liver,* **11**(1), pp. 38-46.

RICHARDSON, M.M., JENNINGS, L.K. and ZHANG, X.A., 2011. Tetraspanins and tumor progression. *Clinical & experimental metastasis,* **28**(3), pp. 261-270.

ROBANUS-MAANDAG, E.C., KOELINK, P.J., BREUKEL, C., SALVATORI, D.C., JAGMOHAN-CHANGUR, S.C., BOSCH, C.A., VERSPAGET, H.W., DEVILEE, P., FODDE, R. and SMITS, R., 2010. A new conditional Apc-mutant mouse model for colorectal cancer. *Carcinogenesis,* **31**(5), pp. 946-952.

ROBERTS, R.B., MIN, L., WASHINGTON, M.K., OLSEN, S.J., SETTLE, S.H., COFFEY, R.J. and THREADGILL, D.W., 2002. Importance of epidermal growth factor receptor signaling in establishment of adenomas and maintenance of carcinomas during intestinal tumorigenesis. *Proceedings of the National Academy of Sciences of the United States of America,* **99**(3), pp. 1521-1526.

RODRIGUES, P., MACAYA, I., BAZZOCCO, S., MAZZOLINI, R., ANDRETTA, E., DOPESO, H., MATEO-LOZANO, S., BILIC, J., CARTON-GARCIA, F., NIETO, R., SUAREZ-LOPEZ, L., AFONSO, E., LANDOLFI, S., HERNANDEZ-LOSA, J., KOBAYASHI, K., RAMON Y CAJAL, S., TABERNERO, J., TEBBUTT, N.C., MARIADASON, J.M., SCHWARTZ, S.,Jr and ARANGO, D., 2014. RHOA inactivation enhances Wnt signalling and promotes colorectal cancer. *Nature communications,* **5**, pp. 5458.

RODRIGUEZ-BOULAN, E. and MACARA, I.G., 2014. Organization and execution of the epithelial polarity programme. *Nature reviews.Molecular cell biology,* **15**(4), pp. 225-242.

RODRIGUEZ-COLMAN, M.J., SCHEWE, M., MEERLO, M., STIGTER, E., GERRITS, J., PRAS-RAVES, M., SACCHETTI, A., HORNSVELD, M., OOST, K.C., SNIPPERT, H.J., VERHOEVEN-

DUIF, N., FODDE, R. and BURGERING, B.M., 2017. Interplay between metabolic identities in the intestinal crypt supports stem cell function. *Nature,* **543**(7645), pp. 424-427.

ROESELERS, G., PONOMARENKO, M., LUKOVAC, S. and WORTELBOER, H.M., 2013. Ex vivo systems to study host-microbiota interactions in the gastrointestinal tract. *Best practice & research.Clinical gastroenterology,* **27**(1), pp. 101-113.

ROMANSKA, H.M. and BERDITCHEVSKI, F., 2011. Tetraspanins in human epithelial malignancies. *The Journal of pathology,* **223**(1), pp. 4-14.

RONAN, T., MACDONALD-OBERMANN, J.L., HUELSMANN, L., BESSMAN, N.J., NAEGLE, K.M. and PIKE, L.J., 2016. Different Epidermal Growth Factor Receptor (EGFR) Agonists Produce Unique Signatures for the Recruitment of Downstream Signaling Proteins. *The Journal of biological chemistry,* **291**(11), pp. 5528-5540.

ROSEN, E.D. and MACDOUGALD, O.A., 2006. Adipocyte differentiation from the inside out. *Nature reviews.Molecular cell biology,* **7**(12), pp. 885-896.

ROUS, B.A., REAVES, B.J., IHRKE, G., BRIGGS, J.A., GRAY, S.R., STEPHENS, D.J., BANTING, G. and LUZIO, J.P., 2002. Role of adaptor complex AP-3 in targeting wild-type and mutated CD63 to lysosomes. *Molecular biology of the cell,* **13**(3), pp. 1071-1082.

RUBINFELD, B., ALBERT, I., PORFIRI, E., MUNEMITSU, S. and POLAKIS, P., 1997. Loss of β-Catenin Regulation by the APC Tumor Suppressor Protein Correlates with Loss of Structure Due to Common Somatic Mutations of the Gene. *Cancer research,* **57**(20), pp. 4624-4630.

RUBINSTEIN, E., ZIYYAT, A., WOLF, J.P., LE NAOUR, F. and BOUCHEIX, C., 2006. The molecular players of sperm-egg fusion in mammals. *Seminars in cell & developmental biology,* **17**(2), pp. 254-263.

RUDDON, R., 2003. What Makes a Cancer Cell a Cancer Cell? In: D.W. KUFE, R.E. POLLOCK, R.R. WEICHSELBAUM, R.C. BAST, T.S. GANSLER, J.F. HOLLAND and E. FREI, eds, *Holland-Frei Cancer Medicine.* 6th edn. Hamilton (ON): BC Decker, .

RUIZ-GARCIA, A., LOPEZ-LOPEZ, S., GARCIA-RAMIREZ, J.J., BALADRON, V., RUIZ-HIDALGO, M.J., LOPEZ-SANZ, L., BALLESTEROS, A., LABORDA, J., MONSALVE, E.M. and DIAZ-GUERRA, M.J., 2016. The Tetraspanin TSPAN33 Controls TLR-Triggered Macrophage Activation through Modulation of NOTCH Signaling. *Journal of immunology (Baltimore, Md.: 1950),* **197**(8), pp. 3371-3381.

RUSTGI, A.K., 2013. BRAF: a driver of the serrated pathway in colon cancer. *Cancer cell,* **24**(1), pp. 1-2.

SACHS, N., KREFT, M., VAN DEN BERGH WEERMAN, M.A., BEYNON, A.J., PETERS, T.A., WEENING, J.J. and SONNENBERG, A., 2006. Kidney failure in mice lacking the tetraspanin CD151. *The Journal of cell biology,* **175**(1), pp. 33-39.

SAINI, S.D., KIM, H.M. and SCHOENFELD, P., 2006. Incidence of advanced adenomas at surveillance colonoscopy in patients with a personal history of colon adenomas: a meta-analysis and systematic review. *Gastrointestinal endoscopy,* **64**(4), pp. 614-626.

SAINT-POL, J., ESCHENBRENNER, E., DORNIER, E., BOUCHEIX, C., CHARRIN, S. and RUBINSTEIN, E., 2017. Regulation of the trafficking and the function of the metalloprotease ADAM10 by tetraspanins. *Biochemical Society transactions,* **45**(4), pp. 937-944.

SALAS, I.,H., CALLAERTS-VEGH,Zsuzsanna, ARRANZ, A.,M., GUIX, F.,X., DÂ€™HOOGE,Rudi, ESTEBAN, J.,A., DE STROOPER,Bart and DOTTI, C.,G., .

SALAS, I.H., CALLAERTS-VEGH, Z., ARRANZ, A.M., GUIX, F.X., DÂ€™HOOGE, R., ESTEBAN, J.A., DE STROOPER, B. and DOTTI, C.G., 2017. Tetraspanin 6: A novel regulator of hippocampal synaptic transmission and long term plasticity. *PLOS ONE,* **12**(2), pp. e0171968.

SARKAR, D., BOUKERCHE, H., SU, Z.Z. and FISHER, P.B., 2004. Mda-9/syntenin: Recent Insights into a Novel Cell Signaling and Metastasis-Associated Gene. *Pharmacology & therapeutics,* **104**(2), pp. 101-115.

SAROSIEK, T. and STELMASZUK, M., 2018. Small intestine neoplasms. *Polski merkuriusz lekarski : organ Polskiego Towarzystwa Lekarskiego,* **44**(260), pp. 45-48.

SASAI, H., MASAKI, M. and WAKITANI, K., 2000. Suppression of polypogenesis in a new mouse strain with a truncated Apc(Delta474) by a novel COX-2 inhibitor, JTE-522. *Carcinogenesis,* **21**(5), pp. 953-958.

SASAKI, N., SACHS, N., WIEBRANDS, K., ELLENBROEK, S.I., FUMAGALLI, A., LYUBIMOVA, A., BEGTHEL, H., VAN DEN BORN, M., VAN ES, J.H., KARTHAUS, W.R., LI, V.S., LOPEZ-IGLESIAS, C., PETERS, P.J., VAN RHEENEN, J., VAN OUDENAARDEN, A. and CLEVERS, H., 2016. Reg4+ deep crypt secretory cells function as epithelial niche for Lgr5+ stem cells in colon. *Proceedings of the National Academy of Sciences of the United States of America,* **113**(37), pp. E5399-407.

SASAKI, T., HIROKI, K. and YAMASHITA, Y., 2013. The role of epidermal growth factor receptor in cancer metastasis and microenvironment. *BioMed research international,* **2013**, pp. 546318.

SATO, T., STANGE, D.E., FERRANTE, M., VRIES, R.G., VAN ES, J.H., VAN DEN BRINK, S., VAN HOUDT, W.J., PRONK, A., VAN GORP, J., SIERSEMA, P.D. and CLEVERS, H., 2011. Long-term expansion of epithelial organoids from human colon, adenoma, adenocarcinoma, and Barrett's epithelium. *Gastroenterology,* **141**(5), pp. 1762-1772.

SATO, T., VRIES, R.G., SNIPPERT, H.J., VAN DE WETERING, M., BARKER, N., STANGE, D.E., VAN ES, J.H., ABO, A., KUJALA, P., PETERS, P.J. and CLEVERS, H., 2009. Single Lgr5 stem cells build crypt-villus structures in vitro without a mesenchymal niche. *Nature,* **459**(7244), pp. 262-265.

SATO, T., VAN ES, J.H., SNIPPERT, H.J., STANGE, D.E., VRIES, R.G., VAN, D.B., BARKER, N., SHROYER, N.F., VAN, D.W. and CLEVERS, H., 2010. Paneth cells constitute the niche for Lgr5 stem cells in intestinal crypts. *Nature,* **469**, pp. 415.

SAWADA, S., YOSHIMOTO, M., ODINTSOVA, E., HOTCHIN, N.A. and BERDITCHEVSKI, F., 2003. The tetraspanin CD151 functions as a negative regulator in the adhesion-dependent activation of Ras. *The Journal of biological chemistry,* **278**(29), pp. 26323-26326.

SCALTRITI, M. and BASELGA, J., 2006. The epidermal growth factor receptor pathway: a model for targeted therapy. *Clinical cancer research : an official journal of the American Association for Cancer Research,* **12**(18), pp. 5268-5272.

SCARPA, M., SCARPA, M., CASTAGLIUOLO, I., ERROI, F., KOTSAFTI, A., BASATO, S., BRUN, P., D'INCÃ , R., RUGGE, M., ANGRIMAN, I. and CASTORO, C., 2016. Aberrant gene methylation in non-neoplastic mucosa as a predictive marker of ulcerative colitis-associated CRC. *Oncotarget,* **7**(9), pp. 10322-10331.

SCHNEEBERGER, K., ROTH, S., NIEUWENHUIS, E.E.S. and MIDDENDORP, S., 2018. Intestinal epithelial cell polarity defects in disease: lessons from microvillus inclusion disease. *Dis Models Mech,* **11**(2),.

SCHNEIKERT, J. and BEHRENS, J., 2007. The canonical Wnt signalling pathway and its APC partner in colon cancer development. *Gut,* **56**(3), pp. 417-425.

SCHRODER, J., LULLMANN-RAUCH, R., HIMMERKUS, N., PLEINES, I., NIESWANDT, B., ORINSKA, Z., KOCH-NOLTE, F., SCHRODER, B., BLEICH, M. and SAFTIG, P., 2009. Deficiency of the tetraspanin CD63 associated with kidney pathology but normal lysosomal function. *Molecular and cellular biology,* **29**(4), pp. 1083-1094.

SCHUTTE, M., RISCH, T., ABDAVI-AZAR, N., BOEHNKE, K., SCHUMACHER, D., KEIL, M., YILDIRIMAN, R., JANDRASITS, C., BORODINA, T., AMSTISLAVSKIY, V., WORTH, C.L., SCHWEIGER, C., LIEBS, S., LANGE, M., WARNATZ, H.J., BUTCHER, L.M., BARRETT, J.E., SULTAN, M., WIERLING, C., GOLOB-SCHWARZL, N., LAX, S., URANITSCH, S., BECKER, M., WELTE, Y., REGAN, J.L., SILVESTROV, M., KEHLER, I., FUSI, A., KESSLER, T., HERWIG, R., LANDEGREN, U., WIENKE, D., NILSSON, M., VELASCO, J.A., GARIN-CHESA, P., REINHARD, C., BECK, S., SCHAFER, R., REGENBRECHT, C.R., HENDERSON, D., LANGE, B., HAYBAECK, J., KEILHOLZ, U., HOFFMANN, J., LEHRACH, H. and YASPO, M.L., 2017. Molecular dissection of colorectal cancer in pre-clinical models identifies biomarkers predicting sensitivity to EGFR inhibitors. *Nature communications,* **8**, pp. 14262.

SEER RESEARCH DATA 1973-2015, 2018-last update, Surveillance, Epidemiology, and End Results (SEER) Program (www.seer.cancer.gov) Research Data (1973-2015), National Cancer Institute, DCCPS, Surveillance Research Program. Available: https://seer.cancer.gov/statfacts/html/colorect.html [August/2018, 2018].

SEIGNEURET, M., 2006. Complete predicted three-dimensional structure of the facilitator transmembrane protein and hepatitis C virus receptor CD81: conserved and variable structural domains in the tetraspanin superfamily. *Biophysical journal,* **90**(1), pp. 212-227.

SEIGNEURET, M., DELAGUILLAUMIE, A., LAGAUDRIERE-GESBERT, C. and CONJEAUD, H., 2001. Structure of the tetraspanin main extracellular domain. A partially conserved fold with a structurally variable domain insertion. *The Journal of biological chemistry,* **276**(43), pp. 40055-40064.

SEIPOLD, L., DAMME, M., PROX, J., RABE, B., KASPAREK, P., SEDLACEK, R., ALTMEPPEN, H., WILLEM, M., BOLAND, B., GLATZEL, M. and SAFTIG, P., 2017. Tetraspanin 3: A central endocytic membrane component regulating the expression of ADAM10, presenilin and the amyloid precursor protein. *Biochimica et biophysica acta.Molecular cell research,* **1864**(1), pp. 217-230.

SETH, S., AGER, A., ARENDS, M. and FRAYLING, I.M., 2018. Lynch Syndrome - Cancer Pathways, Heterogeneity and Immune Escape. *The Journal of pathology,* .

SEUBERT, B., CUI, H., SIMONAVICIUS, N., HONERT, K., SCHAFER, S., REUNING, U., HEIKENWALDER, M., MARI, B. and KRUGER, A., 2015. Tetraspanin CD63 acts as a pro-metastatic factor via beta-catenin stabilization. *International journal of cancer,* **136**(10), pp. 2304-2315.

SHAO, J., WASHINGTON, M.K., SAXENA, R. and SHENG, H., 2007. Heterozygous disruption of the PTEN promotes intestinal neoplasia in APCmin/+ mouse: roles of osteopontin. *Carcinogenesis,* **28**(12), pp. 2476-2483.

SHI, W., FAN, H., SHUM, L. and DERYNCK, R., 2000. The tetraspanin CD9 associates with transmembrane TGF-alpha and regulates TGF-alpha-induced EGF receptor activation and cell proliferation. *The Journal of cell biology,* **148**(3), pp. 591-602.

SHIBATA, H., TOYAMA, K., SHIOYA, H., ITO, M., HIROTA, M., HASEGAWA, S., MATSUMOTO, H., TAKANO, H., AKIYAMA, T., TOYOSHIMA, K., KANAMARU, R., KANEGAE, Y., SAITO, I., NAKAMURA, Y., SHIBA, K. and NODA, T., 1997. Rapid colorectal adenoma formation initiated by conditional targeting of the Apc gene. *Science (New York, N.Y.),* **278**(5335), pp. 120-123.

SHOHAM, T., RAJAPAKSA, R., BOUCHEIX, C., RUBINSTEIN, E., POE, J.C., TEDDER, T.F. and LEVY, S., 2003. The tetraspanin CD81 regulates the expression of CD19 during B cell development in a postendoplasmic reticulum compartment. *Journal of immunology (Baltimore, Md.: 1950),* **171**(8), pp. 4062-4072.

SHOHAM, T., RAJAPAKSA, R., KUO, C.C., HAIMOVICH, J. and LEVY, S., 2006. Building of the tetraspanin web: distinct structural domains of CD81 function in different cellular compartments. *Molecular and cellular biology,* **26**(4), pp. 1373-1385.

SIGISMUND, S., ALGISI, V., NAPPO, G., CONTE, A., PASCOLUTTI, R., CUOMO, A., BONALDI, T., ARGENZIO, E., VERHOEF, L.G., MASPERO, E., BIANCHI, F., CAPUANI, F., CILIBERTO, A., POLO, S. and DI FIORE, P.P., 2013. Threshold-controlled ubiquitination of the EGFR directs receptor fate. *The EMBO journal,* **32**(15), pp. 2140-2157.

SIMPSON, R.J., LIM, J.W., MORITZ, R.L. and MATHIVANAN, S., 2009. Exosomes: proteomic insights and diagnostic potential. *Expert review of proteomics,* **6**(3), pp. 267-283.

SINGH, B., CARPENTER, G. and COFFEY, R.J., 2016. EGF receptor ligands: recent advances. *F1000Research,* **5**, pp. 10.12688/f1000research.9025.1.

SOLDEVILLA, B., RODRIGUEZ, M., SAN MILLAN, C., GARCIA, V., FERNANDEZ-PERIANEZ, R., GIL-CALDERON, B., MARTIN, P., GARCIA-GRANDE, A., SILVA, J., BONILLA, F. and DOMINGUEZ, G., 2014. Tumor-derived exosomes are enriched in DeltaNp73, which promotes oncogenic potential in acceptor cells and correlates with patient survival. *Human molecular genetics,* **23**(2), pp. 467-478.

SONG, N., LIU, S., ZHANG, J., LIU, J., XU, L., LIU, Y. and QU, X., 2014. Cetuximab-induced MET activation acts as a novel resistance mechanism in colon cancer cells. *International journal of molecular sciences,* **15**(4), pp. 5838-5851.

SONOSHITA, M., TAKAKU, K., OSHIMA, M., SUGIHARA, K. and TAKETO, M.M., 2002. Cyclooxygenase-2 Expression in Fibroblasts and Endothelial Cells of Intestinal Polyps. *Cancer research,* **62**(23), pp. 6846-6849.

SORKIN, A. and GOH, L.K., 2009. Endocytosis and intracellular trafficking of ErbBs. *Experimental cell research,* **315**(4), pp. 683-696.

STERK, L.M., GEUIJEN, C.A., VAN DEN BERG, J.G., CLAESSEN, N., WEENING, J.J. and SONNENBERG, A., 2002. Association of the tetraspanin CD151 with the laminin-binding integrins alpha3beta1, alpha6beta1, alpha6beta4 and alpha7beta1 in cells in culture and in vivo. *Journal of cell science,* **115**(Pt 6), pp. 1161-1173.

STIPP, C.S., KOLESNIKOVA, T.V. and HEMLER, M.E., 2003. Functional domains in tetraspanin proteins. *Trends in biochemical sciences,* **28**(2), pp. 106-112.

STROHECKER, A.M., JOSHI, S., POSSEMATO, R., ABRAHAM, R.T., SABATINI, D.M. and WHITE, E., 2015. Identification of 6-phosphofructo-2-kinase/fructose-2,6-bisphosphatase as a novel autophagy regulator by high content shRNA screening. *Oncogene,* **34**(45), pp. 5662-5676.

STUFFERS, S., SEM WEGNER, C., STENMARK, H. and BRECH, A., 2009. Multivesicular

endosome biogenesis in the absence of ESCRTs. *Traffic (Copenhagen, Denmark),* **10**(7), pp. 925-937.

SU, L.K., KINZLER, K.W., VOGELSTEIN, B., PREISINGER, A.C., MOSER, A.R., LUONGO, C., GOULD, K.A. and DOVE, W.F., 1992. Multiple intestinal neoplasia caused by a mutation in the murine homolog of the APC gene. *Science (New York, N.Y.),* **256**(5057), pp. 668-670.

SUZUKI, A., SEKIYA, S., GUNSHIMA, E., FUJII, S. and TANIGUCHI, H., 2010. EGF signaling activates proliferation and blocks apoptosis of mouse and human intestinal stem/progenitor cells in long-term monolayer cell culture. *Laboratory investigation; a journal of technical methods and pathology,* **90**(10), pp. 1425-1436.

SWEETSER, S., SMYRK, T.C. and SINICROPE, F.A., 2013. Serrated colon polyps as precursors to colorectal cancer. *Clinical gastroenterology and hepatology : the official clinical practice journal of the American Gastroenterological Association,* **11**(7), pp. 760-7; quiz e54-5.

TAKAKU, K., OSHIMA, M., MIYOSHI, H., MATSUI, M., SELDIN, M.F. and TAKETO, M.M., 1998. Intestinal tumorigenesis in compound mutant mice of both Dpc4 (Smad4) and Apc genes. *Cell,* **92**(5), pp. 645-656.

TAKEDA, Y., HE, P., TACHIBANA, I., ZHOU, B., MIYADO, K., KANEKO, H., SUZUKI, M., MINAMI, S., IWASAKI, T., GOYA, S., KIJIMA, T., KUMAGAI, T., YOSHIDA, M., OSAKI, T., KOMORI, T., MEKADA, E. and KAWASE, I., 2008. Double Deficiency of Tetraspanins CD9 and CD81 Alters Cell Motility and Protease Production of Macrophages and Causes Chronic Obstructive Pulmonary Disease-like Phenotype in Mice. *The Journal of Biological Chemistry,* **283**(38), pp. 26089-26097.

TALSETH-PALMER, B., 2017. The genetic basis of colonic adenomatous polyposis syndromes. *Hereditary Cancer in Clinical Practice,* **15**, pp. 5.

TAMURA, K., IKUTANI, M., YOSHIDA, T., TANAKA-HAYASHI, A., YANAGIBASHI, T., INOUE, R., NAGAI, Y., ADACHI, Y., MIYAWAKI, T., TAKATSU, K. and MORI, H., 2015. Increased production of intestinal immunoglobulins in Syntenin-1-deficient mice. *Immunobiology,* **220**(5), pp. 597-604.

TANG, X., LIU, H., YANG, S., LI, Z., ZHONG, J. and FANG, R., 2016. Epidermal Growth Factor and Intestinal Barrier Function. *Mediators of inflammation,* **2016**, pp. 1927348.

TANIGUCHI, K., SHAO, Y., TOWNSHEND, R., TSAI, Y., DELONG, C., LOPEZ, S., GAYEN, S., FREDDO, A., CHUE, D., THOMAS, D., SPENCE, J., MARGOLIS, B., KALANTRY, S., FU, J., OÂ€™SHEA, K.Â and GUMUCIO, D., 2015. Lumen Formation Is an Intrinsic Property of Isolated Human Pluripotent Stem Cells. *Stem Cell Reports,* **5**(6), pp. 954-962.

TAURO, B.J., GREENING, D.W., MATHIAS, R.A., MATHIVANAN, S., JI, H. and SIMPSON, R.J., 2012. Two Distinct Populations of Exosomes Are Released from LIM1863 Colon Carcinoma Cell-derived Organoids. *Molecular & Cellular Proteomics : MCP,* **12**(3), pp. 587-598.

TERMINI, C.M. and GILLETTE, J.M., 2017. Tetraspanins Function as Regulators of Cellular Signaling. *Frontiers in cell and developmental biology,* **5**, pp. 34.

TESTA, U., PELOSI, E. and CASTELLI, G., 2018. Colorectal Cancer: Genetic Abnormalities, Tumor Progression, Tumor Heterogeneity, Clonal Evolution and Tumor-Initiating Cells. *Medical Sciences,* **6**(2), pp. 31.

THERY, C., 2011. Exosomes: secreted vesicles and intercellular communications. *F1000 biology reports,* **3**, pp. 15-15. Epub 2011 Jul 1.

THIEN, C.B. and LANGDON, W.Y., 2001. Cbl: many adaptations to regulate protein tyrosine kinases. *Nature reviews.Molecular cell biology,* **2**(4), pp. 294-307.

THORNTON, T.M., PEDRAZA-ALVA, G., DENG, B., WOOD, C.D., ARONSHTAM, A., CLEMENTS, J.L., SABIO, G., DAVIS, R.J., MATTHEWS, D.E., DOBLE, B. and RINCON, M., 2008. Phosphorylation by p38 MAPK as an alternative pathway for GSK3beta inactivation. *Science (New York, N.Y.),* **320**(5876), pp. 667-670.

TILG, H., ADOLPH, T.E., GERNER, R.R. and MOSCHEN, A.R., 2018. The Intestinal Microbiota in Colorectal Cancer. *Cancer cell,* **33**(6), pp. 954-964.

TOH, W.S., LAI, R.C., ZHANG, B. and LIM, S.K., 2018. MSC exosome works through a protein-based mechanism of action. *Biochemical Society transactions,* .

TOMLINSON, I., 2015. An update on the molecular pathology of the intestinal polyposis syndromes. *Diagnostic Histopathology; Mini-Symposium: Pathology of Hereditary Gastrointestinal Neoplasia,* **21**(4), pp. 147-151.

TONG, Y., YANG, W. and KOEFFLER, H.P., 2011. Mouse models of colorectal cancer. *Chinese Journal of Cancer,* **30**(7), pp. 450-462.

TROIANI, T., MARTINELLI, E., NAPOLITANO, S., VITAGLIANO, D., CIUFFREDA, L.P., COSTANTINO, S., MORGILLO, F., CAPASSO, A., SFORZA, V., NAPPI, A., DE PALMA, R., D'AIUTO, E., BERRINO, L., BIANCO, R. and CIARDIELLO, F., 2013. Increased TGF-alpha as a mechanism of acquired resistance to the anti-EGFR inhibitor cetuximab through EGFR-MET interaction and activation of MET signaling in colon cancer cells. *Clinical cancer research : an official journal of the American Association for Cancer Research,* **19**(24), pp. 6751-6765.

TROYER, K.L., LUETTEKE, N.C., SAXON, M.L., QIU, T.H., XIAN, C.J. and LEE, D.C., 2001. Growth retardation, duodenal lesions, and aberrant ileum architecture in triple null mice lacking EGF, amphiregulin, and TGF-alpha. *Gastroenterology,* **121**(1), pp. 68-78.

TSENG, Y.H. and HE, T.C., 2007. Bone morphogenetic proteins and adipocyte differentiation. **3**, pp. 342-360.

TSITSIKOV, E.N., GUTIERREZ-RAMOS, J.C. and GEHA, R.S., 1997. Impaired CD19 expression and signaling, enhanced antibody response to type II T independent antigen and reduction of B-1 cells in CD81-deficient mice. *Proceedings of the National Academy of Sciences of the United States of America,* **94**(20), pp. 10844-10849.

TU, H., AHEARN, T.U., DANIEL, C.R., GONZALEZ-FELICIANO, A.G., SEABROOK, M.E. and BOSTICK, R.M., 2015. Transforming growth factors and receptor as potential modifiable pre-neoplastic biomarkers of risk for colorectal neoplasms. *Molecular carcinogenesis,* **54**(9), pp. 821-830.

UHLEN, M., ZHANG, C., LEE, S., SJOSTEDT, E., FAGERBERG, L., BIDKHORI, G., BENFEITAS, R., ARIF, M., LIU, Z., EDFORS, F., SANLI, K., VON FEILITZEN, K., OKSVOLD, P., LUNDBERG, E., HOBER, S., NILSSON, P., MATTSSON, J., SCHWENK, J.M., BRUNNSTROM, H., GLIMELIUS, B., SJOBLOM, T., EDQVIST, P.H., DJUREINOVIC, D., MICKE, P., LINDSKOG, C., MARDINOGLU, A. and PONTEN, F., 2017. A pathology atlas of the human cancer transcriptome. *Science (New York, N.Y.),* **357**(6352), pp. 10.1126/science.aan2507.

VALLE, L., 2014. Genetic predisposition to colorectal cancer: where we stand and future perspectives. *World journal of gastroenterology,* **20**(29), pp. 9828-9849.

VAN DE WETERING, M., FRANCIES, H.E., FRANCIS, J.M., BOUNOVA, G., IORIO, F.,

PRONK, A., VAN HOUDT, W., VAN GORP, J., TAYLOR-WEINER, A., KESTER, L., MCLAREN-DOUGLAS, A., BLOKKER, J., JAKSANI, S., BARTFELD, S., VOLCKMAN, R., VAN SLUIS, P., LI, V.S., SEEPO, S., SEKHAR PEDAMALLU, C., CIBULSKIS, K., CARTER, S.L., MCKENNA, A., LAWRENCE, M.S., LICHTENSTEIN, L., STEWART, C., KOSTER, J., VERSTEEG, R., VAN OUDENAARDEN, A., SAEZ-RODRIGUEZ, J., VRIES, R.G., GETZ, G., WESSELS, L., STRATTON, M.R., MCDERMOTT, U., MEYERSON, M., GARNETT, M.J. and CLEVERS, H., 2015. Prospective derivation of a living organoid biobank of colorectal cancer patients. *Cell,* **161**(4), pp. 933-945.

VAN DER FLIER, L.G. and CLEVERS, H., 2009. Stem cells, self-renewal, and differentiation in the intestinal epithelium. *Annual Review of Physiology,* **71**, pp. 241-260.

VAN DER WEYDEN, L., ARENDS, M.J., DOVEY, O.M., HARRISON, H.L., LEFEBVRE, G., CONTE, N., GERGELY, F.V., BRADLEY, A. and ADAMS, D.J., 2008. Loss of Rassf1a cooperates with Apc(Min) to accelerate intestinal tumourigenesis. *Oncogene,* **27**(32), pp. 4503-4508.

VAN DEVENTER, S.J., DUNLOCK, V.E. and VAN SPRIEL, A.B., 2017. Molecular interactions shaping the tetraspanin web. *Biochemical Society transactions,* **45**(3), pp. 741-750.

VAN ES, J.H., JAY, P., GREGORIEFF, A., VAN GIJN, M.E., JONKHEER, S., HATZIS, P., THIELE, A., VAN DEN BORN, M., BEGTHEL, H., BRABLETZ, T., TAKETO, M.M. and CLEVERS, H., 2005. Wnt signalling induces maturation of Paneth cells in intestinal crypts. *Nature cell biology,* **7**(4), pp. 381-386.

VAN GIJN, W., MARIJNEN, C.A., NAGTEGAAL, I.D., KRANENBARG, E.M., PUTTER, H., WIGGERS, T., RUTTEN, H.J., PAHLMAN, L., GLIMELIUS, B., VAN DE VELDE, C.J. and DUTCH COLORECTAL CANCER GROUP, 2011. Preoperative radiotherapy combined with total mesorectal excision for resectable rectal cancer: 12-year follow-up of the multicentre, randomised controlled TME trial. *The Lancet.Oncology,* **12**(6), pp. 575-582.

VAN NIEL, G., D'ANGELO, G. and RAPOSO, G., 2018. Shedding light on the cell biology of extracellular vesicles. *Nature Reviews Molecular Cell Biology,* **19**, pp. 213.

VAN NIEL, G., CHARRIN, S., SIMOES, S., ROMAO, M., ROCHIN, L., SAFTIG, P., MARKS, M.S., RUBINSTEIN, E. and RAPOSO, G., 2011. The tetraspanin CD63 regulates ESCRT-independent and -dependent endosomal sorting during melanogenesis. *Developmental cell,* **21**(4), pp. 708-721.

VAN SCHAEYBROECK, S., KELLY, D.M., KYULA, J., STOKESBERRY, S., FENNELL, D.A., JOHNSTON, P.G. and LONGLEY, D.B., 2008. Src and ADAM-17-mediated shedding of transforming growth factor-alpha is a mechanism of acute resistance to TRAIL. *Cancer research,* **68**(20), pp. 8312-8321.

VAN ZELM, M.C., SMET, J., ADAMS, B., MASCART, F., SCHANDENE, L., JANSSEN, F., FERSTER, A., KUO, C.C., LEVY, S., VAN DONGEN, J.J. and VAN DER BURG, M., 2010. CD81 gene defect in humans disrupts CD19 complex formation and leads to antibody deficiency. *The Journal of clinical investigation,* **120**(4), pp. 1265-1274.

VASEN, H.F., TOMLINSON, I. and CASTELLS, A., 2015. Clinical management of hereditary colorectal cancer syndromes. *Nature reviews.Gastroenterology & hepatology,* **12**(2), pp. 88-97.

VENCES-CATALAN, F., RAJAPAKSA, R., LEVY, S. and SANTOS-ARGUMEDO, L., 2012. The CD19/CD81 complex physically interacts with CD38 but is not required to induce proliferation in mouse B lymphocytes. *Immunology,* **137**(1), pp. 48-55.

VENTRESS, J.K., PARTRIDGE, L.J., READ, R.C., COZENS, D., MACNEIL, S. and MONK, P.N., 2016. Peptides from Tetraspanin CD9 Are Potent Inhibitors of Staphylococcus Aureus

Adherence to Keratinocytes. *PloS one,* **11**(7), pp. e0160387.

VLACHOGIANNIS, G., HEDAYAT, S., VATSIOU, A., JAMIN, Y., FERNANDEZ-MATEOS, J., KHAN, K., LAMPIS, A., EASON, K., HUNTINGFORD, I., BURKE, R., RATA, M., KOH, D.M., TUNARIU, N., COLLINS, D., HULKKI-WILSON, S., RAGULAN, C., SPITERI, I., MOORCRAFT, S.Y., CHAU, I., RAO, S., WATKINS, D., FOTIADIS, N., BALI, M., DARVISH-DAMAVANDI, M., LOTE, H., ELTAHIR, Z., SMYTH, E.C., BEGUM, R., CLARKE, P.A., HAHNE, J.C., DOWSETT, M., DE BONO, J., WORKMAN, P., SADANANDAM, A., FASSAN, M., SANSOM, O.J., ECCLES, S., STARLING, N., BRACONI, C., SOTTORIVA, A., ROBINSON, S.P., CUNNINGHAM, D. and VALERI, N., 2018. Patient-derived organoids model treatment response of metastatic gastrointestinal cancers. *Science (New York, N.Y.),* **359**(6378), pp. 920-926.

VOGELSTEIN, B., FEARON, E.R., HAMILTON, S.R., KERN, S.E., PREISINGER, A.C., LEPPERT, M., SMITS, A.M.M. and BOS, J.L., 1988. Genetic Alterations during Colorectal-Tumor Development. *N Engl J Med,* **319**(9), pp. 525-532.

WALLER, A., FINDEIS, S. and LEE, M.J., 2016. Familial Adenomatous Polyposis. *Journal of pediatric genetics,* **5**(2), pp. 78-83.

WANG, H., JIN, H. and RAPRAEGER, A.C., 2015. Syndecan-1 and Syndecan-4 Capture Epidermal Growth Factor Receptor Family Members and the alpha3beta1 Integrin Via Binding Sites in Their Ectodomains: NOVEL SYNSTATINS PREVENT KINASE CAPTURE AND INHIBIT alpha6beta4-INTEGRIN-DEPENDENT EPITHELIAL CELL MOTILITY. *The Journal of biological chemistry,* **290**(43), pp. 26103-26113.

WANG, H.X., LI, Q., SHARMA, C., KNOBLICH, K. and HEMLER, M.E., 2011. Tetraspanin protein contributions to cancer. *Biochemical Society transactions,* **39**(2), pp. 547-552.

WANG, L.K., HSIAO, T.H., HONG, T.M., CHEN, H.Y., KAO, S.H., WANG, W.L., YU, S.L., LIN, C.W. and YANG, P.C., 2014. MicroRNA-133a suppresses multiple oncogenic membrane receptors and cell invasion in non-small cell lung carcinoma. *PloS one,* **9**(5), pp. e96765.

WANG, L. and ZHANG, Q., 2015. Application of the ApcMin/+ mouse model for studying inflammation-associated intestinal tumor. *Biomedicine & Pharmacotherapy,* **71**, pp. 216-221.

WANG, M., ZHAO, C., SHI, H., ZHANG, B., ZHANG, L., ZHANG, X., WANG, S., WU, X., YANG, T., HUANG, F., CAI, J., ZHU, Q., ZHU, W., QIAN, H. and XU, W., 2014. Deregulated microRNAs in gastric cancer tissue-derived mesenchymal stem cells: novel biomarkers and a mechanism for gastric cancer. *British journal of cancer,* **110**(5), pp. 1199-1210.

WANG, Y., TONG, X., OMOREGIE, E.S., LIU, W., MENG, S. and YE, X., 2012. Tetraspanin 6 (TSPAN6) negatively regulates retinoic acid-inducible gene I-like receptor-mediated immune signaling in a ubiquitination-dependent manner. *The Journal of biological chemistry,* **287**(41), pp. 34626-34634.

WEE, P. and WANG, Z., 2017. Epidermal Growth Factor Receptor Cell Proliferation Signaling Pathways. *Cancers,* **9**(5), pp. 52.

WEIGAND, K.M., SWARTS, H.G., FEDOSOVA, N.U., RUSSEL, F.G. and KOENDERINK, J.B., 2012. Na,K-ATPase activity modulates Src activation: a role for ATP/ADP ratio. *Biochimica et biophysica acta,* **1818**(5), pp. 1269-1273.

WHO, W.H.O., 2015-last update, Cancer [Online]. Available: http://www.who.int/mediacentre/factsheets/fs297/en/ [08/25, 2018].

WIESE, K.E., NUSSE, R. and VAN AMERONGEN, R., 2018. Wnt signalling: conquering

complexity. *Development (Cambridge, England),* **145**(12), pp. 10.1242/dev.165902.

WILHELM, S.M., DUMAS, J., ADNANE, L., LYNCH, M., CARTER, C.A., SCHUTZ, G., THIERAUCH, K.H. and ZOPF, D., 2011. Regorafenib (BAY 73-4506): a new oral multikinase inhibitor of angiogenic, stromal and oncogenic receptor tyrosine kinases with potent preclinical antitumor activity. *International journal of cancer,* **129**(1), pp. 245-255.

WILLETT, C.G., BOUCHER, Y., DI TOMASO, E., DUDA, D.G., MUNN, L.L., TONG, R.T., CHUNG, D.C., SAHANI, D.V., KALVA, S.P., KOZIN, S.V., MINO, M., COHEN, K.S., SCADDEN, D.T., HARTFORD, A.C., FISCHMAN, A.J., CLARK, J.W., RYAN, D.P., ZHU, A.X., BLASZKOWSKY, L.S., CHEN, H.X., SHELLITO, P.C., LAUWERS, G.Y. and JAIN, R.K., 2004. Direct evidence that the VEGF-specific antibody bevacizumab has antivascular effects in human rectal cancer. *Nature medicine,* **10**(2), pp. 145-147.

WILSON, K.J., MILL, C., LAMBERT, S., BUCHMAN, J., WILSON, T.R., HERNANDEZ-GORDILLO, V., GALLO, R.M., ADES, L.M., SETTLEMAN, J. and RIESE, D.J.,2nd, 2012. EGFR ligands exhibit functional differences in models of paracrine and autocrine signaling. *Growth factors (Chur, Switzerland),* **30**(2), pp. 107-116.

WONG, V.W.Y., STANGE, D.E., PAGE, M.E., BUCZACKI, S., WABIK, A., ITAMI, S., VAN, D.W., POULSOM, R., WRIGHT, N.A., TROTTER, M.W.B., WATT, F.M., WINTON, D.J., CLEVERS, H. and JENSEN, K.B., 2012. Lrig1 controls intestinal stem cell homeostasis by negative regulation of ErbB signalling. *Nature cell biology,* **14**(4), pp. 401-408.

WOOD, L.D., PARSONS, D.W., JONES, S., LIN, J., SJÖBLOM, T., LEARY, R.J., SHEN, D., BOCA, S.M., BARBER, T., PTAK, J., SILLIMAN, N., SZABO, S., DEZSO, Z., USTYANKSKY, V., NIKOLSKAYA, T., NIKOLSKY, Y., KARCHIN, R., WILSON, P.A., KAMINKER, J.S., ZHANG, Z., CROSHAW, R., WILLIS, J., DAWSON, D., SHIPITSIN, M., WILLSON, J.K.V., SUKUMAR, S., POLYAK, K., PARK, B.H., PETHIYAGODA, C.L., PANT, P.V.K., BALLINGER, D.G., SPARKS, A.B., HARTIGAN, J., SMITH, D.R., SUH, E., PAPADOPOULOS, N., BUCKHAULTS, P., MARKOWITZ, S.D., PARMIGIANI, G., KINZLER, K.W., VELCULESCU, V.E. and VOGELSTEIN, B., 2007. The Genomic Landscapes of Human Breast and Colorectal Cancers. *Science,* **318**(5853), pp. 1108-1113.

WRIGHT, M.D., GEARY, S.M., FITTER, S., MOSELEY, G.W., LAU, L.M., SHENG, K.C., APOSTOLOPOULOS, V., STANLEY, E.G., JACKSON, D.E. and ASHMAN, L.K., 2004. Characterization of mice lacking the tetraspanin superfamily member CD151. *Molecular and cellular biology,* **24**(13), pp. 5978-5988.

WRIGLEY, J.D., AHMED, T., NEVETT, C.L. and FINDLAY, J.B., 2000. Peripherin/rds influences membrane vesicle morphology. Implications for retinopathies. *The Journal of biological chemistry,* **275**(18), pp. 13191-13194.

WU, J., JIAO, Y., DAL MOLIN, M., MAITRA, A., DE WILDE, R.F., WOOD, L.D., ESHLEMAN, J.R., GOGGINS, M.G., WOLFGANG, C.L., CANTO, M.I., SCHULICK, R.D., EDIL, B.H., CHOTI, M.A., ADSAY, V., KLIMSTRA, D.S., OFFERHAUS, G.J., KLEIN, A.P., KOPELOVICH, L., CARTER, H., KARCHIN, R., ALLEN, P.J., SCHMIDT, C.M., NAITO, Y., DIAZ, L.A.,Jr, KINZLER, K.W., PAPADOPOULOS, N., HRUBAN, R.H. and VOGELSTEIN, B., 2011. Whole-exome sequencing of neoplastic cysts of the pancreas reveals recurrent mutations in components of ubiquitin-dependent pathways. *Proceedings of the National Academy of Sciences of the United States of America,* **108**(52), pp. 21188-21193.

XIAO, H., YIN, W., KHAN, M.A., GULEN, M.F., ZHOU, H., SHAM, H.P., JACOBSON, K., VALLANCE, B.A. and LI, X., 2010. Loss of single immunoglobulin interlukin-1 receptor-related molecule leads to enhanced colonic polyposis in Apc(min) mice. *Gastroenterology,* **139**(2), pp. 574-585.

YAMADA, Y. and MORI, H., 2007. Multistep carcinogenesis of the colon in Apc(Min/+) mouse. *Cancer science,* **98**(1), pp. 6-10.

YAMANE, L., SCAPULATEMPO-NETO, C., REIS, R.M. and GUIMARAES, D.P., 2014. Serrated pathway in colorectal carcinogenesis. *World journal of gastroenterology,* **20**(10), pp. 2634-2640.

YAMASAKI, M., EMOTO, H., KONISHI, M., MIKAMI, T., OHUCHI, H., NAKAO, K. and ITOH, N., 1999. *FGF-10 Is a Growth Factor for Preadipocytes in White Adipose Tissue.*

YAMAZAKI, Y., OKAWA, K., YANO, T., TSUKITA, S. and TSUKITA, S., 2008. Optimized proteomic analysis on gels of cell-cell adhering junctional membrane proteins. *Biochemistry,* **47**(19), pp. 5378-5386.

YANEZ-MO, M., SILJANDER, P.R., ANDREU, Z., ZAVEC, A.B., BORRAS, F.E., BUZAS, E.I., BUZAS, K., CASAL, E., CAPPELLO, F., CARVALHO, J., COLAS, E., CORDEIRO-DA SILVA, A., FAIS, S., FALCON-PEREZ, J.M., GHOBRIAL, I.M., GIEBEL, B., GIMONA, M., GRANER, M., GURSEL, I., GURSEL, M., HEEGAARD, N.H., HENDRIX, A., KIERULF, P., KOKUBUN, K., KOSANOVIC, M., KRALJ-IGLIC, V., KRAMER-ALBERS, E.M., LAITINEN, S., LASSER, C., LENER, T., LIGETI, E., LINE, A., LIPPS, G., LLORENTE, A., LOTVALL, J., MANCEK-KEBER, M., MARCILLA, A., MITTELBRUNN, M., NAZARENKO, I., NOLTE-'T HOEN, E.N., NYMAN, T.A., O'DRISCOLL, L., OLIVAN, M., OLIVEIRA, C., PALLINGER, E., DEL PORTILLO, H.A., REVENTOS, J., RIGAU, M., ROHDE, E., SAMMAR, M., SANCHEZ-MADRID, F., SANTAREM, N., SCHALLMOSER, K., OSTENFELD, M.S., STOORVOGEL, W., STUKELJ, R., VAN DER GREIN, S.G., VASCONCELOS, M.H., WAUBEN, M.H. and DE WEVER, O., 2015. Biological properties of extracellular vesicles and their physiological functions. *Journal of extracellular vesicles,* **4**, pp. 27066.

YANG, S., ZHOU, X., LI, R., FU, X. and SUN, P., 2017. Optimized PEI-based Transfection Method for Transient Transfection and Lentiviral Production. *Current protocols in chemical biology,* **9**(3), pp. 147-157.

YANG, X., CLAAS, C., KRAEFT, S.K., CHEN, L.B., WANG, Z., KREIDBERG, J.A. and HEMLER, M.E., 2002. Palmitoylation of tetraspanin proteins: modulation of CD151 lateral interactions, subcellular distribution, and integrin-dependent cell morphology. *Molecular biology of the cell,* **13**(3), pp. 767-781.

YANG, Y. and MLODZIK, M., 2015. Wnt-Frizzled/planar cell polarity signaling: cellular orientation by facing the wind (Wnt). *Annual Review of Cell and Developmental Biology,* **31**, pp. 623-646.

YANG, Y.G., SARI, I.N., ZIA, M.F., LEE, S.R., SONG, S.J. and KWON, H.Y., 2016. Tetraspanins: Spanning from solid tumors to hematologic malignancies. *Experimental hematology,* **44**(5), pp. 322-328.

YASUHIRO, Y. and HIDEKI, M., 2007. Multistep carcinogenesis of the colon in ApcMin/+ mouse. *Cancer Science,* **98**(1), pp. 6-10.

YEUNG, L., HICKEY, M.J. and WRIGHT, M.D., 2018. The Many and Varied Roles of Tetraspanins in Immune Cell Recruitment and Migration. *Frontiers in immunology,* **9**, pp. 1644.

YOUNG, M., ORDONEZ, L. and CLARKE, A.R., 2013. What are the best routes to effectively model human colorectal cancer? *Molecular oncology,* **7**(2), pp. 178-189.

YOUNG, M. and REED, K.R., 2016. Organoids as a Model for Colorectal Cancer. *Current Colorectal Cancer Reports,* **12**(5), pp. 281-287.

YUN, S., KWAK, Y., NAM, S.K., SEO, A.N., OH, H.K., KIM, D.W., KANG, S.B. and LEE, H.S., 2018. Ligand-Independent Epidermal Growth Factor Receptor Overexpression Correlates with Poor Prognosis in Colorectal Cancer. *Cancer research and treatment : official journal of Korean Cancer Association,* .

ZHAI, Z., YU, X., YANG, B., ZHANG, Y., ZHANG, L., LI, X. and SUN, H., 2017. Colorectal cancer heterogeneity and targeted therapy: Clinical implications, challenges and solutions for treatment resistance. *Seminars in cell & developmental biology,* **64**, pp. 107-115.

ZHANG, B., YIN, Y., LAI, R.C. and LIM, S.K., 2014. Immunotherapeutic Potential of Extracellular Vesicles. *Frontiers in Immunology,* **5**, pp. 518.

ZHANG, H., LI, Z.L., YE, S.B., OUYANG, L.Y., CHEN, Y.S., HE, J., HUANG, H.Q., ZENG, Y.X., ZHANG, X.S. and LI, J., 2015. Myeloid-derived suppressor cells inhibit T cell proliferation in human extranodal NK/T cell lymphoma: a novel prognostic indicator. *Cancer immunology, immunotherapy : CII,* **64**(12), pp. 1587-1599.

ZHANG, L., AALKJAER, C. and MATCHKOV, V.V., 2018. The Na,K-ATPase-Dependent Src Kinase Signaling Changes with Mesenteric Artery Diameter. *International journal of molecular sciences,* **19**(9), pp. 10.3390/ijms19092489.

ZHANG, L. and WRANA, J.L., 2014. The emerging role of exosomes in Wnt secretion and transport. *Current opinion in genetics & development,* **27**, pp. 14-19.

ZHANG, S., ZHANG, Y., QU, J., CHE, X., FAN, Y., HOU, K., GUO, T., DENG, G., SONG, N., LI, C., WAN, X., QU, X. and LIU, Y., 2017. Exosomes promote cetuximab resistance via the PTEN/Akt pathway in colon cancer cells. *Brazilian journal of medical and biological research = Revista brasileira de pesquisas medicas e biologicas,* **51**(1), pp. e6472-431X20176472.

ZHANG, X.A., LANE, W.S., CHARRIN, S., RUBINSTEIN, E. and LIU, L., 2003. EWI2/PGRL associates with the metastasis suppressor KAI1/CD82 and inhibits the migration of prostate cancer cells. *Cancer research,* **63**(10), pp. 2665-2674.

ZHAO, B., WANG, L., QIU, H., ZHANG, M., SUN, L., PENG, P., YU, Q. and YUAN, X., 2017. Mechanisms of resistance to anti-EGFR therapy in colorectal cancer. *Oncotarget,* **8**(3), pp. 3980-4000.

ZHAO, M., MISHRA, L. and DENG, C.X., 2018. The role of TGF-beta/SMAD4 signaling in cancer. *International journal of biological sciences,* **14**(2), pp. 111-123.

ZHOU, J., FUJIWARA, T., YE, S., LI, X. and ZHAO, H., 2014. Downregulation of Notch modulators, tetraspanin 5 and 10, inhibits osteoclastogenesis in vitro. *Calcified tissue international,* **95**(3), pp. 209-217.

ZHU, Y., AILANE, N., SALA-VALDES, M., HAGHIGHI-RAD, F., BILLARD, M., NGUYEN, V., SAFFROY, R., LEMOINE, A., RUBINSTEIN, E., BOUCHEIX, C. and GRECO, C., 2017. Multi-factorial modulation of colorectal carcinoma cells motility - partial coordination by the tetraspanin Co-029/tspan8. *Oncotarget,* **8**(16), pp. 27454-27470.

ZIMMERMAN, B., KELLY, B., MCMILLAN, B.J., SEEGAR, T.C.M., DROR, R.O., KRUSE, A.C. and BLACKLOW, S.C., 2016. Crystal Structure of a Full-Length Human Tetraspanin Reveals a Cholesterol-Binding Pocket. *Cell,* **167**(4), pp. 1041-1051.e11.

ZUIDSCHERWOUDE, M., GOTTFERT, F., DUNLOCK, V.M., FIGDOR, C.G., VAN DEN BOGAART, G. and VAN SPRIEL, A.B., 2015. The tetraspanin web revisited by super-resolution microscopy. *Scientific reports,* **5**, pp. 12201.